SYSTEM STUDIES IN COLUMN CRYSTALLISERS

by

C. BATES

A thesis is submitted for the
Degree of Doctor of Philosophy,
The City University, Department
of Industrial Chemistry, London.
November, 1981

TABLE OF CONTENTS

List of Tables

Lists of Figures

List of Photographs

ACKNOWLEDGEMENTS

The author would like to express his gratitude to Dr. [redacted] for advice, guidance and encouragement given throughout the project. I would also like to thank Mr. [redacted], for his technical advice and assistance with assembly of the experimental equipment. I am indebted to my colleagues, Dr. [redacted], Mr. [redacted] and Miss [redacted], for their assistance during the course of the work and especially to my wife for her invaluable help with the preparation of the thesis.

DECLARATION

"I grant powers of discretion to the University Librarian to allow this thesis to be copied in whole or in part without further reference to me. This permission covers only single copies made for study purposes, subject to normal conditions of acknowledgement."

ABSTRACT

The process of column crystallisation was initially developed for the small scale production of ultra-pure organic compounds. The original units were small bench scale systems producing only a few grams of purified product. The work presented in the thesis is the scale up of a Schildknecht column to give a unit capable of producing several kilograms of purified product, continuously. A 100 millimetre diameter column crystalliser was designed and constructed, the layout being based upon results from the 50 millimetre diameter column. The equipment assembled is capable of processing a range of aqueous and organic, binary, eutectic mixtures. The column is able to operate batchwise or continuously.

Systems investigated on the 100 millimetre column include ~ desalination and ethanol concentration. Waste effluent recovery and heavy water regeneration were evaluated on the 50 millimetre column. Operation of the columns is optimised for the above systems, the parameters investigated being, speed of rotation of the transport conveyor, crystal production rate, product removal rate and reflux ratio. In order to elucidate the dominant factors in the purification process, an extractive washing model is utilised to calculate values of the diffusion and mass transfer groups. The important factors controlling the separation efficiency of the columns are the axial diffusion of impurity and the mass transfer between the adhering and free liquids around the crystal phase. The variation in these two parameters for each column is discussed. An attempt at simplifying the mathematical model is presented. The aim is to develop an equation capable of predicting key parameters rapidly, that is, product purity and column length. Also the effects of speed of rotation of the helical transfer unit on mean crystal size is reported.

List of Symbols

a	Area available for mass transfer between adhering and reflux liquids per unit volume of the column (L^{-1})
A	Column cross section normal to flow direction (window area defined by conveyor and annulus) (L^2)
C	Crystal production rate ($M.T^{-1}$)
D	Coefficient of diffusion ($L^2.T^{-1}$)
F	Feed flow rate ($M.T^{-1}$)
H_E	Separation factor for the enriching section, defined by equation (3.48) (L)
H_S	Separation factor for the stripping section, defined by equation (3.57) (L)
H_Φ	Separation factor for the enriching section, operating the column at total reflux, defined by equation (3.59) (L)
K	Mass Transfer coefficient between adhering and free liquids (LT^{-1})
L	Reflux liquid stream rate ($M.T^{-1}$)
L'	Adhering liquid stream rate ($M.T^{-1}$)
L_E	Enriched product stream rate ($L^3.T^{-1}$)
L_S	Stripped product stream rate ($L^3.T^{-1}$)
L_P	Purification section length (L)
M_D	Mass transfer rate of impurity due to axial dispersion ($M.T^{-1}$)
M_K	Mass transfer rate of impurity from adhering liquid to reflux liquid ($M.T^{-1}$)
R_E	Product offtake ratio ($R_E = L_E/C$)
Y	Impurity content of reflux liquid ($M.M^{-1}$)
Y'	Impurity content of adhering liquid ($M.M^{-1}$)
Y_E	Impurity content of enriched stream ($M.M^{-1}$)
Y_F	Impurity content of feed stream ($M.M^{-1}$)
Y_P	Defined by equation (3.49) ($M.M^{-1}$)
$\bar{Y}_P$	Defined by equation (3.56) ($M.M^{-1}$)
Y_S	Impurity content of stripped stream ($M.M^{-1}$)

Y_{ϕ} Impurity content of reflux liquid at the feed point $(M.M^{-1})$

Y_{Φ} Free liquid composition at the top of the purification section when operating the column at total reflux $(M.M^{-1})$

Y* Impurity content of stripped stream at zero stream rate $(M.M^{-1})$

Z Distance in the column measured from the freezing section (L)

Z_F Distance of the feed point from the freezing section (L)

Z* Distance from the feed point to a point located in the column $(Z-Z_F)$ (L)

Greek Symbols

α Ratio of adhering liquid stream to crystal rate

ε Impurity content of solid phase $(M.M^{-1})$

η Volume fraction of free liquid

ρ Density of liquid phase $(M.L^{-3})$

CHAPTER 1

(1) Introduction

The process of fractional crystallisation is used for the separation and purification of components and is achieved by the dissolution and formation of crystals. If a solvent is present, the pure product is crystallised out and this is fractional crystallisation from solution, for example, the separation of a mixture of salts with water. In the case of a phase transition without the addition of a solvent, the process is fractional solidification, for example, the separation of two salts from a melt as it is allowed to cool. One can achieve the same result when crystallising out a component from a binary solution, for example, a salt and water mixture which forms a eutectic. Upon cooling, either ice or pure salt separates out from solution and both are considered fractional solidification since no third component was added as solvent. This last point is very important for a purification, since with fractional crystallisation from solution, one has solvent as a possible product contaminant, whereas this is eliminated with fractional solidification.

Crystallisation has been used to improve the standard of living of man for several thousand years. The crystallisation of both salt and sugar are by far the oldest and probably among the most important of crystallisation activities. Bennett[1] cites the crystallisation of sugar by the Persians in 500 A.D. as one of the earliest instances where the people collected syrups and boiled them to produce a purified form of crystalline sugar. For many centuries man has been aware that sea-ice has a lower salt content than the sea and in many instances has been used to supplement supplies of fresh water. This phenomenon had been observed by Nebbia[2] in the sixteenth century with his studies on the freezing of salt water. He noted the effects of the initial salt

concentration on the final product quality and how by subsequent freezing/melting the salt concentration could be reduced to only a trace. Detailed investigation by Buchanan[3] on his Antarctic cruise identified the constituents of the sea-ice, and that the success of the purification was determined by how the ice was melted. In this instance, the pure solvent had frozen out rejecting the brine, the "pockets" of brine being removed by drainage and washing as the ice melted.

Industrial crystallisation, though one of the oldest chemical engineering unit operations, still remains one of the last to yield to quantitative analysis and is one of the most difficult to operate continuously in a steady state manner. Crystallisation offers several advantages as a general method of separation and purification. The first, and perhaps most important, stems from the fact that the crystalline state is the most ordered one. In general, the crystallising substance which first separates from any solution is highly pure, even when the solution itself contains considerable quantities of contaminants. In fractional solidification the separation is a phase transition between solid-liquid and as such is analogous to fractional distillation, where the transition is between a vapour and a liquid phase.

The separation of two or more liquids by fractional distillation is well known. The separation depends on the concentration differences between two phases at equilibrium, and is in effect a countercurrent method which operates continuously. Until recently there has been no method whereby solid/liquid separation could be carried out continuously in one apparatus. With fractional solidification one utilises a column very similar to a packed distillation column and operates on concentration differences between the solid and liquid phases. The process is both countercurrent

and continuous in operation and suffers some of the limitations of a distillation column, that is, attainment of equilibrium and mass transfer effects. With distillation one only achieves slight enrichment at each stage and multi-stage processes are required for really good separations. A good industrial fractionating column may contain as many as a hundred plates and be capable of separating closely boiling liquids on a very large scale. Since the degree of purification of a single crystallisation is so high, one or two recrystallisations will produce material of exceptionally high purity. This is the case with fractional solidification and one achieves high degrees of purity with a smaller number of theoretical plates in the column.

The two processes differ in that with fractional solidification it is common to have low solubility in the solid phase, whereas liquid mixtures usually exhibit complete mutual miscibility. Changes in pressure have only a small effect on the solid-liquid phase equilibria as opposed to vapour-liquid equilibria. Alternatively by changing the phase of the mixture to be separated from liquid to solid rather than liquid-vapour, the energy requirements are less since the latent heat of fusion is usually much less than the latent heat of vaporization. With a fractional crystallisation process it is possible to separate systems that were uneconomical for distillation because of low relative volatilities, close solubilities or sensitivity to small increases of temperature during processing.

Examples of commercial industrial crystallisation processes which have achieved importance are numerous. Various systems have been treated and fractional crystallisation is used for separating and purifying numerous organics and for concentrating aqueous systems. An early success using a countercurrent fractional solidification process was achieved by Arnold[4][5] of the Philips Petroleum Company. He conceived a process for the production of pure p-xylene

from a mixture of its isomers. From typical feed stocks containing 22 per cent p-xylene, (the remaining 78 per cent being o, m-xylene plus ethyl benzene) high purity streams of p-xylene were produced of 94 to 98.7 per cent purity.[6] The process has now become commercially established, and during the early 1960's plants were regularly producing more than 60,000 metric tons/annum of product with a purity greater than 99 per cent. This process has overcome the problems associated with the fractional distillation of the xylene isomers. The system utilises an external chiller to produce a crystal slurry which is then treated in a column to effect the separation.

Organics have also been purified in single stage treatment systems based upon the concepts of the Schildknecht[7] column. The original equipment was designed for small scale production of high purity materials and these have subsequently been developed into industrial units. One modern system, the K.C.P. Crystal Purifier,[8] uses a slightly modified purification column and commercial plants in Japan are producing 5,000 metric tons/annum of p-dichlorobenzene of 99.99 per cent purity. These are just two examples from the many available for the production of purified organic chemicals. Fractional crystallisation has also been applied successfully to aqueous systems, the major development being in the recovery of waste or polluted water for reuse. The main efforts have been in the field of desalination of sea water for the production of potable water on a commercial scale. The increase in population has placed further demands on the existing natural water supplies. The conventional methods of damming valleys to produce huge reservoirs is not adequate to respond to short-term shortages. Between the conception of the idea to build a reservoir and actually obtaining water from it, requires many years of planning and construction. One also has to consider the land one loses by flooding valleys, in arid areas this could

result in the loss of the only fertile strips of land available. Apart from this, the damming of major water sources has often led to unforseen social and environmental problems, for example, the change of lifestyle for people below the dams, brought about by landscape changes arising from the loss of running water. Lastly we have seen failures in some of these well-designed dams and no structure can be considered totally safe when containing many millions of gallons of water.

Short term rapid solutions are required to solve the problem of augmenting the existing water supply. Ennis[9] has analysed the problems faced by the United States and has been able to show that the daily average water demand has already exceeded the available supply when considered as a whole. The solution to the problem is complex, the available water is distributed over the face of the earth in a very uneven manner: less than 0.027 per cent of the total water is fresh and immediately available. In fact most of the fresh water is locked up in the Arctic and Antarctic ice caps and it has been estimated[10] that if an iceberg measuring 2700 by 2700 by 250 metres was towed at a speed of half a knot from the Amery ice shelf to Australia, 30 per cent would arrive intact. The water would by worth $5.5 millions, that is, about 10 per cent of the cost of a similar quantity of desalinated water, compared with a towing cost of $1.0 millions. Unfortunately this is only speculation and one could not guarantee the success of such a venture.

Some 97 per cent of the water available on the earth (13×10^8 km^3) is found in the large oceans and compared to this the lower seven miles of the earth's atmosphere only contains 13×10^3 km^3, this is, 0.000053 per cent of the total water - an abundant source of drinking water is potentially available from the sea. Freeze crystallisation has been applied to this as a means of producing potable water. Research commenced around the 1940's and has progressed

to the point where several large freeze desalination plants are producing potable water,[11] for example, Colt Industries have several large field test sites:

(a) 250,000 U.S. g.p.d. plant at Eilat, Israel

(b) 100,000 U.S g.p.d. plant on St. Croix U.S. Virgin Islands

A spin-off from the desalination programme has been the use of these various crystallisation techniques to treat industrial waste water. Several schemes have been proposed by Campbell and Emmermann[12] to recover water and chemicals from metal finishing wastes and other systems containing dissolved organic and inorganic materials.

In most of these applications, crystallisation is competing with other established methods, particularly so in the desalination field where distillation processes have been in use for many years. However as the problems of energy usage and conservation become more important, the real advantages to be gained from crystallisation processes will be realised. Provided certain process considerations are satisfied, that is, the freezing point temperature does not fall much below $-10^{\circ}C$, and one can achieve a sufficient recovery, then energy consumption is very favourable.

CHAPTER 2

Literature Survey

(2.1) Continuous Crystallisation

The various crystallisation processes have been differentiated by Nyvlt[13] according to the mode of inducing supersaturation in the solution:

(a) crystallisation through cooling

(b) crystallisation through evaporation, with constant heat input

(c) crystallisation with adiabatic evaporation of solvent

(d) crystallisation through salting-out from solution by another substance with a common ion which reduces the solubility of the crystallising substance

(e) crystallisation induced by the addition of a second solvent that reduces the solubility of the crystallising substance

(f) crystallisation involving chemical reaction, such as the addition of a new gaseous or liquid component, electrolysis or thermal decomposition.

The first three methods are most common. All the crystallisation processes referred to can be carried out using discrete batches or, where the economics are favourable, continuously. By suitable selection of geometric configuration and mode of agitation, one can produce a range of crystallisers suitable for industrial applications and those currently available have been reviewed by Banforth.[14]

We shall limit our interest to processes where the crystallisation is through cooling, and the separation and purification

is achieved in one piece of equipment. One of the early techniques to utilise crystallisation for the production of high purity compounds, was zone-melting, which was described by Pfann[15] in 1952. His original concept was for the purification of a binary solid-solution alloy,but he observed that this technique could be applied to other materials. The material to be purified was cast into a small tubular container, surrounded by a narrow heating band, which was able to traverse the length of the tube. As the heater moved slowly up the column a liquified zone of material ascended the column at a few inches per hour. Because pure crystalline material tends to separate from any melt, the material which crystallised from the lower end of the liquified band was purer than the material which dissolved from the upper end. The impurities were thus concentrated in the molten band and eventually reached the top of the column. The process can be repeated many times and it is possible to produce exceptionally pure material.

This topic has received much scientific investigation and Herrington[16] has produced a monograph devoted to the zone-melting of organic substances, which gives a thorough account of published work on various types of zone-melting systems and the physico-chemical essentials of the process of zone-melting. This work has been actively pursued in Russia where it was initially developed for the production of the very pure semiconductors required for radioelectronics. They have also used zone-melting for the separation of isotopes and have applied the technique to the purification of a variety of organic substances - paraffins, aromatics, ferments, antibiotics, etc. One particular topic which has been studied has been the purification of monomers for the production of more stable, higher grade polymers.

Anikin[17] has carried out detailed studies on the purification of methyl methacrylate and styrene to establish the distribution of impurity in purified substances and the ultimate purity obtainable in the samples.

There have been several variations upon the basic technique described. Eldib[18] has produced a separation technique called zone precipitation, based upon the differences in solubilities of waxes. Here the mixture to be separated is treated with a solvent until a gel is formed, the solvent itself does not have to solidify. A zone in the cclumn is heated and is liquified, and as this hot zone is traversed, the liquid behind it solidifies and rejects the most soluble components. Thus after the heater has traversed the entire slab, the solids of greatest solubility will be depleted behind it and concentrated in the direction of movement. Another technique has been described by Vol'pyan[19], that of the zone crystallisation of liquid. Normally the charge to be purified is first completely crystallised, and then one or more molten zones passed through it. However with (Z.C.L.) one does the opposite and a solid zone is passed through the liquid mixture. Theoretical investigations have been undertaken by Fedorova[20] and Filippov[21] but their detailed discussion is beyond the scope of the present investigations.

Although zone-melting was very successful for producing very pure materials, the quantities available were small and the process was difficult to operate continuously. Industry required large tonnage processes that could be automated and run continuously to compete with established methods. One of the first serious attempts to achieve this was made by the Philips Petroleum Company. While working in the field of crystallisation, Arnold[4][5] invented

a new continuous countercurrent fractional solidification process analogous to continuous fractional distillation. His proposed system could be carried out in a horizontal tank or a continuous vertical tower along which a temperature gradient had been established. The apparatus was filled with a saturated multi-component solution which upon encountering the lower temperature zone formed crystals of one component. The crystals were transported, by gravity or mechanical means, from the lower temperature zone to the higher temperature zone, countercurrently to the saturated solution, and purified crystals discharged as product.

Developing the ideas of Arnold, Philips of the U.S.A. produced a small countercurrent crystal-purification column whose construction and operation were described by McKay[22]. The equipment consisted of a column in which a reciprocating porous piston compressed a crystal slurry contained therein. Crystals were melted by a base heater, the mother liquor being withdrawn under vacuum through the porous piston, while the high-purity product drained from the base of the column. He studied various organic and aqueous systems but generally yields were not high, for example, an average of 1.82kg/hr using a 50 mm diameter column.

In 1961 Schildknecht[23] produced the results of his work on the purification of organic systems using a small column. The column was 13-15 cms in length and contained an effective charge of 7-10 g of substance. Crystal production, purification and separation were carried out in the one column, unlike McKay's column where the crystals were produced by an external scraped surface chiller. The column was composed of two fixed glass tubes, one placed inside the other, and an exact fitting steel spiral, which was rotated by external means around the inner tube. Cooling was applied at one end of the tubes while the opposite ends were heated, the crystals

produced in the lower temperature end being transported by the rotating spiral and melted at the opposite end. Schildknecht found that a spiral rotation of 80-150 r.p.m. produced the best separations. His initial runs were batch but by providing an inlet in the middle part and outlets at the top and bottom parts, the column could be operated continuously. An important observation made by Schildknecht was the much reduced processing times in column crystallisations, over those of zone-melting, to produce comparable separations, that is, a factor of 100 times greater for zone-melting.

Schildknecht's work contained no theoretical calculations that would enable column performance to be predicted in advance. Anikin[17] prepared a theory of crystallisation columns to explain the purification mechanism,and deduced an equation which predicted the purity of the substance after purification in a given volume of the column. His purification mechanism was based upon successive recrystallisations taking place in the column, until the decrease in impurity concentration brought about by crystallisation of the liquid was balanced by diffusion of impurity from the liquid. Concurrently with this work Yagi and Inoue[24] were carrying out investigations of the countercurrent crystallisation column based upon McKay's design. They analysed the various phenomena in the purification process, that is, the relation between the falling rate of the porous piston and the heat supplied at the bottom of the column, the effect of pressure on the purifying capacity of the equipment, temperature distribution and concentrations of products. From their results the transfer coefficient and H.T.U. of the column were estimated.

Due to continuing success with the piston type of column Philips had continued further development work and the original apparatus had been scaled up to pilot plant. McKay and Goard[25] described the operation of such a pilot scale unit, an external scraped surface chiller was still used, feeding crystals into the

purification column. Energy for crystal movement and reflux driving force were supplied by a pulse unit in the product line, the mother liquor was removed through a wall filter. McKay was able to demonstrate the reliability of the process and its suitability for commercial expansion. The design was patented in 1965[26].

In 1967 McKay and Goard[27] published further work which analysed the effects of process variables; crystals size, bed porosity, mother liquor viscosity and resolidification of reflux liquid, on the performance of the column. They also described the scale up of the process for p-xylene purification which had been developed by Philips[28]. The pulsed crystal purification columns had been successfully scaled up thirteen-fold over the pilot plant columns. The commercial units were operating continuously with a high on-stream factor and were producing products of greater than 99 plus weight percent p-xylene from feed stocks of 68-72 percent p-xylene. A typical column of cross-section 1000 cm^2 produced 530 Kg/hr of product and the projected capacity for p-xylene production in 1967 was 130,000 tons/yr.

Now that column crystallisation was established more research was being conducted into modelling the various systems. Powers[29] and his co-workers compared the two distinct types of columns, end and centre-fed. They examined the applications and results obtainable from the equipment, plus the operating variables associated with each. Powers developed a model which considered the two extremes of solid solubility, that is, a eutectic system (little or no solid solubility) and a system forming a solid solution. In the former case purification by washing was the dominant mechanism and in the latter it was by recrystallisation. The mass transfer between adhering and free liquids and diffusion along the column determined the purification/separation obtainable. Concurrently Devyatykh[30]

developed his theory for countercurrent crystallisation columns of the Schildknecht type by assuming that for certain cases, separation was accomplished not by repeated recrystallisation of the mixture in the column but by mass exchange between the solid and liquid phases moving in counterflow to one another, that is, diffusion in the solid phase.

Arkenbout[31][32] developed his work on the concepts of theoretical plates and transfer units for countercurrent separation processes in exchange columns, to include a mathematical description of countercurrent crystallisation. He derived an expression for the interfacial mass transfer in which the contribution of both recrystallisation and extractive washing were considered. The equation covered the whole range of solid solubilities. Many researchers were now carrying out experimental work using column crystallisers. Malyusov[33] attempted to elucidate the separation mechanism by relating the height of an equivalent separation stage to process variables. He studied the effects of speed of rotation of the spiral and clearance between spiral and column walls. The latter value determined the crystal size and at the smallest clearances the highest efficiencies were obtained, confirming the hypothesis that the separation was controlled by a diffusion process.

Development of a Schildknecht column was undertaken by Betts[34] with the objectives of investigating the applicability of this crystalliser to separations and purifications of industrially important materials, and to optimise the design and operation of the column based upon experimental and theoretical considerations. He investigated many organic and aqueous systems and demonstrated the success of this type of column to their separation and purification. However, feed rates used in this study adversely affected performance when increased above 500 g/hr. Betts made some quantitative observations about crystal size and shape but did not include any

theoretical treatment in this paper. Initiation of the development of commercial scale columns was undertaken by Messrs. Newton Chambers Engineering Limited[35] while the Coal Tar Research Corporation took out a patent[36] on a pulse fed column of similar design. A horizontal scraped surface crystalliser was also described by Armstrong[37][38] who indicated its potential in dewaxing of petroleum oils, para-xylene separation and fatty acid preparations.

Theoretical investigations of column crystallisers were undertaken, Albertins & Powers[39] modelled a column operating at steady state under batch conditions. The crystals were conveyed through the column by a rotating and oscillating spiral. They measured the composition profiles directly for the eutectic system Benzene/cyclohexane, taking into account the impurity associated with the crystal phase to explain the observed concentration profiles. They concluded that axial dispersion and impurity level in the crystal phase together limited the separation that was achieved, that is, they neglected the washing of the adhering liquid. Player[40] also presented a mathematical analysis of column crystallisation, which distinguished between the mode of purification in the end-fed, porous piston column and the centre-fed Schildknecht column. The temperature and composition profiles observed in these two types of columns differ markedly in that a sharp discontinuity is observed in the former but not in the latter. This arises from the mode of operation of the columns. The end-fed porous piston relies on refreezing in a compact bed of crystals while the centre-fed column operates with a freely moving slurry. It relies on the washing action to produce pure crystals rather than displacement of adhering mother liquor since with a feed containing only 1-5% impurity refreezing would be minimal.

A mathematical analysis of a continuous column crystalliser was presented by Bolsaitis[41] for the crystallisation of p-xylene from xylene mixtures. He divided the crystalliser into two sections:

a crystalliser-crystal settler, whose performance was characterised by a stripping efficiency, and a countercurrent washing section. The stripping efficiency was defined as the fraction or percentage of crystallisable material removed from the solution entering the crystallisation section. The crystals formed were transported out of this section into the enriching section of the column, under the influence of gravitational, buoyant and viscous drag forces. The effect of the spiral as the transporting mechanism of the crystals was not confirmed by the experimental work. However the equation describing the enriching section can only be applied in special cases, that is, when the molar volumes of crystallising component and impurity are approximately equal.

Steady state batch operation of a column crystalliser was again studied by Gates & Powers[42], this time extending the systems to cover the range of solid solubilities. Gates found that a model which incorporated the washing of the adhering liquid together with the axial dispersion and impurity associated with the crystal phase, provided a more consistent fit of Albertins[39] data. Again it was found that the rate controlling step in effecting separation was the mass transfer between countercurrently passing streams of crystal and liquid, but axial diffusion limited the final separation. The eutectic system Benzene/cyclohexane was again investigated by Henry and Powers[43] under continuous flow operation. The variables investigated were :

(a) Terminal stream flow rates (i) feed rate
(ii) bottom product rate
(iii) overhead product rate
(iv) internal crystal rate

(b) Feed composition

(c) Feed position

The spiral agitation conditions were not varied.

A mathematical model based on axial dispersion and mass transfer, together with consideration of impurity content of the crystal phase, was developed for the enriching and stripping section composition profiles. Axial dispersion was found to be the dominant mechanism limiting separation, and the primary variable which determined the product purity was the enriching section product: crystal rate ratio. A correlation of crystal phase impurity composition with the "bottoms" product composition showed that the minimum level of impurity associated with the crystal phase was attained when the stripping section was flushed with feed material, or when the enriching section was operated at conditions approaching total reflux. The ultimate purity that can be obtained with complete washing is the crystal phase composition.

Schildknecht[44] also reported the operation of a continuous column crystalliser. In his previous work he had experienced problems with column blockage arising from agglomeration of crystals. Like the previous workers he had modified his columns to operate with an oscillatory motion of the rotating spiral. He observed good separations for the azobenzene-stilbene system, total solid solubility, with rotational speeds of 70-80 r.p.m. at medium amplitudes (3 to 6 mm) and oscillations of 180-330 times/min. His 250 ml column produced good separation up to a throughput of 130 g/hr. He also reported work on a semitechnical scale column (approximately 2 litres capacity) for the purification of sea water and a micro-column for the rapid purification of substances in the milligram quantities.

Large scale crystallisation processes were now being developed, one such process was invented by Brodie[45] at the Sydney plant of Union Carbide. The product processed was para-dichloro-benzene and purities of 99.99 percent were achieved from 75:25 mixtures of the p- and o- isomers[46]. The Brodie purifier utilised

a long horizontal and somewhat tapered body in which crystals grew while passing countercurrently against an overhead flow of liquid. There are three general process zones: recovery, refining and purification with the feed entering between the recovery and the refining section. The temperature gradient throughout the unit is maintained by cooling, countercurrently, the external walls of the recovery and refining sections. A scraper conveyor of helical design transports the crystals along the horizontal recovery and refining sections to a vertical purification section. A vertically mounted agitator provides for uniform crystal settling, to build up a uniform moving bed, that is subjected to a countercurrent reflux stream. Near the base of this zone the crystals are completely melted to form a liquid reflux and product. The process has been developed and industrial units have been installed in many countries[47], for example, units are currently operating in Japan purifying 7,200 tonne/an. naphthalene and 6,000 tonne/an. para-di-chlorobenzene for Nippon Steel Chemicals and Hodogaya Company.

Variations on the basic column theme have also been developed. Matz[48] described a vertical countercurrent crystalliser in which the Helix was driven in the opposite direction to a central cored shaft, through which the heat transfer medium circulated. Arkenbout[49] replaced the rotation and oscillation of the Helix with a vibratory motion applied to the column. The column contained sieve discs upon which steel balls rested, as the column vibrated the balls were set into vigorous and irregular movements. He compared the operation of his column to that of Philips and Brodie and discussed the various process parameters affecting the separation achieved. The advantages claimed for the column were that purification was not only achieved by washing but also by continuous, repeated recrystallisation brought about by the grinding of the crystals during passage through the column. Also mechanically the

column was simple to operate, had a high separating efficiency per sieve disc and was amenable to scale up operations.

Development of a Schildknecht column was also undertaken by Hobson and McGrath[50]. Initial work on a 50 mm diameter column, 90 cm length with an internal volume of 1 litre was used to construct a 100 mm diameter column, 1500 mm in length with an internal volume of 3.8 litres. Due to mechanical difficulties, the larger column was never operated under steady state conditions for sufficient time for the analysis of column operation. The development and successful operation of the 100 mm diameter column, together with a theoretical study of the 50 mm diameter column were subsequently reported[51].

As an alternative to a spiral conveyor for crystal transport, Moyers[52] described a column which featured a wall scraper and a porous piston which rotated and reciprocated as a unit. The purification section was free from internal constrictions. The crystals were formed in the top portion of the column, the movement down the column being controlled with the porous piston. Liquid feed entered the middle of the column, mother liquor flowed overhead from the freezer and product was withdrawn as a liquid melt from the base. The crystals were compacted into a dense bed as opposed to a high porosity crystal slurry normally used in screw conveyor columns. Moyers also used a different approach to modelling the column. He described a non-adiabatic, plug flow axial dispersion model to describe freezer, heater, stripping and enrichment sections . He did not consider interphase transport terms since he concluded that axial dispersion and bulk flow effects had been shown by others to dominate column performance. He reported axial dispersion coefficients of 0.2-0.3 cm^2/S and concluded that the dense-bed column crystalliser exhibited near plug flow characteristics for both solid and liquid phases.

The processes available for separating adhering mother liquor and crystal slurry were examined by Wells[53]. Two cases were considered, that of a single stage crystallisation, utilising a filter or centrifuge for crystal slurry separation, and a multi-stage crystallisation unit exemplified by a Schildknecht column. In the former the adhering liquid was removed from the crystals by using a wash process in conjunction with the filter or centrifuge. In the latter the mother liquor was displaced from the crystals by the countercurrent wash of melted crystal product. Models describing both systems were presented, the column model being based on the developments of Henry[43] and modified by Wells for running the column under economic operating conditions. The axial dispersion was considered more dominant than mass transfer at the low refluxes considered. Models relating product composition to product offtake, feed composition and the height of the purification section were presented for eutectic and solid solution systems.

Russian workers have continued to carry out work on column crystallisers. Devyatykh[54] et al have studied the longitudinal mixing in a continuous countercurrent flow column crystalliser. The upper part of the column contained a scraped surface crystalliser utilising a short spiral of rectangular cross-section, the rest of the column being agitated by a spiral stirrer attached to the base of the helical screw. Utilising a diffusion model they determined the coefficient of longitudinal mixing and evaluated the effects of flow rate and crystal production rate on the magnitude of the coefficient. The coefficient was evaluated using the pulsed feed of an indicator substance, that is, a tracer into the system. Devyatykh[55] and his co-workers carried out further work on a similar column to the above, but this time the spiral crystal stirrer was not attached to the coolable copper rod and rotating stirrer. The scraper and spiral

stirrer were put in motion by separate drives and it was possible to evaluate the effect of the loosener (spiral stirrer) rate on the separating power of the column. An important factor identified was an increase in separating power of the crystallisation column with a decrease in mean crystal size resulting from increasing loosener rotation rate. When the loosener rotation rate increased there was a reduction in the portion of solid phase and an increase in the intensity of longitudinal mixing showing the need for selecting the optimum value for the loosener rotation rate.

Developments in the field of continuous fractional crystallisation have been rapid and already the established processes are being challenged. The Kureha Chemical Industry Company of Japan have recently introduced their compact crystal purifier [56] based upon a precrystalliser and a column containing a screw conveyor. Crystals are introduced at the base and transported up the purifier, while reflux fluid flows down the column under gravity. Reduction of 30-50 per cent in capital costs as well as 50 per cent reduction of energy costs and 50 per cent reduction in required plant area have been claimed by the manufacturers. The simplified design of their crystalliser over the Brodie Purifier promises sizeable maintenance - cost reductions according to Kureha.

(2.2) Continuous Crystallisation applied to Freeze Separation/ Concentration Processes

Introduction

Investigations have been undertaken to develop continuous crystallisation processes for industrial use. There are several industrial systems currently in use treating organic mixtures. There has also been much work carried out to develop continuous crystallisation processes for aqueous systems, notably the removal of salts from sea water to produce potable water. The processes investigated in this work are of this latter type, aqueous, eutectic-forming systems operating above the eutectic point. The separations considered were :

(a)	Removal of salt from sea water	: Desalination
(b)	Ethanol concentration	: Fermentation products concentration
(c)	Heavy Water Concentration	: Upgrading/regeneration of heavy water to reactor grade quality
(d)	Waste effluent treatment	: Recovery of water/chemicals for reuse and pollution control

A brief background of each system investigated is presented below.

(2.2) (a) Desalination

Introduction

A supply of potable water is vital to the development of any country. It has been estimated[57] that rain precipitates some 340×10^{12} g.p.d. over the earth's surface; unfortunately the distribution is random and about 60% of the earth is arid or semi-arid. The problem is to extract the water from its various sources. The ocean holds 97% of the earth's water with 2% frozen in the two polar ice caps, this accounting for 75% of the fresh water

of the world. Of the 1% of liquid fresh water, some is ground water and difficult to extract, leaving a possible 0.6% of the total water of the earth available to man.

If one wishes to augment the natural supplies then desalination will have to be employed. The techniques available are:

(i) Distillation

(ii) Ion exchange

(iii) Reverse osmosis

(iv) Electrodialysis

(v) Freezing

(vi) Hydrate formation

Distillation is the most developed technique, many of the industrial installations being based upon this. Much of the desalination development has been in the U.S.A. Strobel[58] and Ennis[9] have carried out economic investigations for desalination, and in his projected role for desalination, Strobel predicted the following trends:

Year	1980	2000	2020
Desalting Capacity	510 M.G.D.	3090 M.G.D.	5700 M.G.D.

TABLE (2.1)

(M.G.D. = millions of gallons per day) In 1971 Desalting capacity = 56 M.G.D. Ennis has also suggested that by the 1970's costs for producing potable water by conventional methods (reservoirs, aquifiers) will be comparable when considering plants of 50 M.^{us}G.D. or over.

In January 1975, the total world desalting capacity was analysed by Morris[59], and showed the following trends: 318 M.^{us}.G.D. for sea water and 120 M.^{us}.G.D. for brackish water. Almost 40% of the installed capacity was Multiple Effect distillation, membranes and freezing contributing virtually zero. The distillation

processes were dominated by Multi-Stage-Flash, accounting for some 90% of installed capacity. The only large orders for M.S.F. in the 150-200 M.^{us}G.D. were for the oil-rich countries; elsewhere it had declined, reflecting the energy costs associated with desalination.

In the U.K. desalination expertise has been developed, the main outlets being the Middle Eastern countries. Desalination plants for producing drinking water have not been installed in our country. However various studies[60] have shown that our demand for water will have doubled by the end of the century. As a result, it will be necessary to construct over the next 30 years, water conservation projects with a total capacity equivalent to those constructed in the last century. There is a possibility to augment these resources - artificial recharge of aquifiers, recycling of used water, but these must be used with care. Israel's water system operates virtually within a closed cycle and they are extremely dependent upon recycling waters for irrigation, etc. Recently it has been reported[61] that there is an alarming accumulation of minerals, chloride salts, pesticides, fertilizers, nitrates and detergents in their coastal aquifiers and it appears desalination will be inevitable before the end of the century.

In their latest report[62] the Water Resources Board analysed the need for desalination and concluded that it was not economically viable, at least for the period up to the end of the century. Ours was a problem of distribution rather than deprivation. These findings have been criticised by Silver[63] as being short-sighted and he advocates a more enlightened policy towards desalination by distillation or reverse osmosis. One of the main drawbacks to implementing this policy would be the necessity to site the desalination plants on areas of unpolluted coast line. Butler[64] cites the example of the (M.S.F.) plant at Terneuzen in Holland, in the heart of the refineries/petrochemical complex where the desalinated

water produced is unfit to drink.

The arguments for or against desalination are complex. We have seen that from an energy point of view costs are always higher for desalination than conventional supply. However where energy is cheaper, conditions more amenable and water is not easily obtained, desalination is the only answer. In his assessment of the desalination technology, Heckroth[65] compared the major systems available other than distillation and freezing and concluded that although the technology was advancing, for municipal water use there was only one conclusion; "The future of desalting was bright but costs must drop".

Distillation Desalination

The various desalination processes can be represented thus:

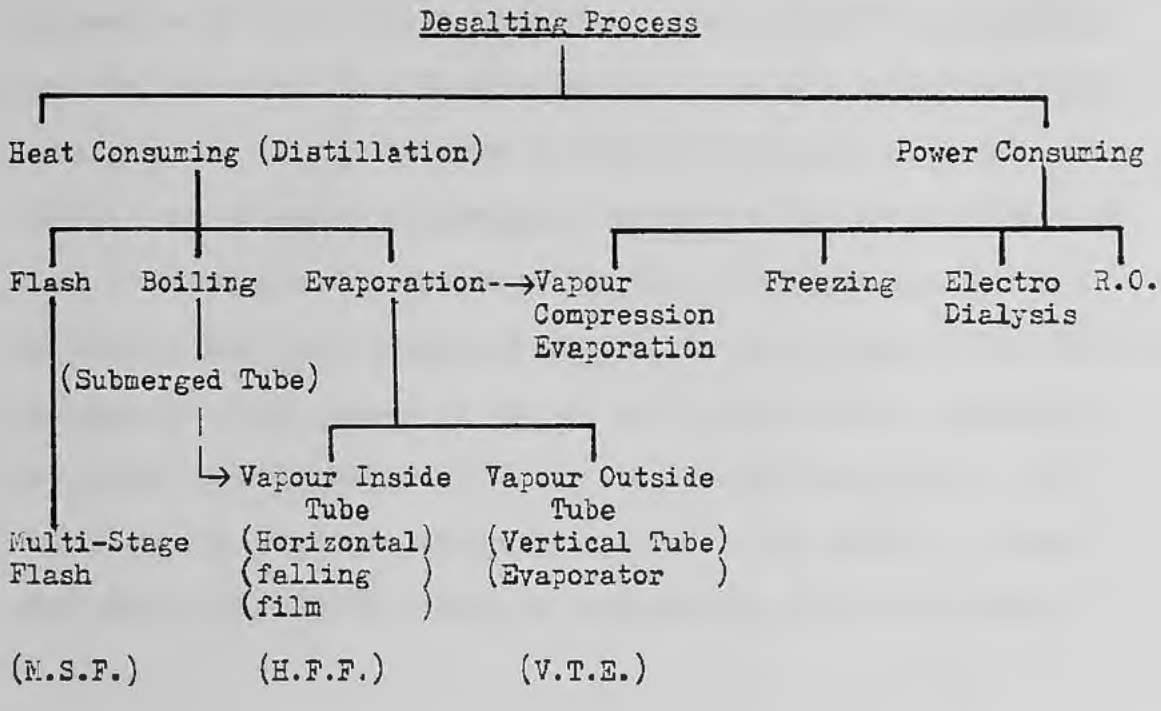

FIG.(2.1)

The two main distillation processes are the (M.S.F.) and Multiple effect (M.E.) of which the (H.F.F.) and (V.T.E.) are examples. A very comprehensive account of the development and operation of these systems has been presented by Porteous[66], in his book, Saline Water Distillation Processes.

Original desalination plants were on single effect and produced only one pound of distillate per pound of steam; some land-based plants used three effects, but these plants were costly to build and expensive to operate. A growing demand led to the M.S.F. process "taking-off" in the late fifties and much of the pioneering work was carried out by Professor R. S. Silver[67] and Dr A. Frankel[68] who also produced designs for improving the multiple effect process.

The two most common types of multiple effect are the V.T.E. and H.F.F. In the first, brine entering an effect flows across the

upper tube plate, through a distributor nozzle to form a liquid film which flows down the inside of the tube. Steam condenses on the outside of the tube, forming product distillate, causing evaporation of brine inside the tube. Steam formed by evaporation from the brine acts as a heating medium in the next effect and brine leaving the bottom of the tubes is feed for the next. In the H.F.F. the situation is reversed, horizontal bundles of tubes have steam condensing on the inside of the tubes transferring heat to the evaporating brine cascading freely over the outside of the tubes. Unevaporated brine passes to the top of the next effect, operating at a lower pressure where it flashes to a lower temperature. It then passes on to the outside of the tubes of the effect. Steam generated in one effect passes to the next and acts as a heating medium.

The most widely used technique today is the M.S.F., accounting for some 97% of the world capacity for desalting.(57) In this system a large number of stages operate together at successively lower pressures. The condensing of the vapours to pre-heat the sea water occurs countercurrently to the multi-stage flash to give a cooling evaporation and heating-condensation heat interchange. There is no evaporation heat transfer surface but there is a condensation heat transfer surface. In the early plants the flash evaporation and condensation were rather turbulent giving rise to major energy losses; this was overcome with the development of the controlled flash evaporation process — C.F.E.

The major problem encountered in the above methods is the production of scale as the hot brine deposits carbonates and the like. This requires that the brine undergoes a suitable pre-treatment. Corrosion is also a problem, more so in the M.S.F. because of increased concentrations and elevated temperatures. Also the brine temperature determines the flash range which can be obtained and

output is directly related to flash range. Likewise the multiple effect process is limited by the elevation of the boiling point with concentration, reducing the number of stages to twelve for practical purposes. In his assessment of the various distillation processes Pugh[69] believes that the M.E. processes have inherent advantages which will (a) enable them to compete with the M.S.F. and (b) potentially produce water 20% more cheaply.

Research is continuing on ways to make evaporation processes more attractive but unfortunately the escalating spiral of construction and energy cost has become a major factor in the assembly of these plants. Developments for the future include combining the (M.S.F. /M.E.) via a steam compressor to produce a hybrid process known as the Vapour Compression Evaporator—V.C.E. which would combine well with nuclear desalination. A review of the new developments in distillation desalination has recently been presented by Veenmon.[70] He not only describes the mechanism of the processes but provides a comparison of the investment or capital costs, energy costs, operating and maintenance costs for the processes.

Solar Desalination

In order to reduce energy requirements several attempts have been made to utilise solar radiation. Sheth[71] et al proposed using solar radiation under retarded evaporation conditions, that is, using the temperature difference between the surface sea water and deep sea water. The process would require storage of heated sea water which would be fed into a heat exchanger, under vacuum, wherein the warm sea water would partially flash evaporate. True Solar distillation systems have been erected on several of the Greek Islands[72] and Australia. The stills comprise a brine pool with associated radiation-absorbent liner, a supporting structure and a glass or plastic cover. An inlet for feed water, distillate removal from the glass and a reject brine outlet are required. Porteous[66] has described the construction of such stills on the Island of Aldabra. Attempts at cheapness of construction using plastic roofs, light supporting structures and polythene lined brine pools have not proved an economic, durable method, viz. the Syrni still constructed by Delyannis and Piperoglous has required modifications to change the plastic roof to a glass one.

Reverse Osmosis Desalination

Desalination techniques based on membranes have been developed and have been described in various texts.[74] Reverse Osmosis is a general term applied to a membrane process for separation and concentration of substances in solution. It usually consists of allowing a solvent to preferentially pass through a membrane normally described as semi-permeable. The product is thus enriched in solvent, leaving a concentrated solution on the opposite side of the membrane. The process takes place at ambient temperature and thus no phase change is involved. Normally "osmosis" describes the flow of solvent through a semi-permeable membrane from a less concentrated solution to an area of higher concentration. The normal osmotic flow of

solvent can be reversed on application of hydraulic pressure to the more concentrated solution if such pressure is in excess of the normal osmotic pressure, hence the term Reverse Osmosis.

The preparation and operation mechanisms have been extensively studied[75] and new membranes are being constantly developed especially in the desalination field.[76] One of the main drawbacks to the process is the increased hydraulic pressure required for increased salinity together with the sensitivity of the membranes to the state of the incoming feed. Thus most R.O. plants operate using brackish water and a basic plant requires pretreatment cartridge filters and chemical feeders; high pressure pumps and post treatment equipment. The problems of suspended and colloidal material build up on the surface of the membrane - fouling - and its effects on the membrane flux have been a major problem in the successful operation of many plants. Various design modifications have been studied and developed[77] to reduce this problem and R.O. modules have been developed to handle many separation problems. A related process utilising membranes is electrodialysis;[78] the process is based upon a cell constructed from a large number of membrane - separated compartments across which an electrical potential can be applied. The membranes are chosen to be ion selective and the saline solution passes over the surface of the membranes. The stack is arranged such that positive and negative electrodes terminate the stack at each end, and when a D.C. potential is applied the cations migrate towards the cathode through the cation-permeable membranes into the concentration solution. Further migration is prevented by the anion selective membrane next in line. The cations are thus retained in these brine compartments. A similar process occurs with the anions. Thus one gets two streams building up, a concentrated or waste stream and a diluting or product stream.

Like the R.O. plants they also are used on brackish waters and suffer similar problems during operation. The problems encountered are polarisation and scaling, this is where there is enrichment of salt concentration near the surfaces of the membranes facing the brine compartments and a corresponding depletion in the fresh water compartments. The polarisation factor exerts a considerable influence on the economics of electrodialysis. A recent estimate of membrane desalting capacity is[70] :

Reverse Osmosis	518 Plants	632 x 10^3 m^3/day
Electrodialysis	85 "	138 " "
Electrodialysis-reversing	86 "	58 " "

TABLE(2.2)

for plants with capacities of 95 m^3/day or more.

Ion Exchange Desalination

Ion exchange processes have also been applied to desalination[79] but for conventionally, chemically regenerated ion exchange, chemical cost normally confines the process to treating waters of 800 p.p.m. or less Total Dissolved Solids.[80] The continual regeneration of the exchange resins and the complexity of running the systems limits their use to where a high quality product is required. An interesting solution to this problem has been developed by Sirotherm, I.C.I. Australia[80] for producing boiler water for a Soda Ash factory. They have produced a resin that can be regenerated by washing with hot water. The process operates on short cycle times, 55 minutes for absorption and 14 minutes for regeneration and despite problems with dissolved oxygen levels, the resins performance has been to specification.

Freezing Processes for desalination

Presently we are faced with the dilemma of increasing energy costs plus reductions in supplies and as such any process capable of reducing energy demands[57] is worthy of consideration. To this end much work has been carried out on developing desalination by freezing and in 1952 The Office of Saline Water (O.S.W.) was created in the U.S.A. to carry out research and development in desalination.

As we have seen natural freeze desalination has been known for many years. In the colder regions of the earth, the ocean freezes to form an ice layer which is composed of pure ice and pockets containing concentrated salt water. Annual thaws provide water for downward washing action which eventually leaves the uppermost ice layers free of brine. This ice when melted, provides potable water. Such techniques were reported by Nebbia[2] for sea water purification where a repeated freezing/melting technique reduced the salt concentration to only traces, the final level being dependent upon the initial salt concentration.

It was recognised that such techniques were useful in augmenting ships' water supplies. A more detailed understanding of the freezing process was provided by Buchanan.[3] His early investigations were directed towards explaining the purity variations of ice he collected from the sea or glaciers. He identified the brine "pockets" in the ice as the source of the inhomogeneities in the product water and was able to publish quantitative data for the freezing of salt water. It was some years later before the idea of incorporating the freezing phenomenon was utilised in a working process. In the early 1940's various schemes were proposed and patents granted. All employed virtually the same process steps (a) freezing, (b) separation-washing, (c) condensing-melting and (d) heat exchange. The developments of modern processes have

followed these steps differing mainly in the detail for carrying out the various operations.

Freeze Desalination

The freezing of ice can be accomplished directly on a surface cooled by mechanical refrigeration. Weiss[11] summarised the various disadvantages associated with the method and concluded it was not a viable method for commercial production of fresh water. The processes chosen differ principally in whether the refrigerant is the water itself or an immiscible secondary refrigerant. The former is designated a primary refrigerant process and the latter a secondary refrigerant process. Commercially the primary refrigerant process is known as Vacuum Freezing, Vapour Compression or Vacuum Flash Freezing. The process has been extensively described in the literature[81][82][83][84] and developed commercially in America by the Carrier Corporation, Colt Industries and also in Israel by the Israel Desalination Engineering (Zarchin Process) Limited.

In the process, feedwater is passed through a heat exchanger and is cooled by the product and brine streams leaving the process, to within a few degrees of its freezing point. The feed enters the crystalliser where the refrigerant (water vapour) is evaporated by vacuum, thus removing heat from the feed water and forming ice. The refrigerant vapour is pumped out of the crystalliser by a compressor and is recontacted with ice that has been washed and it gives up its latent heat by condensing. This causes the ice to melt. The melted ice becomes the product and is pumped out of the process in heat exchange with the feed. The ice is pumped from the crystalliser to a counter washer as a slurry with the concentrated feed water.

The Secondary Refrigerant Process has also been extensively developed by Struthers[83] (S.S.I.C.), Blaw-Knox,[83] Avco Systems Division[85] and Simon-Carves (U.K.A.E.A.)[86][87] using Butane or other immiscible fluorocarbon liquids as the refrigerant medium.

Sea water, filtered and pre-cooled in a primary heat exchanger, is fed into a crystalliser, into which liquid butane is injected. The butane boils under reduced pressure and the resultant cooling effect leads to the formation and growth of ice crystals from the water. The ice/brine slurry so produced is passed to a wash column separator where the brine is drained off and the ice washed with a small fraction of product water. The washed crystals then pass into a melter vessel, in which they are brought into contact with butane gas fed from the crystalliser through a low-pressure compressor. The crystals melt in contact with the compressed gas, most of which, in turn, condenses on the melting ice, and the two immiscible liquids are then separated in a decanter.

The major development in the U.K. undertaken by Simon-Carves Limited, U.K.A.E.A. and the Government was to construct a 4500 m^3/day (1.M.G.D.) pilot plant on a site at Ipswich. From previous work with a laboratory-scale plant (45.5 m^3/day) (10,000 G.D.) Simons scaled up to the pilot plant which was to be used to demonstrate the feasibility of a 5 M.G.D. commercial plant. It was believed at the time that costs from desalinated water from freezing would fall below those for other processes and conventional water schemes[60] and there was a potential market in Northern Europe for these systems. However this was not realised and faced with rising development costs, the plans were shelved in 1972.

Experience has shown that difficulties in the design and operation of the steps following the initial freezing have been responsible for most of the operating costs. Critical points appear to be the wash separators, the heat exchangers, the melters and the compressors. However Bardhun[88][89] in his reviews has also highlighted problems associated with the use of Butane and its derivatives, namely the formation of various hydrates together with

the ice. Elimination of this problem has been achieved by the suitable choice of refrigerant and improved dispersion of refrigerant in the sea water; Gibson et al[90] used spray nozzles and Freon -114 in their system. Carrier[91] has experimented with Octafluoro-cyclobutane C-318 which satisfies all the requirements but is very expensive to use. The use of liquid Natural Gas[92][93] has also been considered but would be difficult to use in a crystalliser.

Another problem is the emulsification of liquid refrigerant in the slurry with drop sizes ranging from a few to a hundred microns. Avco Corporation experienced this with Freon-114 refrigerant[88] and likewise the U.K.A.E.A. in their butane desalination plant. Denton et al[94] carried out experiments on methods to remove the dissolved and entrained butane and also to improve the melting of the ice to facilitate butane disengagement. If the butane is not removed there is a gradual coalescence of these droplets in the wash column, reducing porosity irregularly, and giving poor washing results. Another requirement is that one has to strip not only the dissolved butane from the water and brine products, but also to remove as much as ten times this amount of emulsified butane. Failure to achieve this renders the water unpalatable and it exceeds the limit for butane in drinking water of 0.1 mg/l[94] determined chromographically.

Investigations of the washing and melting of the ice have been carried out. The only successful washing device has been the countercurrent wash column[91] and the operational characteristics have been described by Grossman,[95] Schwartz and Probstein.[96][97] Experimental work and theoretical models have been used to describe column performance, the most successful systems operating under pressure rather than gravity. A unit throughput of thirty times that obtainable in a gravity column has been achieved using the

pressure column, allowing these columns to be reduced in size.

An interesting development described by Snyder[98] was the use of hydrate formation for desalination. In this process the water solidifies and precipitates at higher temperature and pressure than does pure ice, due to the presence of a hydrating agent. The solid contains no salt and has 5-15 mole percent of hydrating agent which, since it is insoluble in water, separates when the ice melts. The brine slurry and hydrates are treated in a wash column very similar to the one used in a conventional S.R.F. process. Hydrating agents described include chlorine, methyl bromide, $C Cl_2 F_2$ and Propane[83]. One of the main problems with the hydrate process has been the production of large correctly-shaped crystals for easy washing since smaller crystals tend to produce compacted beds of low permeability.[91]

Several other schemes for desalination using freezing have been proposed. Ashley[99] described an indirect freezing system using a helical agitation unit. Sea water enters the helical passageway at the top of the freezing section and as it passes down, forms an ice slurry. The ice converges towards the centre of the passageway while the brine remains close to the refrigerant surface. The ice slurry and brine are separated in a gravity wash column. Less complicated systems have been described by Johnson[99] and Curran.[100] Both use conventional indirect freezing and rely upon freezing a portion of the impure water onto the cold surface. By careful balancing of refrigerant and sea water flows it is possible to remove pure ice from the vessel walls using a scraper, or by simultaneous melting and draining.

Freezing processes were also investigated to solve the problem of handling large volumes of waste brine.

The Eutectic Freezing Process has been developed by A.V.C.O.[101][93] and involves four principal unit operations:

(a) Crystallisation of salt hydrate

(b) Separation of ice and hydrate crystals from a eutectic slurry

(c) Counter-current washing of eutectic ice

(d) Drying of the hydrate crystals

The system is a development of the AVCO Crystalex™ process, except the freezing is continued until the eutectic temperature is reached, 23.3% Sodium Chloride and -6°F, whereupon the ice and salt crystallise simultaneously. The relationship of freeze-based systems to other desalination processes has been presented as follows:[69]

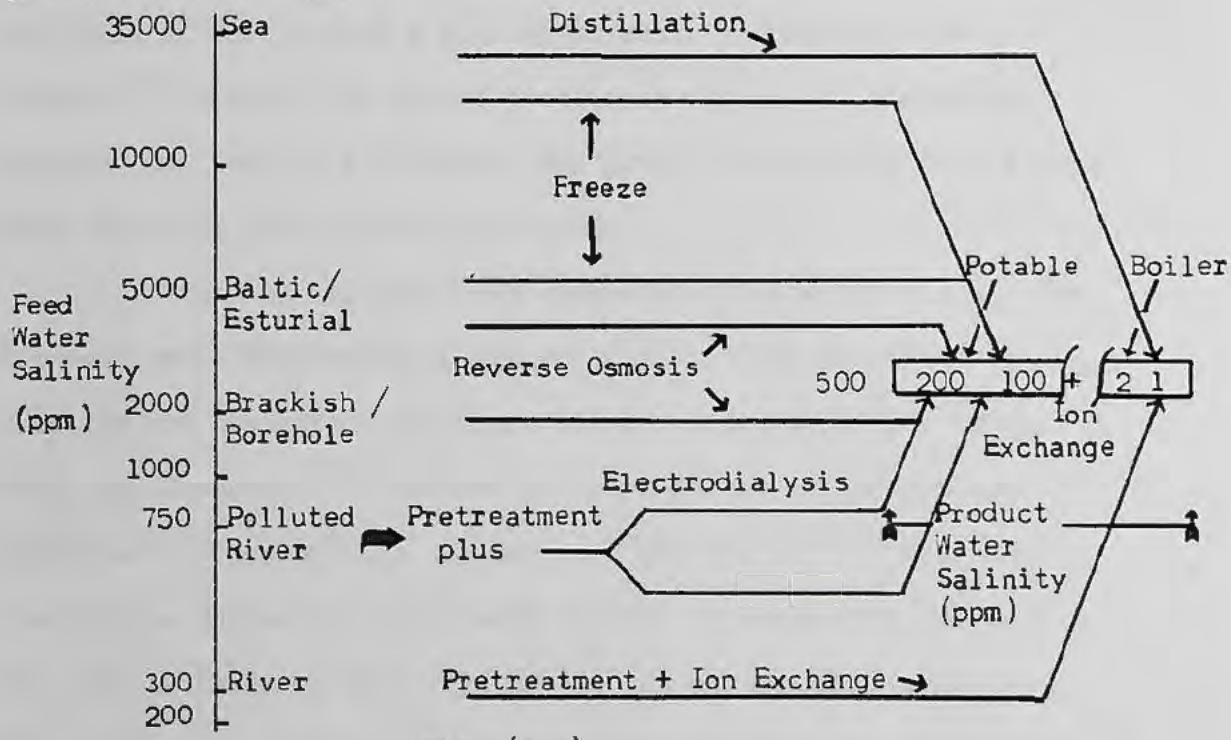

FIG. (2.2)

The application of various desalination processes

Presently there are no major S.R.F. schemes operating and much of the pilot plant work in America has ceased, one of the last being that of A.V.C.O. at Wrightsville Beach in 1975.[93] The U.K.A.E.A. has continued to examine the S.R.F. project,[102] and has proposed an integral design incorporating the four main process stages which would be capable of producing water at a cost lower

than those of competing systems.

Review of Desalination Research

The interest in desalination has stimulated much research into the crystallisation processes occurring during the freezing of salt water solutions. Various workers have studied agitation, heat transfer to suspended particles, ice nucleation rates, heat transfer to evaporating droplets, effects of residence time, etc, all with the idea of improving performance of the crystalliser. Early work reported by Harriot,[103] on ice growth in a direct contact, butane-cooled, stirred tank, showed this occurred one quarter to one half times as fast as predicted from heat transfer correlations. He also analysed the effects of crystal shape on diffusion of salt around a growing crystal. Fernandez and Bardhun[89] studied the growth process at the tip of a growing dendrite and were able to relate the growth rate in the a-axis with water velocity and applied subcooling.

Research had also been conducted outside the U.S.A., the Japanese being interested in the concentration of sea water by freezing, and the effective use of the constituents of sea water. Umano and Kawasaki[104] carried out work on the nucleation and growth of ice crystals in sea water. Orcutt[83][105] had also studied the nucleation and growth applied to the S.R.F. process. His model considered the influence of the refrigerant phase on nucleation rate and the crystal size distribution in the crystalliser. He considered two growth mechanisms: a heat transfer limited growth, or growth accompanied by agglomeration, this latter providing the best agreement between observed and calculated size distributions. Orcutt and Cary[106] also studied the process of liquid mixing in the freezer crystalliser vessel and were able to relate the degree of mixing to the power input to the agitators and their position in the vessel.

The mechanism of salt rejection during the freezing of sodium chloride solution was described by Terwilliger and Dizio[107]. They wished to describe mathematically the system for sodium chloride solution undergoing solidification and experiencing solute redistribution, and also to analyse the factors responsible for controlling salt segregation. Utilising a new experimental technique they were able to monitor the sodium chloride rich boundary layer, and determine both the liquid and solid phase solute distributions. This was found to depend upon:

(a) the liquid phase interface concentration which is controlled by the supercooling

(b) the thermal driving force imposed to initiate and maintain freezing.

On the same theme Janzow and Chao[108][109] studied the mechanism of salt entrainment for ice crystallised from brine. Their original concept had been for a desalination system using pre-cooled hollow pellets, which simultaneously served as artificial nucleation sites and carriers of ice crystals as they traversed through the brine. In their study, ice was grown on one of these pellets and by varying the brine velocity and subcooling, the effect on salt entrainment was studied. They concluded that the brine adhering to the thin plates of ice was retained in the interstices by capillary forces, and as such they were unable to produce pure ice even after subjecting the pellets to a rinsing treatment. During this study they also observed the formation of large crystals of plate-like ice in the bulk of the slowly traversing brine. The phenomenon took place only when ice crystals were simultaneously grown on a chilled solid surface elsewhere in the brine, inducing the free ice crystallisation.

Studies of ice crystallisation by direct contact refrigeration were reported by Margolis et al.[110] They studied

the effects of driving force, residence time and agitation rates on the crystal size distribution, in a small continuous ice crystalliser. The important results were:

(a) that higher agitation rates gave smaller crystals

(b) that crystal size was not reduced by halving the residence time from 13 to 6.5 minutes.

The crystals produced were observed and photographed showing them to be disc-shaped and larger than those predicted by permeability measurements. Modelling of the batch crystallisation process for the ice-brine system was undertaken by Wey and Estrin.[111] They considered the crystallisation processes as being described by a population balance, plus material and energy balance equations. A general size-dependent growth model, based upon diffusion-controlled growth mechanisms, and a simple power law for the nucleation rate involving the supersaturation and total surface area, were included. The results revealed that the heat transfer properties of the crystalliser, the level of agitation, the coolant temperature and the number of seeds markedly affected the final distribution.

Desalination by Continuous Column Crystallisation has been described by Hobson and McGrath.[50] Subsequent work has been carried out to develop the system[51] and produce a dynamic model, which describes the operation of the column, based on experimental and computer simulation work.[112] From the model the behaviour of the column could be predicted for the freezing section, so far as nucleation and growth of solids present, were concerned.

Evan et al[88] also studied nucleation rates in an ice crystalliser, assuming primary nucleation was negligible and secondary nucleation occurred at rates controlled by the rate of removal of nuclei growing on existing crystals. They also proposed detailed models for these nucleation rates observed. Kane and his co-workers[113] also investigated the kinetics of the secondary nucleation of ice

and its implications to the operation of continuous crystallisers. Nucleation rates were determined for a wide range of solution subcoolings, refrigerant subcooling, agitation power, impellor configuration and salt concentration. The average crystal size was found to be most sensitive to the solution subcooling, but relatively insensitive to the refrigerant subcooling, degree of agitation and type of agitator over the operating conditions considered. Similarly they believed that new nuclei resulted from shearing dendrites or surface irregularities on the surface of the parent crystals. The results also suggested that nucleation occurred due to collision of crystals with the crystalliser, and possibly from fluid shear effects. Crystal-crystal collision nucleation was negligible at the ice concentrations used.

(2.2.) (b) Ethanol Concentration

The production and concentration of ethanol by fermentation and distillation is a very ancient science. Alcohol was known to the ancients as they witnessed its evaporation on boiling, the first aqueous solutions being produced around the 12th Century, when it was extolled for its curative effects. The various fermentation and distillation techniques have been described by Austin,[114] where he makes the point that the fermentation process is similar for all sugars, the end use determining any variations. Distillers require the maximum alcohol obtainable, while the brewer has flavours, colour, etc., to consider. These latter points are worthy of consideration as Richie[115] indicates that the problem with distilling fermented fruits is the loss of some of the original flavours, e.g. fusel oils which contribute to the bouquet of the wine are often high boiling and tend to concentrate in the "tails" during distillation.

The manufacture of ethanol has been based upon the abundance of cheap raw materials e.g. in Germany alcohol is produced almost exclusively by fermentation, whereas in the U.S.A. synthetic alcohol is produced from cheap ethylene. The production of ethanol by fermentation is limited by the tolerance of the yeast to the increasing ethanol and original sugar concentration, e.g. with sacchromyces, the initial sugar concentration must not exceed 12-15%. Thus in wine production one normally produces 9-12% by volume of alcohol which has to be upgraded by some physical concentration technique to produce fortified wines or spirit. The possibility of ethanol concentration was suggested by Betts[34] with a view to reducing transport costs when shipping wines and beers.

Beer concentrates were also produced by McKay[27] from the pilot plant, Philips piston crystalliser. A beer containing 4.9%

by volume was cooled in a chiller to about 26°F to form a slurry containing 40 wt% ice crystals. Upon processing in the column a beer concentrate of about 6% by volume alcohol was produced, which on reconstitution to the original strength gave a beer equal in taste and analysis to the original feed. A beer concentrating plant based on this was described by McKay,[28] the efficiency was such that the melted crystals were removed as 99.97% pure water product which was reused for normal brewery operations. The system operated under positive, carbon dioxide pressure and as all the solids handling occurred within the equipment, the beer did not contact the atmosphere.

Another field of interest centred around ethanol has developed from its use as a fuel energy source. As an alternative to methane generation, a number of fermentation technologists are looking at the production of ethanol from crops and wastes. Humphries[116] has concluded that with vacuum fermentation the process could be economically attractive; however, the economic bottleneck is the separation of the alcohol from the aqueous fermentation medium, that is, the high costs associated with distillation. Laboratory studies[117] have produced ethanol from corn stalks by hydrolysis with sulphuric acid to produce a mixture of glucose and xylose which can be fermented using a suitable yeast. Current estimates are that a ton of corn would produce 415 lbs (188 kgs) of ethyl alcohol based on 90% conversion of the hexosans and pentosans. The proposed system uses a distillation column to upgrade a feed of approximately 3% ethanol from the fermentation process. The ethanol produced in this manner can be blended with conventional petroleum, extending the supplies of the primary fuel. Countries with abundant corn supplies have launched into this technology and currently "gaso-hol" is undergoing tests in several countries. It is feasible

in the near future that ethanol will supplant petroleum as the main fuel for motor vehicles, especially in countries able to produce corn products on a vast scale.

(2.2) (c) Deuterium Oxide Production and Concentration

Deuterium, heavy hydrogen, was first identified by H. C. Urey and his co-workers in 1931. Both deuterium and its oxide, heavy water, immediately became of interest in chemical and biochemical research. About ten years later, at the inception of the wartime atomic energy project, it was recognised that heavy water would be an excellent moderator for a nuclear reactor producing plutonium. With the rapid expansion of the nuclear programme in the 1950's, the demand for greater quantities of heavy water increased and it was necessary to proceed rapidly with the design and construction of large new production facilities.

From early research, the accepted figure for the Deuterium: Hydrogen in naturally occurring waters was 1:6900, that is 0.0145 mole percent Deuterium Oxide. The possible exchange reactions were:

$$H_2 + D_2 \rightleftharpoons 2\ HD$$

$$H_2O + D_2O \rightleftharpoons 2\ HDO$$

which, due to the low concentration of starting material, would have to be carried out with multiple cascades to give stagewise enrichment. In his early review of enrichment processes Augood[118] quotes the current price for Deuterium Oxide as 70,000 pounds per ton. The techniques for mass production had to be developed rapidly and various systems were based upon Distillation, Chemical Exchange and Electrolysis. Early distillation processes were described by Selak,[119] the first was based on the differences in boiling points between water and deuterium oxide. The distillation was carried out under vacuum, the final product being treated by electrolysis.

In the plant the H_2O was stripped from the slightly less volatile heavy water (HDO and D_2O) giving concentrations of 90% D_2O. The process was not economic and design capacity was not achieved in the plants primarily due to the low plate efficiencies in the initial stages of the distillation train. A typical plant described by Augood[118] for a designed production rate of 1 ton D_2O per twenty-eight days, consisted of 15 sets of 8-column elements, 72 - 100 feet high. White[120] also concluded that distillation was too costly as a primary process but that it was feasible using high performance columns for high D_2O concentrations, e.g. 99.8%. A similar process for hydrogen distillation was also developed,[119] taking advantage of the higher separation factor for H_2/D_2, requiring fewer theoretical stages for a given separation. Besides the problems of working near absolute zero, the processes required very pure hydrogen to prevent column blockages.[120]

Chemical exchange reactions for hydrogen and deuterium were carried out over catalysts[118] or chemical compounds,[121] however the processes were never extensively developed, since, despite the high separation factor (3.87), the equilibrium rate was slow. Electrolysis[118] was also developed for heavy water production. In the process, the ratio of light hydrogen to heavy hydrogen in the gas evolved at the cathode is higher than that in the electrolyte; thus, the heavy hydrogen content of the electrolyte increases severalfold. Since deuterium would be lost in the hydrogen gas evolved from a cell containing water rich in the heavy component, liberated gases were burned and the resultant product passed back into the system at a suitable stage. This latter operation for deuterium recovery has been the subject of many patents.[122][123][124] The electrolytic process is expensive to operate in the initial stages of concentration but is often used for the upgrading of an already concentrated stream.

Another important source of heavy water has been from processes based upon deuterium enrichment by isotope exchange reaction. Early examples[125][126] were based upon the exchange reaction of several isotopic species in hydrogen and water vapour in the presence of a catalyst, such as platinum or palladium. The first large scale production using this isotopic exchange principle was at Trail in the U.S.A. in June 1943. The plant employed existing electrolytic hydrogen facilities to convert water from the exchange tower, to hydrogen, to be scrubbed by the water coming down the tower.[127] Other processes for concentrating deuterium oxide by isotope exchange between water and hydrogen sulphide in staged pairs of hot and cold isotope exchange towers, have been described by Thayer.[128] Here the process is based upon the equilibrium:-

$$H_2S + HDO \underset{COLD}{\overset{HOT}{\rightleftharpoons}} H_2O + HDS$$

In the exchange process, water entering the system flows downwards through the cold tower and then the hot tower, countercurrent to the hydrogen sulphide streams. The water is progressively enriched in deuterium as it passes through the cold tower and progressively depleted in deuterium as it passes through the hot tower. Since the converse is true with respect to the hydrogen sulphide stream, the gas and liquid streams between the towers are enriched in the deuterium isotope. A portion of the enriched water is extracted from the water stream as product, the depleted water disposed of as waste, and the hydrogen sulphide stream continuously recycled as separating agent.

Industrial installations using this type of system have been described by Bebbington.[129] The Dana and Savannah River Plants extract the D_2O from natural water using the G.S. Process[130] to a concentration of 15-20%, from there, by vacuum distillation to

90-95% and by electrolysis to 99.8%. The basic element of the G.S. Process is a pair of gas-liquid contacting towers, one at 30°C (cold) and 120-140°C (hot). Water passes down the cold tower and then through the hot tower countercurrent to H_2S gas at a pressure of 275 p.s.i. Many variations of these processes have been covered by patents. Other systems capable of undergoing this isotope exchange, e.g. a hydrogen/ammonia system have been reviewed by Barr.(127)

Other techniques have also developed; Chopey(131) used an electrolysis of natural water to give a stream of 0.15% HD which was subjected to a two stage rectification process to yield 99.8% deuterium oxide. The rectification steps used specially developed Kuhn columns for the separation of components with close boiling points. Another method(132) described the contacting of steam with a stream of finely divided particles of a metal capable of reducing water under the reaction conditions prevailing. Initial contacting at elevated temperatures 350-900°C and super atmospheric pressures gave rise to a deuterium containing hydrogen stream and particles of metal oxide. By further contacting at high pressure but reduced temperature, 100°C, the deuterium replaces a portion of the molecularly-bound hydrogen in the water and the deuterium-containing hydrogen is simultaneously impoverished in deuterium.

With the greater use of deuterium oxide, a need has arisen for treating degraded heavy water, such that re-enrichment can be achieved economically. The concentration requirements vary widely with the operating conditions of the reactor so any re-concentration apparatus must ensure efficient recovery of the heavy water, be cheap to operate and should easily respond to changes in the feed concentration. Losses of heavy water and reduction in its concentration are unavoidable due to (a) leakage from the heavy water loop, including pumps,and (b) losses in the regeneration and replacement

of ion-exchange resin in the heavy water purification system. Two possible systems based upon electrolysis or rectification have been described, [133] the choice of process depending upon the amount of degraded heavy water requiring treatment. Schotten [134] describes a re-concentration system for the Savannah River Plant, based upon fractional distillation under vacuum, however the energy expenditure is very high. Typical degradation rates required an annual rework of about 0.05 kgs of D_2O at a concentration of 84 wt.% per pound of system inventory. Of this total 0.02 kgs D_2O at 91 wt.% was generated as overheads from the reactor-integrated still, and 0.03 kgs at 71 wt.% from leaks, spills, drains, etc. Clearly a system is required that can treat such waste streams as these to restore the heavy water to its working concentration of 99.5 wt.%.

By utilising the difference in freezing point of water and heavy water, 3.8°C, it should be possible to separate the two components using multi-stage crystallisation. The success of such a system would depend upon there being sufficient theoretical stages in a column to elevate the concentration of heavy water from approximately 80 wt.% to 99.5 wt.%.

(2.2) (d) Waste Effluent Recovery

A problem associated with technological and industrial expansion is the increasing volume of effluent or pollutants requiring treatment. Consents for discharge of wastes to sewers are becoming more stringent and less easy to avoid. Industry is being forced to pay, and pay heavily, for the wastes it produces. As dumping costs rise it is economic sense for the various industries to treat their own effluents. Also it is a fact that the supply of suitable waste dumps is not inexhaustible and thus we are only postponing the day when we have to get to grips with the pollution problem. Any process which can be applied to solve some of the problems is worthy of consideration.

The problem can be divided into two parts, the main requirement can be for the removal of a high volume diluent, water, for recycle and reuse, or the production of a concentrated stream from the waste effluents for processing or recovery. The various methods for achieving a reduction in the toxic portion of the effluent can be summarised as:

(a) Dilution

(b) Destruction

(c) Recovery

(a) Involves the loss of water and/or chemicals while (b) requires the addition of more chemicals. The conventional techniques based on these approaches have been described by Besselievre.[135] Typical interception methods used were (a) fine screening, (b) solids-separation by settlement with the possibility of a precipitation stage, (c) oxidation stage for stabilisation of organics, (d) polishing phase and (e) solids disposal of the accumulated sludges. Whilst these methods are still widely used the complexity of the incoming effluent has increased and often more sophisticated techniques are required to deal with chemicals, toxins, etc.

There have been many different approaches to solving the various problems, many of these have come from systems developed in other fields. Typical examples of these have been the spin-off of various desalination techniques for the treatment of various waste water streams. In many instances the systems developed could not cope with the very high volumes required in desalination to put them in an economic operating bracket. Some of the systems described were pilot scale test units originally used for desalination. Campbell and Emmerman[12] described such a project for the treatment of the rinse waters from a metal-finishing production line. The advantages they saw for using freezing were that as the water was removed by freezing, the freezing point of the concentrate was only moderately lower than that of fresh water, thus one could achieve high volumes of water for reuse. Also the concentrate streams were reduced in volume and their composition was unchanged, enabling them to be destroyed or recycled.

The various process systems utilising freezing have been described by Fraser and Johnson,[136] they are based upon the Vacuum-Freezing Vapour Compression, Secondary Refrigerant, Vacuum-Freezing Ejector Absorption and the Crystalex™ Process. The main applications identified have been for (a) paper mills, (b) metal finishing, (c) chemical wastes, (d) acid-rinse waters, (e) tanneries and textiles. The various processes have been used for (a) concentration for by-products recovery, (b) concentration for reuse in the process, (c) concentration for disposal. A typical mobile unit supplied by Colt Industries was able to produce 100,000 G.P.D. of fresh water effluent of 50-500 mg/L T.D.S. from a feed of 5,000 - 40,000 Mg/L T.D.S.[82] The Colt Industries process was based upon the Vacuum-Freezing Vapour Compression system while a system based on Secondary Refrigerant was tested by AVCO, that is, their Crystalex™ process.[137]

The basic components of the system were a direct-contact crystalliser, surface-type melter-condenser and a pressurised wash column. To demonstrate the applicability of the process to waste streams containing heavy metal salts, approximately 100 µg/ml of Calcium, Chromium, Nickel and Zinc ions were added to a 3% Sodium Chloride solution and used as a feed. Typical results obtained at throughputs of over 600 G.P.D. are displayed in Table(2.3)

Metal	Feed mg/L	Product mg/L	Percentage Removal
Ca^{2+}	105	0.40	99.62
Cr^{6+}	110	0.23	99.80
Ni^{2+}	105	0.44	99.58
Na^{+}	11,800	47.00	99.60
Zn^{2+}	100	0.34	99.66

TABLE(2.3)

All the ions were reduced in the same ratio regardless of initial concentration and the total solids removal was better than 99.5%

The other main area of process development has been the use of Reverse Osmosis techniques. These have found applications in various process industries, for example, the treatment of metal finishing wastes, cheese industries, paper and pulp,and concentration of nuclear wastes. Their uses in these various processes have been described by McNulty,[138] with particular emphasis on the use of membranes for the treatment of very toxic effluents, for example, cyanide waste streams.

The success of the various freezing processes in the treatment of waste effluent streams suggests another useful application of Column Crystallisation. This is particularly so when

the volume of waste to be treated is not large and a high quality water effluent is required for reuse, or a concentrated waste effluent stream is required for further recovery of by-products.

CHAPTER 3 Theory: Mechanism of crystallisation

(3.1) Supersaturation and metastability

If a saturated solution is cooled then in the absence of solid phase, appreciable crystal nucleation begins only if a certain level of supersaturation is exceeded. All the kinetic processes of crystallisation may be considered to be similar to those occurring during a chemical reaction. Their driving force is the supersaturation defined as the difference between the concentration of a supersaturated solution, C, and a solution just saturated, Cs, at the same temperature. A supersaturated solution is a requirement for crystallisation to take place. Early work on the stability of supersaturated solutions has been reviewed by Van Hook,[139] with note to the work of Ostwald on "supersolubility" and his introduction of the terms metastable and labile, which are best illustrated graphically.

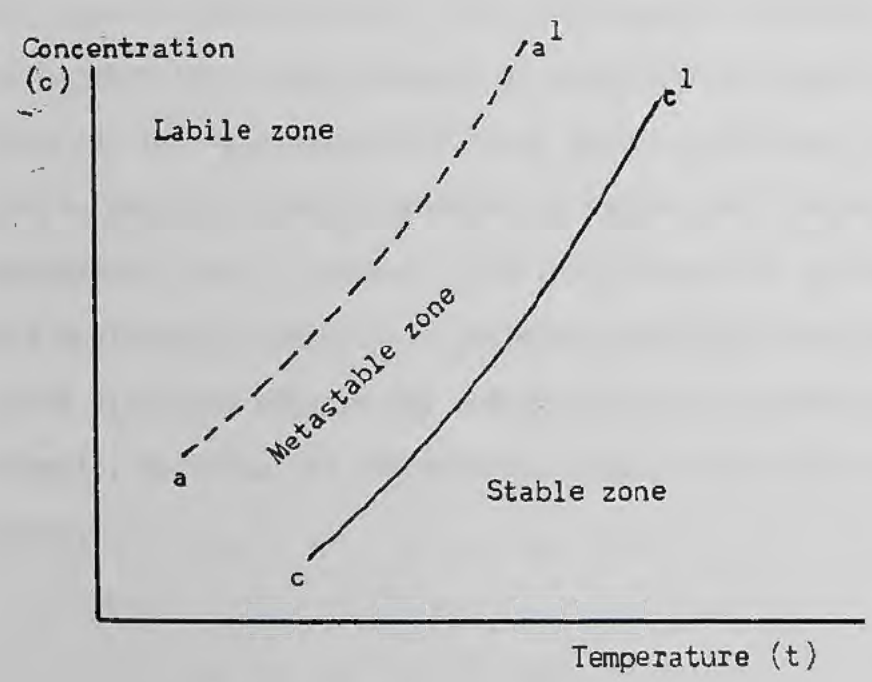

(FIG. 3.1)

Concentration - temperature relation for saturated solutions

Labile zone	:	spontaneous crystallisation
$a - a^1$	:	supersolubility curve (metastability limit)
$c - c^1$	:	normal solubility curve
Metastable zone	:	supersaturated zone between two curves where spontaneous crystallisation is impossible, requires initiation
Stable zone	:	unsaturated zone, crystallisation is impossible

In contrast to the solubility curve, the supersolubility curve does not depend just on the temperature and composition of the solution. This is because the onset of spontaneous crystallisation depends on time, other conditions being equal. The formation of nuclei in a solution is facilitated by the presence of a large amount of dissolved matter, high concentration and a low temperature. Consequently the position of the metastability limit varies not only with the concentration and temperature but also with the mass of the solution. Also most agitated solutions nucleate spontaneously at lower degrees of supercooling than do quiescent ones, that is, the supersolubility curve tends to approach more closely the solubility curve in agitated solutions, and the width of the metastable zone is reduced. Similarly excessive cooling does not aid nucleation, there is an optimum temperature required beyond which viscosity effects may reduce nucleation drastically, for example, reducing the temperature causing the solution to set to a glass.

(3.2) Nucleation

The various methods of nucleation have been represented by Mullin[140] thus:

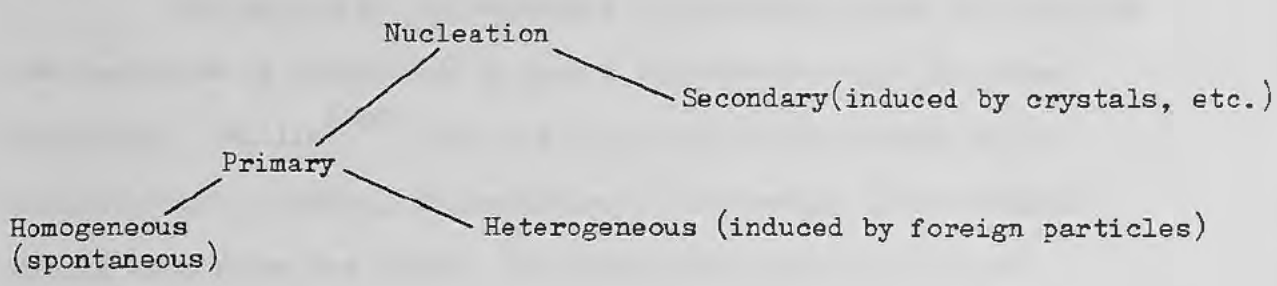

FIG.(3.2) Modes of Nucleation

The term "primary" is for all cases of nucleation homogeneous or heterogeneous in systems that do not contain crystalline matter. On the other hand, nuclei generated in the vicinity of crystals present in a supersaturated system corresponds to "secondary" nucleation, this is the case normally encountered in most crystallisers where the crystal nuclei are formed in a suspension of crystals. It is most likely that all these types of nucleation proceed simultaneously in an industrial crystalliser but it may be presumed that secondary nucleation will be largely prevailing, while the homogeneous nucleation mechanism will be of very little or no importance.

(3.2) (a) Formation of nuclei in a perfectly clean solution

A perfectly clean solution is defined as a solution which is free of solid nuclei of the solute and of solid-particle impurities of any other substance (only real solutions approach this perfect case). The formation, spontaneously, of nuclei, in such solutions has been questioned on many occasions. These doubts are due to the fact that there is a definite correlation between the appearance of crystallisation centres and the presence of various types of impurities; also it has been found that supersaturated solutions can be stored for a long time without any visible changes;

moreover, some substances cannot be crystallised at all from "pure" solutions.

The nature of nuclei formed in perfectly clean solution,and the mechanism of nucleation in such a solution have not yet been determined. Mullin[140] has this to say about the formation of nuclei: "Most probably, the mechanism of nucleation is as follows. Minute structures are formed, first from the collision of two molecules, then from that of a third with the pair and so on. Short chains may be formed initially, or flat mono-layers, and eventually the lattice structure is built up." Whilst this is a simplified approach, it describes the nucleation mechanism well. The construction process, which occurs very rapidly, can only continue in local regions of high supersaturation and many of the "sub-nuclei" redissolve because they are extremely unstable. If a nucleus grows beyond a critical size, it becomes stable under the average conditions of supersaturation obtained in the bulk of the fluid.

This concept of critical size has been developed from the chemical theory of nucleation, stemming from the work of Gibbs et al.[141] The formation of a liquid droplet or solid particle within a homogeneous fluid demands the expenditure of a certain quantity of energy in the creation of the liquid or solid surface. Therefore the total quantity of work, W. required to form a stable crystal nucleus is equal to the sum of the work required to form the surface Ws (a positive quantity), and the work required to form the bulk of the particle, Wv (a negative quantity).

$$W = Ws + Wv \qquad (3.1)$$

When considered in terms of the modified Gibbs-Thompson equation for the vapour pressure of a liquid drop, one can obtain a measure of the work of nucleation, W, in terms of the degree of

supersaturation,[139] that is:

$$W = \frac{16\pi\sigma^3 M^2}{3(RT\rho \ln S)^2} \qquad (3.2)$$

σ = surface energy of droplet per unit area

M = Molecular weight

ρ = density of droplet

T = absolute temperature

R = gas constant

S = supersaturation

This equation tells us when the system is only just saturated, S = 1 lnS = 0, the amount of energy for nucleation is infinite, that is, a saturated solution cannot nucleate spontaneously; but if sufficient energy is injected, spontaneous nucleation is theoretically possible at any degree of super-saturation.

The free energy changes associated with the process of homogeneous nucleation have been explained by Mullin[140] et al with the following equation:

$$\Delta G_{crit} = \frac{16\pi\sigma^3}{3(\Delta G_v)^2} = \frac{4\pi\sigma r_c^2}{3} \text{ since } r_c = \frac{-2\sigma}{\Delta Gv} \qquad (3.3)$$

ΔG_v = excess free energy between a very large particle ($r = \infty$) and the solute in solution.

r_c = critical nucleus

Graphically:

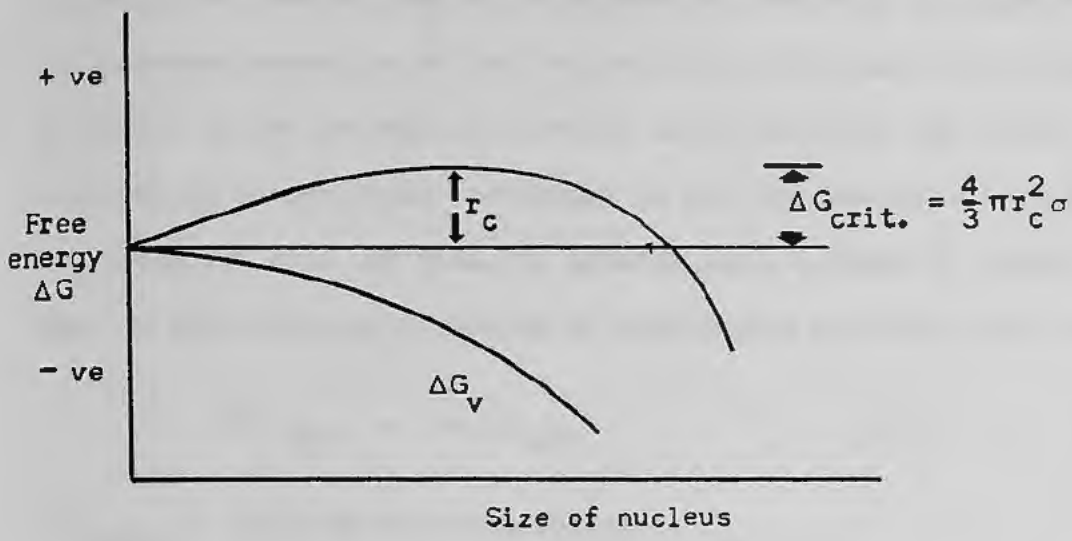

FIG.(3.3)

Free energy diagram for nucleation, explaining the existence of a "critical" nucleus

The graph indicates the behaviour of a newly created crystalline lattice structure in a supersaturated solution with its size. The critical size r_c represents the minimum size of a stable nucleus, whichever course it then follows must result in a reduction of the free energy.

(3.2) (b) Influence of impurities on the formation of nuclei.

Heterogeneous and Secondary nucleation

The formation of nuclei under real conditions usually takes place in heterogeneous systems, which are supersaturated solutions containing various solid particles. In heterogeneous solutions the mechanism varies from one case to another, depending on the amount and nature of solid impurities present in such solutions. The various theories for the mechanism have been discussed by Nyvlt,[13][142] dividing secondary nucleation into two groups:

(1) nucleation due to abrasion

(2) nucleation due to boundary layer

Khamskii[143] distinguishes between other crystallising centres, for example, seeds, particles of substances isomorphous

with the crystallising substance and forming solid solutions with it, particles forming regular intergrowths, particles of substance which absorb molecules of the crystallising substance. The formation of nuclei in the presence of various solid particles and solid surfaces is easier, since the change in the free energy necessary for the formation of a new phase in heterogeneous systems is smaller than in the formation of nuclei in homogeneous solutions, that is:

$$\Delta G'_{crit} = \phi \Delta G_{crit} \qquad (3.4)$$

$\Delta G'_{crit}$ = heterogeneous conditions

ϕ = less than unity

One of the important factors for controlling the nucleation process is the interfacial energy, σ , which for a two solids and liquid system can be represented as follows:

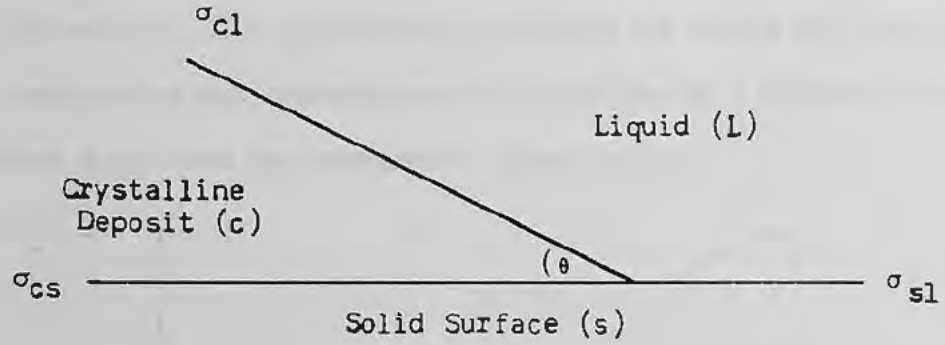

FIG.(3.4)

Interfacial Energy relationship

σ_{cl} = solid crytalline phase c, and liquid l, σ_{sl} = foreign solid surface s and liquid l, σ_{cs} = solid crystalline phase and foreign solid surface.

Resolving these forces in a horizontal direction

$$\sigma_{sl} = \sigma_{cs} + \sigma_{cl} \cos\theta \qquad (3.5)$$

or

$$\cos\theta = \frac{\sigma_{sl} - \sigma_{cs}}{\sigma_{cl}} \qquad (3.6)$$

θ = angle of contact between crystalline deposit and foreign solid

The factor ϕ in equation can be expressed as [140]

$$\phi = \frac{(2 + \cos\theta)(1 - \cos\theta)^2}{4} \qquad (3.7)$$

Thus when $\theta = 180^\circ$, $\cos\theta = -1$ and $\phi = 1$

(a) $$\Delta G'_{crit} = \Delta G_{crit} \qquad (3.8)$$

when θ lies between 0 and 180° $\theta < 1$; therefore

(b) $$\Delta G'_{crit} < \Delta G_{crit} \qquad (3.9)$$

when $\theta = 0$, $\phi = 0$

(c) $$\Delta G'_{crit} = 0 \qquad (3.10)$$

For case (a) the overall free energy of nucleation is the same as that required for homogeneous nucleation (i.e. spontaneous). For case (b) nucleation is easier to achieve because the overall excess free energy required is less than that for homogeneous nucleation, and lastly, in case (c), the free energy of nucleation is zero, which corresponds to the seeding of a supersaturated solution with crystals of the solute. The relationship between the ratio of free energies of homogeneous and heterogeneous nucleation as a function of the contact angle can be represented graphically.

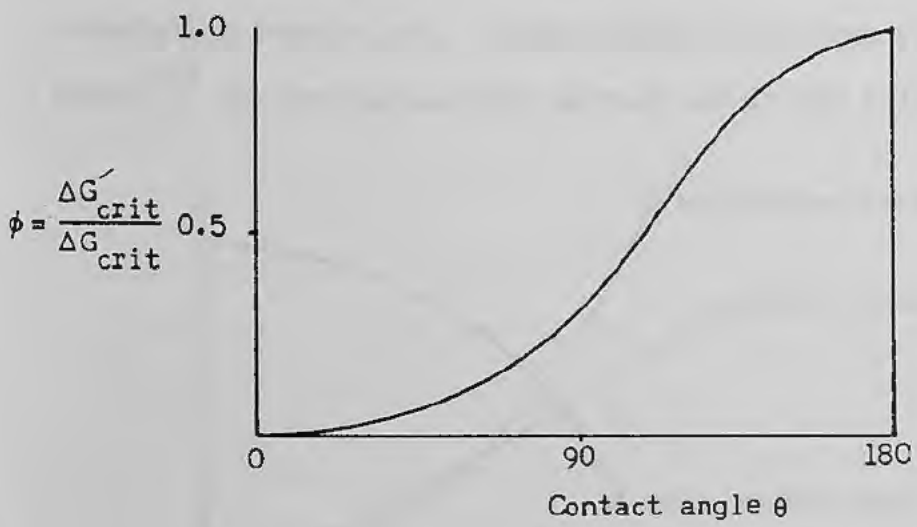

FIG.(3.5)

Ratio of free energies of homogeneous and heterogeneous nucleation as a function of the contact angle.

(3.2) (c) Nucleation Rate

The rate of nucleation J, e.g. the number of nuclei formed per unit time per unit volume, can be expressed in the form of the Arrhenius reaction equation.

$$J = A \exp(-\Delta G/kT) \qquad (3.11)$$ k = Boltzmann constant

For the nucleation of water droplets from supersaturated water vapour, the factor A has been estimated as 10^{25}; giving the rate of nucleation J as the number of nuclei per second per cm^3. Equation (3.11) may be evaluated using the Gibbs-Thompson relationship* and equation(3.3) ($\ln S = \frac{2M\sigma}{RT\rho r}$)* to give:

$$J = A \exp\left(- \frac{16\pi\sigma^3 V^2}{3k^3T^3(\ln S)^2} \right) \qquad (3.12)$$

where σ = surface energy per unit area (interfacial tension)

V = molecular volume

S = Supersaturation

T = absolute temperature

This equation indicates that three main variables govern the rate of nucleation: temperature T; degree of supersaturation S; interfacial tension σ. These effects have been represented by Nyvlt[13] for crystallisation carried out in the metastable zone;

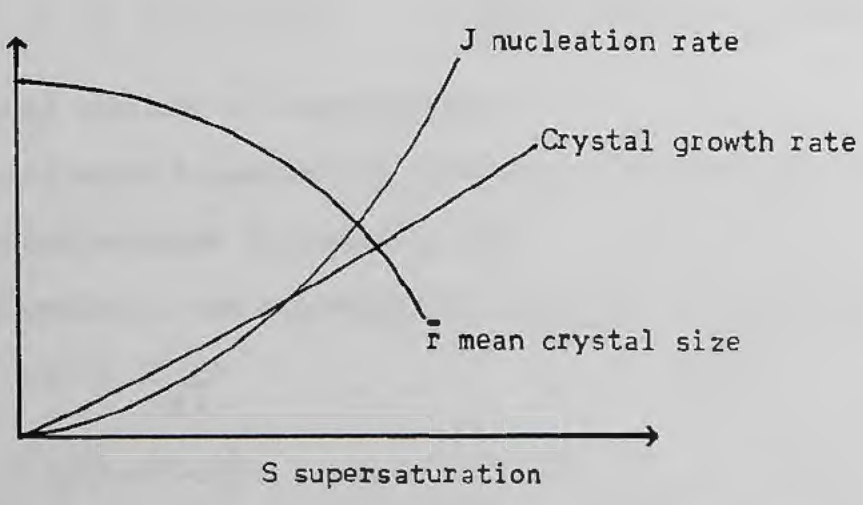

(FIG. 3.6)

Effect of increasing supersaturation on nucleation and crystal growth rates.

When a certain level of supersaturation is reached, that is, on the boundary of the metastable zone, the nucleation rate increases rapidly and consequently the average size of the crystals formed $\bar{r}$, diminishes strongly.

The lack of success of this rate equation, for homogeneous nucleation to explain the behaviour in actual crystallisers, where the nucleation is heterogeneous or secondary, has prompted workers to examine empirical relationships to express the kinetics of nucleation. The power-law dependence of nucleation rate J, on supersaturation, has become a commonly used relationship, viz:

$$J = K_n \cdot \Delta c_{max}^m \qquad (3.13)$$

K_n = nucleation rate constant

m = 'order' of the nucleation process

Δc_{max} = maximum allowable supersaturation

The validity of the equation has been demonstrated by Nielsen,[144] since it can be derived from the classical nucleation relationship, equation (3.12)

$$J = A \exp\left(- B (\ln S)^{-2} \right) \qquad (3.14)$$

The nucleation rate may be expressed in terms of the rate at which supersaturation is created by cooling.

$$J = q.b \qquad (3.15) \qquad b = -\frac{d\theta}{dt} \text{ (temperature change)}$$

b = rate of creation of supersaturation

q = mass of solid deposited per unit mass of free solvent present when the solution is cooled by $1^{\circ}C$.

q is a function of the concentration change of the crystallising species.

$$q = E \frac{dc^*}{d\theta} \qquad (3.16)$$

where $E = R/\left(1-c(R-1)\right)$

R = ratio of molecular weights of hydrate:anhydrous salt

c = solution concentration expressed as mass of anhydrous salt per unit manufactured solvent.

The maximum allowable supersaturation, ΔC_{max}, may be expressed in terms of the maximum allowable undercooling, $\Delta\theta_{max}$.

$$\Delta C_{max} = \left\{\frac{dc^*}{d\theta}\right\} \Delta\theta \text{ max} \qquad (3.17)$$

Equation 13 can now be rewritten as

$$E \left\{\frac{dc^*}{d\theta}\right\}_b = K_n \left[\left\{\frac{dc^*}{d\theta}\right\} \Delta\theta \text{ max}\right]^m \qquad (3.18)$$

which on taking logarithms

$$\log b = (m-1) \log \left\{\frac{dc^*}{d\theta}\right\} - \log E + \log K_n + m \log \Delta\theta_{max} \qquad (3.19)$$

indicating that the dependence of log b on log $\Delta\theta_{max}$ is linear, and the slope of the line is the "order" of the nucleation process m. The assumption made here is that the size of stable nuclei, the nucleation rate constant and the order of nucleation are independent of the process conditions. Nyvlt[13][142] has described an apparatus and experimental technique to determine the relation between log b and log ΔC_{max}; however, work is still progressing on the interpretation of these experimentally determined quantities.[145] An area of active research has been in the field of nucleation and growth of ice crystals in secondary refrigerant freezing processes. Orcutt[105] has carried out investigations of these processes and has developed a model which gives a realistic, sudden increase in the nucleation rate at an appropriate temperature, viz:

$$\frac{\text{Number of nuclei formed}}{\text{unit time - unit surface area}} = B_o (\Delta T_s)^n \qquad (3.20)$$

B_o = nucleation rate constant

n = constant

ΔT_s = $(32-104\ X_s-T_s)^\circ F$

T_s = temperature of the bulk brine

X_s = concentration salt, weight fraction T.D.S.

Making $n > 1$ gives a rate which increases rapidly as ΔT_s increases. Similar relationships were also found by Wey and Estrin,[146] who found that the crystallisation characteristics of ice crystals from a 3% brine solution could be modelled from moments of the density function from data obtained from crystal size distribution measurements. They found that within the range of operating conditions, the nucleation rate could be correlated by a power law model:

$$B_o = K_N \cdot (\Delta c^*)^{1.8} \cdot \mu_2^{0.2} \qquad (3.21)$$

$$K_N = 26.2\ (P/V)^{0.52} \qquad (K_N = K_O\ (P/V)^n)$$

B_o = nucleation rate $n^o/sec/cc$

$K_N K_O$ = proportionality constants in secondary nucleation expression

P/V = Power dissipation per unit volume ergs/sec/cc

Δc^* = overall supersaturation g/cc

μ_j = J^{th} moment of distribution function n

$$\left(\mu_j = \int_0^\infty n\, L^j\, dL\right) \qquad n^o/\ cm^j/cc$$

(3.3) Crystal Growth: mechanism and rate

The growth of crystals is governed by at least two processes:

(a) The diffusion of particles to the surface of a growing crystal.

(b) Their incorporation in the structure of the crystal lattice by

(i) adsorption of a particle by the surface

(ii) migration along the surface

(iii) final incorporation in the lattice.

The rate of crystal growth is influenced by the same factors as the nucleation process: temperature, rate of stirring, presence of impurities, degree of supersaturation, viscosity, etc.

The growth of a crystal can be represented by the time dependence of the linear dimensions, the surface, the volume or the mass of a crystal. The most common term is the linear growth rate, which is understood to mean the rate of displacement of a face at right angles to its plane, the rate of motion of a face of a crystal parallel to itself.

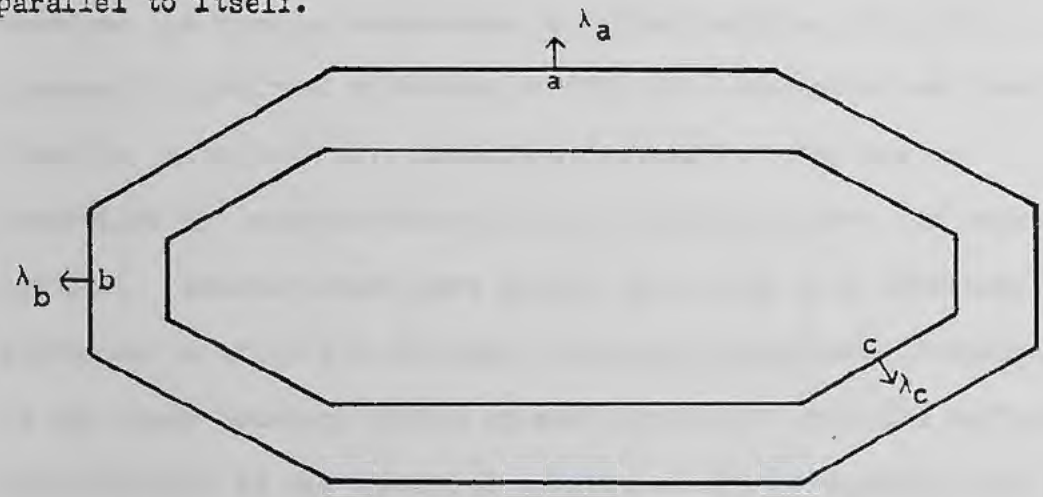

$\lambda_{a,b,c}$, ---- linear growth rate functions

(FIG. 3.7)

Schematic representation of growing crystals which retain their shape

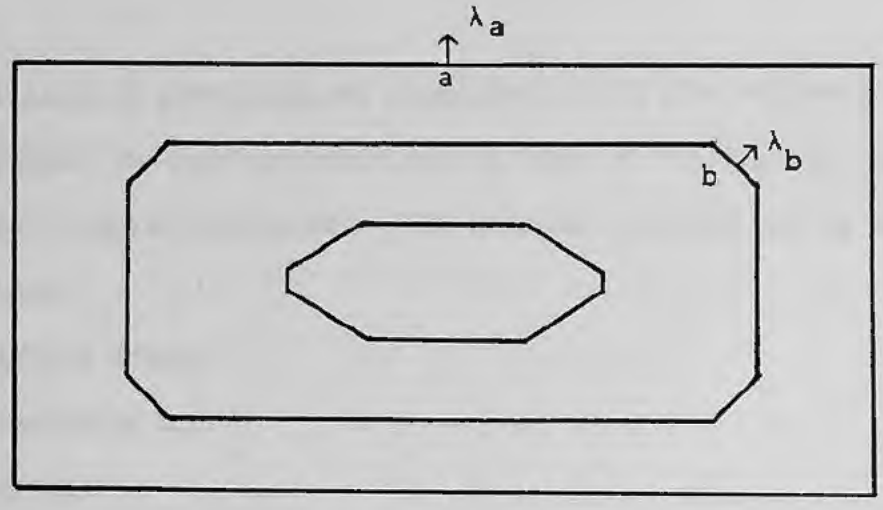

(FIG. 3.8)

Schematic representation of a growing crystal which changes its shape

The difference between the linear rates of growth of individual crystal faces may alter its habit because of the increases of the size of some faces and the disappearance of others. Usually, those faces disappear which have the highest linear growth rates.

The kinetics of crystallisation will be determined by the slowest of the interdependent processes (a) and (b). Nyvlt[13] has examined the various mechanisms and given examples where the process in unstirred solutions is diffusion controlled, and where there is sufficient mass transfer, the reaction kinetics are controlled by incorporation of ions or molecules into the crystal lattice. However cases have arisen where even with stirring, diffusion is still the limiting factor, and turbulance, developing at the phase boundary during crystal growth, has provided sufficient mass transfer in the unstirred solution. Nyvlt suggests that by comparing the activation energy of the process with that of diffusion, the effects of admixtures, stirring and the kinetics of dissolution and crystallisation, one will be able to ascertain which step determines the crystallisation kinetics.

Several theories of crystal growth have been advanced, Nyvlt has concluded that most are not suited to the practical

crystallisation situation, and concludes that it is relevant only to represent the most probable growth rate of the crystals by the simplest possible relations. The various theories can be divided as follows:

(a) Surface Energy

(b) Adsorption Layer

(c) Kinematic

(d) Diffusion

It is the latter, Diffusion process, which Nyvlt considers the most applicable to practical use. The various other mechanisms have been extensively described by Mullin,[140] Strickland-Constable,[147] Khamskii.[143]

The basis of the diffusion theory is that the deposition of solid on the face of a growing crystal is a diffusional process. It was also assumed that crystallisation was the reverse of dissolution and that the rates of both processes were governed by the difference between concentration at the solid surface and in the bulk of the solution. The various concentration driving forces can be represented thus:

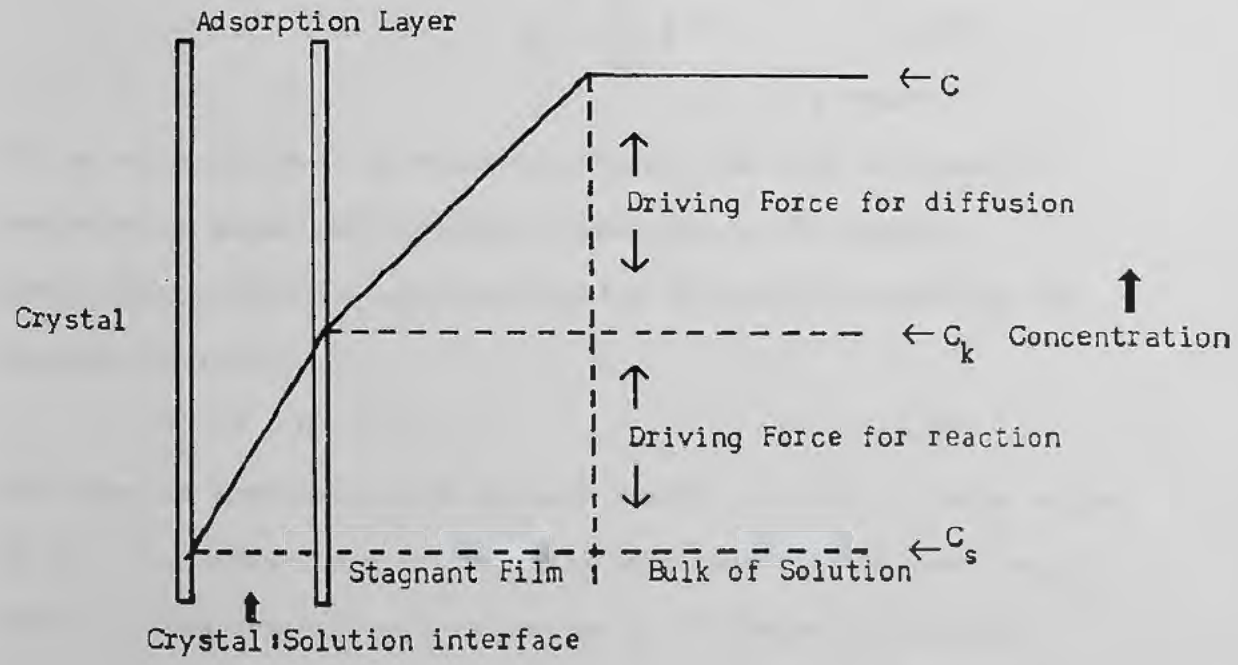

(FIG. 3.9)
Concentration Driving Forces near the crystal surface

It should be noted that the driving forces will rarely be of equal magnitude, and the concentration drop across the stagnant film is not necessarily linear. The solution concentration close to the crystal surface is controlled by a dynamic balance between diffusion-controlled mass transfer, for example.

$$\text{rate is } \frac{dG'}{dT} = \frac{DA}{\delta} (C-C_k) \qquad (3.22)$$

C_k = solute concentration in the solution at the Crystal:Solute interface

A and δ = area and thickness of the absorbed layer

D = Diffusion coefficient

and the rate of reaction when the solute molecules arrange themselves into the crystal lattice, for example,

$$\text{rate is } \frac{dG'}{dT} = k' A(C_k - C_s) \qquad (3.23)$$

k' = rate constant

In order to eliminate the difficulties involved in measuring interfacial concentration, an "over-all" concentration driving force $(C-C_s)$ is used, since at steady state the uptake of particles and their removal by diffusion balance, that is, equation(3.22) and(3.23) can be modified thus,

$$\frac{dG}{dT} = k' A \left(C-C_s - \frac{dG}{dT} \cdot \frac{\delta}{DA}\right)^n \qquad (3.24)$$

n = order

If the value of DA/δ is relatively large, the last term can be neglected in equation(3.24).This corresponds to the crystal growth being controlled by the kinetics of particle uptake by the lattice, that is,

$$\frac{dG}{dT} = k' A (C-C_s)^n \qquad (3.25)$$

For cases of extremely rapid surface reaction, that is, large values of k' , the latter term on the right hand side of(3.24)must tend to zero, and the crystallisation process is diffusion-controlled.

$$\frac{dG}{dT} = \frac{DA}{\delta} (C-C_s) \qquad (3.26)$$

If the surface reaction is determined by 1st order kinetics, then n = 1 and equation(3.24)becomes:

$$\frac{dG}{dT} = \left\{ \frac{\delta}{D} + \frac{1}{k'} \right\}^{-1} A\ (C-C_s) \qquad (3.27)$$

k_2 = crystallisation rate constant for 1st order reaction.

or $\frac{dG}{dT} = k_2 AP$

P = Supersaturation

The validity of this assumption is questionable as many inorganic salts crystallising from aqueous solution give an overall growth rate order, n, in the range 1.5 - 2. Mullin[140] has extended the rate equation to take account of a non-linear dependency of surface integration on concentration driving force. The resulting equation is complex and can only be solved explicitly for simple cases, the relationship between the various coefficients, DA/δ and k', and k_2 not being clearly defined. In practice it has been found that the crystallisation rate can be represented by the empirical relation

$$dG/dT = k_2 AP^n \qquad (3.28)$$

over a limited concentration range. The value of n may be equal to unity, but may also assume other, larger values. Experimental investigations have given rise to relationships of this form e.g. when Umano and Kawasaki[104] studied the nucleation and growth of ice crystals in sea water. They found that the quantity of ice produced, x g/min, during the period of rapid rise in temperature after nucleation had the following relationship:

$$\frac{dx}{dt} = 21.S.\theta^2 \qquad (3.29)$$

S = surface area crystal (cm^2)

θ = degree of supercooling (^oC)

That is to say, the rate of precipitation of ice crystals immediately after nucleation, is proportional to the square of the

degree of supercooling. Also, when the nucleation was completed and nuclei were growing into grains, the relationship between the degree of supercooling and the rate of growth was:

$$\frac{dx}{dt} = 5.75 \times 10^{-3} \; s\theta \qquad (3.30)$$

showing first order dependence, with the value of k_2 (equation 3.28) for the rate constant being 5.75×10^{-3} $^{o}C^{-1}$ cm^2.

(3.3) (a) Factors influencing the rate of crystal growth

It has been observed that growth rates increase when a solution is being stirred. This can be explained as stirring allows the crystals to be contacted by fresh supersaturated solution at the same time decreasing the thickness of the adsorption layer. Increased stirring does not produce larger crystals since one promotes the formation of nuclei and one has to use an optimum stirring rate to produce large crystals. Aggregation of crystals is also reduced by agitation. The topic has been the subject of many investigations to determine the precise effects taking place in a crystalliser. Generally one can show from the Diffusion theory (Equation 3.27), that:

$$k_2 = \frac{D}{\delta + (D/k)} \qquad (3.31)$$

In a solution that is highly agitated $\delta \ll D/k$, so that measurements of k_2 and extrapolating to infinite stirring rates facilitate the determination of k. If the value of the diffusion coefficient is known, one can then determine the dependence of the thickness of the diffusion layer on the agitation intensity.

An increase in temperature generally leads to an increase in crystallisation rate, however nucleation rate increases more rapidly with increasing temperature than the growth rate. The temperature and viscosity effects on growth are related; uniformity and size of crystals is best achieved in low suspension viscosities. The relative supersaturation has no direct effect on the crystallisation constant, whereas at very high values the instances of lattice defects

increase which accelerates the crystallisation process, as these imperfect crystals grow faster than the more perfect ones.

The addition of soluble admixtures has a deleterious effect on the crystallisation rate. This could arise from the fact that these absorbed particles must be displaced by the crystallising substance, or the work required to locate the crystallising substance in the lattice is greater due to the presence of these particles. Lastly the effects of pressure on the crystallisation rate are very small. This can be explained by considering the insensitivity of the mean intermolecular spacings in solution to pressure increases.

The whole process is very complex and for an ionising solute crystallising from aqueous solution, Mullin[140] has postulated the following:

(1) Bulk diffusion of solvated ions through the diffusion boundary layer
(2) Bulk diffusion of solvated ions through the adsorption layer
(3) Surface diffusion of solvated or unsolvated ions
(4) Partial or total desolution of ions
(5) Integration of ions into lattice
(6) Counter-diffusion of released water through adsorption layer
(7) Counter-diffusion of water through boundary layer.

Which step dominates is difficult to elucidate and presently no theory fully explains all the observable phenomena.

(3.4) Influence of Impurities on the Crystallisation Kinetics/ Crystal quality

The presence of certain impurities, often very small traces, can have profound effect on the crystallisation process. For instance, nucleation may be retarded or crystal growth suppressed entirely. Savanoe[148] has examined the various mechanisms by which impurity can result in the crystals. The first and most important are the impurities arising from adhering mother liquor. Traditionally a centrifuge or filter has been used to reduce the amount of mother liquor adhering to the crystal surface. The efficiency of the separation process depends to a large extent on the uniformity of the crystals and the relative amount of crystal surface per unit weight of crystalline material. It has been estimated[148] that for a system where the mother liquor contains water (as a solute) and impurity in the ratio of 15 to 1, by reducing the moisture content from adhering mother liquor after the centrifuge to 1%, the percentage of impurity from adhering mother liquor will be reduced to $^{1}/_{15}^{th}$ of 1% or approximately 0.07%. Further improvement can be realised by removal of surface impurities with a solvent wash.

Recent work by Nakai and Miyake[149] on the benzene/cyclohexane eutectic system have confirmed these observations. Using a cooling-batch-type crystalliser to produce benzene crystals, the cyclohexane impurity in scale and bulk crystals was measured. From their experiments they concluded that the impurity in the bulk crystals, such as agglomerates, is higher due to the inclusion of mother liquor, than that of scale crystals, having a plate-like, rigid form. Also they found that washing both types of crystals with liquid benzene markedly elevated the purity of the crystals. Wells et al[53] adopted a heuristic approach to assist process selection of unit stages in producing organic chemicals by crystallisation. They were

particularly concerned with improving performance with respect to removal of adhering mother liquor from the crystal slurry. They examined the use of centrifuges and filters in conjunction with various wash procedures. Of particular interest was the investigation of the operation of a Schildknecht Column for the purification of benzene from a benzene/cyclohexane mixture. The amount of impurity associated with the solid phase X was approximated by the linear function

$$X = 0.0004\ Ym \qquad (3.32)$$

Ym = mother liquor composition (mole fraction)

Furthermore they were able to show that for a particular column length a lower limit of product purity was achived for a given mother liquor composition. This they were able to demonstrate by centrifuging the product from the column and then washing the crystals in the centrifuge by partial melting of the crystals. The initial centrifuging operation reduced by at least a factor of ten the impurity associated with the crystals while the latter stage showed only a marginal improvement. This prompted them to suggest the integration of multi-stage and single stage units as economic, particularly with the Schildknecht Column. This would enable the size of the column to be reduced whilst maintaining a high purity product by incorporating a centrifuge in the process.

Secondly, impurity can become attached to the crystal by adsorption. Garrett[150] has examined this particular phenomenon with particular reference to the use of various compounds as habit modifiers in industrial crystallisation processes. There is as yet no generally accepted theory to explain the mode of action of habit modifying impurities, but it is clear that different impurities can act in different ways. In his observations, Garrett has noted the many varied modes of adsorption taking place and their effects on the crystal growth. Since there is a dynamic equilibrium between

the crystal surface and the solution for both the impurity and the crystallising solid, the impurity is not necessarily fixed once it has joined the crystal surface. It may effectively block further growth for a time, but eventually may be desorbed and replaced by the parent solid, that is, growth is only retarded.

In some cases adsorption is sufficient to block the growth completely, of one face, and as a result modification of the crystal occurs. In some instances the amount of material adsorbed may be too small to be noticed but where the crystallisation rate is such that complete overgrowth can occur, then significant amounts of the impurity will be retained. Conversely impurities with only a small fraction of their bulk contributing to the absorbing charge would be expected to be susceptable to desorption, other things being equal. Likewise impurities with weaker charges would again undergo desorption and in these cases high concentrations of materials are required to produce significant modification.

Thirdly, impurity can be introduced by inclusion of mother liquor in the growing crystal. The lower the supersaturation, the more regularly do crystals grow. Higher ranges of supersaturation induce flawed growth and allow mother liquor to be included between layers of crystallites, as well as between crystal aggregates. Mullin[140] describes an interesting phenomenon, usually associated with crystallisation from the melt, but also readily observable in crystallisation from solution. When a crystal grows in an impure system, impurity is rejected at the solid-liquid interface. If the impurity cannot diffuse away fast enough it will concentrate near the crystal face and decrease the equilibrium melting point. Thus the supercooling is reduced and the growth rate is retarded. The equilibrium saturation concentration of the bulk solution will be lower than that at the interface, so the temperature driving force increases over a short distance from the crystal face towards the

bulk solution.

This 'constitutional supercooling' causes interfacial instability, the growing interface breaking up into thin fingers which allows the heat of crystallisation to be dissipated. The regions between the projections entrap impure solution and a succession of inclusions may be left behind. With high constitutional supercooling (high level of impurity) dendritic branching generally occurs, giving rise to problems during the subsequent solid-liquid separation and drying operations.

(3.5) Crystal impurities arising during the freezing of a eutectic system in a continuous column crystalliser

Many classes of liquid/solid binary systems exist. However the systems of industrial importance are usually eutectic or solid-solution forming. Most organic binary mixtures are eutectic-forming, as in the case of benzene/cyclohexane, and it is possible to obtain pure crystals in a single theoretical stage, except at the eutectic point. The various phase relationships can be explained as follows. If a liquid mixture of two similar components A and B is cooled, solid will commence to separate at a definite temperature, namely the freezing point. The actual value will depend on the ratio of A:B and if one plots a series of compositions varying from pure A to pure B, the corresponding curves are obtained:

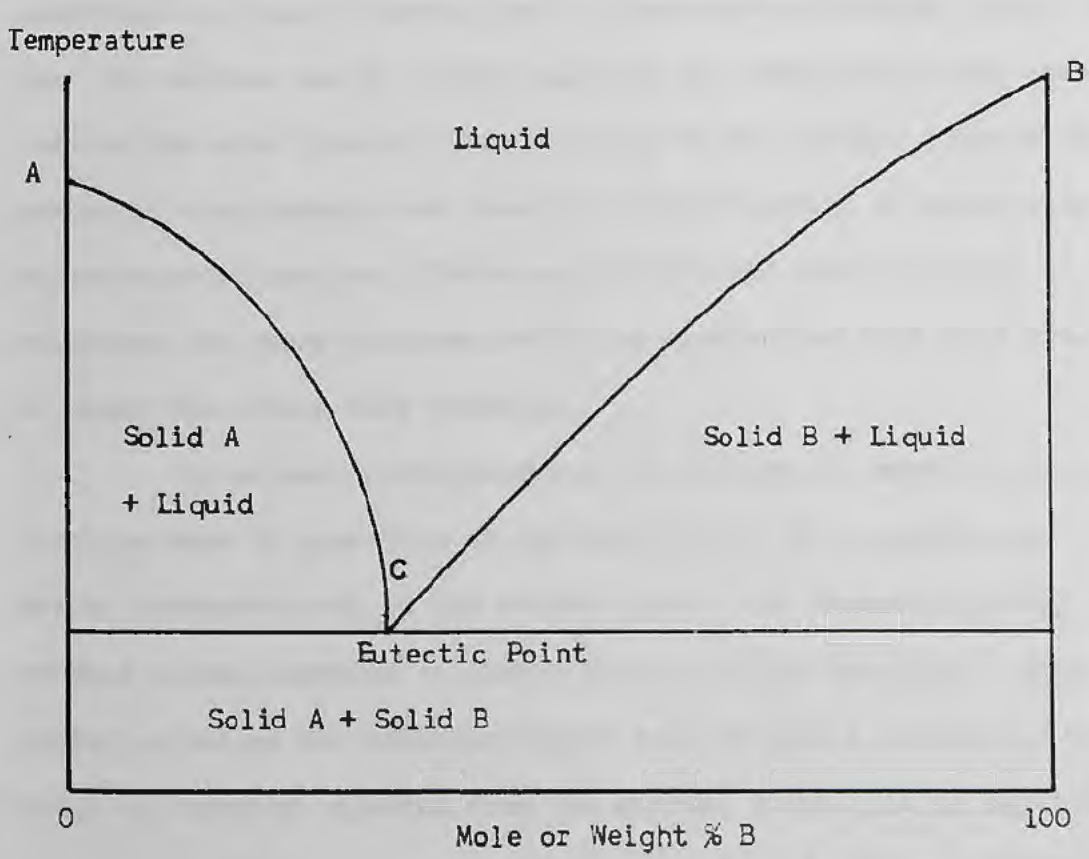

FIG. (3.10)

Phase diagram for a simple binary system

The points A and B are the freezing points of the pure components. The addition of B to A lowers the freezing point along AC and for A added to B lowers the freezing point of the latter along BC. If the freezing point and composition of a given mixture are such as to fall on the curve AC, the solid which separates is pure A and similarly for the curve BC. At the point C where the curves AC and BC meet, the eutectic, both solids A and B are in equilibrium with the liquid phase. In column crystallisation, separations are not carried out in the eutectic region. It is stressed that this representation is an idealised description and often the accuracy of literature versions of both types of phase diagram is questionable. Since a pure phase cannot exist in equilibrium with an impure one, from thermodynamic considerations Cutts and Wells[151] allowed for this deviation from ideality by modifying the phase diagram, for the benzene/cyclohexane system, such that the solidus was at a fine angle to the temperature axis rather than on the axis itself. This position of the solidus affects the purity of the crystals and thus the possible extent of separation in column crystallisation. Cutts and Wells found that for solid solutions the phase diagrams predicted separations that were greater or lower than those they obtained.

In column crystallisation the sources of impurity can come from the mode of operation of the equipment. The crystals are moving countercurrent to the reflux liquid, but because of drag effects a small portion of liquid rises with the crystals. This stream is called the adhering liquid and contains a relatively high level of impurity rejected from the crystal phase. It is continually contacted with a countercurrent stream of liquid of lower impurity content. Thus there is a driving force to reduce the concentration imbalances and the impure crystals are being 'washed' free of this

adhering impurity. This continual washing establishes an axial composition gradient in the column and the axial dispersion in the reflux liquid acts to oppose the separation. It is also possible for impurities to be associated with the crystals. This can be caused by either volumetric liquid inclusions or by the trapping of impurities on the irregular surface of the crystals. It is doubtful if the washing process is able to remove any of this impurity associated with the crystal phase.

In the case where there is solid-solubility then impurity removal is dependent upon the temperature gradient in the column. Impure crystals become unstable at higher temperatures in the purification section and undergo partial or total melting. Simultaneously the reflux liquid undergoes partial freezing. Thus by this continual melting and refreezing a composition gradient is established.

Early investigation of column crystallisers did not include all the possible sources of impurity in their models. Powers[152] proposed a model where the purification of a system, with negligible solid solubility, was limited by axial dispersion and washing of the adhering liquid associated with the crystals. When Albertins[39] investigated the benzene/cyclohexane system, he found that it was necessary to include the impurity associated with the crystal phase to explain his experimental concentration profiles. He neglected the washing of the adhering liquid and concluded that the separation was limited by the axial dispersion and the impurity associated with the crystals. Gates[42] who extended this study found that by including all modes of impurity transfer/removal, the experimental data gave a more consistent fit to the model. The final investigations were carried out by Henry,[43] who, using the same binary system as above, operated the column crystalliser in a continuous mode, as opposed to the Total Reflux investigations of the previous workers.

Henry developed a model which included the transfer of impurity by axial dispersion, washing of impurity from the adhering liquid, and the impurity associated with the crystal phase when the column operated with continuous product removal. In cases where the washing was complete, that is, most of the crystal phase was returned to the column as reflux, a region of constant impurity composition develops in the portion of the purification section near the melting section. This occurs when the reflux, or free-liquid, composition approaches that of the crystal phase impurity composition, $\mathcal{E}$. For the benzene/cyclohexane system, Henry found that this crystal phase impurity composition was related to the mother liquor composition of the freezing section. For a perfectly mixed freezing section this is equal to the bottom composition Y_s, that is:

$$\mathcal{E} = 1.42 \times 10^{-3} (Y_s) \quad (43) \qquad (3.33)$$

Impurities are concentrated in the freezing section to a higher degree with total reflux than with continuous flow operation. Consequently $\mathcal{E}$ is higher for total reflux than for continuous flow operations. The implications are that purer material can be obtained with continuous flow than with total reflux operation for small values of product removal : crystal production rate. The $\mathcal{E}(Y_s)$ dependence provides a constraint on the maximum product purity that can be attained for a single pass for a given feed composition. When the freezing section (c.f. stripping section in Henry's model) is flushed, that is, bottom product removal (L_s) : feed rate (F) ≈ 1, the composition approaches a minimum value equal to the feed composition. Consequently, the minimum value of the crystal phase composition is proportional to the feed composition (Y_F),

$$\mathcal{E}_{min} = 1.42 \times 10^{-3} (Y_F) \quad (43) \qquad (3.34)$$

The washing which occurs in the purification section does not affect the crystal phase composition, for systems of limited solid solubility. Therefore, multiple-stage or cascade operation must be employed to achieve a product composition less than ε_{min}. As reported previously, this was confirmed by Wells et al[53] who by centrifuging their product from the column were able to reduce the impurity significantly. Henry also found that there was a lower limit of product offtake (L_E) : crystal rate (C) below which no further purification was achieved. Thus for maximum purity the ratio of $(L_E)/(C)$ should be chosen such that the impurity content of the product (Y_E) is just equal to the crystal phase impurity.

(3.6) Mathematical Model of a Column Crystalliser

The model for systems of limited solid solubility includes the effect of axial diffusion of impurity, induced by the rotating and oscillating conveyor, and the mass transfer between the adhering and free liquids. The crystal phase composition is considered to be a constant in the purification section. This accounts for any inclusion phenomena that may occur during the freezing process. The column is operated with countercurrent flow, that is, a portion of the crystals are melted and the liquid generated in the melting section is used to wash the adhering liquid. The various flow streams are represented schematically in the column as follows:

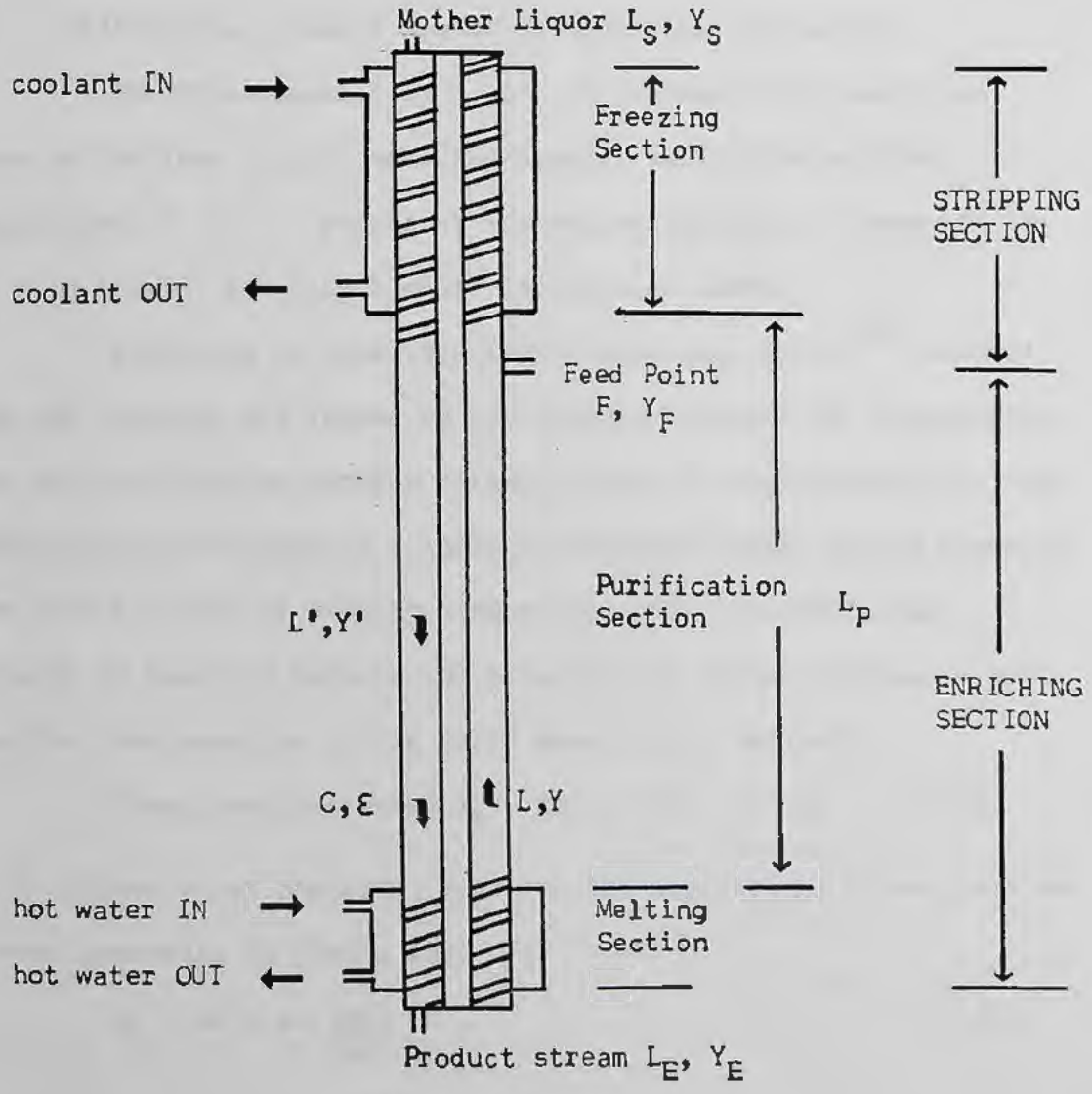

FIG. (3.11)

Schematic representation of a column crystalliser

These can also be considered if one takes a differential element of the purification section, the phase flows in the purification section for a eutectic binary are:

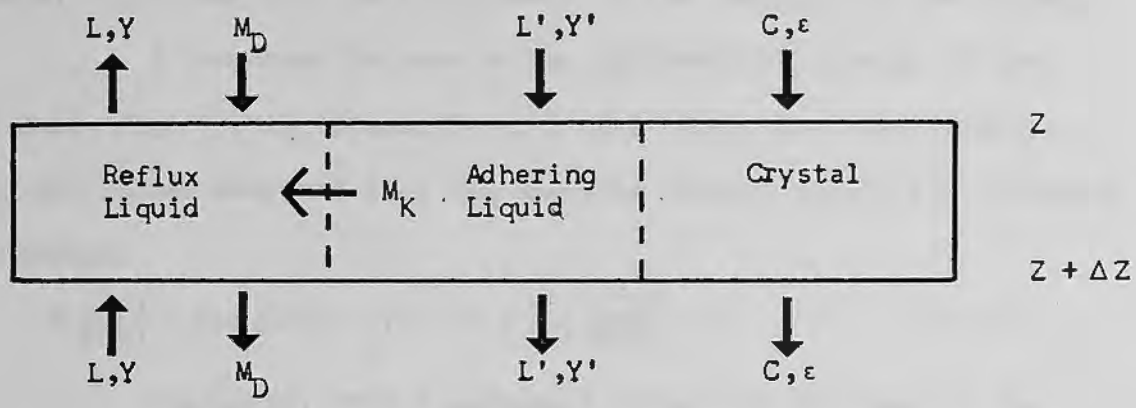

FIG. (3.12)

Differential element across the purification section

The flows denoted by L, L' , C represent the mass flow rates of the free liquid, adhering liquid, and crystals. The compositions Y, Y' , ε represent the weight fraction of impurity of the free liquid, adhering liquid, and crystal phase.

Referring to eutectic-forming binaries, Henry[43] assumed that the crystals are formed in the freezing section and transported down the purification section without change in composition (ε). The crystals are surrounded by a layer of adhering liquid having constant flow rate (L') but of varying composition (Y'). A continuous exchange of impurity between the adhering and reflux liquids is then feasible (back-washing of the solid phase) at a rate of:

$$\text{(Mass transfer rate) } M_K = K a A \rho (Y' - Y)\, dz \qquad (3.35)$$

Axial dispersion of impurity, opposing the separation, takes place at a rate (according to Fick's Law) of:

$$M_D = -D \rho A \eta \left(\frac{dy}{dz}\right) \qquad (3.36)$$

It is assumed that solid and liquid flow rates, mass transfer and diffusion coefficients are constant, the column is at steady state and that adhering liquid flow rate, L' , is proportional to solids flow rate, C and the ratio is independent of the position in the column.

A component balance on the differential element of free liquid, Fig. (3.12) between Z and Z + ΔZ (where Z is the position in the column measured from the freezing jacket) yields the following equation.

$$L\left(\frac{dy}{dz}\right) + KaA\rho\,(Y' - Y) + D\,\rho\,A\,\eta\left\{\frac{d^2y}{dZ^2}\right\} = 0 \qquad (3.37)$$

Similarly, from a component balance at the base of the purification section:

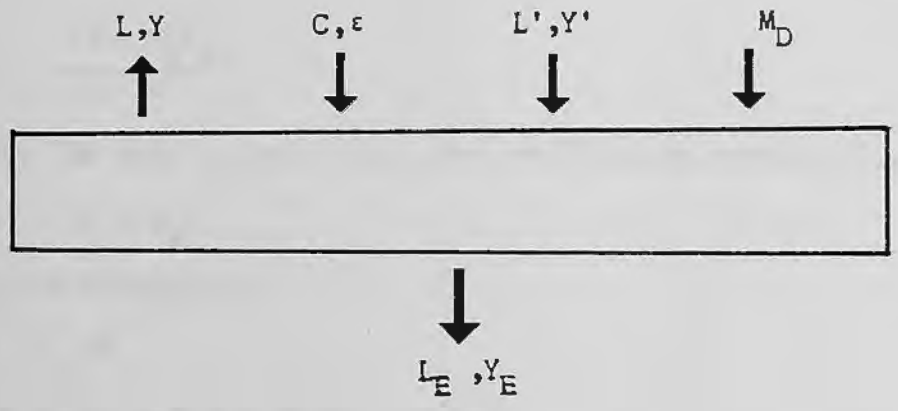

FIG. (3.13)

Component balance at the base of the purification section

$$C\varepsilon + L'\,Y' - D\rho\,A\,\eta\left\{\frac{dy}{dz}\right\} = LY + L_E\,Y_E \qquad (3.38)$$

And a mass balance about the same point yields,

$$L = L' + C - L_E \qquad (3.39)$$

It is now possible to solve equations (3.38) (3.39) and (3.37) after simplification of the latter. Experimental results have shown[43] that the term (d_2Y/dz^2) may be neglected.(x) This is known as the Transport Equation approach and equation (3.37) becomes,

$$L\left\{\frac{dy}{dz}\right\} + KaA\rho\,(Y' - Y) = 0 \qquad (3.40)$$

(x)- - See Appendix (A·5)

Equations (3.38) (3.39) and (3.40) can now be solved; eliminating Y′we have a first order differential equation describing the enriching section,

$$\left\{\frac{L\,L'}{(Ka\rho A} + D\,\rho\,A\eta\right\}\frac{dy}{dz} + (L - L')Y = C\varepsilon - L_E Y_E \qquad (3.41)$$

That is,

$$\left\{\frac{1}{(L - L')}\right\}\left\{\frac{L\,L'}{(Ka\rho A} + D\rho A\eta\right\}\frac{dy}{dz} + Y = \frac{C\varepsilon - L_E Y_E}{L - L'} \qquad (3.42)$$

That is,

$$H_E\frac{dy}{dz} + Y = Y_P \qquad (3.43)$$

Where,

$$H_E = \frac{1}{(L - L')}\left\{\frac{(LL'}{(K\rho aA} + D\,\rho\,A\,\eta\right\} \qquad (3.44)$$

And,

$$Y_P = \frac{C\varepsilon - L_E Y_E}{L - L'} \qquad (3.45)$$

Note From the mass balance about the purification section (3.39)

$(L - L') = (C - L_E)$

and from the assumptions

$$a = L'/C \qquad (3.46)$$

Then $(L \times L') = a(1 + a)C^2 - a L_E C$ (3.47)

Thus (3.44) can be rewritten,

$$H_E = \frac{1}{(C - L_E)}\left[D\rho A\eta + \frac{a(1 + a)\,C^2 - aL_E C}{KaA\rho}\right] \qquad (3.48)$$

and (3.45) $Y_P = \dfrac{(C\varepsilon - L_E Y_E)}{C - L_E}$ (3.49)

The solution of (3.43) is thus:

$$\int\frac{dy}{Y - Y_P} = -\int\frac{dz}{H_E} \qquad (3.50)$$

$$\log_e (Y - Y_P) = \frac{-z}{H_E} + C \qquad (3.51)$$

The boundary condition of the purification section is defined at $Z = Z_F$ (the feed-point) where $Y = Y_\phi$, the composition of the reflux stream before meeting the feed.

$$\therefore C = \text{Log}_e (\bar{Y}_\phi - Y_P) + Z_F/H_E \qquad (3.52)$$

Hence the solution $\log_e \left[\frac{Y - Y_P}{Y_\phi - Y_P}\right] = \frac{-(Z - Z_F)}{H_E}$ (3.53)

That is $\frac{(Y - Y_P)}{(Y_\phi - Y_P)} = \exp. \frac{-(Z-Z_F)}{H_E}$ (3.54)

This is a general solution describing the concentration profile in the enriching section. A detailed derivation of equation (3.41) can be found in the work of Gladwin.[153]

Similarly a set of equations for the stripping section can be obtained.

$$\frac{(Y - \bar{Y}_P)}{(Y_\phi - \bar{Y}_P)} = \exp. \frac{-(Z - Z_F)}{H_S} \qquad (3.55)$$

where

$$\bar{Y}_P = (C\varepsilon + L_S Y_S) \Big/ (C + L_S) \qquad (3.56)$$

and

$$H_S = \frac{1}{(C+L_S)} \left[D \rho A \eta + \frac{a(1 + a) C^2 + a L_S C}{KaA\rho}\right] \qquad (3.57)$$

For total reflux operation, the value of L_E is zero and the equation for the enriching section (3.54) becomes:

$$\frac{(Y-\varepsilon)}{(Y_\Phi - \varepsilon)} = \exp. -Z/H_\Phi \qquad (3.58)$$

where Y_Φ is the free liquid composition at the top of the purification section. Then:

$$H_\Phi = \left[\frac{D\rho A\eta}{C} + \frac{a(1 + a)C}{KaA\rho}\right] \qquad (3.59)$$

Equation (3.58) can be used to predict the purification section composition profile, but in this case an initial condition is used rather than terminal-stream material balances as with continuous flow work. This can be achieved by equating the amount of impurity initially in the column to the impurity in the column at steady state. (See Albertins[39]).

To carry out design calculations, the operating conditions F, Y_F, L_E, C, L_P and Z_F are needed to constrain the problem for fixed-conveyor agitation conditions. The above design method is empirical, because the mass transfer factors H_E and H_S and the crystal phase composition ε must be determined from experimental data.

Design Equation

The separation in the enriching section ($^{Y}E/^{Y}\phi$) can be estimated for eutectic systems by developing an approximate design equation. By considering the various purification mechanisms operating in the column and introducing specific simplifying assumptions, as proposed by Wells et al[53], it is possible to produce an equation which relates product composition, ^{Y}E, product offtake ratio ^{R}E, feed composition ^{Y}F, and purification section length ^{L}P. For eutectic systems the following expression may be derived (see Appendix A1),

$$Y_E = \varepsilon + \left[\frac{1 - R_E}{\alpha - R_E + 1}\right] \alpha Y_F \cdot \exp. \left[\frac{-L_P (1 - R_E) C}{D \rho A \eta}\right] \quad (3.60)$$

where $D \rho A \eta$ represent the axial dispersion of impurity in the column.

CHAPTER 4

Experimental

4. Introduction

As we have seen, crystallisation techniques have some very real advantages to offer in the field of industrial processes. The design and operation of crystallisation apparatus is still largely empirical as many of the crystallisation phenomena are not fully understood. Crystallisation has become important as a method of purification and as a method of providing crystalline materials in the desired size range. Broadly, crystallisers may be classified according to whether they are batch or continuous in operation; the latter being further divided into linear and stirred types. Crystallisers can also be classified according to the method by which supersaturation is achieved. The main feature of the crystalliser used is the method by which the size of the product is regulated, this being a fundamental dependent of the nucleation process.

The crystalliser is operated such that the product produced falls within a desired size range; many crystallisers circulate the mother liquor removing the crystals in the classifier. The fines, as such, are returned to the process, for dissolution or to continue growing. Separations based on crystallisation rarely achieve product purities indicated by phase equilibria for a variety of reasons. High impurity levels result because mother liquor is often occluded in crystal imperfections and is entrapped in crystal agglomerates. The crystal is further contaminated by the large amount of mother liquor held in the crystal mass by surface tension and capillary forces. Impurities are also adsorbed on the crystal surface by chemisorption.

To obtain a product of desired purity by crystalliaation, the amount of impurity in the crystal and/or the adhering liquid must be reduced. In conventional processes of crystallisation, this reduction may require several pieces of equipment and repeated handling of the solid phase. The impurity in the crystal itself can only be removed by repeated melting and recrystallisation at successively higher temperatures. The amount of adhering liquid can be reduced by filt ration, centrifugation, washing or by a combination of these processes.

Column crystallisation, on the other hand, is a technique whereby the crystals are obtained at high levels of purity in a single piece of equipment. There have been several column configurations described in which this has been achieved. Common to all the processes is a purification section in which the solid phase and free liquid are contacted whilst experiencing a temperature gradient throughout the section. This differential countercurrent contacting of crystals and liquid is a relatively new method for separation and purification.

The various columns used by previous workers are presented in Table (4.1). The columns (1) and (2) used in the present investigations are significantly larger than those previously studied. This will enable the effects of scale up to be studied, especially the transportation of crystals at greater column dimensions.

Investigator		Outer Tube I.D.mm	Inner Tube O.D.mm	Height mm	Approx. Volume mls.	Remarks
Bolsaitis (41)		25	15	867	270	enriching & stripping section 434 mm long.
Moyers (52)		25	/	600	295	no internal tube, a scraper & piston only in the freezing section
Schildknecht (44,7) (proposed)	a.	16	8	150	20	ultrapurification
	b.	25	15	700	220	
	c.	40	16	520	550	semi-technical scale
	d.	100	/	2000	/	
Betts (34)	a.	25	12	500	190	column manufactured by
	b.	51	31	850	1100	Messrs. Newton Chambers
Powers and Albertins (39)		26	11	610	270	Total reflux \ steady
Gates (42)		26	13	545	220	Total reflux / state
Henry (43)		32	11	618	440	Continuous-Steady state
Cutts and Wells (151)		51	36	690	700	column manufactured by Messrs. Newton Chambers
Present study column 1.		50	/	930	1000	no internal screw tube support but a solid Archimedean screw conveyor
column 2.		100	/	1420	9000	

Table (4.1) Column configurations used in other studies.

(4.1) Materials : Chemicals

(i) Sodium Chloride - 56 lb bags, technical grade from I.C.I

(ii) Industrial Methylated Spirits - approximately 95% ethanol and 5% methanol for use in the column.

Absolute Ethanol for standard solutions.

(iii) Deuterium Oxide (98.8% pure) from A.E.R.E. Winfrith, Dorset.

(iv) Metal Salts, Analar Grade, B.D.H Poole, Dorset.

$NiCl_2\ 6H_2O$

$CrCl_3\ 6H_2O$

$CdCl_2\ 2.5H_2O$

$ZnCl_2$

$FeCl_3$

Analytical Equipment

(i) Pye E7566/4 conductivity bridge with 1 ml microcell type E7598/B, used for the measurement of the conductivity of Sodium Chloride solutions and the mixed metal salt solutions.

(ii) Pye 104, flame ionisation detector (F.I.D.) G.L.C.

Carrier gas : Nitrogen

Fuel : Hydrogen : Air

Column: PEG 400 M for the analysis of ethanol/water. 20% by wt. on Chromosorb W; 100-120 mesh as support. A sample injection 0.5 μL.

(iii) Calculating Digital Density Meter DMA 45, Anton Paar, Austria.

Thermostated with a Grant water bath to $\pm$ 0.5°C for measurement of density change in the water/deuterium oxide system. Sample requirement 0.7 ml.

(4.2) Previous development of the 100 mm diameter column

A 100 mm diameter column crystalliser, of similar configuration to the 50 mm diameter crystalliser, had been assembled. The column consisted of three flanged, stainless steel sections, bolted together giving a total length of 1500 mm. The Archimedean screw conveyor was constructed from nylon supported on a heavy central rod of mild steel. The screw pitch was 25 mm, with a flight thickness of 6 mm. The annular space between the tube wall and central screw boss was 12 mm. Tolerance on the tube wall: screw interface was 0.076 mm on the diameter at 0°C, at 20°C the screw could not rotate within the tubes. The effective working volume of the column was 3800 mls, some 67% being occupied by the screw. A schematic is presented in Fig. (4.1)

ANCILLARY EQUIPMENT

FIG. (4.1)

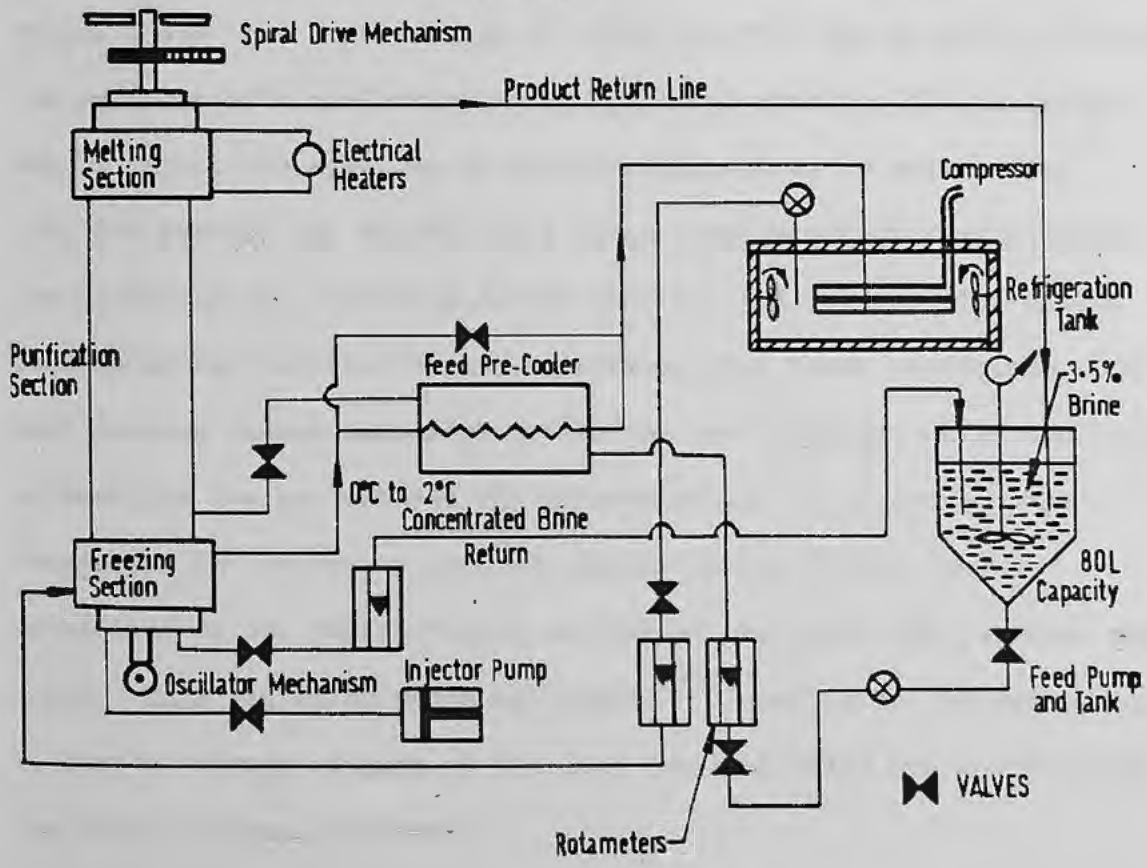

Fig. (4.1)

Column and ancillary equipment, October 1974

The operation of this column was described in detail by Hobson.[50] The initial runs with the freezing section mounted at the top of the column proved unsuccessful and the configuration was inverted. When operating the column continuously, great care had to be taken to control the screw speed. As the screw speed was increased, separations increased but at the expense of more frictional heat input. Because of the close tolerance of the rotating surfaces, localised heating of the liquid to above 20°C would cause the spiral to jam. Refrigerant circulation also required careful monitoring to prevent blockage due to excess freezing, and similarly the column was very sensitive to heat inputs at the top of the column.

Initial results at low flow rates were encouraging but the operation of the column became unstable and difficult to control as they increased. With aqueous solutions great difficulty with controlled ice nucleation within the freezing section was experienced. Hobson found that supercooling of -10°C to -14°C had no effect without the presence of a nucleating agent (phloroglucinol). His technique was to inject the agent as an aqueous suspension, in crushed ice, into the base of the column via a large bore peristaltic pump,which was supplying the ice/brine slurry feed for the column. The column cooling became critical during operation under these conditions, too much cooling caused excessive nucleation and blockage, while too little allowed the ice to melt and the phloroglucinol to disperse. The reason for the necessary step of nucleating the feed brine was attributed to the "mirror"-like surface of the screw and internal tube walls. This was later shown by Gladwin[153] not to be the cause, and in fact a "mirror" finish on the heat transfer walls was a prerequisite for steady column operation.

The solution to the problems proposed by Hobson[50] was the removal of the freezing section from the column and conversion to a Butane freezer based on a Draught Tube principal with self-induced agitation. The ice/brine slurry from the freezer would be fed by impellor into the base of the column and the ice crystals transported upwards by the screw's rotation. Wash water would be provided as a reflux fraction of the ice melted at the top and concentrated brine would be removed from the column base. The melting section could be supplied with heat from the condensation of the recompressed butane.

(4.3) Improvements and modifications to the 100 mm diameter column

Sections of the column requiring design modifications.

Screw conveyor

The design of the screw reduced the working volume of the column considerably. The central steel shaft made the assembly heavy and difficult to rotate and the energy expended in cooling it was unproductive. The number of flights was excessive, giving a high contact area for the column walls and conveyor. The screw must be able to rotate in a water filled column at room temperature, thereby reducing frictional contacts and preventing seizure of the conveyor. The final screw conveyor should be as light as practically possible to reduce the load on the motor.

Freezing section

This was formed from "Calorex-D-Tubing" wrapped around the stainless steel tube in a spiral, insulated on the outside.

Melting Section

A heating system was required that was easy to control and had a fast response.

Feed

It was considered impractical to use an ice/brine slurry. Also the use of nucleating agents was considered undesirable. The problems associated with the use of butane were too numerous to make the construction of a pilot scale column crystalliser feasible.

Modifications carried out

Screw

The Archimedean screw was constructed from nylon flight segments fixed around a 25 mm diameter polypropylene shaft. The flights were assembled so as to provide a continuous path for the transport of solid phase. All the flights were machined to ensure a constant radius on the screw and free rotation in the column. The

dimensions of the screw are given in Fig. (4.2).

Purification section

The stainless steel column was replaced with a thick-walled perspex column of the same dimensions. This was to allow the build-up of the crystal bed to be observed. The stainless steel freezing section and melting section were bolted on to screwed rods set in the perspex flange. The dimensions of the section are given in Fig. (4.3).

Melting section

Several types of heating devices were used, depending upon the configuration of the column. When the melting section was mounted at the top of the column, the following system was used. A polythene crystal trap was mounted on the top of the steel flange into which was placed a copper coil hot water heater, centrally around the central axis. When the melting section was mounted at the base of the column, it was provided with two means of melting the crystals. Around the outer wall of the section a waterproof hot foil heating tape was secured while a copper coil hot water heater was mounted in the base plate of the column. The coil was sealed to the base plate and extended up the column to the end of the last screw flight. The dimensions are given in Fig. (4.4).

Freezing section

A nylon jacket was fabricated to fit over the stainless steel tubing. The cooling jacket was lagged with polystyrene foam. The feed inlet was located 5 mm below the jacket. The internal surface of the freezing section was honed to within $\pm$ 5 thou. of parallel and polished to a mirror finish. Periodically the column was repolished. The dimensions are given in Fig. (4.5).

A COMPARISON OF THE TRANSPORTATION SCREWS

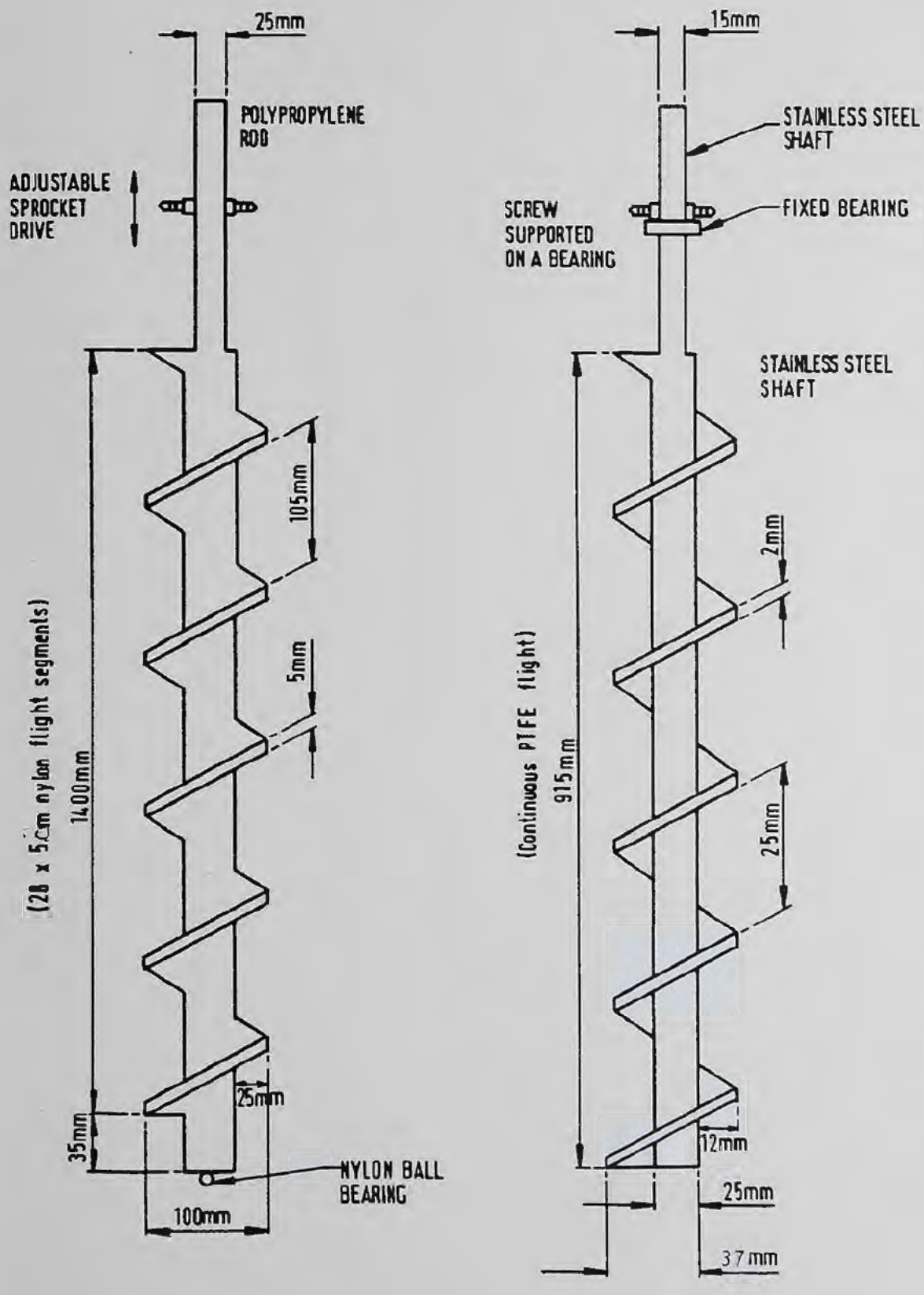

100mm NYLON CONVEYOR

50mm PTFE CONVEYOR

FIG. (4.2)

DESIGN OF PERSPEX PURIFICATION SECTIONS

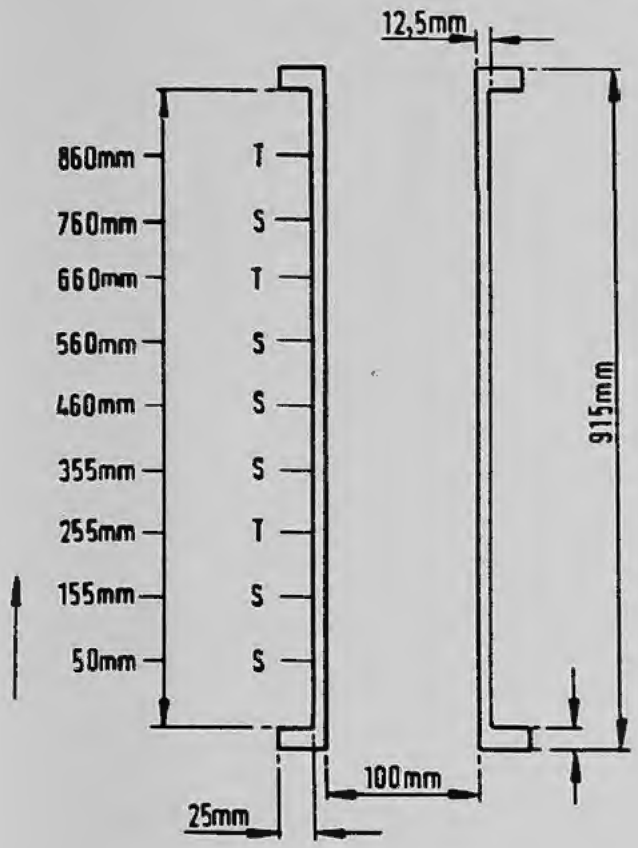

FLANGES : 12 bolt fixing (S/S)

TUBE WALL THICKNESS: 12,5mm

SAMPLE TUBES: 6mm O.D.
3mm I.D.
(Stainless steel)

S : Sample point

T : Thermocouple probe

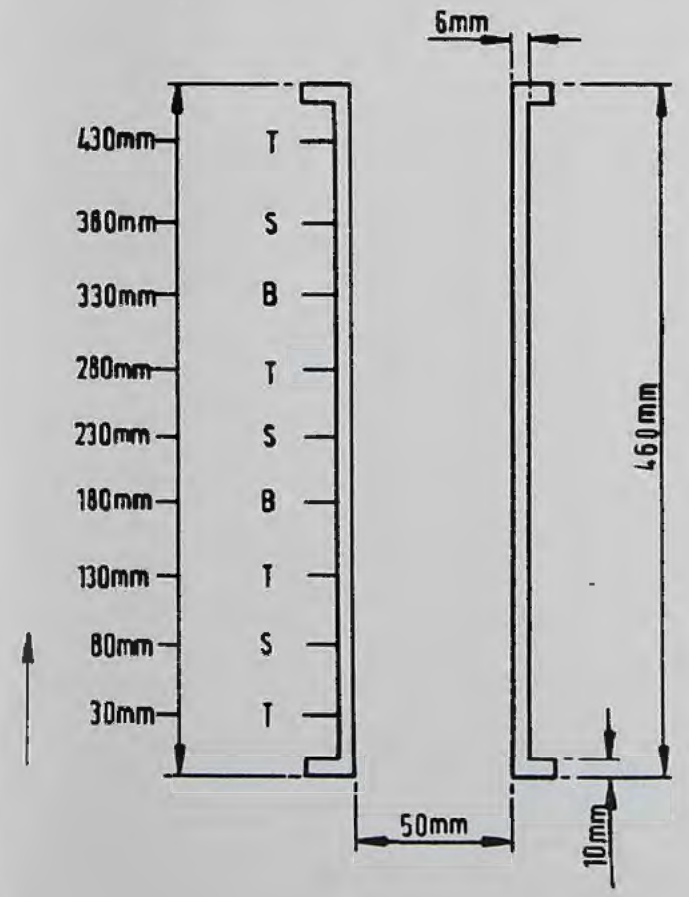

FLANGES : 4 bolt fixing (S/S)

TUBE WALL THICKNESS : 6mm

SAMPLE TUBES: 6mm O.D.
3mm I.D.
(Stainless Steel)

S: Sample Point.

T: Thermocouple probe.

B: Blanked off.

FIG. (4,3)

DESIGN OF THE COLUMN MELTING SECTIONS

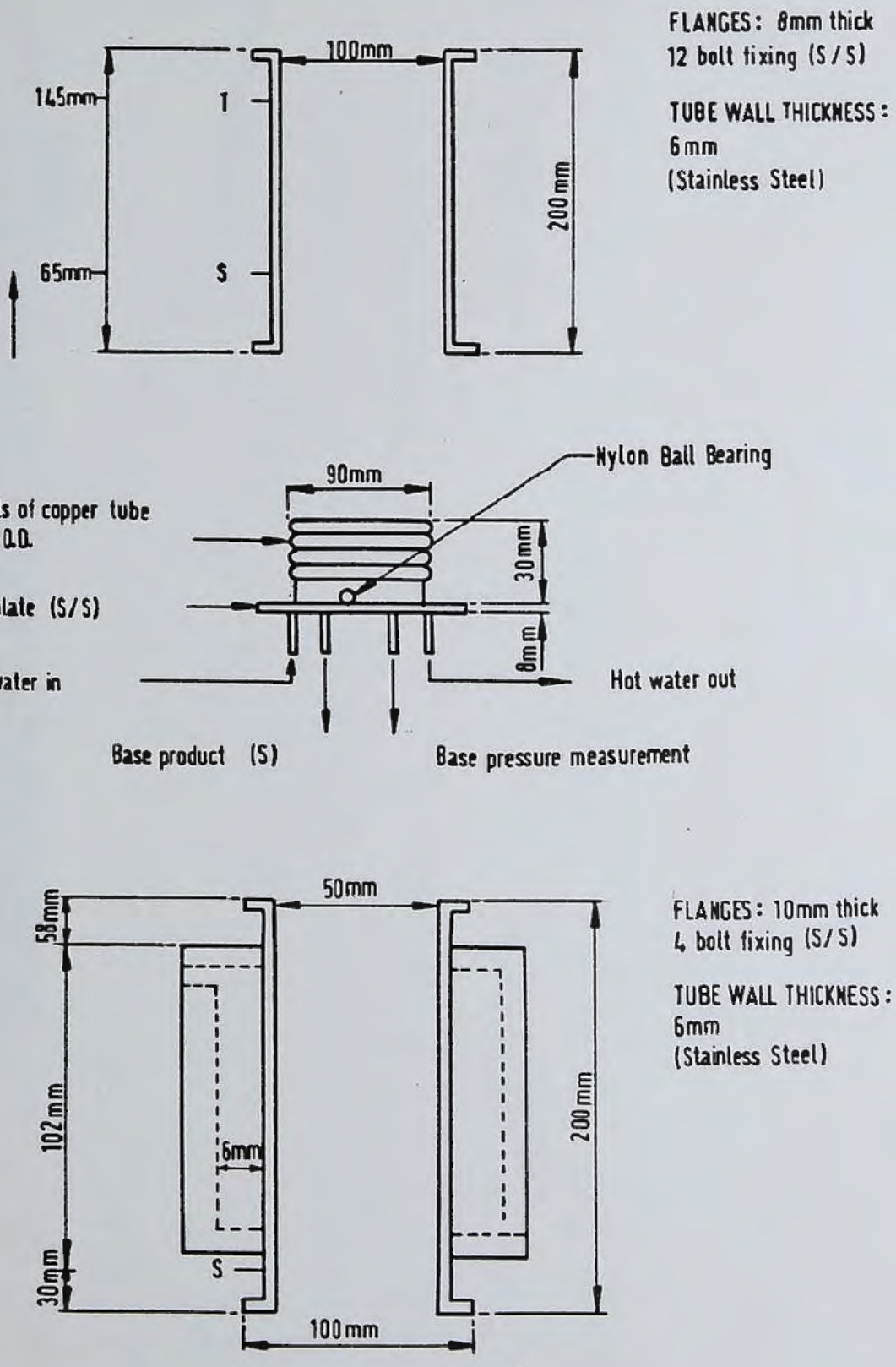

FIG. (4·4)

DESIGN OF THE FREEZING SECTIONS

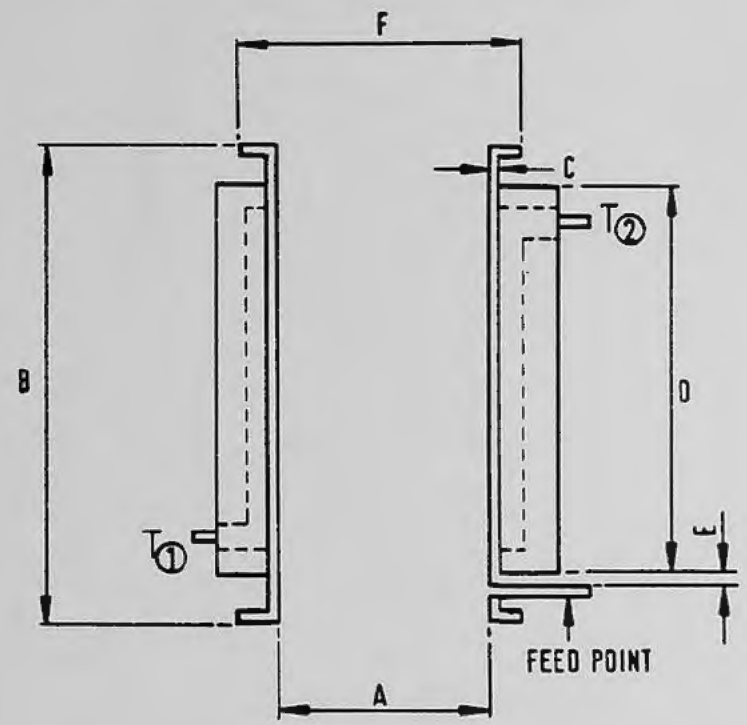

T: Thermocouple points

$T_{①}$: Coolant IN $T_{②}$: Coolant OUT

Dimensions (mm)	(A)	100	50
	(B)	305	330
	(C)	2,0	1,6
	(D)	240	240
	(E)	5	5
	(F)	160	100

Volume of freezing section 625 mls 250mls

FIG. (4·5)

Miscellaneous improvements

The original column was cooled by a mixture of 50/50 (by weight) anti-freeze/water solution contained in a 90 litre tank. The $\frac{1}{2}$ H.P. refrigeration unit reduced the temperature to -15°C. This unit was used to cool the stirred feed tank. A larger refrigeration system was used for cooling the freezing section. The coolant was calcium chloride (S.G. 1.28) contained in a 350 litre, insulated tank, cooled to -35°C and stirred by recirculation from the main refrigerant pump.

The feed was contained in an 80 litre, stirred, jacketed vessel, where the temperature could be controlled by regulation of cooling flow. The refrigerant was circulated using a glandless, magnetically driven centrifugal pump, the flow being indicated on a rotameter. For continuous operation the feed and base product were pumped using Watson-Marlow (MHRE 100) metering peristaltic pumps. These were resistant to corrosion and effectively controlled the flow-rates of the two streams.

The screw conveyor was driven by a 3 phase $\frac{1}{3}$ H.P. Kopp variator motor. This motor worked at constant torque and voltage providing constant driving power at low rotational speeds. Transmission of power was via gear cogs and chain drive, allowing for variation in speed of rotation from 40 to 150 r.p.m. The temperature gradient in the column was measured using J-type iron/constantan thermocouples sealed in stainless steel. The output from these thermocouples was displayed on a Honeywell 12 point recorder.

A schematic of the modified equipment, assembled for continuous operation is presented in Fig. (4.6).

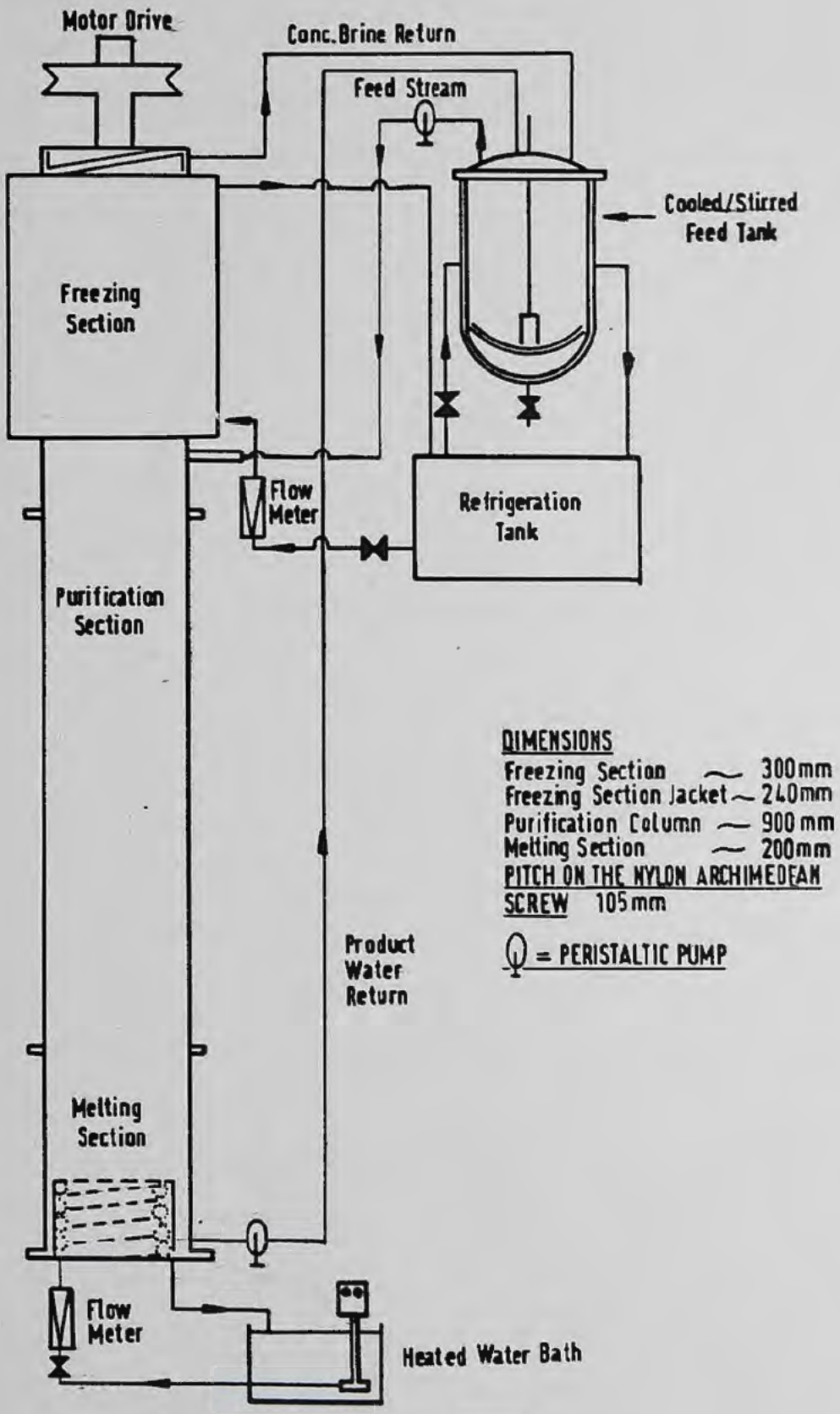

100mm diameter column and associated equipment

FIG. (4.6)

(4.4) Column Operation ; Total Reflux and Continuous

The column was assembled with thefreezing section at the base and the melting section at the top, the crystals being transported upwards. The general procedure adopted for start up in both Total Reflux and Continuous work was as follows:

The operation of the system was begun by precooling the feed. This was accomplished by pumping refrigerant from the smaller unit around the jacket of the feed tank. The feed was continuously stirred to prevent any localized under cooling and ice nucleation. On average the precooling of 80 litres of feed required $1\frac{1}{2}$ hours to bring the temperature almost to the freezing point. In the initial work a feed solution of 3.5% wt/wt Sodium Cloride in water was used giving a freezing point of - 1.98°C.

The feed was then pumped via the peristaltic pump to the column. Once the column was filled with feed the screw drive system was switched on and the screw speed adjusted to the required value and checked with a stop-watch. For a continuous run the feed rate and "base" product (pure stream) were checked and calibrated. Once these were fixed the temperature recorder was switched on and the refrigerant in the large refrigerant tank cooled to give a temperature of - 30 to - 35°C.

The pump to circulate refrigerant from the large tank to the column was switched on and the flow was controlled using a rotameter, while some of the refrigerant was recycled directly back to the tank. The temperatures were carefully monitored and recorded every $\frac{1}{4}$ hour throughout the experiment. The location of the various sample and temperature points is indicated in Figs (4.3) - (4.5). The time for build-up of a crystal bed was $1\frac{1}{2}$ - 2 hours depending upon the crystal production rate. Once the column was filled with crystals, liquid samples were taken along the length of the column. A 5 ml syringe

was used to take the samples, which were stored in sealed sample bottles until they reached room temperature (usually about 20 minutes). The salt concentration (NaCl) in the water was determined using a conductivity bridge. Hourly samples were taken for at least three hours after the column had initially filled with crystals. In the continuous work it took about three hours, after crystals initially filled the column, to reach steady state, whereas it took about two hours in the total reflux runs. Steady state conditions were indicated by a straight line plot on semi-log paper for the log of concentration versus position in the column.

The other parameters measured throughout the experiment were the purified (base) product and the concentrated (top) product rates. These two streams were recombined in the feed tank where the concentration was monitored for any fluctuations. The build-up of crystals into a packed bed was indicated by an increase in the current drawn by the motor. Under normal operation of a water filled column a current of 0.5 amps was drawn. Any increase in this value indicated a build-up of crystals or that a blockage had occurred in the freezing section. When the freezing section was at the top and crystals were transported downwards, it was possible to observe the build-up of crystals by an increase in pressure measured at the base. For steady column operation it required the balancing of heat input into the melting section to give a steady pressure of 4 to 5 pounds per square inch. The pressure gauge also indicated a blockage in the freezing section since the reduced flow of top product was reflected by an increase in base pressure.

The systems studied in the column were aqueous and did not require any special handling techniques. Where necessary individual sampling techniques were modified to suit the different systems/ analytical method.

(4.5.a.i) Operational Conditions : Desalination

The initial column evaluation was conducted using the sodium chloride/water system. A feed solution of 3.5% wt/wt sodium chloride in tap water was adopted, this enabling a comparison of the separations obtained on the column with other processes used for conventional desalination. The parameters varied are listed below and divided into:

(i) Column effects:

(a) Geometry of the Archimedean screw, annular space, angle of flights and length.

(b) Direction of crystal transport, ascending or descending the column.

(c) Position of feed into the column.

(ii) Operational effects:

(a) Screw speed variations.

(b) Size and shape of crystals.

(c) Crystal production rate, undercooling and flow of refrigerant.

(d) Heat input to melt crystals.

(e) Feed rate.

(f) Feed temperature.

(g) Product removal rate.

(h) Impurity fraction of the feed.

The first runs performed were batch or Total Reflux in nature. These initial runs were investigatory in nature to evaluate the column performance and reliability of the ancillary equipment. The column was operated with the freezing section at the base, transporting the crystals up the column. It soon became obvious that the crystals reaching the top of the column could not be melted at a steady rate and crystal mass was transporting out of the column.

The trap was added to contain the crystal mass and the crystals emerging from the top of the column were contacted by a heated copper coil. Refrigerant was circulated around the freezing section, varying the temperature from -17°C to -20°C. The screw speed was varied from 54 r.p.m. to 74 r.p.m. In all cases, the build up of a crystalbed was found to be difficult and the purification obtained was confined to the top 200 mm of the column.

In order to improve performance a feed precooler was used, plus ice in the brine slurry. This improved the rate of formation of crystals and a concentration gradient was established. Unfortunately a significant reduction in impurity was only observed in the top 200 mm of the column. A typical concentration gradient being:

Top	- 12,000 p.p.m.
Initial Feed charge	- 33,000 p.p.m.
Base	- 58,000 p.p.m.

Difficulty was experienced with the precooler in the initial filling of the column. Due to the low feed:refrigerant rate, frequent blockages occurred. The copper coil heater was proving difficult to regulate. An excess of melted crystals would descend the column destroying the concentration gradient that had been established, a typical concentration profile is shown in FIG. (5.1.a). To improve crystal production rate, the refrigerant temperature was further decreased. This produced an initial increase in the crystal mass which soon decreased as the freezing section rapidly blocked. Increasing the screw speed from 54 r.p.m. to 74 r.p.m. while progressively reducing the cooling temperature to below -20°C did not solve the problem. The increased screw speed caused crystals to be transported up the column at a rate which exceeded the capacity of the melting section.

At this point several modifications were made to the apparatus to enable it to operate under more controlled conditions.

(1) A smaller cog drive was attached to the motor reducing the minimum screw speed to 42 r.p.m.

(2) A new copper coil was fabricated and mounted above a polypropylene disc fixed to the central screw shaft. The disc was designed to hold the crystals back in the column and force them outwards over the copper coils. This allowed for a reduced heat input to the coils and hence more controlled melting. Both designs are shown in FIG. (4.7)

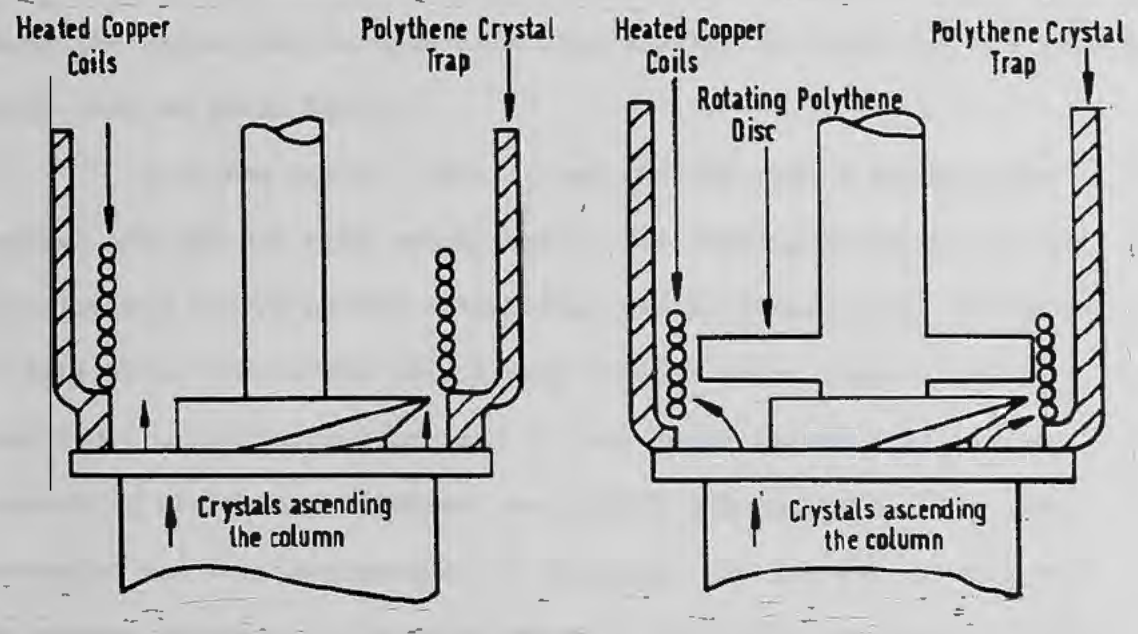

FIG. (4.7) Melting section details

The previous experiments were repeated and the column was found to be more responsive to control and it was possible to build up a crystal bed and achieve separation down the column. A typical concentration profile is shown in FIG. (5.1.b). The column was now reliable to operate and it was decided to convert the system for continuous operation, that is, a removal of product from the top, a concentrated stream at the base with the crystals transported upwards.

Continuous Operation

The column was assembled as for the previous runs, feed entered the column just above the freezing section and was metered via the peristaltic pump. A similar pump was also used to remove the concentrated stream from the base, the product stream being the overflow from the column. Five runs were carried out, varying the screw speed from 42 to 50 r.p.m. Base product removal and crystal production rate were also varied, the results are summarised in TABLE (5.2), and a typical concentration profile is given in FIG. (5.1.c). Once again, purification was limited, the separation being towards the top of the column as before. In all cases the concentration gradients were similar to those for the initial trial runs at Total Reflux.

From the initial runs it was obvious that a homogeneous crystal bed had not been established. The washing of impurity from the crystals ascending the column was totally inadequate. The means of generating the reflux liquid with the hot water copper coil required constant attention when in use, since excess "hot" water descending the column rendered the crystal bed unstable. The feed precooler was very susceptable to blockage. At the end of each run the volume of free liquid draining from the column averaged 4 litres indicating that the crystals were present in a "mush" rather than a packed bed.

In view of the number of problems encountered with transporting the crystals up the column, whilst having the freezing section at the base, it was decided to reverse the column configuration.

Modifications to the experimental equipment

The column was assembled with the freezing section at the top and the melting section at the base. The latter section was equipped with two means of melting crystals, a hot foil tape and a

small copper coil. A pressure gauge was also added to register a build up of crystals. The feed entered the column 5 mm below the freezing jacket, the pure product being removed from the base and the concentrated stream leaving as overflow. The feed precooler was also removed, the feed temperature being regulated in the jacketed feed tank.

The same operating conditions as previously used were employed. From a consideration of the densities of the system (Ice = 0.92 g/ml and 3.5% by wt NaCl solution = 1.025 g/ml) ice crystals would be expected to rise. This was observed, as they rose they were compacted together and transported down the column by the screw. In this way a uniform continuous crystal phase was seen to descend the column. However after several hours of operation a blockage of the freezing section occurred, evidenced by the lack of crystal transport and an increase in the waste stream. Increasing the feed rate to the column did not prevent blockage. In order to increase the agitation in the freezing section a liquid pulse was introduced, but failed to improve the situation. Several more runs were carried out at progressively increasing screw speeds, but the problem persisted.

Upon dismantling the freezing section after such a blockage, it was found to contain a large plug of ice, equal in length to the freezing section (see Plate 4.2).

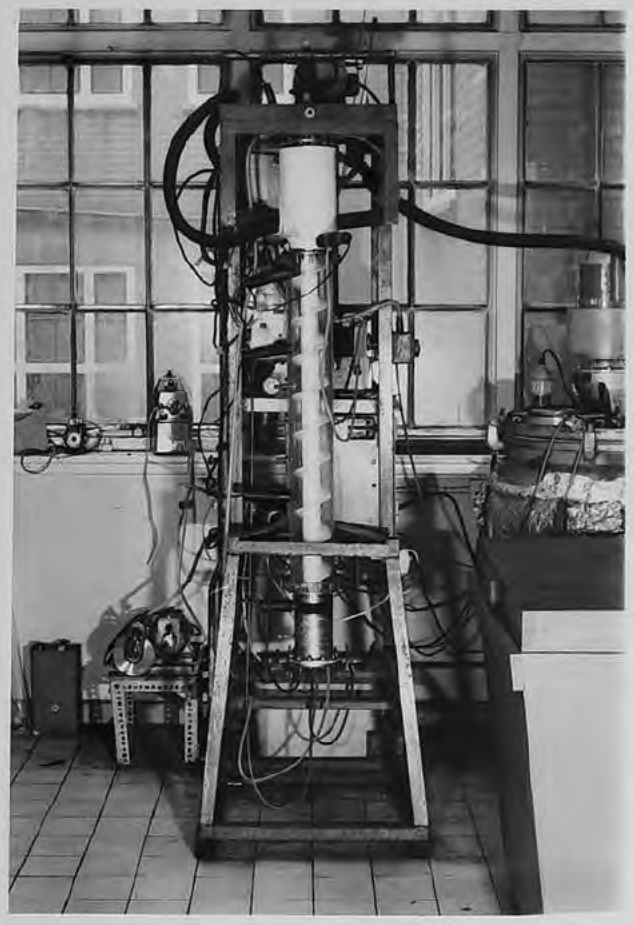

PLATE (4.1)

General view of the 100 mm column crystalliser, assembled in configuration (B)

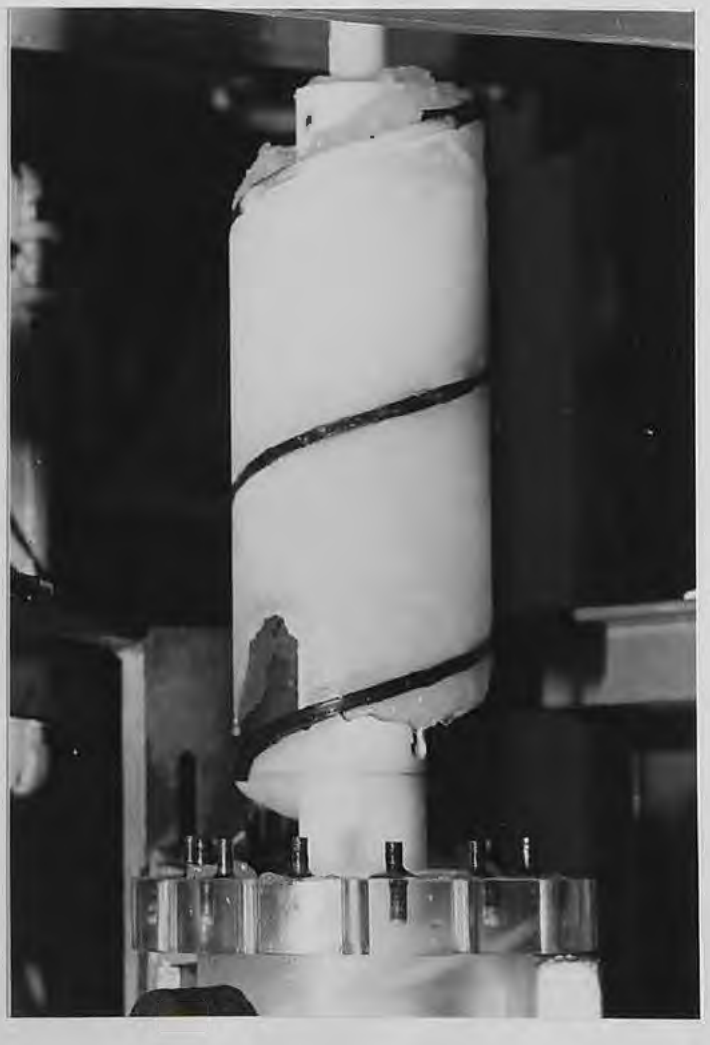

PLATE (4.2)

Termination of an experimental run due to blockage of the freezing section

The outer edge was firm and glass-like, while the inner mass was a compacted "mush". The central portion of the ice plug was hollow allowing the passage of feed solution but no further crystal production. An examination of the inner surface of the freezing section showed that the surface had been abraded by intermittent contact with the nylon flights. The surface was buffed with a 100 mm high speed mop impregnated with a stainless steel abrasive,and finally finished with a very mild abrasive and soft polish. Upon reassembly the column performed well and did not block and the system was operated, varying the parameters which are listed below.

(a) The effects of screw speed on the enriched product purity, over the range of 50 to 100 r.p.m. were investigated.

(b) By choosing a suitable screw speed the variation in the concentration of sodium chloride in the free liquid for increasing feed rate was determined.

(c) These two sets of experiments had been carried out at constant crystal production rate, hence the variation in the impurity content of the enriched product with increasing crystal production was assessed.

(d) The effects of the variation of the various product streams was also considered, that is, the ratio of product to feed and product to crystal production rate (Reflux Ratio) on the enriched product purity.

Note

The experiments carried out in (a) were performed at a high and low crystal production rate for each screw speed. The effects of increasing the crystal production rate were not possible beyond 0.6 g/sec in the present column. At low crystal rates the pressure generated at the base was 3-4 p.s.i., upon increasing to the above production

rate, this increased to 10-12 p.s.i. An increase in current drawn (from 0.5 Amps to 1.0 Amps) also occurred. At these very high crystal rates there was a tendency for the Archimedean screw to be driven out of the column or for the driven pin on the screw drive to shear. To prevent this required careful control of the melting section. However, the best separations were achieved under these conditions.

From the work on the 50 mm column, the best feed position had been as near to the freezing section as possible. In the present experiments this was kept fixed 5 mm below the freezing jacket. Alse mechanical oscillation of the transport screw was not employed, as this had been found to increase the transport of impurity down the 50 mm column.

Analytical Procedure

The column was always sampled in the order of increasing impurity, that is, from the pure product to the impure concentrated stream. A minimum of 2 mls of sample were removed, twice, from each sample point, the first sample being discarded. Samples were allowed to equilibrate with room temperature before a measurement of conductivity was made. The unknown concentrations were then determined by comparison with a prepared calibration curve of known sodium chloride solutions in water. After each sample reading the 1 ml micro cell was flushed twice with distilled water and dried with a tissue.

(4.5) (a) (ii) Screw conveyor: further modification

At the termination of the initial desalination experiments, it was decided to investigate the possibilities of modifying the screw so as to simplify the operation of the column. The nylon Archimedean screw was replaced with a much shorter mild steel screw with more efficient 'scrapers' and facility for the removal of ice samples for microscopic study. Figure (4.8) shows the design of the new screw.

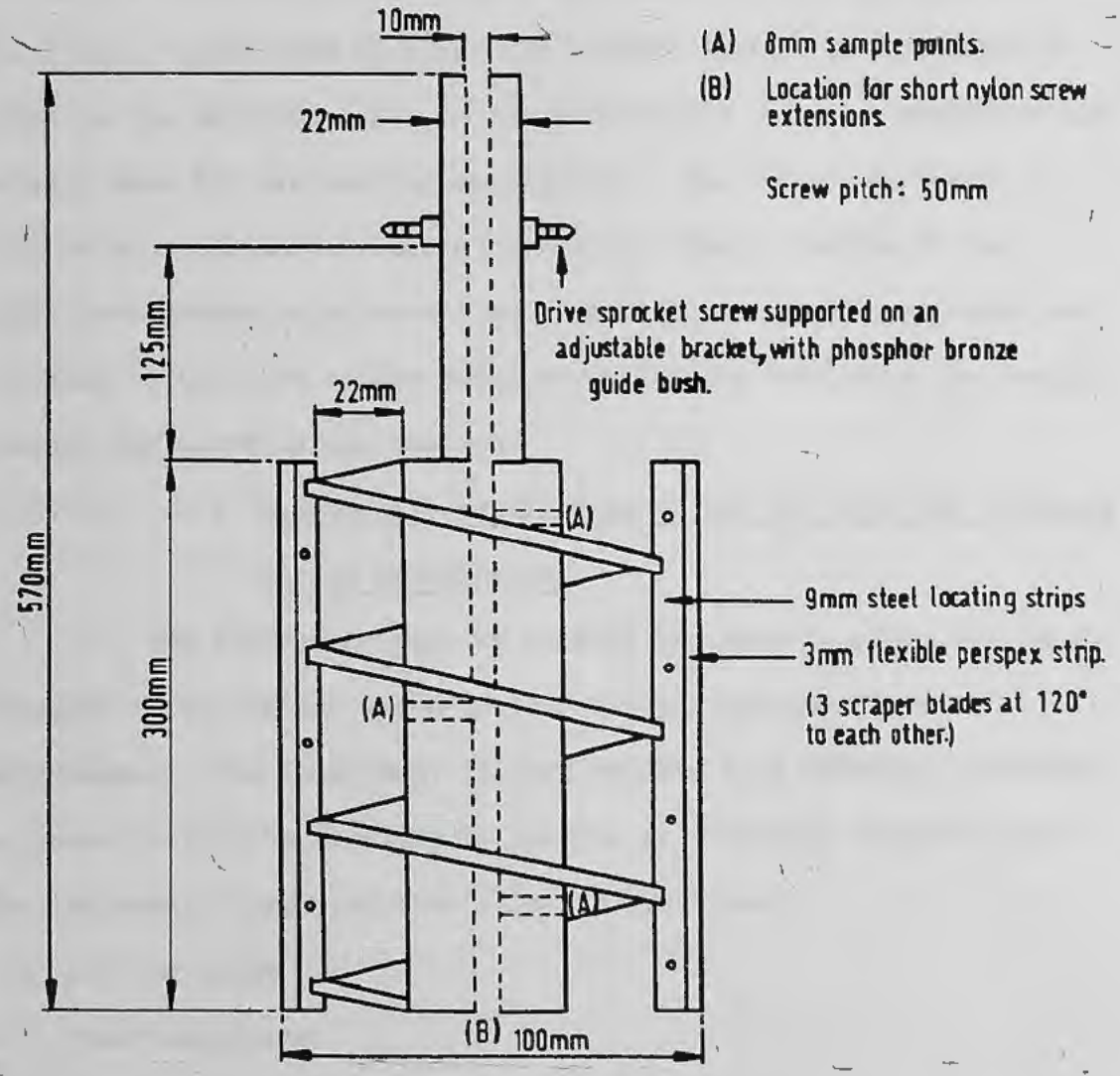

Fig. (4.8) Design of scraped surface metal screw

The screw was fabricated around a steel shaft to which a spiral of mild steel was welded. Three strips of perspex 12.5 mm wide, 2 mm thick and 270 mm long were fitted vertically and equidistant from each other on the outer side of the spiral. These are fixed within a steel bracket which gives them rigidity to perform the function of ice scrapers, removing ice from the inner heat transfer surface of the freezing section.

A hole was drilled through the steel shaft from top to bottom and connecting holes (four) were drilled from the side to allow the crystal mush to enter the central shaft. By inserting a probe to the required depth it was possible to remove a sample of the crystal mush for microscopic examination. The screw was coated with an epoxy primer to reduce corrosion. Short lengths of the nylon Archimedean screw were also assembled such that they could be attached to the base of the metal screw thereby extending its length through the purification section.

(4.5) (a) (iii) Microscopic examination of the ice crystals produced during desalination

The instrument used to measure the crystal sizes and shapes produced in the column was a Leitz,cooling stage,polarising microscope.. The instrument is very similar to a standard laboratory microscope with the facility to operate at different temperatures. The instrument comprises the following functions:

(1) Cooling stage

(2) Polarising lens

(3) An attached photo tube for photomicrography

(4) Compensators

(5) Rotating stage

The cooling stage corresponds in size and shape with the circular revolving stage of the Leitz polarising microscope. The

cooling stage contains a built-in electric heater with automatic thermo-regulator, a cooling coil, a built-in thermometer and various inlet and outlet connections to the cooling unit (a Kryomat 1700). The cooling stage was also fitted to take a calibrating thermometer, a guard tube and nitrogen chamber to prevent any condensation at lower temperatures. The calibrating thermometer gives the exact temperature of the object mounted on the microscope.

The Kryomat 1700 was used to circulate methanol, which could be cooled to -30°C, in a well-insulated temperature controlled bath, by means of an air-cooled compressor. A circulating pump supplied the coolant through the insulated connecting tubes to the stage to cool the object on the stage. Regulating the flow of coolant adjusted the operating temperature of the cold stage.

General Procedure

(1) Samples withdrawn from the column were stored in a well insulated container, cooled to the freezing point of the crystals.

(2) The microscope and Kryomat 1700 were switched on about 10 minutes before taking measurements.

(3) The temperature of the cooling stage was set.

(4) When the temperature was reached, crystals were transferred on to the glass slide already mounted on the stage. A pre-cooled transfer pipette was used.

(5) The nitrogen chamber and guard tube were then placed over the sample to exclude external interference.

(6) The microscope was adjusted to get the best view and photographs of the ice crystals taken.

(7) In order that the actual size of the ice crystals could be measured from the photomicrographs, an object of known size was placed on the microscope stage, and using the same magnification, photographs of the object were taken.

(8) Comparison of the object size with the size obtained from photomicrography measurement enables a factor difference to be calculated and hence, the magnification contributed by the camera.

(9) This factor gives the overall magnification of the ice crystals viewed through the camera, and for that specific objective used. Hence, the size of the ice crystals can be determined.

Note: Objectives of 4 x MF and 10 x MF were used in this work.

To ensure that the cooling stage temperature did not cause an increase or decrease in crystal size whilst they were viewed through the microscope eyepiece, photomicrographs of the ice crystals were taken at different intervals of time. The ice crystal sizes determined were then compared for any increase or decrease in size. Also, a set time for viewing crystals was used, once this period had expired, fresh crystals were used to replace the old ones.

(4.5) (b) Operational Conditions : Ethanol concentration

In order to obtain further data on the effects of scale up from a 50 mm diameter column to a 100 mm diameter column a second system was processed on the large unit. Once again it was an aqueous, binary eutectic system of ethanol in water. The initial concentration of industrial methylated spirits (I.M.S.) was undertaken on the 50 mm diameter column, using a feed of 10% by wt I.M.S. in water. This was used as feed for the present studies. Due to the low specific gravity ethanol (0.789 g/ml) and the lower freezing point, the ethanol remains liquid at the top of the column, the ice crystals being displaced down the column by the screw. Thus the tendency for the crystals to migrate to the top of the freezing section should be less in the ethanol water system than the desalination system.

However from the previous work, the column configuration was chosen such that the freezing section was at the top of the column, the crystals being transported down, through the purification section into the melting section. With this system the column was being operated in a reverse manner. Normally the top, concentrated stream would be the impure product, by virtue of its lower freezing point, and would be considered waste. In this case the concentrated stream is an upgraded product of ethanol in water.

The column was operated as before except this time the feed tank was cooled to -4.5°C, just above the freezing point of the feed. The crystals produced in the freezing section were of a "mush" form and were easily transportable. The following variables were investigated.

(a) Effect of screw speed at a (i) High Feed:High Product removal rate
(ii) Low Feed :Low Product removal rate
for speeds from 34 - 104 r.p.m.

(b) Effect of feed position.

(c) Effect of top product removal rate

(d) Crystal production rate

(e) Effect of liquid pulses on the ethanol concentration down the column.

Analytical Procedure

Samples from the column were collected as before and sealed in sample bottles using airtight suba seals. 0.5μL samples were then injected on to the G.L.C. and the unknown concentrations determined by comparison of peak heights with those for standard solutions. G.L.C. conditions used were:

Column oven temperature	80°C
Detector oven temperature	100°C
Nitrogen flow rate	40 ml/min

Hydrogen flow rate	45 ml/min
Air flow rate	600 ml/min
Amplifier attenuation	5×10^4

Column 1530 mm by 4 mm diameter

(4.5) (c) Operational Conditions : Waste effluent recovery

It is possible to consider using column crystallisation for several reasons . It is undesirable to discharge quantities of effluent to waste causing pollution,and there is an expensive loss of chemicals that could be recovered and recycled. The development of such a system for the recovery/removal of mixed metal ions was carried out on the 50 mm diameter column crystalliser. An initial attempt had been made to recover copper as copper sulphate from an aqueous feed on this column. This had been partially successful and showed that copper sulphate solution could be concentrated from 3% by wt salt in water up to 9%. Above this concentration problems were encountered with the nucleation of ice, that is, hard needle-like crystals were formed in preference to a "mush" and column blockage occurred.

The feed solution prepared was based upon that for a typical metal finishing plant effluent stream. This simulated effluent stream had been previously used by Campbell and Emmermann[12] in their development ofan S.R.F. process for the recycling of water from metal finishing wastes. An analysis of the feed solution is presented below:

Ni^{2+}	=	100 mg/L	
Cr^{3+}	=	104 mg/L	
Cd^{2+}	=	113 mg/L	All salts weighed as chlorides
Zn^{2+}	=	100 mg/L	
Fe^{3+}	=	112 mg/L	

The metal salts were dissolved in an aqueous solution of 30,000 mg/L Sodium Chloride in water. The feed solution was a straw-coloured liquid.

The 50 mm diameter column was assembled as per the 100 mm diameter column and all the runs were continuous. A pure "water" product was removed from the base and a concentrated salt stream from the column overflow. The parameters investigated were :

(a) Effect of screw speed on product purity, from 52 - 120 r.p.m.

(b) Effect of feed position on product purity.

(c) Effect of enriched product removal rate on the impurity content of the enriched stream.

(d) Effect of crystal production rate on product purity.

Analytical procedure

Conductivity measurements were used to obtain the concentration profile down the column. The unknown concentration was determined from a prepared calibration curve. The calibration curve was prepared as follows: six standard solutions were prepared from analar metal salts, in which the ratios of the metal ions were the same as they were in the feed solution, for example, the Ni^{2+} concentration varied from:

Std. (1)	Std. (2)	Std. (3)	Std. (4)	Std. (5)	Std. (6)
27 mg/L	50 mg/L	74 mg/L	100 mg/L	126 mg/L	151 mg/L

while the ratio of Ni^{2+}: Cr^{3+}: Cd^{2+}: Zn^{2+}: Fe^{3+} remained constant.

A plot of conductivity versus concentration was a straight line passing through the origin. The concentrations of the individual metal ions in the feed and product were also determined using Atomic Absorption Spectrophotometry. This allowed an accurate estimation of the level of removal of the various metals to be made.

(4.5) (d) Operational Conditions: Heavy water regeneration/upgrading

The application of column crystallisation to this system is for the recovery and upgrading of heavy water for reuse. When heavy water has been used in the moderator circuit of a reactor its concentration gradually falls, due to ingress of water and other contaminants into the system. Normally a reactor plant has to treat an impure, contaminated, heavy water recycle stream of 80% D_2O and upgrade it to 99.9% D_2O before it can be reused in the main system. Initial work on the 50 mm diameter column suggested that it was possible to separate water and heavy water. The experimental work on concentration of deuterium oxide was hindered by two major problems. The first of these was developing an analytical technique that would respond to the changes in ratio of water to heavy water. The other problem concerned the actual crystal form the heavy ice took. Pure water and heavy water nucleate and grow as needle-like crystals and as such were not transportable.

This last problem was solved by using a 3% ethanol solution as a habit modifier. This allowed the formation of the characteristic crystal mush and it was possible to transport the ice/heavy ice mixture. However using a habit modifier gave rise to problems with the analysis (for ethanol is 0.7893 g/ml). The original method of measuring the density by weighing was determined to have an accuracy of 1 - 2%, however the method was long and tedious to perform. To overcome this and improve reproducability and accuracy, an automatic digital density meter was used for the exact measurement of density changes down the column. The following shows the densities of the pure components as measured on the Anton Parr DMA 45:

	Density g/ml 30°C
Pure D_2O	1.1039 1.1041 (two separate samples)
Pure C_2H_5OH	0.7810
Pure H_2O	0.9957

The freezing point for a mixture 80% D_2O, 17.5% H_2O, 2.5% C_2H_5OH was + 2.5°C. The freezing point for pure D_2O + 4.0°C. The density of the above mixture is 1.0740 g/ml which indicates that it is possible to detect the changes in density as the ratio of water : heavy water varies.

The 50 mm diameter column was assembled as previously with the freezing section at the top and the crystals transported downwards through the purification section into the melting section. The column was operated with continuous feed, product removal from the base and a "concentrated" overflow from the top. The various parameters investigated were the effects of:

(a) Screw speed

(b) Moving the feed point down the column

(c) Increasing the reflux ratio

(d) Increasing the crystal production rate

Analytical procedure

In a simple, two component eutectic system, it is easy to measure the increase of one component relative to the other, for as one increases the other decreases and vice versa. In the present system changes in the compositions relative to each other are measured using G.L.C. (for the ethanol) and density determinations. Thus the changes in density can arise from the change in the ratio of ethanol to water and not from an increase in heavy water concentration. That is, as the density increases down the column, the ethanol concentration decreases, the problem arises in deciding if the increase in density is due solely to the replacement of ethanol by water. To verify this, sample feedstock solutions were prepared varying the concentration of ethanol in each and then the density measured. A graph of percentage ethanol versus density is plotted, and the straight line extrapolated to zero ethanol concentration, which corresponds to a H_2O : D_2O system.

In each case the weight fraction of D_2O was kept as constant as possible.

In an experimental run using this feedstock, a density gradient is established down the column simply by removing the ethanol, and we can predict the final density of the expected H_2O : D_2O mixture. Since the freezing point of the stock solution is above 0°C, pure water cannot freeze out. The heavy water component when pure freezes at +4°C, and will freeze out at the column operating temperature. In the experimental runs, the densities measured were greater than those predicted from the graph, indicating that the increase was due to the enrichment of the D_2O fraction by crystallisation, above 0°C.

Ethanol impurity : determined by G.L.C. using the same conditions as the ethanol concentration work.

Density Measurement

The sample is introduced into a U-shaped sample tube which is rigidly supported at its open ends. The sample tube is electromagnetically excited to vibrate at its natural frequency. From the frequency change caused by a specific sample inside the sample tube, the density of the sample is calculated. Since the mass of the sample participating in the vibration is established in this way, there is no need for measuring either weight or volume. Viscosity or surface tension of the sample do not affect the result.

For the instrument calibrated with air and distilled water, and thermostated to ±0.5°C, it has the following precision and range:

$\pm$ 1 x 10^{-4} g/ml in the range 0 to 1.5 g/ml

$\pm$ 5 x 10^{-4} g/ml in the range 0 to 3.0 g/ml

Temperature range of sample -10 to +60°C

Sample size, minimum 0.7 ml.

The sample is normally injected into the sample tube with a hypodermic syringe. The sample tube has to be completely filled,

without any entrapped gas or solids. At the completion of a reading, the sample is sucked out out of the sample tube which is washed with a suitable solvent and dried with the built-in air compressor.

Chapter 5 Results and Observations

(5.1) Desalination: effect on separation of column variables.

The variables investigated were:

(a) Screw Speed

(b) L_E = product flow rate

(c) C = solids flow rate in the enriching section

(d) L_E/C = fraction of melted solid removed from column

(e) L_E/F = pure product/feed rate

(f) F = feed rate

Variables held constant

(a) Y_F = feed composition (3.5% by wt. NaCl impurity)

(b) Z_F = feed position

(c) Freezing section, purification section, melting section lengths

Mathematical Treatment of Results

The mathematical analysis, described by Powers,[43] for predicting the performance of column crystallisers operating under Total Reflux and Continuous operation, was applied to desalination in the pilot plant continuous column crystalliser. The two parameters controlling the separation in the column are the axial diffusion of impurity and the mass transfer between the adhering liquid and the free liquid.

The concentration profiles for the enriching section were measured and are described by Powers' solution:

$$\frac{Y - Y_P}{Y_\phi - Y_P} = e^{\frac{-(Z-Z_F)}{H_E}} \qquad (3.54)$$

where $H_E = \frac{1}{(C-L_E)} \left[D\rho A\eta + \frac{a(1+a)C^2 - aL_E C}{KaA\rho} \right]$ (3.48)

and $Y_P = \frac{(C\varepsilon - L_E Y_E)}{C - L_E}$ (3.49)

Equation (3.54) can be rewritten:

$$\ln (Y - Y_P) = \frac{-(Z - Z_F)}{H_E} + \ln (Y_\phi - Y_P)$$

If $(Z - Z_F)$ is written Z^* (i.e. the distance from the feed point to the sample point)

$$\ln (Y - Y_P) = \frac{-Z^*}{H_E} + \ln (Y_\phi - Y_P) \qquad (3.54)$$

Using two column positions, from the experimentally determined concentration profile, equation (3.54) could be solved from simultaneous equations where Z_1^*, Z_2^*, Y_1, Y_2 are known and only Y_P and H_E need to be evaluated. If Z_1^* is chosen each time such that $Z_2^* = 2Z_1^*$, then

$$Y_P = \frac{Y_1^2 - Y_2 Y_\phi}{2Y_1 - Y_\phi - Y_2} \qquad (5.1)$$

In the case of each graph six values of Y_P were calculated and the average determined such that a plot of $\ln (Y - Y_P)$ vs Z^* gave a best-fit straight line. The slope of the line is $-1/H_E$.

Using equation (3.48), the D and Ka values were determined using the measured value of L_E and C. The evaluation of the constants α and η is given in the appendix. By choosing a series of crystal production rates and/or base product rates a series of simultaneous equations can be formed and solved for the D and Ka values. It is now possible to use these calculated values, in equation (3.54) to give a theoretical separation value for H_E at different crystal production rates and/or base product rates. This enables a series of theoretical plots of impurity vs. position in the column to be constructed and compared with the experimentally measured concentration profiles.

From equation (3.49), knowing C, L_E, Y_E and Y_P; ε the solid phase impurity level was calculated for that particular set of operating conditions.

Screw Speed r.p.m.	D cm^2 sec^{-1}	Ka sec^{-1}
100	3.13×10^{-2}	1.07×10^{-4}
60	2.65×10^{-2}	1.09×10^{-4}

Crystals transported downwards

TABLE (5.1)

Calculated Values for D and Ka for the Desalination System

The desalination of "seawater" was carried out in the column at Total Reflux and Continuous operation. The initial batch runs were designed to test the operational reliability of the column and ancillary equipment.

(a) Total Reflux : Column configuration (A)

The column was operated with the freezing section at the base, the crystals being transported up through the purification section and melted at the top of the column. The difficulty in building up a crystal bed and establishing controlled melting of the crystals prevented any significant separation in the column. A typical concentration profile is shown in Fig. (5.1), curve (a). By carrying out several design modifications, a reduction in drive speed and use of an improved melter, it was possible to build up a crystal bed and achieve separation down the column. A typical concentration profile showing the improvement is presented in Fig. (5.1), curve (b).

This is a characteristic concentration profile curve, showing an impurity gradient of approximately 2000 ppm at the pure end, down to 78,000 ppm at the concentrated impurity end, the point of inflection being around the mid portion of the column. Whilst

separation was limited to the upper portion of the column it indicated that the desalination system could be treated on the column. Further investigations were carried out by operating the column in the same configuration but with a continuous supply of feed. The results of these initial investigations are presented in Table (5.2) and a typical curve shown in Fig. (5.1) (c).

Run	Crystal rate g/sec	Product stream rate g/hr	Waste stream rate g/hr	Screw speed r.p.m.	Enriched product composition p.p.m.
DS 1	0.407	4192	9030	40	15,000
DS 2	0.460	3698	7500	40	14,000
DS 3	0.492	6206	2910	40	16,500
DS 4	0.412	2318	6110	45	12,000
DS 5	0.409	1828	3550	50	16,500

TABLE (5.2)

Parameters for initial investigation of Column Crystallisation under Continuous operation

The performance of the column, operating in this mode, has been described in section (4.5) (a). Comparison of this concentration profile to the two previous Total Reflux runs shows a more uniform concentration gradient in the column. A purification gradient has been established down to the feed point and the top stream impurity composition is much reduced. However the problem of operating the column, for long periods, with a stable crystal bed makes this column configuration unfavourable. The mass of crystals ascending the column cannot be dealt with easily. The fine control of energy input cannot be achieved with the present melting section configuration.

On the positive side, the column demonstrated that it could handle impure streams of feed material and reduce the impurity levels, operating continuously. Whilst the bench scale columns have operated successfully under Total Reflux, the 100 mm diameter column does not give useful separations with the present system. There is no advantage from operating the column under Total Reflux or with the freezing section at the base.

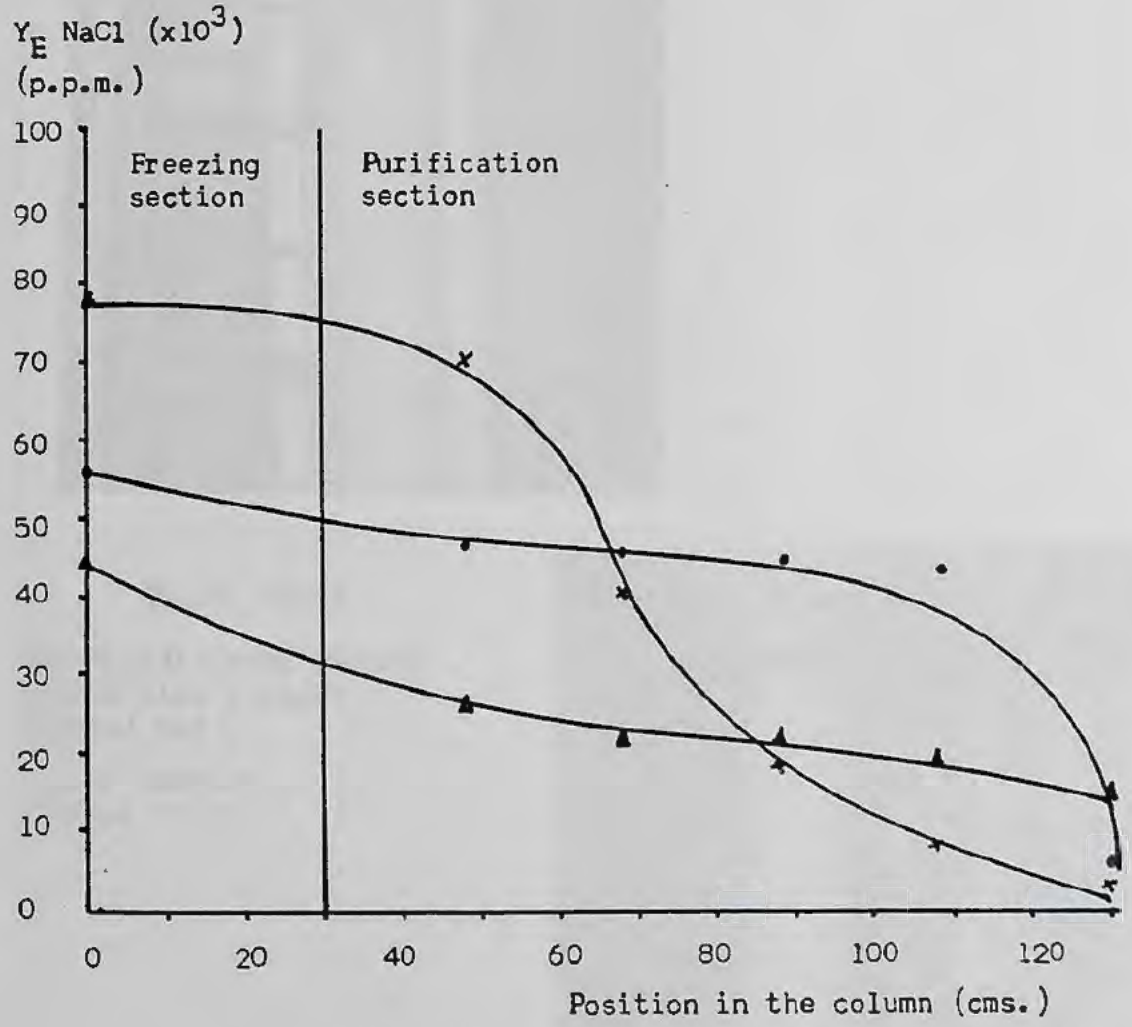

	Refrigerant temp. (°C)	Screw speed (r.p.m.)	Feed concentration (p.p.m.)	
(a) • —— •	-18 to -20	54	30000	Total reflux
(b) × —— ×	-20	42	30000	Total reflux
(c) ▲ —— ▲	-24	45	35000	Continuous - configuration (A)

FIG. (5.1)

Concentration profiles for the initial evaluation runs

PLATE (5.1)

Column Crystalliser operating in configuration (B)

(1) Purification section partially filled with descending crystals

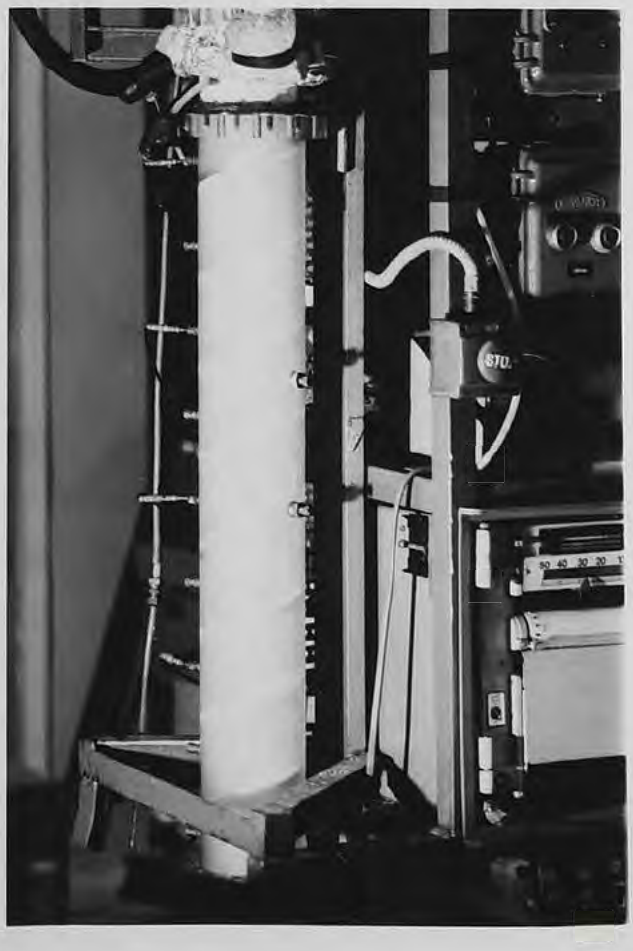

PLATE (5.2)

(2) Purification section packed with a dense crystal bed

(c.f. section (c))
(page 147)

Continuous Operation: Column configuration (B)

With the column operating, in the reverse mode, optimisation runs were carried out to determine the most favourable conditions for steady state operation. From the concentration profiles of these runs the various column parameters were calculated. A summary of the variables is presented in Table (5.3), the individual concentration profiles in Table (5.4),(5.5).

(a) Screw Speed Fig. (5.2)

The spiral rotation rate was varied over the range 50 - 100 r.p.m., most of the subsequent runs being carried out at fixed rotation rates of 60 r.p.m. or 100 r.p.m. The peak level of impurity occurred around 80 r.p.m. although the magnitude of impurity variation over the rotation range was not excessive. At rates of 50 to 100 r.p.m. there was little change in separation at the higher levels of solid flow rate, C. However, at the lower level of C, the separation was reduced. This is as expected since at lower solids production,the slurry viscosity is reduced rendering the transfer of impurity by axial diffusion easier. Since the spiral rotation is the only agitation in the column this determines the effectiveness of the mass transfer of impurity, i.e. how effective is the washing of the adhering liquid from the solid phase. Thus a balance,between the two extremes of excess impurity diffusion down the column and zero mass transfer, has to be achieved at a compromise screw speed.

Calculated values for the Diffusion (D) and Mass Transfer (Ka) terms at 60 r.p.m. and 100 r.p.m., in the column, are very similar (see Table (5.1)), showing that at these two spiral rotation rates there is no enhancement of one effect over the other. However, for the desalination system the values of the diffusion coefficients are so low that the diffusion effects are minimised at the measured conditions.

Desalination : Experimental Runs Table (5.3)

Run No	Feed Rate (g/hr)	Feed Composition (ppm NaCl)	Screw Speed (rpm)	Enriched Product Rate (g/hr)	Enriched Product Comp^{n} (ppm NaCl)	Crystal Direction	Crystal Rate (g/sec)	
DS 1	13000	30,000	40	4192	15,000	F.S. ↑	0.407	Continuous
DS 2	11100	30,000	40	3698	14,000	base	0.460	"
DS 3	8935	30,000	40	6206	16,500	↑	0.492	"
DS 4	8361	30,000	45	2318	12,000		0.412	"
DS 5	5329	30,000	50	1828	16,500	↑	0.409	"
DS 8	8592	30,000	50	2000	1,500	F.S. ↓	0.591	"
DS 9	8900	35,000	50	2000	2,500	top	0.574	"
DS 12	7072	34,000	60	2450	12,000		0.443	"
DS 16	7891	33,000	60	2950	19,000	↓	0.478	"
DS 17	7249	35,000	60	2100	8,000		0.478	"
DS 18	8317	36,000	60	2150	5,000		0.478	"
DS 20	8639	38,000	60	2150	4,000	↓	0.514	"
DS 21	7405	33,000	60	2120	5,000		0.547	"
DS 25	6600	33,000	60	700	3,800		0.554	"
DS 26	6447	32,000	60	700	4,000	↓	0.529	"
DS 29	6848	35,000	80	1600	5,000		0.590	"
DS 30	5700	35,000	80	1500	15,000		0.572	"
DS 31	6448	36,000	100	1576	3,250	↓	0.485	"
DS 32	6252	36,000	100	1693	4,000		0.520	"
DS 33	5520	35,000	100	1308	6,200		0.390	"
DS 34	6710	38,000	100	1442	5,250		0.443	"
DS 35	7600	36,000	100	1475	6,500	↓	0.470	"
DS 36	6650	37,000	100	1524	5,000		0.542	"
DS 37	7753	36,000	100	1469	3,000		0.527	"
DS 38	6710	35,000	100	1292	3,500		0.491	"
DS 40	2575	36,000	100	900	4,500	↓	0.445	"

F.S. Freezing Section base -- (configuration A) top -- (configuration B)

Desalination : Experimental Results Table (5.4)

Distance From Freezing Section (cms)	Concentration of NaCl in Free Liquid : Concentration Profile (p.p.m.)											
	DS 1A	DS 1B	DS 1C	DS 1D	DS 1E	DS 1F	DS 1	DS 2	DS 3	DS 4	DS 5	
-30.0	55000	77500	86000	78000	66000	72000	44000	45000	47000	44000	51500	Base of Column
19.0	46000	69500	51000	49500	51000	47000	30000	31500	33000	30000	31500	
39.0	45500	38500	43000	39000	37000	45000	24000	30000	30500	22000	30500	
59.0	46000	17500	34000	28000	35000	44000	20500	22500	20500	20000	30500	
79.0	45000	8500	22500	13000	28000	22500	19500	20000	20500	20000	30000	
89.0	37500	5000	-	-	-	-	19500	20000	18500	18500	30000	
100.0	5000	3500	8500	4500	8000	4500	15000	14000	16500	12000	16500	Top of Column
Crystal Direction	↓	↓	↑	↑	↑	↑	↓	↓	↓	↓	↓	
Screw Speed (r.p.m.)	54	42	60	80	100	120						
Crystal Rate (g/sec)	0.310	0.305	0.340	0.317	0.335	0.335						

Runs DS 1A - 1F Total Reflux

DS 1A,1B - DS 1-5 Freezing Section at the base of the column (configuration A)

DS 1C - 1F Freezing Section at the top of the column (configuration B)

Desalination : Experimental Results Table (5.5)

Distance from the freezing section(cms)	Concentration of NaCl in the Free Liquid (values x 10^3) : Concentration Profiles (p.p.m.)																			
	DS 8	DS 9	DS 12	DS 16	DS 17	DS 18	DS 20	DS 21	DS 25	DS 26	DS 29	DS 30	DS 31	DS 32	DS 33	DS 34	DS 35	DS 36	DS 37	DS 38	DS 40
-30.0	58.5	61.0	55.0	46.0	49.5	47.0	61.0	47.0	49.5	55.5	55.5	69.5	55.5	47.0	49.5	49.5	44.0	47.0	52.5	64.0	47.5
19.0	33.0	44.0	44.0	35.0	41.0	38.5	49.5	33.0	25.0	30.0	34.0	44.0	26.5	31.0	31.5	33.0	41.0	44.0	19.0	41.0	46.5
39.0	24.0	30.0	34.0	31.0	33.0	33.0	44.0	31.0	13.0	20.0	22.5	32.5	12.5	30.0	30.0	30.0	32.0	38.0	14.0	27.0	45.5
59.0	15.0	17.5	33.0	22.0	31.0	30.5	20.5	17.5	7.0	11.0	12.5	20.0	6.5	16.5	24.0	18.5	30.0	31.0	5.0	6.5	44.0
79.0	12.0	11.0	32.5	19.5	27.5	20.0	10.0	10.5	5.0	5.5	6.5	11.0	3.5	7.0	14.0	8.5	20.5	20.0	3.5	6.5	27.0
89.0	1.2	8.1	30.0	19.5	18.5	17.5	9.0	7.0	3.8	5.5	5.5	7.0	3.8	5.5	9.0	7.0	16.5	12.5	3.3	4.5	19.0
108.0	/	/	9.0	17.0	13.5	10.0	6.0	5.5	3.5	4.0	4.5	6.5	3.3	4.5	6.3	5.3	12.0	4.5	3.3	3.5	7.0
113.0	1.5	2.5	12.0	19.0	8.0	5.0	4.0	5.0	3.8	4.0	5.0	5.0	3.3	4.0	6.2	5.3	6.5	5.0	3.0	3.5	4.5

Runs DS 8 - DS 40 Crystals transported downwards

/ --- NO sample obtainable

Freezing section at the top of the column (configuration B)

FIG. (5.2)

Effect of screw speed on enriched product purity for crystals transported downwards.

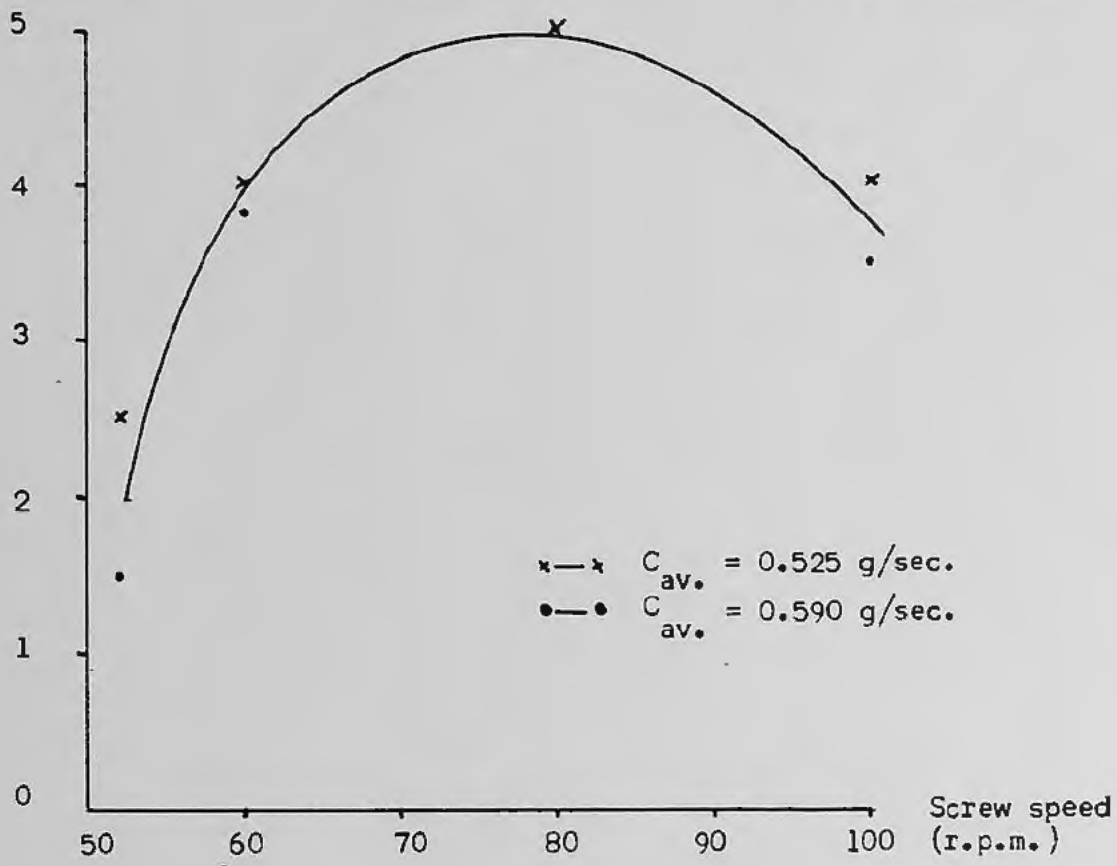

FIG. (5.3)

Variation in the concentration of NaCl in the free liquid when increasing the feed rate, for the same crystal production rates.

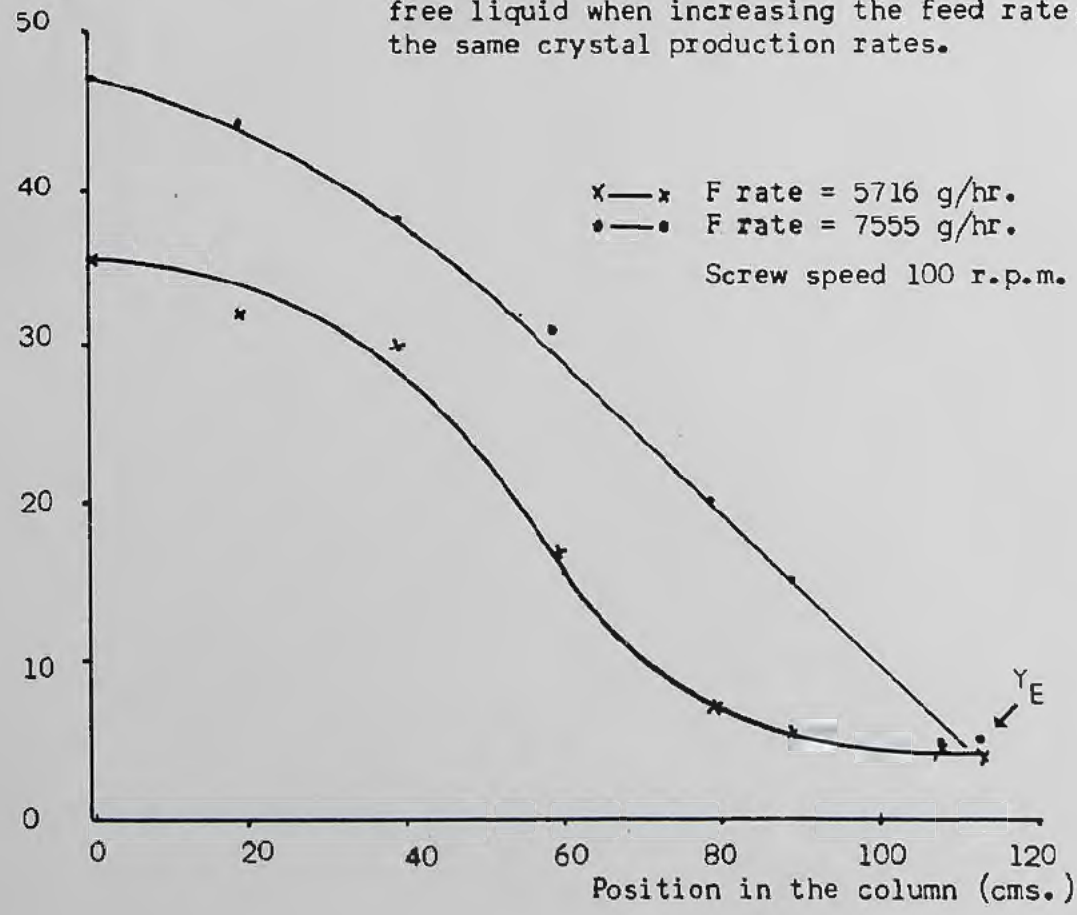

(b) Feed Rate Variation (Fig. 5.3)

The effects of operating the column under varying rates of feeding, whilst maintaining the same conditions of crystal production C, and base product rate L_E, followed the expected trend. As the feed rate increased, the transfer of impurity down the column increased. As L_E was fixed, the excess feed material was removed in the overflow waste stream L_S, thus the flow of liquid through the freezing section increased and the effective crystal production rate decreased. This reduction in solids production did not allow a compacted crystal bed to be built up, hence the fall-off in impurity removal.

(c) Crystal Rate (Fig. 5.4)

As seen in the previous optimisation runs, the solids production rate is a key parameter in determining the separation achieved in the column.

In Equation (3.48), the term appears as $\left(\frac{1}{C - L_E}\right)$ and C^2 in the mass transfer segment. Thus as C is increased, the first term decreases whilst the latter increases. In practical terms, at low values of solids production, the diffusion can be expected to contribute significantly to the impurity levels down the column. As solids production increases, it is predicted that mass transfer should be more dominant. Therefore an increase in crystal production rate should improve the purification. This trend was observed over a range of values of C = 0.390 g/sec to C = 0.527 g/sec.

This was the maximum solids production that could be achieved without the problem of column blockage from excess crystal hold-up in the freezing section. A visual indication of solids production was the base operating pressure. At low values of C, a typical pressure of 3-4 p.s.i. was generated. As C increased, the base pressure increased to 10-12 p.s.i. At these higher pressures a dense crystal bed was formed as opposed to a crystal slurry. It was possible to inject air at a sample point and follow its descent

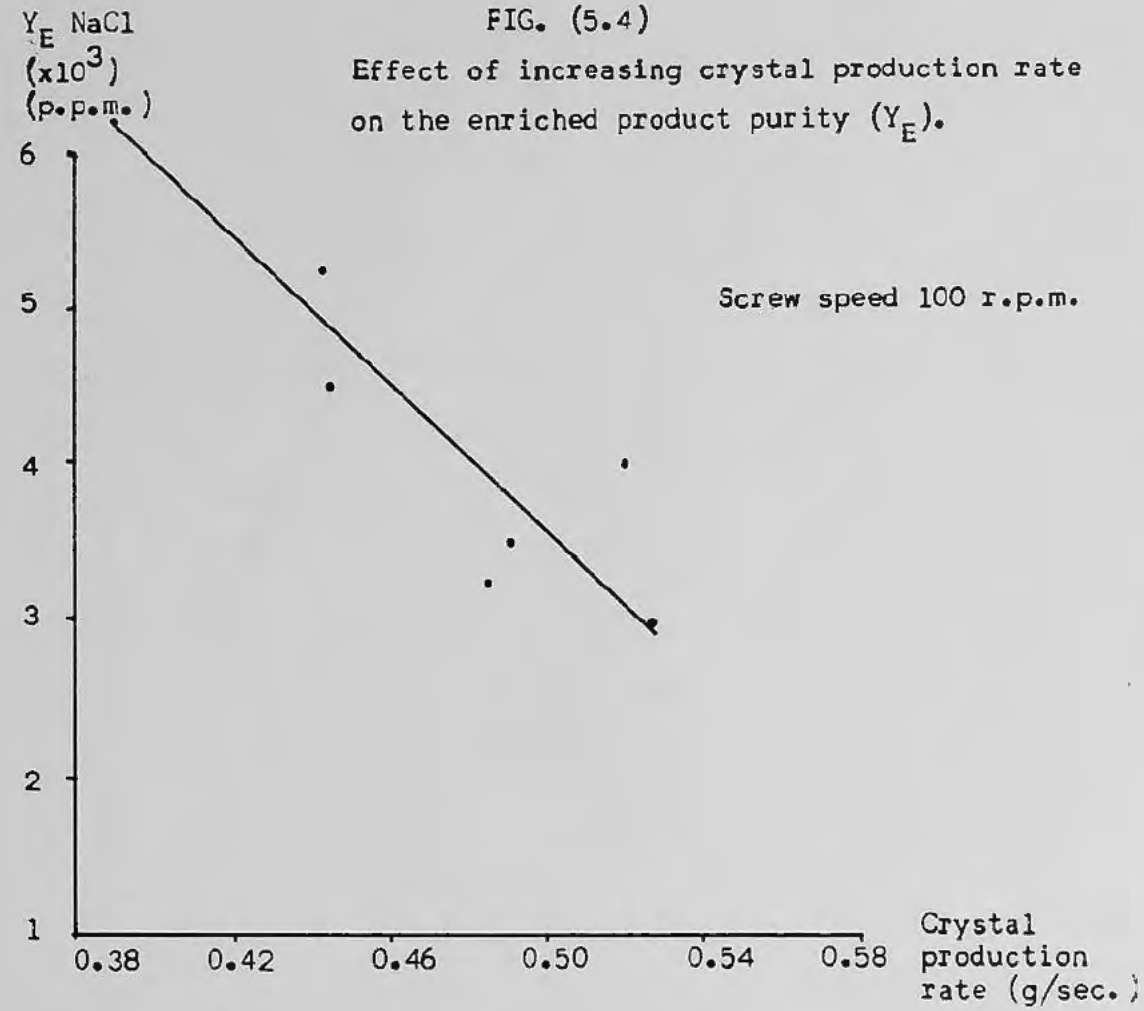

FIG. (5.4)

Effect of increasing crystal production rate on the enriched product purity (Y_E).

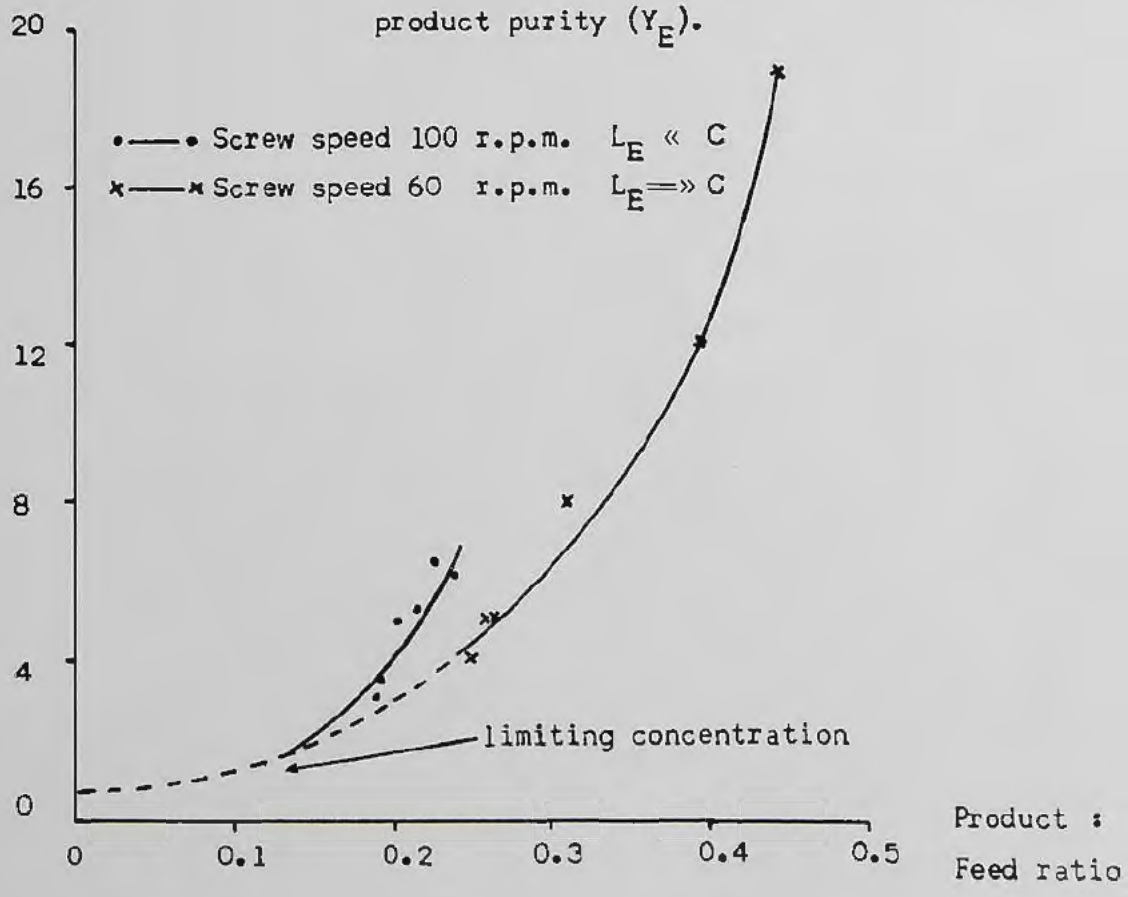

FIG. (5.5)

Effect of product ratio on the enriched product purity (Y_E).

down the column, whereas with the crystal slurry it diffused upwards.

(d) Product ratio removal rate Fig. (5.5)

An important factor in any process is the quantity of purified material obtained per unit time from the equipment. Crystals produced in the freezing section are purified by a washing mechanism as they descend through the purification section. Obviously, the impure crystals have to be contacted with purer free liquid to achieve this. The source of this washing liquid is from a recycle of a portion of the pure feed. It can be seen that this determines the quantity of pure product one can remove from the column, and as such one can operate between the two extremes of a high volume/low purity product and a low volume/high purity product. Another constraint upon the product removal rate is that for equation (3.48) to be valid,

$$H_E = \frac{1}{(C-L_E)} \left[D\rho A\eta + \frac{a(1+a)C^2 - a L_E C}{KaA\rho} \right] \qquad (3.48)$$

then $C > L_E$, to give meaningful values for D and Ka. In practice a compromise is chosen such that a reasonably pure product is obtained.

(e) Reflux Ratio FIG. (5.6)

This is defined as the fraction of melted solids removed from the unit, that is, the ratio of pure product flow rate to solids flow rate L_E/C. This is a measure of the quantity of liquid returned to the column for the washing of the impurity from the crystals. The column can operate between the two extremes of:

$R_E = 1.0 \quad L_E = C$ (no reflux liquid)

and $R_E = 0.0 \quad L_E = 0$ (no product)

If the washing of impurity from the crystals was complete, then at low values of R_E the enriching section product should have zero or minimum impurity. Examination of FIG. (5.6) shows an upturn, that is, below a certain value of R_E there is no improvement in product purity. There is a lower limit of product impurity content of 3,000 p.p.m. which represents a value beyond which improvement on this specific apparatus is difficult to achieve with an economic reflux. A value of 500 p.p.m. was found for the desalination system on the 50 m.m. column.

In an effort to simplify the study of the effects of process parameters, Wells[53] stated that under economic operating conditions, $D\rho A\eta \gg LL'/K\rho a A$ (3.44) especially at <u>low</u> refluxes, and that the adhering liquid at the feed point had the same composition as the feed, Y_F. The resulting simplified design equation,

$$Y_E = \varepsilon + \left[\frac{1 - R_E}{\alpha - R_E + 1}\right] \alpha Y_F \quad \exp.\left[\frac{-L_P (1 - R_E) C}{D \rho A \eta}\right] \qquad (3.60)$$

is derived in Appendix (A.1)

To test the validity of applying this equation, with the restrictions stated, the impurity content of the enriched product was measured at various reflux ratios and the theoretical value of impurity content for those ratios calculated. The results are summarised in Table (5.6).

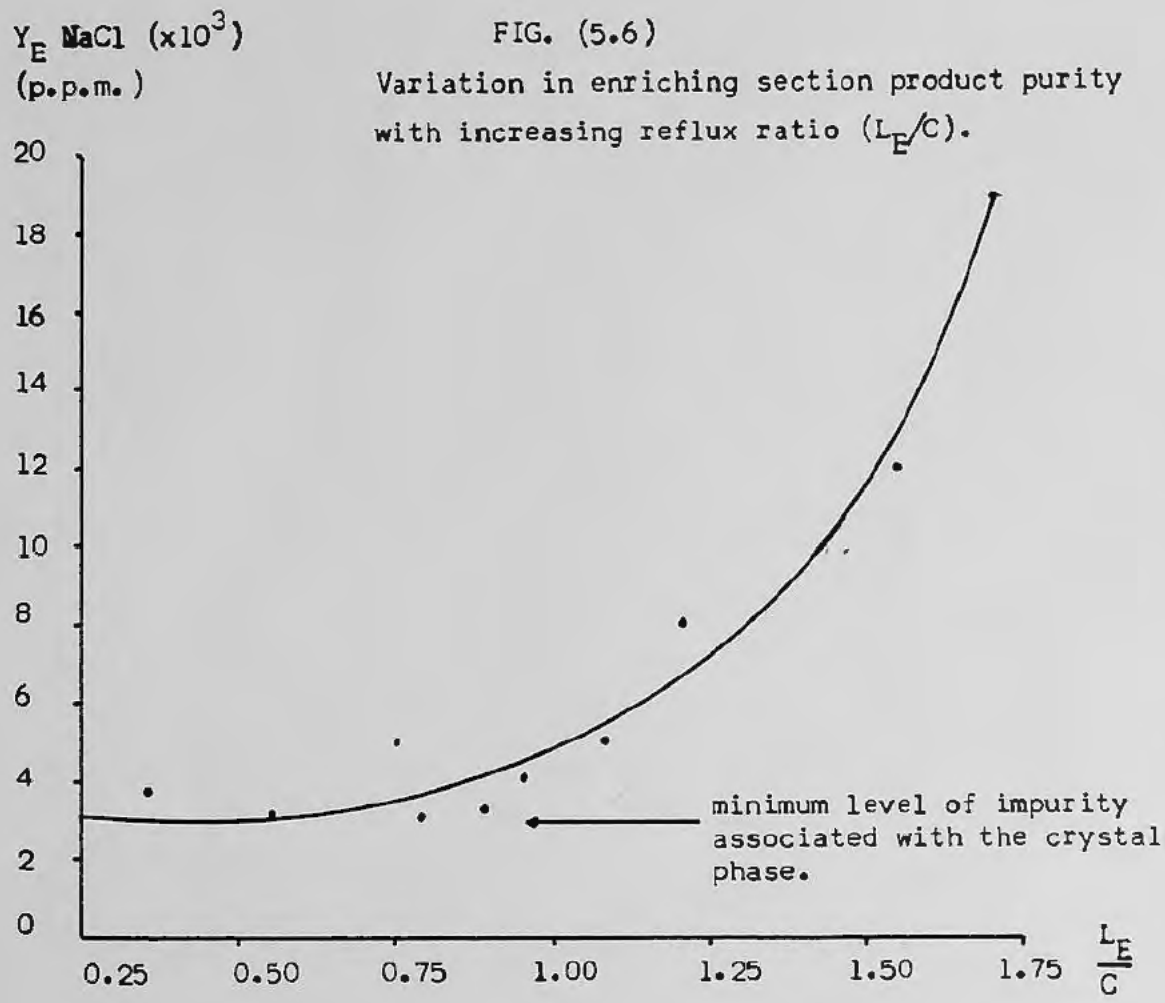

FIG. (5.6)

Variation in enriching section product purity with increasing reflux ratio (L_E/C).

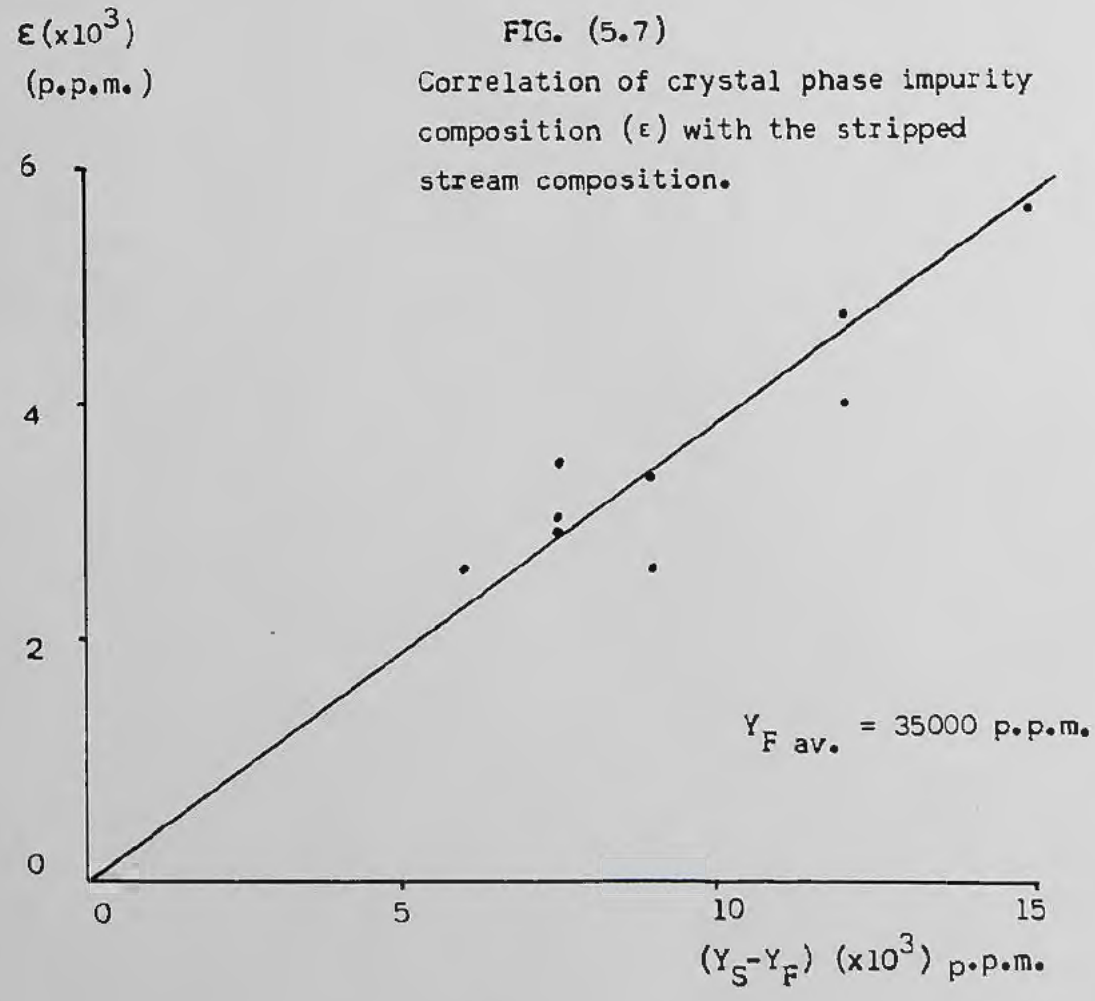

FIG. (5.7)

Correlation of crystal phase impurity composition (ε) with the stripped stream composition.

D.S Run	Reflux Ratio R_E	Y_E (Theoretical)	Y_E (Measured)	Percentage Difference
25	0.723	2617	3800	45.0
26	0.756	3428	4000	16.7
31	0.902	2922	3250	11.0
32	0.905	3585	4000	11.6
33	0.932	5857	6200	5.9
34	0.904	4799	5250	9.6
36	0.782	4020	5000	24.4
38	0.731	2912	3500	20.2
40	0.562	3031	4500	48.5

TABLE (5.6)

Values of R_E for which Equation (3.60) is valid

Constants used to calculate Y_E (Theoretical) in Equation (3.60)

L_P = 90 cms ρA = 90.95 Y_F = 35,000 p.p.m. D = 0.029 $cm^2 sec^{-1}$

α = 0.265 η = 0.267

When $R_E \ll 1$, then Y_E (Theoretical) and Y_E (Experimental) are very similar. When operating the column with little reflux, that is, maximising product, Equation (3.60) gives a good estimation of the impurity content of the enriched stream.

(f) Impurity associated with the crystal phase

In the development of the original model it was envisaged that impurity could be entrapped in the crystal matrix or exhibit slight solid solubility. The amount of impurity associated with the crystal phase is governed by the crystal growth kinetics which result from particular conditions in the freezing section.

The impurity composition in the crystal phase, ε, can be calculated from the values of Y_P, in the rearranged equation (3.45),

$$\varepsilon = \frac{Y_P\ (C - L_E) \ + \ L_E\ Y_E}{C} \qquad (3.45)$$

The values of ε were related to the composition of the freezing section, taken as the impurity content of the stripped stream, Y_S. This assumes that the freezing section is perfectly mixed. The values of ε were calculated for fixed conveyor rotation rates. A plot of ε versus $(Y_S - Y_F)$, FIG. (5.7), indicates that ε does increase with Y_S. The ε, $(Y_S - Y_F)$ data exhibit a linear relationship. A least square fit of the data gives the following relation:

$$\varepsilon = 0.33\ (Y_S - Y_F) \ + 519 \qquad (5.1)$$

In his work on Benzene/Cyclohexane, Henry[43] concluded that such a linear dependence was to be expected if impurity was entrained as liquid inclusions.

The dependence of ε on the stripped stream composition, Y_S, imposes a restriction on the ultimate purity that can be achieved with the column crystalliser. The minimum value of Y_S occurs when the stripping section is flushed with feed material, that is:

$$Y_{S\ (min)} \ = \ Y_F$$

Such a condition would correspond to zero product removal. The minimum value of impurity associated with the crystal phase, $\varepsilon(min)$, corresponds to $Y_S(min)$. For the particular system under consideration equation (5.1) predicts that,

$$Y_S(min) \ = Y_F, \ \ \varepsilon_{(min)} \ = 519 \text{ p.p.m.}$$

At typical levels of mother liquor concentration in the freezing section during an experimental run, equation (5.1) predicts the value of $\varepsilon_{(min)}$, for example

when Y_S = 45,000 p.p.m. $\varepsilon_{(min)}$ = 3820 p.p.m.

If we have complete washing of adhering liquid from the crystals, then the product impurity is determined by the crystal phase impurity. Therefore one would predict that in the above case, the minimum level of product impurity is $\varepsilon(\text{min})$, that is,

$$\varepsilon_{(\text{min})} = Y_E = 3820 \text{ p.p.m.}$$

To produce material purer than $\varepsilon_{(\text{min})}$ would require a second pass through the crystalliser.

The parameter controlling the impurity removal is the reflux ratio R_E. Examination of Fig. (5.6) illustrates that the product purity reaches a limiting value as R_E is decreased. Further reductions in R_E do not improve product quality. Impurities that can be removed by the washing process have reached a minimum and at this point $Y_E \Omega \varepsilon$. From Fig. (5.6),

when $R_E = 0.8$ $\quad Y_E = 3{,}400$ p.p.m. $\quad (\Omega \varepsilon)$

This value compares well with that predicted by equation (5.1), for continuous column operation.

When the column is operated at Total Reflux, the $\varepsilon(Y_S)$ dependence infers that the base level of impurity should be greater since the mother liquor concentrations are significantly higher in the freezing section. At Total Reflux, the concentration profile is described by equation (3.58).

$$\frac{Y - \varepsilon}{Y_\Phi - \varepsilon} = \text{exp.}^{-Z/H_\Phi} \qquad (3.58)$$

Values of ε calculated for the Total Reflux runs are compared with the mother liquor composition in the freezing section.

ε calculated ppm	Y_S (average conc^n) F/S p.p.m.	Y_E base impurity p.p.m.
8475	70,350	8500
4379	68,825	4500
5505	64,375	8000
4500	60,500	4500

TABLE (5.7)

Calculated ε values for Total Reflux conditions

There are insufficient Total Reflux experiments for a detailed analysis. However the ε (Y_S) dependence shows a similar trend to that observed for Continuous operations. The measured base impurity levels, Y_E, are of the same order as the calculated values for the crystal phase impurity. However these ε values, although towards the top of the range for crystal phase impurity in the Continuous operation, are not greatly in excess of them. It would appear that operating the column at Total Reflux does give rise to a slight increase in residual base impurity levels.

The high value of R_E for the continuous runs, allows for reasonable levels of product draw-off without significant reduction in product purity. With the smaller columns previously investigated it was necessary to operate at much lower values of R_E (approximately 0.4) to achieve the maximum product purity. However the product purity achieved in the columns was greater than in the 100 m.m. diameter column, for example,

25 mm Dia.	$R_E = 0.35$	$Y_E =$ 57 p.p.m. Ref(43)
100 mm Dia.	$R_E = 0.80$	$Y_E = 3400$ p.p.m.

It is apparent that the narrow bore columns are much more sensitive to product removal rates/washing efficiency than the column under investigation. Consequently there are no advantages from operating the 100 m.m. diameter column with high reflux return rates as the improvement in product quality is not realised.

It would appear that there is a reduction in the washing efficiencies achieved as the diameter of the column is increased. The sensitivity of the smaller diameter columns to reflux ratio levels indicates that there is efficient contacting of the impure and pure phases. This is to be expected, since the level of mixing must be higher by virtue of the column geometry. With the 100 m.m. diameter column, the working volume is increased and the potential for zones of low mixing to exist is high. This would be especially true when the column is operating with a densely packed crystal bed requiring the reflux liquid to diffuse through the packed crystal bed rather than be mixed with the crystals. In this situation it is not unreasonable to postulate that some of the adhering liquid will not be contacted by reflux liquid.

The use of an Archimedean Screw for crystal transport produced low levels of mixing within the purification section of the column. Once the crystals were packed into a dense bed there was little chance for them to undergo physical movement as a result of rotation of the screw. At high screw speeds it was possible to observe the formation of a clear channel at the base of each screw flight as crystals were compacted under the influence of the rotational forces. A portion of reflux liquid ascending the column would do so by these channels, thereby giving rise to reduced contacting between the crystals and wash liquid.

(g) Screw conveyor modifications

The function of the Archimedean Screw is to prevent the build-up of solid on the heat transfer surface and facilitate transport of the crystals out of the freezing section preventing screw seizure. The use of this type of conveyor gives rise to engineering difficulties and is not amenable to scale up to larger units. However it is necessary to use a transport device since it has been observed that crystal transport is not significantly influenced by gravity even when the crystal phase is denser than the liquid phase[154]. As a compromise the freezing section was fitted with the three bladed, scraped surface screw, illustrated in Fig. (4.8). This short screw was suspended in the freezing section from an overhead bearing eliminating the problems of driving a long screw in the column.

In use, the short screw was easier to drive and several experimental runs were attempted, the column operating in configuration (B). The initial cooling produced crystals as before and these were observed descending the column into the perspex purification section. A slight zone of turbulence was present just below the end of the screw flights. As the crystal mass increased it formed small aggregates of crystals which, due to buoyancy and thermal effects, ascended the column and formed a packed mass at the base of the freezing section. The turbulence in this portion of the purification section was reduced and the crystal leaving the freezing section had to displace this crystal plug down the column. This reduced the transport of the crystals from the freezing section, causing crystal hold-up and eventual column blockage.

Variations in feed rate, screw speed and cooling rate did not improve the crystal transport. The feed position was relocated from the base of the freezing section to the hollow central shaft of the short screw, thereby increasing mixing in the freezing section.

Similar results were obtained. The metal screw was then assembled in the column with short sections of the nylon Archimedean Screw attached to the end, each one projecting further into the purification section. The column was operated at the same settings as for the previous experiments. Again the crystals were observed leaving the freezing section, travelling down the short lengths of attached screw and forming a crystal plug in the quiescent zone of the purification section. As the length of the attached screw increased, so the zone of crystal compaction moved down the purification section, resulting in the eventual blockage of the freezing section, as before.
It was not possible to operate the column for extended periods using any of the shorter screw conveyors . For successful crystal transport from the freezing section, through the purification section, a full-length screw was required.

(h) Microscopic examination of the crystals

By the nature of a continuous crystallisation process one does not produce a product of completely uniform size. The processes of nucleation, growth, dissolution, attrition, etc. give rise to a crystal product covering a range of sizes. It is not possible to measure or define absolutely the size of an irregular particle, so in order to characterise the product, one employs a size distribution estimation. For the column crystalliser this was achieved using a photomicroscopy method.

The mean crystal size was determined by statistical calculation using the formula:

$$\bar{d} = \frac{\sum f_i \, d_i}{\sum f_i} \qquad (5.3)$$

This calculation of the mean crystal size is based on the number of crystals found by photomicroscopic examination. Ths value for $\bar{d}$ can be expressed as the modal or median diameters; both are determined from frequency plots (size interval versus number of

particles in each interval). The modal diameter is the value at the peak of the frequency curve, whereas the median value divides the distribution equally. If the distribution curve is Gaussian, the two diameters coincide.

In the cases where sieving of the produce is possible then other methods can be used ranging from a simple arithmetic mean to a value obtained on a weight basis. The root mean square diameter is often used when surface properties are important, according to Mullin[140] the formula:

$$\bar{d} = \sqrt{\frac{\sum nd^2}{\sum n}}$$

n = fi = number of crystals

$\bar{d}$ = equivalent diameter of the crystals

can be used provided certain assumptions for the crystals are made. There are numerous other methods available for estimating the "average" diameter but as yet no one technique is generally applicable. Therefore, all calculations based on an average diameter are prone to error and it is necessary to specify how the values of $\bar{d}$ have been been calculated.

Using equation (5.3) the ice crystal size was measured as a function of screw speed, the column operating under continuous flow conditions. The effects of the screw speed are presented in Fig. (5.8) and a photomicrograph of the ice crystals shown in Plate (5.3).

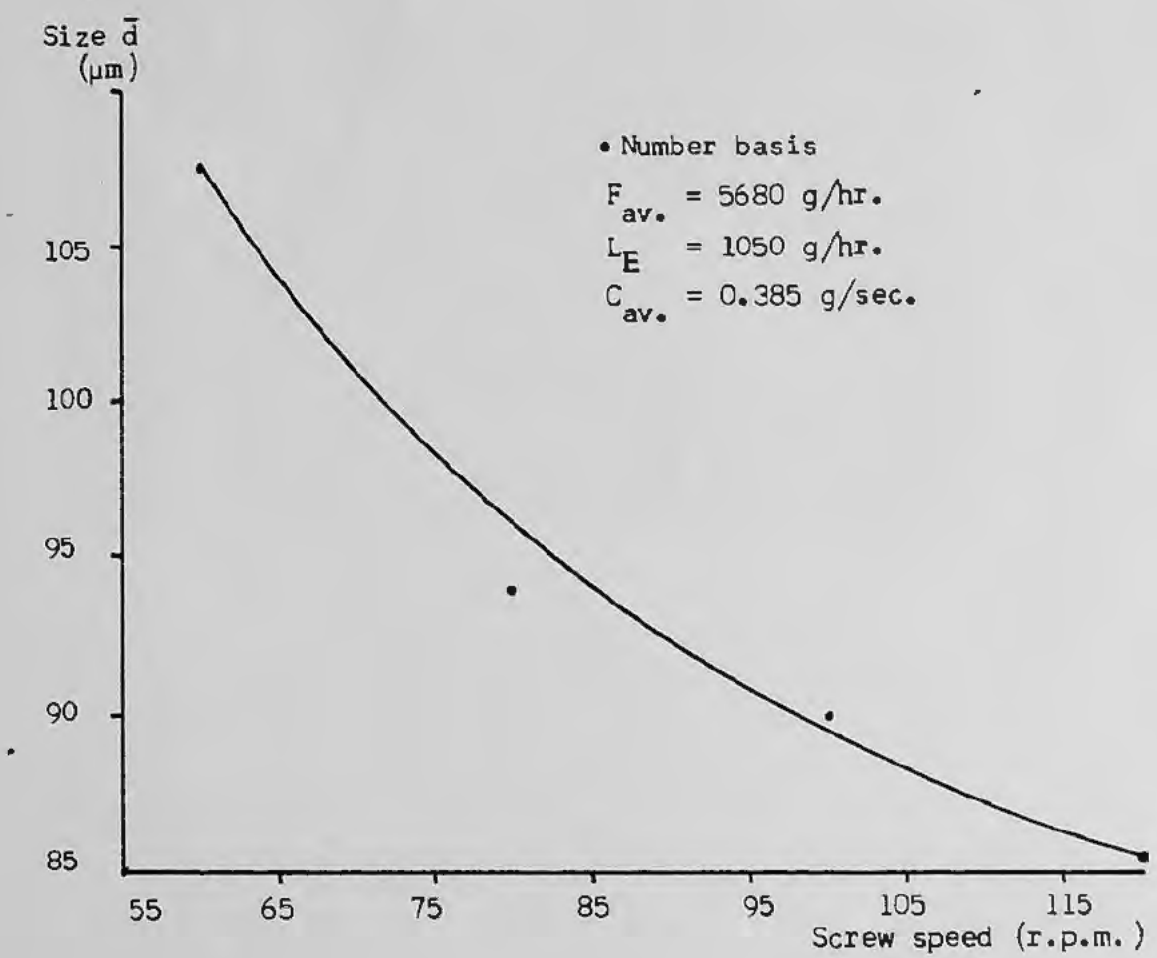

FIG. (5.8)

The effect of screw speed on crystal size under continuous flow conditions

Whilst this is not an exhaustive study of the parameters effecting crystal size, it was found that the mean crystal size varied with the change in one of the important operating parameters, the screw speed. As the screw speed increased, so the size was found to decrease. This is as expected since an increase in screw speed subjects the crystals to greater mixing with subsequent increase in attrition, that is, small corners and edges of the thin ice crystals were broken by increased crystal/crystal and crystal/crystalliser

contacts. This is shown in the crystal photomicrograph Plate (5.3). The crystal sizes were found to vary from 88 μm to 108 μm .

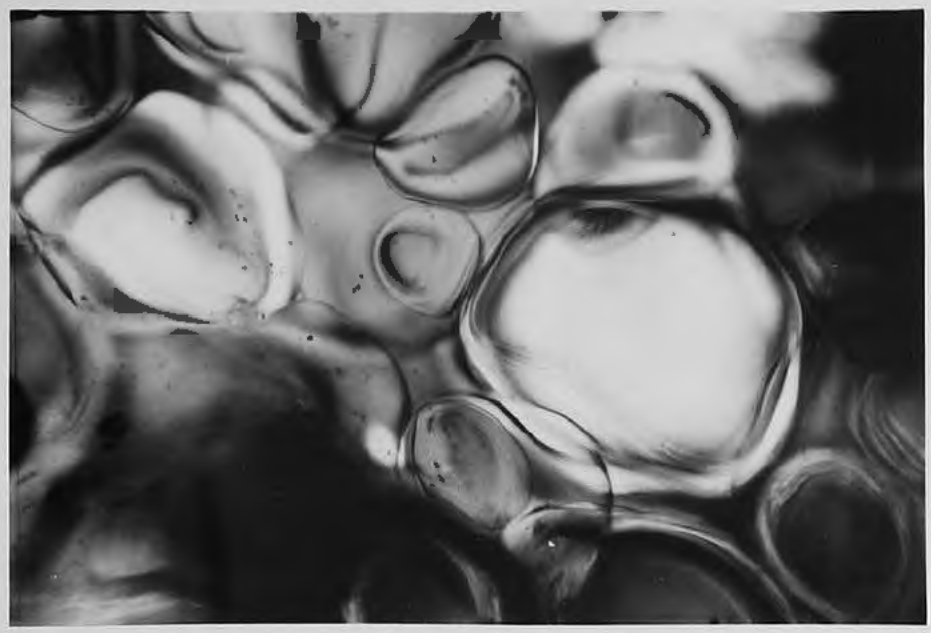

PLATE (5.3)
Photomicrograph of ice crystals (x 100 MF.)

(5.2) Ethanol Concentration

The use of the column crystalliser for the concentration of ethanol required that the samples be taken from the stripping section. With the column operating in configuration (B) this is from the feed point below the freezing section to the overflow point at the top of the freezing section. Normally the stripped stream would be a concentrated waste, however with this system it is the ethanol enriched product. It was hoped that the short screw conveyor tested in the desalination work (see section (5.1.g)) would enable samples to be removed from the freezing section for analysis of the stripping section. However due to the problems encountered when using this modified screw, a full length nylon conveyor was used .

The stripping section concentrations were measured for liquid entering and product leaving the section over a range of crystal production rates.

The variables investigated were:

(a) Screw speed for (i) High F : High L_E) over a range
(ii) Low F : Low L_E) 34 - 104 r.p.m.

(b) Z_F = feed position

(c) L_S = top product removal rate

(d) C = solids flow rate in the stripping section

(e) Introduction of a liquid pulse

The variables held constant:

(a) Y_F = feed composition (10% by wt I.M.S. in water)

(b) Freezing section, purification section, melting section lengths

(c) F = feed rate

Mathematical Treatment of results

The concentration profile for the stripping section is described by equation (3.55):

$$\frac{Y - \bar{Y}_P}{Y_\phi - \bar{Y}_P} = \exp. \frac{-(Z - Z_F)}{H_S} \qquad (3.55)$$

where $\bar{Y}_P = (C\,\varepsilon + L_S\,Y_S) / (C + L_S)$ (3.56)

and $$H_S = \frac{1}{(C + L_S)}\left[D\eta A\rho + \frac{a(1+a)\,C^2 + a L_S\,C}{KaA\rho} \right] \qquad (3.57)$$

For a range of crystal production rates at fixed top product rate, L_S, a series of simultaneous equations were derived and solved for D and Ka values. Using these values, substituted in equation (3.57), a theoretical value of H_S was calculated which allowed the concentration of ethanol in the top product stream to be estimated and compared with the experimentally measured value. See Appendix (A.3)

Calculated values for the column parameters were:

$Ka = 2.67 \times 10^{-4}$ sec^{-1}

$D = 0.71$ $cm^2\ sec^{-1}$ at 34 r.p.m.

Both values show an increase in magnitude of approximately 2.5 over those calculated for the desalination system. Hence we can expect both the diffusion down the column and mass transfer between the adhering and free liquids to determine the magnitude of the separation factor H_S.

Continuous Operation : Column configuration (B)

The column was operated with the freezing section at the top, the crystals produced being transported down through the purification section to the base melting section. From the concentration profiles of the runs the various column parameters were calculated. A summary of the variables is presented in Table (5.8), the concentration profiles in Table (5.9).

Ethanol concentration : Experimental Results Table (5.8)

Run Number (ET)	Feed rate (g/hr.)	Feed composition % EtOH by wt	Distance of feed point from freezing section (cms)	Top product rate (ml/hr)	Top product composition % EtOH by wt	Base product rate (ml/hr)	Base product composition % EtOH by wt	Crystal rate (g/sec)	Screw speed (r.p.m.)
1	4400	10.0	0.5	1030	16.7	4020	6.7	0.324	34
2	3400	10.5	0.5	3150	16.4	1025	2.6	0.342	34
3	4300	9.0	0.5	1520	13.5	3500	6.3	0.367	34
4	4000	11.0	0.5	880	15.4	3800	10.5	0.351	44
5	3350	11.2	0.5	2700	12.8	970	3.3	0.351	44
6	4000	10.3	0.5	1100	15.1	3650	9.6	0.336	54
7	3400	11.1	0.5	3080	14.5	1060	9.5	0.326	54
8	3500	10.6	0.5	3070	14.5	1080	9.3	0.367	74
9	4450	9.6	0.5	1090	12.8	4300	8.3	0.342	104
10	3700	9.8	0.5	3090	13.1	1260	8.4	0.364	104
11	4450	9.4	0.5	1480	12.6	3950	8.9	0.362	88
12	4250	9.8	0.5	1230	13.8	3980	8.5	0.353	64
13	3550	9.2	0.5	3060	12.9	1160	2.0	0.359	64
14	3450	9.1	0.5	3000	11.9	1090	1.7	0.330	40
15	4350	9.4	10.0	1270	13.2	3960	6.5	0.397	34
16	4250	9.5	20.0	1200	14.2	3940	3.8	0.390	34
17	4000	9.3	35.0	1120	16.2	3640	6.3	0.411	34
18	4400	9.1	50.0	1410	16.1	3880	8.3	0.371	34
19	4300	9.3	70.0	1250	15.8	3930	7.2	0.384	34
20	3750	9.1	0.5	470	15.9	4000	9.4	0.378	34
21	4500	9.1	0.5	2000	13.4	3570	8.2	0.379	34
22	4750	9.6	0.5	2530	13.6	3300	8.3	0.416	34
23	4500	9.7	0.5	1440	13.6	3950	8.3	0.315	34
24	4100	10.3	0.5	1730	13.6	3180	5.2	0.301	34
25	4450	9.5	0.5	1420	12.5	3930	7.6	0.261	34
26	4200	10.5	0.5	1470	12.1	3550	4.0	0.346	34

Ethanol concentration : Experimental Results Table (5.9)

Distance from the feed point (cms.)	Concentration of Ethanol in the Free Liquid (% by wt) : Concentration Profiles													
	ET 1	ET 2	ET 3	ET 4	ET 5	ET 6	ET 7	ET 8	ET 9	ET 10	ET 11	ET 12	ET 13	ET 14
-30.0	16.7	16.4	13.5	15.4	12.8	15.1	14.5	14.5	12.8	13.1	12.6	13.8	12.9	11.9
19.0	13.1	14.7	11.4	13.1	12.2	12.1	9.6	11.5	12.8	9.4	11.7	8.0	8.5	10.8
39.0	12.9	15.4	12.2	13.0	11.7	11.1	8.8	11.3	11.3	8.4	11.4	9.3	8.5	9.7
59.0	13.0	12.2	8.2	13.1	11.1	11.2	8.9	10.6	10.9	7.4	10.1	9.4	7.6	7.8
79.0	12.6	9.4	7.9	12.3	10.4	10.2	9.5	9.9	10.5	7.7	10.2	8.9	6.8	5.6
89.0	11.9	7.0	6.7	12.2	8.4	9.3	8.9	9.9	10.3	8.2	8.8	8.2	6.4	5.2
108.0	9.7	3.3	6.3	10.7	3.7	9.9	8.9	9.9	10.3	8.4	8.3	8.0	3.0	1.8
113.0	6.7	2.6	6.3	10.5	3.3	9.6	9.5	9.3	8.3	8.4	8.9	8.5	2.0	1.7

Ethanol concentration : Experimental Results Table (5.9) Continued

Distance From the feed point (cms.)	Concentration of Ethanol in the Free Liquid (% by wt) : Concentration Profiles												
	ET 15	ET 16	ET 17	ET 18	ET 19	ET 20	ET 21	ET 22	ET 23	ET 24	ET 25	ET 26	
-30.0	13.2	14.2	16.2	16.1	15.8	15.4	13.4	13.6	13.6	13.6	12.5	12.1	Crystals transported downwards.
19.0	10.1	10.9	12.3	11.1	10.8	11.7	8.9	9.2	10.7	11.9	11.6	10.2	
39.0	9.6	12.1	11.0	10.8	9.9	11.9	7.2	9.6	11.1	11.2	12.0	9.1	
59.0	11.4	11.9	12.2	9.1	9.5	11.0	6.6	8.2	9.8	9.5	13.5	8.1	Freezing section at the top of column. Configuration (B)
79.0	10.6	8.6	11.7	8.7	9.4	10.3	6.3	8.0	9.6	7.7	10.0	9.0	
89.0	8.6	9.3	11.7	8.7	5.5	8.6	5.4	7.6	8.8	5.8	9.9	5.5	
108.0	6.5	4.7	8.0	6.4	6.1	8.3	5.3	7.3	7.3	4.3	6.8	4.5	
113.0	6.4	3.8	6.3	8.3	7.2	9.4	8.2	8.3	8.3	5.2	7.6	4.0	

(a) Screw speed (Fig. 5.9)

The ratio of the stripping section length to the enriching section length is 0.27, that is, it compromises the freezing section of the column. This section does not operate with a compacted bed as does the enriching section but with a crystal slurry. The stripping section will be more sensitive to the mass flow rates into and out of the section. The effects of the screw speed were investigated at the two extremes of flow conditions, that is, with a high feed rate to the column together with a high base removal rate, and with a low feed rate to the column and a low base removal rate. In the first case the predominant flow is down the column, from the stripping section, the direction reversing for the second case giving a high value for L_S. The value of Y_S depends upon the concentration of ethanol entering the stripping section.

Operating with a high base product rate decreases the purification towards the top of the column, thus the liquid stream entering the stripping section is enriched in ethanol. When the column is operated with a low base product removal, the stripping section is flushed with liquid at the feed concentration. Also there is less opportunity for removal of adhering liquid from the crystals due to the reduced contact time for the wash liquid and crystals in the stripping section.

As seen in Fig. (5.9) a low screw speed gives similar ethanol concentrations in the top product stream. Under these conditions the diffusion and mass transfer effects are balanced. An increase in screw speed multiplies the diffusion effects with a reduction in the ethanol concentration of the top product stream. The initial rapid reduction for the low base product removal case is a result of the increased diffusion together with a reduction in washing efficiency as the crystals leave the stripping section at a greater rate. A further increase in screw speed improves the removal

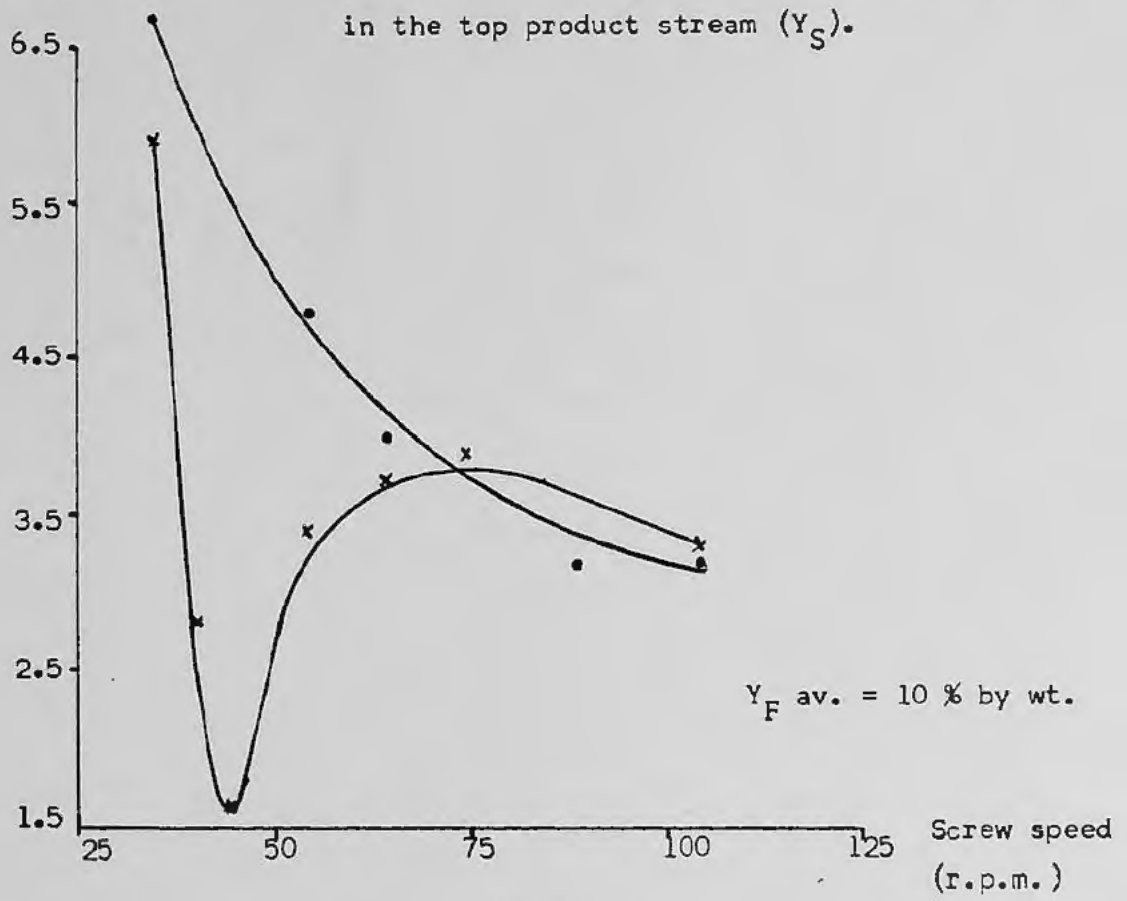

FIG. (5.9)

Effect of screw speed on ethanol enrichment in the top product stream (Y_S).

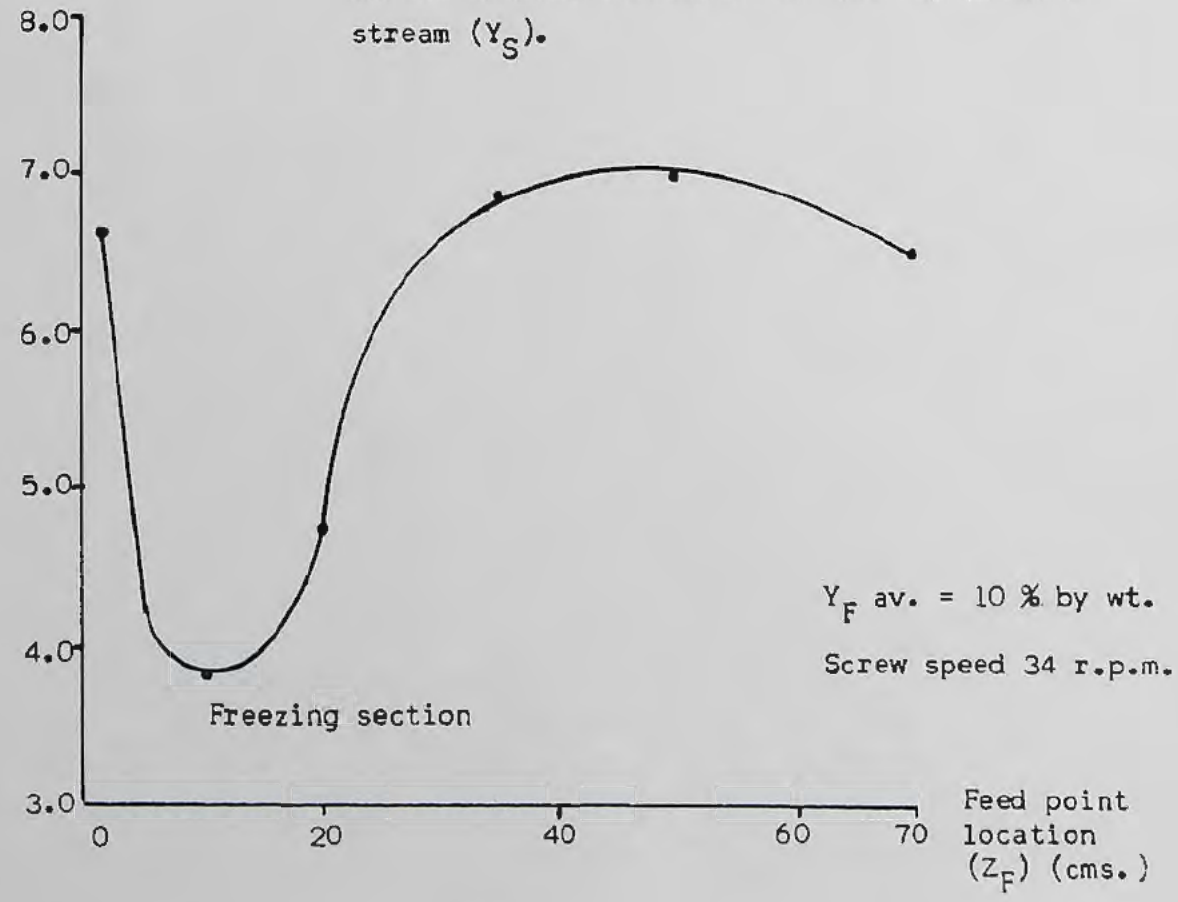

FIG. (5.10)

Effect of moving the feed point down the column on the ethanol enrichment in the top product stream (Y_S).

of ethanol from the adhering liquid by free liquid thereby elevating the ethanol concentration of the free liquid.

(b) Feed position Fig. (5.10)

The effect of moving the feed position down the purification section is shown in Fig. (5.10). This is effectively increasing the length of the stripping section approaching the system of the centre-fed column. The ratio of stripping section length to enriching section length has increased progressively to 0.71. Previous work with the 50 mm diameter column has shown a reduction in ethanol concentration in the overhead product as the above ratio increased to 0.67. This was caused by a reduction in washing efficiency as the purification section was shortened. An initial reduction in ethanol concentration was observed in the 100 mm diameter column, however as the feed point was moved down the purification section, it returned to its initial value.

This demonstrates the reduced sensitivity of the larger column to the changes in internal flows. With the much reduced washing section length it was still possible to remove ethanol from the adhering liquid. However, as the feed position approached the base of the purification section, a slight upward trend of increased ethanol concentration in the base product was observed. That is, there was a slight reduction in the washing efficiency with increased ethanol diffusion down the column, into the melting section.

(c) Top product removal rate Fig. (5.11)

When the column is operated at a constant feed rate and fixed feed impurity level, the overhead or top product rate is determined by the removal of base product. As we see from Fig. (5.11) operating with a high base product removal rate gives the optimum ethanol enrichment in the top product. The reflux stream entering the stripping section has an increased ethanol content. As a result

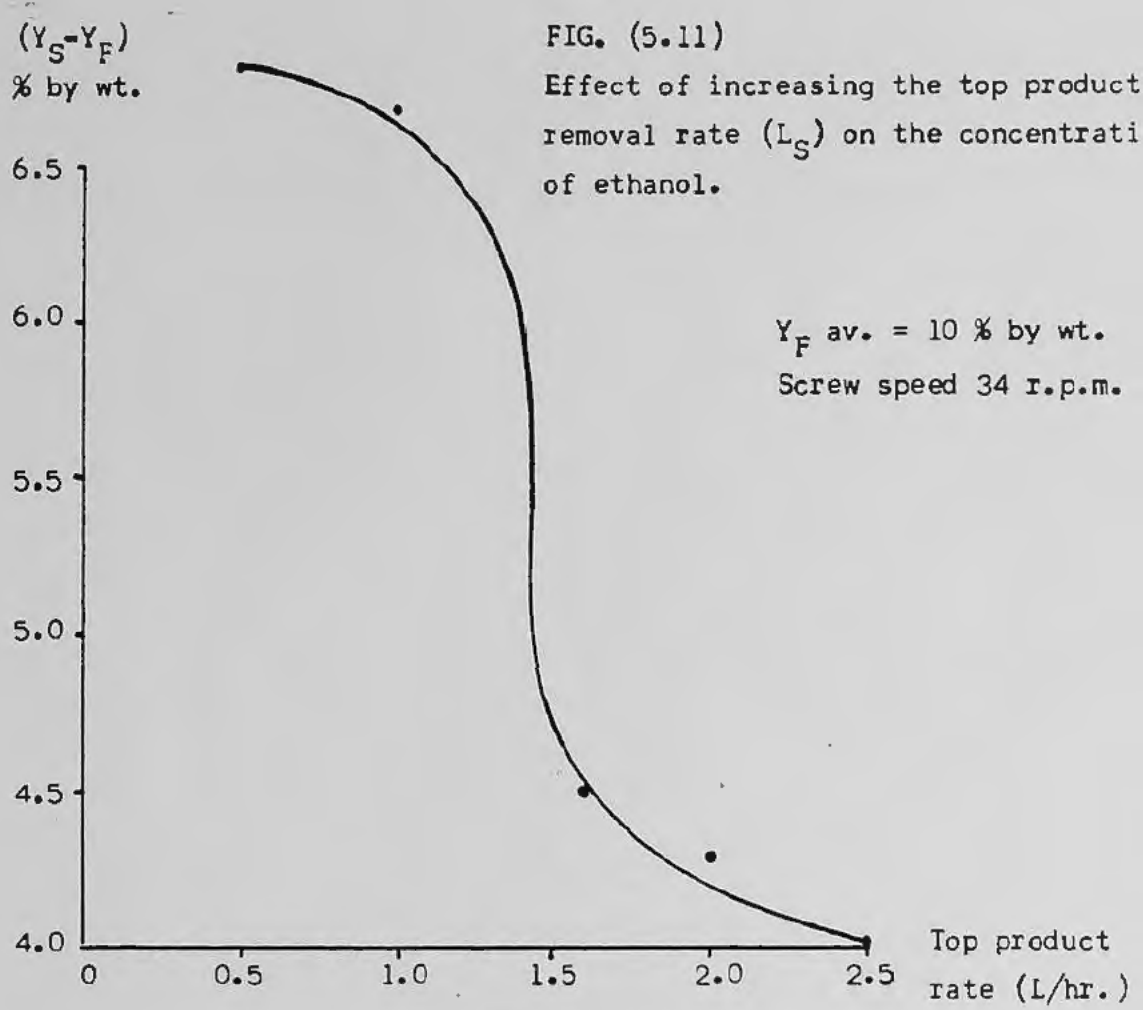

FIG. (5.11)
Effect of increasing the top product removal rate (L_S) on the concentration of ethanol.

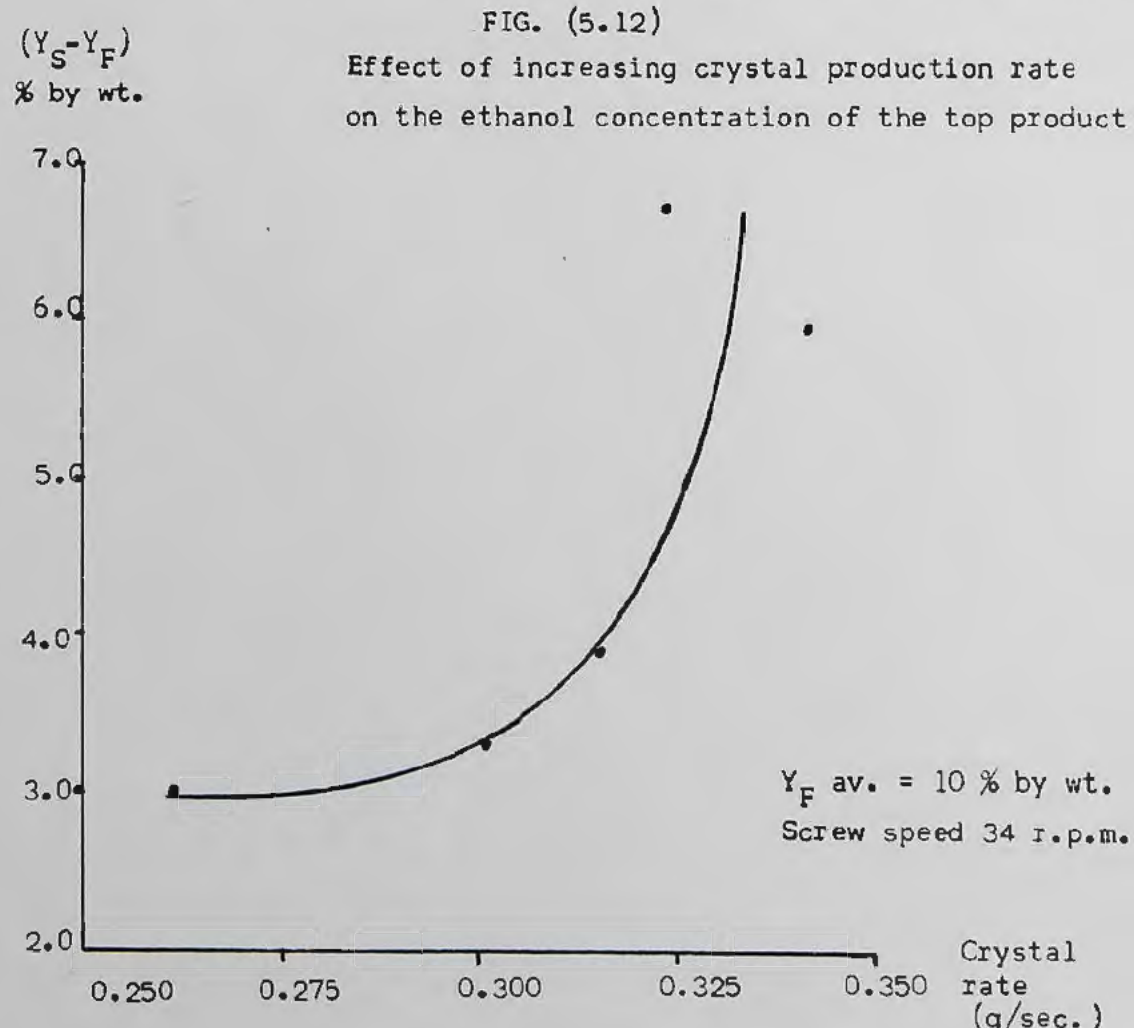

FIG. (5.12)
Effect of increasing crystal production rate on the ethanol concentration of the top product

of the low flow conditions in the section the crystals and ascending liquid stream have an increased contact time. The combination of the two maximises the ethanol enrichment in the overhead product. Reduction of the base product removal rate gives a corresponding increase in the overhead product rate, and a decrease in the ethanol content of the stream. For very low base product removal rates the stripping section is flushed with liquid at or very close to that of the feed stream to the column.

(d) Crystal production rate Fig. (5.12)

In the mathematical analysis of the stripping section, the crystal production appears as $(C + L_S)$ in the diffusion term and C^2 in the mass transfer term, that is:

$$H_S = \frac{D\eta A\rho}{(C + L_S)} + \frac{a(1 + a)\, C^2 + aL_SC}{(C + L_S)\, Ka\, A\rho} \qquad (3.57)$$

As the crystal production increases there should be a reduction in the diffusion together with an increase in the mass transfer as predicted by equation (3.57). Here we are looking for large values of H_S since these give rise to high values of Y in equation (3.55). This means the free liquid entering the stripping section is enriched in ethanol. As crystal production increases the ethanol concentration of the stripped stream should increase (since H_S is increasing) and there is no theoretical limit to the crystal production rate.

This trend is observed in Fig. (5.12), the ethanol concentration increasing markedly above a crystal production rate of 0.300 g/sec. However the limiting factor to increased crystal production is the capacity of the refrigerant system to maintain these levels. This maximum was 0.342 g/sec., on a continuous basis, for the series of crystal production rate investigations.

(e) Effect of liquid pulsing on column performance

Previous attempts had been made to use an oscillating motion coupled with the rotation of the screw conveyor. The screw was oscillated through a set distance at a fixed frequency with the object of improving mass transfer, whilst not increasing the effects of axial diffusion. Mechanical oscillation of the 50 mm diameter screw(amplitude 6 mm, frequency 104 per minute) destroyed the concentration gradient in the column with diffusion of impurity down the column. The injection of a liquid pulse into the column had less severe effects, but the increased diffusion negated any improvement in washing efficiency.

Mechanical oscillation of the 100 mm diameter screw was not investigated, however the effect of introducing a liquid pulse at the feed point was studied. This was achieved using a variable stroke length displacement pump. A comparison of concentration profiles for runs with and without pulsing are shown in Fig. (5.13). There was a reduction in ethanol concentration in the overhead product and a reduction in the ethanol concentration of the free liquid in the purification section. The use of a liquid pulse improved the washing of adhering impurity from the crystals without increasing the diffusion down the column. Operating the column in the conventional sense, that is, removal of most of the ethanol from the enriched product, the liquid pulse reduced impurity levels down the column. However with the present system, this reduced the concentration of ethanol in the liquid entering the stripping section, with the subsequent reduction in its concentration in the overhead product. Generally it appears using columns with a small cross-sectional area, the adhering impure liquid can be successfully removed at the level of agitation generated from the use of a screw conveyor alone.

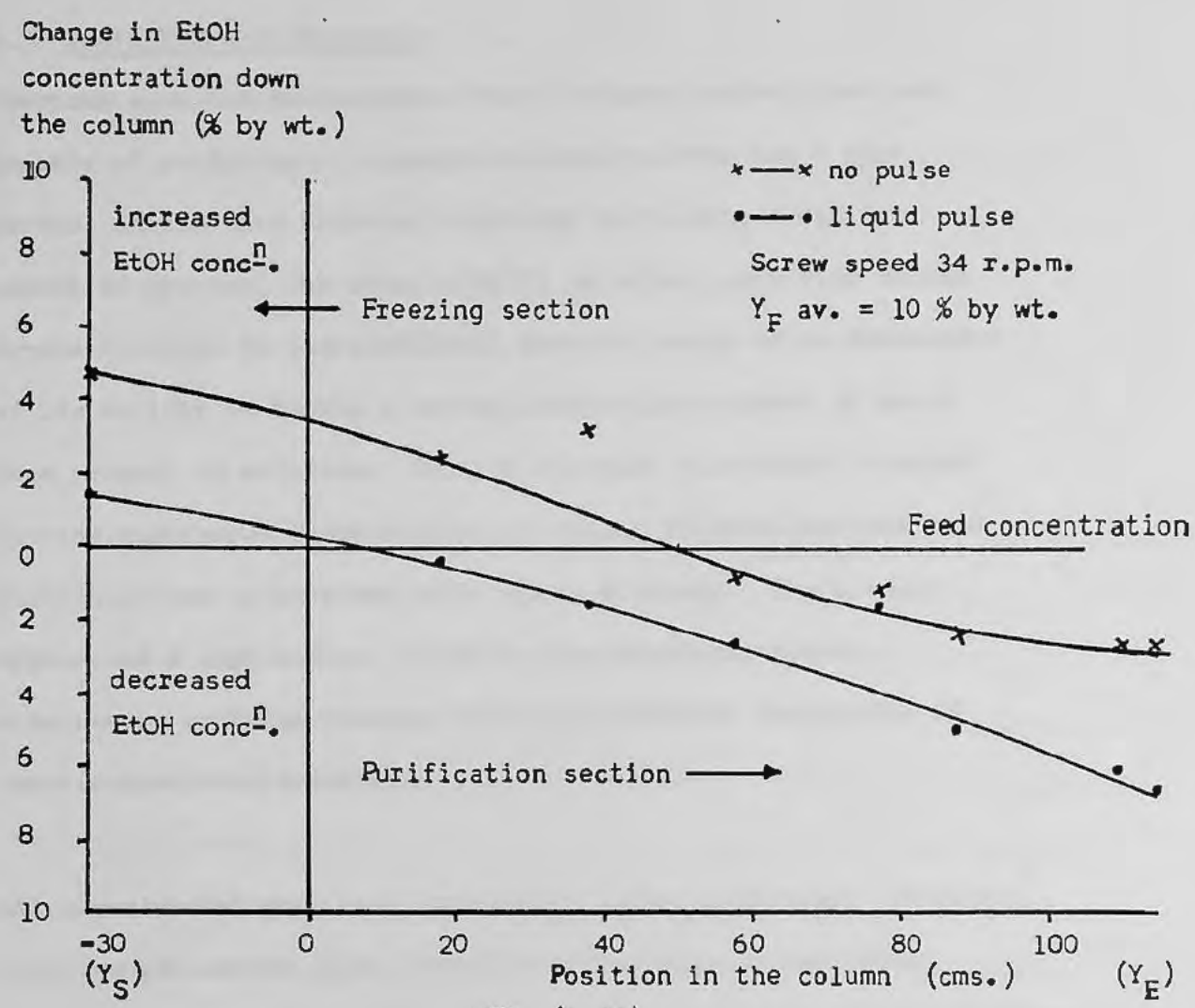

FIG. (5.13)

Effect of liquid pulse on the Ethanol concentration profile

5.3 Waste Effluent Recovery

Previous work had demonstrated that a column crystalliser was capable of producing a concentrated waste stream and a pure product stream when treating solutions containing a minimum number of species, for example Na:Cl in water. Applying column crystallisation to waste effluent recovery would allow assessment of its ability to handle a system containing a number of metal ions present in solution. Earlier attempts to produce a system for the continuous concentration of copper sulphate had not been successful due to problems with column blockage. The present system had a high sodium chloride concentration, thereby eliminating problems arising from the nucleation and growth of non-transportable crystals.

All experimental runs were carried out under continuous operation, the same parameters being recorded as for runs in the 100mm diameter column. The mathematical analysis used for the desalination work was applied to the 50mm diameter column. Over a range of crystal production rates equations (3.48) (3.49) and (3.54) were evaluated and the Diffusion, D, and Overall Mass Transfer terms, Ka, determined for the set operating conditions.

The variables investigated were:

(a) Screw speed

(b) Increasing (Z_F), moving the feed position down the column

(c) L_E = product flow rate

(d) C = solids flow rate in the enriching section

The variables held constant were:

(a) Y_F = feed composition

(b) Freezing section, purification section, melting section lengths.

Calculated values for the column parameters were:

$$Ka = 9.96 \times 10^{-3} \quad sec^{-1}$$

$$D = 0.44 \quad cm\ sec^{-1} \quad \text{at 60 rpm}$$

Over the range of crystal production rates investigated, the contribution of the values of D and Ka, in equation (3.48), in determining the separation achieved, indicates that the diffusion will be more important than the overall mass transfer in establishing the impurity distribution in the column. In the 100mm diameter column, the values were such that the overall mass transfer term was dominant, suggesting that diffusion down the column had little effect upon the final separation achieved. Operating the smaller column for maximum separation required the supression of parameters promoting axial diffusion, whilst at the same time maintaining the removal of adhered impurity by washing.

Continuous Operation: Column configuration (B)

A summary of the experimental variables is presented in Table (5.10) together with the relevant concentration profiles in Table (5.11).

Waste Effluent Recovery : Experimental Results Table (5.10)

Run Number (WE)	Feed Rate (g/hr.)	Feed Composition (p.p.m.)	Distance of feed point from freezing sectn	Crystal Rate (g/sec.)	Enriched Product Rate (g/hr.)	Enriched Product Composition (p.p.m.)	Screw Speed (r.p.m.)
1	1070	36000	0.5 (cms.)	0.178	363	5000	52
2	1107	34500	0.5 "	0.185	367	7000	60
3	1029	34500	0.5 "	0.193	366	4500	76
4	1099	35500	0.5 "	0.193	362	4000	60
5	1130	35500	0.5 "	0.229	370	7000	100
6	1105	35500	0.5 "	0.216	353	8500	120
7	1113	36000	0.5 "	0.226	353	3500	60
8	1085	35000	6.0 "	0.196	358	11000	60
9	1142	35000	18.0 "	0.202	357	12000	60
10	1092	36000	24.0 "	0.203	359	17500	60
11	1159	35000	0.5 "	0.233	513	7500	60
12	1140	34500	0.5 "	0.277	664	12500	60
13	1150	34500	0.5 "	0.237	830	19500	60
14	1110	33500	0.5 "	0.181	360	9500	60

Waste Effluent Recovery : Experimental Results Table (5.11)

Distance from the feed point (cms)	Concentration of salts in the Free Liquid (p.p.m.) : Concentration Profiles (values x 10^3)													
	WE 1	WE 2	WE 3	WE 4	WE 5	WE 6	WE 7	WE 8	WE 9	WE 10	WE 11	WE 12	WE 13	WE 14
-31.5	47.5	47.5	52.0	52.0	52.0	49.0	56.0	47.0	47.0	45.0	64.0	68.0	68.0	45.5
12.0	24.5	27.5	23.5	27.0	23.5	23.0	27.0	27.0	31.0	24.5	23.0	31.0	31.5	24.0
24.0	17.5	17.5	16.5	22.5	20.0	16.0	18.0	21.0	29.0	24.5	13.5	27.0	24.0	17.5
36.0	12.5	12.5	7.0	11.5	12.5	12.5	7.5	15.0	18.5	20.0	10.5	16.5	22.5	17.5
62.0	5.0	7.0	4.5	4.0	7.0	8.5	3.5	11.0	12.0	17.5	7.5	12.5	19.5	9.5

Freezing section at the top of the column (configuration B)

Runs WE1 to WE14 Crystals transported downwards

A comparative analysis for the column operating at low product removal rate with a high crystal production rate is presented in Table (5.12). The concentration of the various metals being determined by A.A.S. The concentrations of metal ions in the product are very low and are comparable to those obtained by Campbell and Emmerman [12] using a S.R.F process.

Element	Concentration in Feed m_g/L	Concentration in Product mg/L	Percent removal
Nickel	101	0.58	99.43
Chromium	99	0.10	99.89
Cadmium	113	0.16	99.86
Zinc	178	0.98	99.45
Iron	129	0.25	99.81

Table (5.12) Metal ion separation test results

Notes: The impurity content of the product stream was 150 mg/L, determined from conductivity measurements, hence the major impurity in the product stream was sodium chloride. This corresponded to an average removal level of 99 percent, the sodium chloride concentration being taken as the difference in the product analysis above.

These low levels of impurity are obtained only under carefully controlled conditions, these being determined by the screw speed, crystal rate, and base product removal rate. Generally the level of impurity in the base product is much higher, approximately 3500 mg/L, allowing easier operation of the column under continuous conditions for extended periods. To obtain these low levels in a practical system would require the use of multiple pass or a cascade system.

(a) Screw Speed

The speed of rotation of the screw was investigated over the range of 50 to 120 rpm. The screw speed determines the level of mixing, within the column, hence at low screw speed, agitation is less than at the higher screw speeds. For this system, where the diffusion is expected to be the controlling factor limiting the separation, greater screw speeds will increase mixing and transport of solid material down the column, with the resultant increase in axial diffusion of impurity. This effect is observed in Fig (5.14) where minimum impurity levels are obtained at 60 rpm. Below this value the slight increase in impurity is due to a reduction in washing efficiency which is to be expected with the lower levels of agitation. However as the screw speed is increased up to 120 rpm, the impurity levels in the product stream rise, due to the diffusion of impurity down the column. The overall mass transfer rate does not increase correspondingly, hence an increase in impurity associated with the crystal phase.

(b) Feed Position

The influence of feed position on product quality is shown in Fig (5.15). The effect of increasing Z_F is to increase the impurity in the product. This behaviour is predicted by equation (3.54) which describes the concentration profiles in the enriching section. As with the 100 mm diameter column the best separations were achieved with Z_F at a minimum, any increase in this value reducing the length of the enriching section. This has two consequences, the purification section length is effectively reduced, decreasing washing capacity and efficiency, and axial diffusion exerts a greater effect upon the concentration gradient in the enriching section. The immediate increase in impurity of the product demonstrates how much more sensitive is the 50 mm diameter column to changes in operating conditions.

FIG. (5.14)

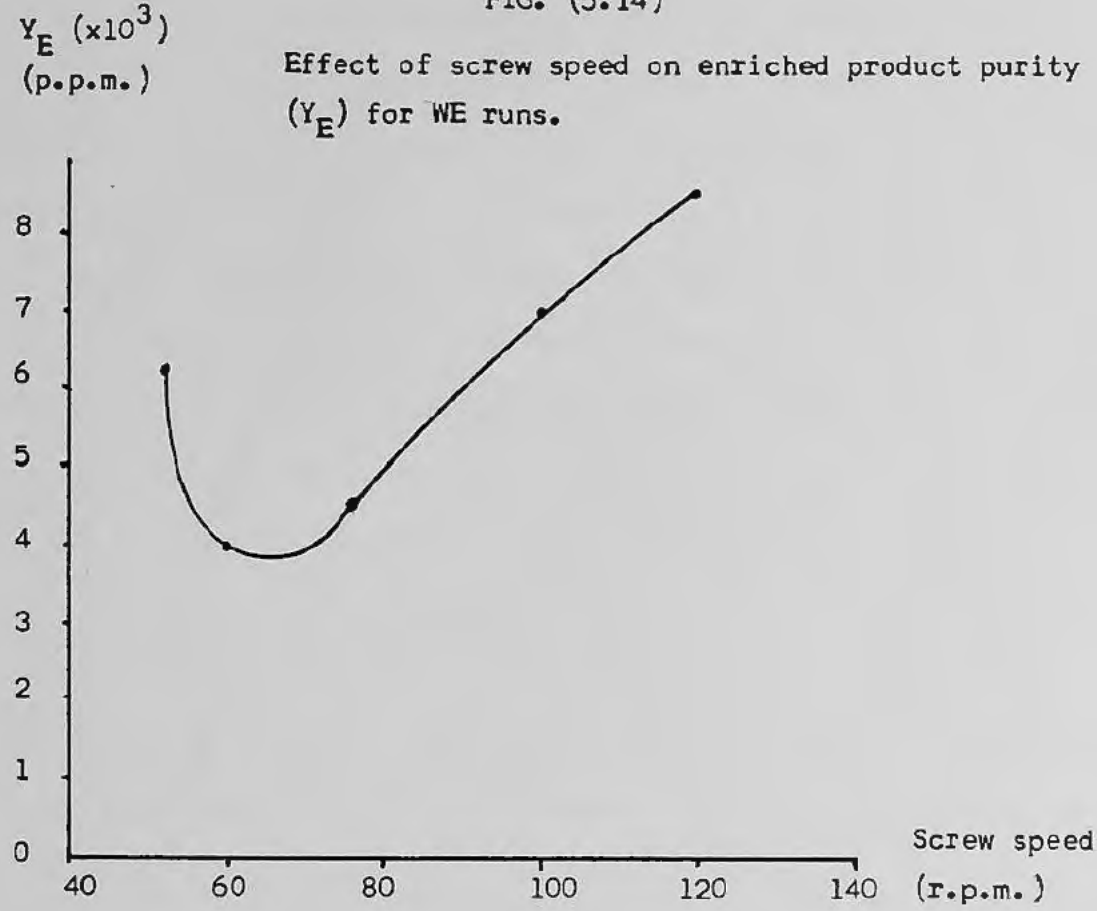

Effect of screw speed on enriched product purity (Y_E) for WE runs.

FIG. (5.15)

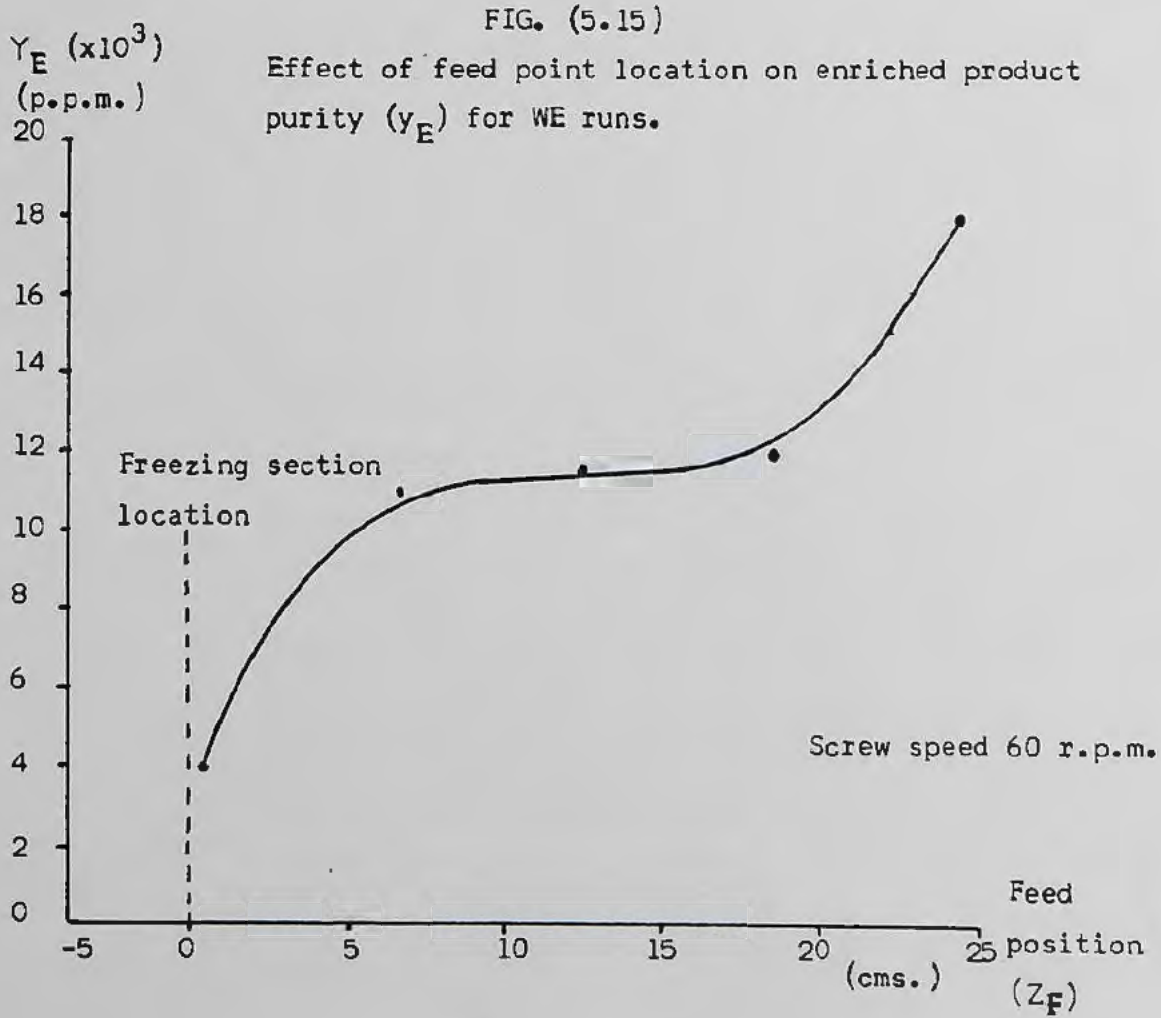

Effect of feed point location on enriched product purity (y_E) for WE runs.

(c) Product removal rate

The impurity level of the product is governed by the quantity of adhered impurity associated with the crystals after their passage through the purification section. The driving force for impurity removal is the concentration difference between the stream of free liquid and the layer of adhered impure liquid around the crystals. This has been expressed as the quantity of reflux liquid returned to the column, and it has been shown that for the 100mm diameter column, base product removal rates could be high without significant reduction in product purity. However the ultimate purity of product was correspondingly low. This was attributed to the lower levels of mixing and reduced contacting of reflux liquid in the column. A comparison with the 50mm diameter column showed how much more effective were the mass transfer processes, hence the rapid response of the column to changes in operating conditions.

Examination of Fig (5.16) shows the effect of increasing the enriched product removal rate on the impurity level of the product. As the value of L_E increases, there is a corresponding increase in Y_E. This increase is predicted from equation (3.48). As the magnitude of $(C-L_E)$ decreases there is an upward trend in the H_E values which corresponds to a reduction in the separation achieved. Removing more product reduces the quantity of reflux liquid in the column ($R_E = L_E/C$) which adversely affects the washing efficiency. When $L_E \gg LS$ there is an increased flow through the enriching section (co-current with and in the direction of crystal transportation), hence an increase in the impurity by axial diffusion down the column. For a base product removal rate of 830 g/hr, the product purity is only reduced to two thirds of the feed impurity.

(d) Crystal production rate

The effects of increasing crystal production rates have been previously discussed in the desalination system. Here the 100mm diameter column operated over a range of C = 0.396 to 0.527 g/sec. With the present study the effective working range was found to be 0.181 to 0.225 g/sec, comparable to those measured for the desalination system investigated in earlier work on the column. The experimental results are presented in Fig (5.17), a point to note is the levelling from 0.200 g/sec to 0.225 g/sec. Reduction in impurity over this range is only 750 mg/L. Operating the column at crystal production rates in excess of 0.225 g/sec made column operation for extended periods unstable, that is, column blockage in the freezing section occurred. This tailing off in impurity removal can be explained in terms of reduced washing efficiency. The more crystals produced, the more compacted is the crystal bed. Contacting of the reflux liquid with adhered impure liquid is subject to rate controlling diffusion processes.

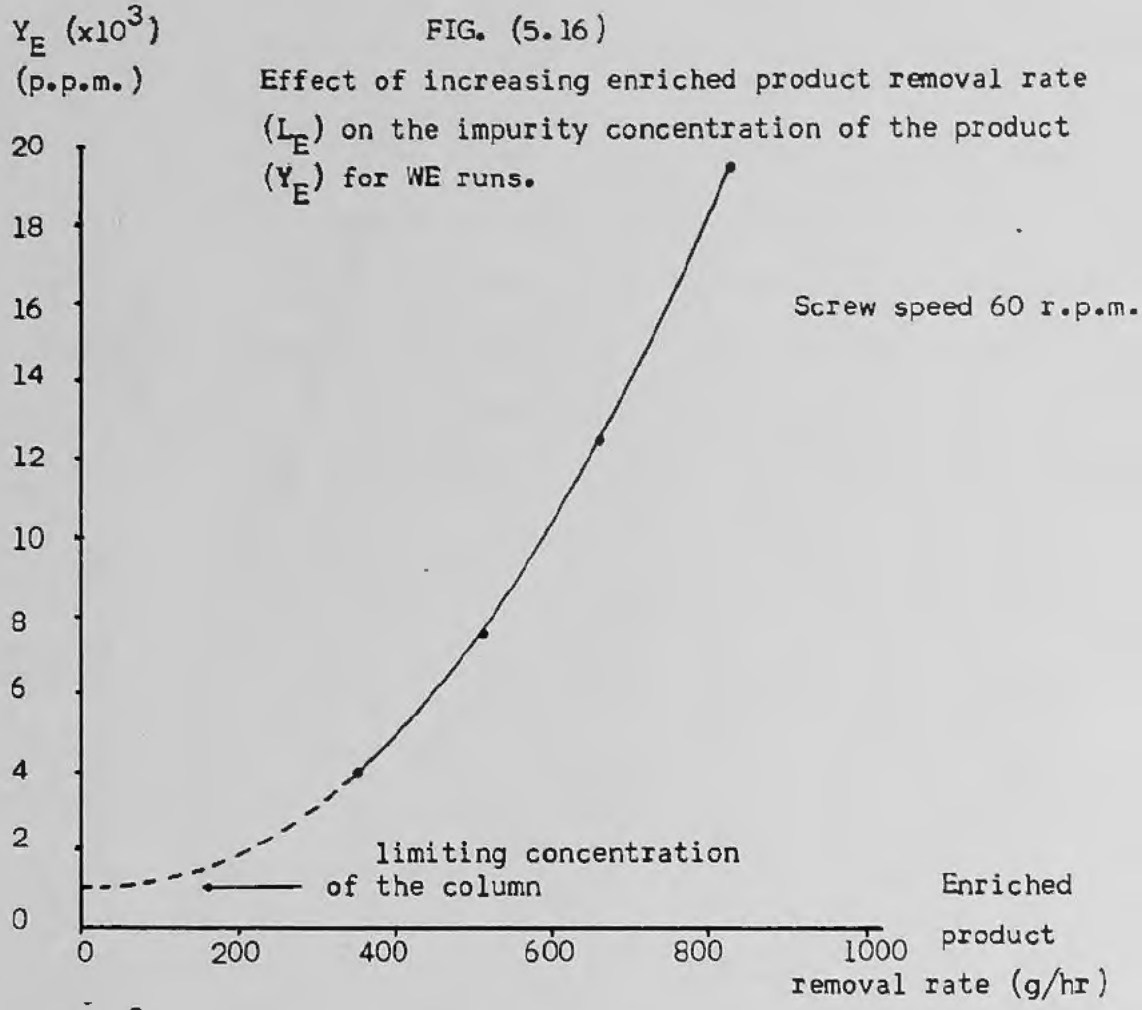

FIG. (5.16)

Effect of increasing enriched product removal rate (L_E) on the impurity concentration of the product (Y_E) for WE runs.

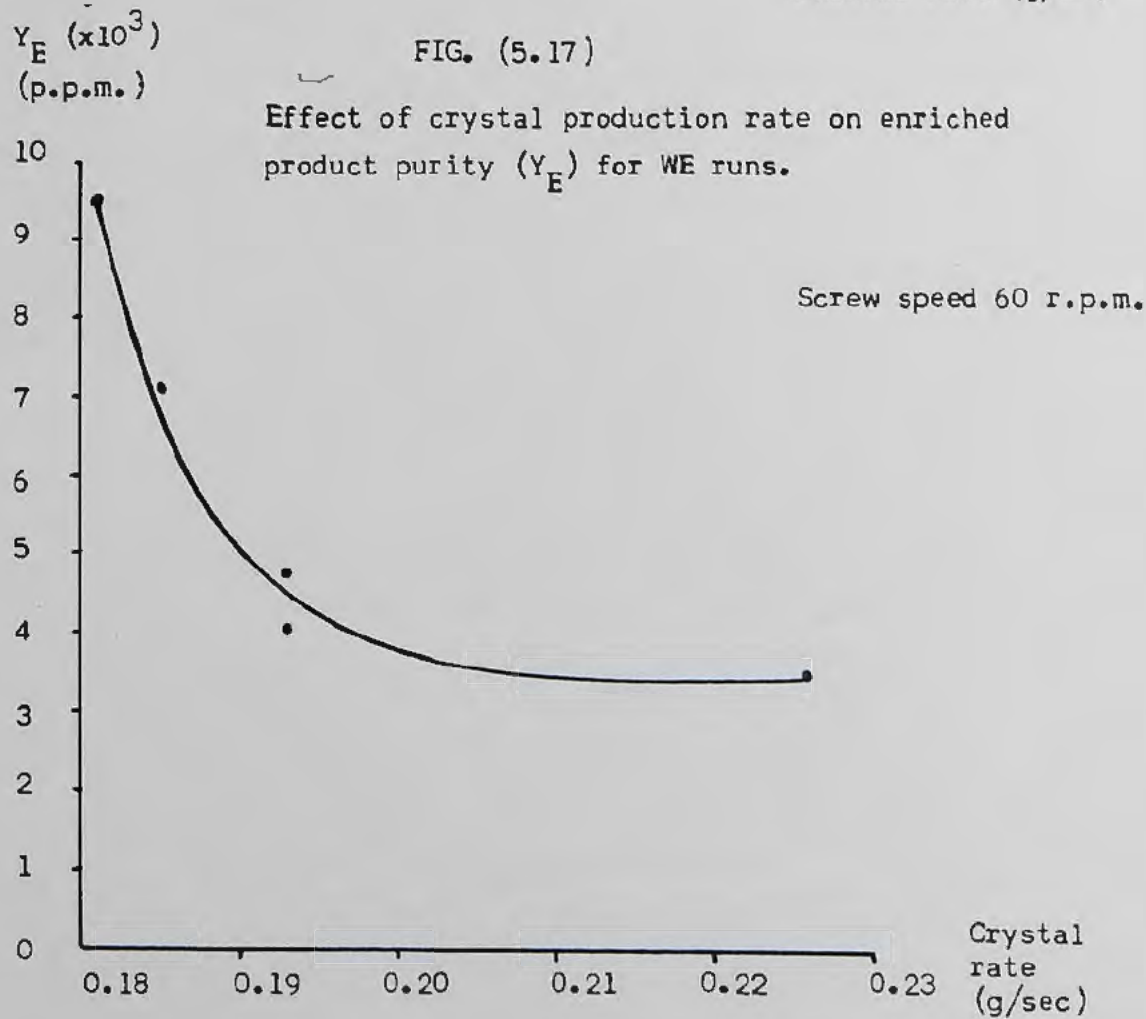

FIG. (5.17)

Effect of crystal production rate on enriched product purity (Y_E) for WE runs.

(5.4) Heavy Water Regeneration

Previous work with the water : heavy water system had shown the necessity for using a crystal modifier to produce crystals that could be transported with the screw conveyor. Introduction of a third component into the system made the analysis of the component concentrations more difficult. Ethanol was used in the experimental runs since it was miscible with the aqueous components, and it was possible to remove it from the product streams during crystallisation. This gave a product stream, ethanol-free, and a waste stream enriched in ethanol. The initial analytical technique required the accurate weighing of 10 mls of the feed, base and top products. It was not possible to sample the length of the column and obtain a concentration profile. However it was calculated that an upgrading of the heavy water concentration from 75% to 80% was possible at a screw speed of 60 rpm.

Using the calculating digital density meter it was possible to remove samples along the whole length of the column and obtain an accurate density measurement to four places of decimal. Since this technique was more accurate and reproducable than a simple weighing of a sample, it was possible to monitor the changes in density down the column, whilst varying different operational parameters. The problems associated with the variation in ethanol concentration along the column were discussed in section 4.5 (d), the correlation between the percentage of ethancl in the mixture and the density of the mixture is shown in fig (5.18). For the prepared standard solutions the percentage of heavy water was maintained as close to 79.5% as was possible, the variations being the ratio of water to ethanol.

On the same graph is plotted a series of feed stock solutions used in the experimental runs. In this case the percentage of heavy water in the mixture averaged 79.9%, hence the higher density readings observed for the same ethanol concentration. Extrapolation of this line back to zero ethanol concentration, gives the density readings we should obtain if the removed ethanol was replaced by water, there being no increase in the heavy water concentration. Density values recorded for experimental runs, where the feed concentration of heavy water was in the range 79.5% to 79.9%, exceeded the predicted values, showing there had been a slight enrichment in the heavy water component.

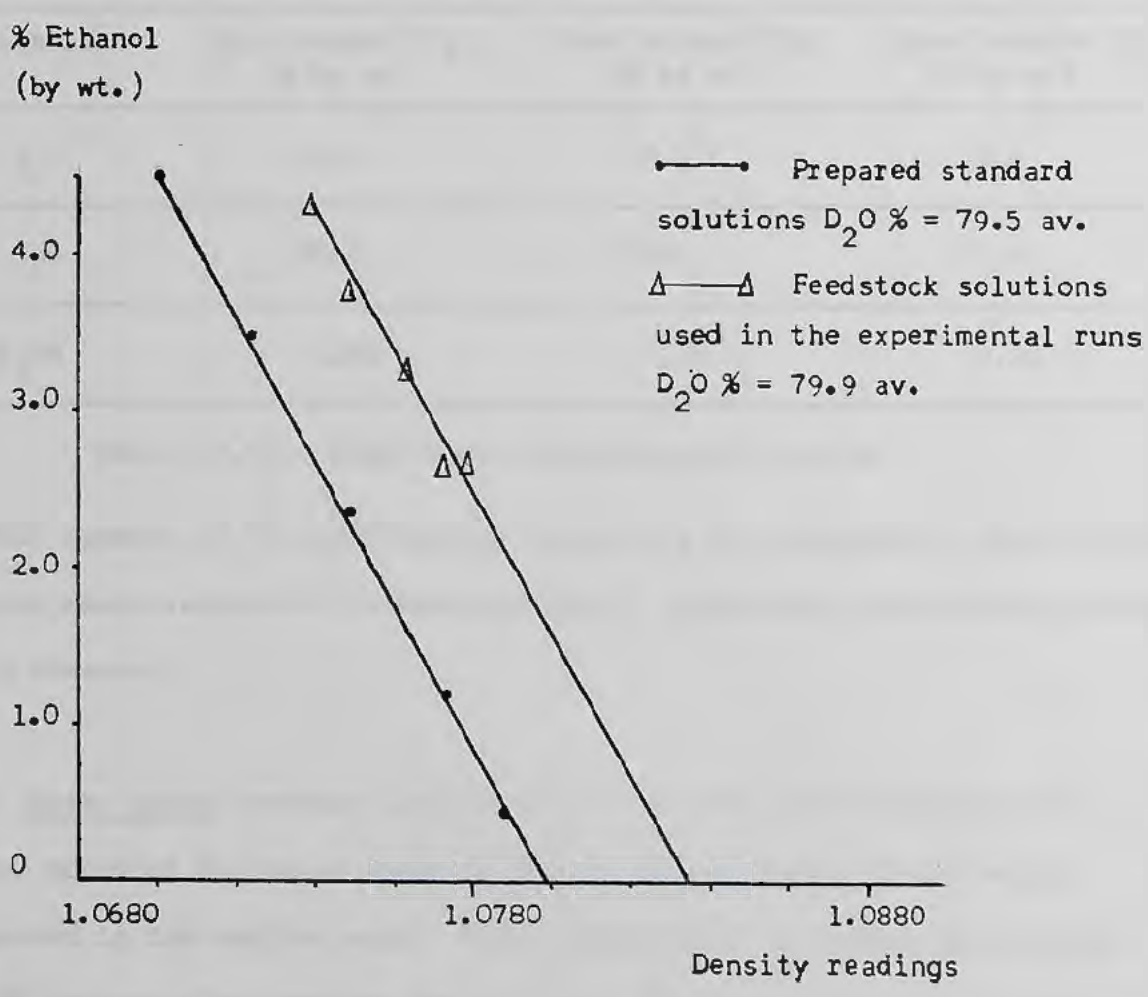

Fig (5.18)

Correlation of ethanol concentration of the mixture with the density of the mixture

Optimisation of the heavy water: water system was carried out as with previous investigations, the main operational parameters varied being; screw speed, feed point location, changes in reflux ratio and crystal production rates.

A mathematical treatment of the results was not possible because the concentration gradients were such that there was little enrichment of D_2O above the feed concentration. The maximum increase recorded was 2.32% for C = 0.254 g/sec and screw speed = 60 rpm. The variation in the concentration of the three streams is shown below, a typical concentration gradient being:

Component	Top Product (Y_S) (% by wt)	Feed Stream (Y_F) (% by wt)	Base Product (Y_E) (% by wt)
H_2O	16.2	17.2	18.4
D_2O	79.2	79.6	81.4
C_2H_5OH	4.58	2.88	0.20

Table (5.13) Heavy water concentration profile

A full summary of the experimental parameters is presented in Table (5.14). Within small variations in the heavy water enrichment the following trends were observed.

(a) Screw Speed Maximum enrichment of the heavy water occurred at a screw speed of 60 rpm as shown in Fig (5.19), a similar trend being observed in the earlier work. This maximisation of column performance at 60 rpm was also recorded for the Waste Effluent regeneration work, the minimum levels of impurity being achieved at this point. The ethanol does not freeze out and is discharged, elevated in concentration in the overhead product. This allows a small fraction of the heavy

Heavy Water Regeneration : Experimental Results Table (5.14)

Run No	Feed compⁿ % ETOH > % D_2O by wt >	Feed point Z_F cms	Feed rate (g/hr)	Enriched product (g/hr)	Enriched compⁿ % by wt	Crystal rate (g/sec)	Screw speed (rpm)
1	3.01 79.98	0.5	970	230	0.67 81.43	/	52
2	4.14 79.63	0.5	1024	221	0.03 81.95	0.254	60
3	2.64 84.80	0.5	950	218	0.04 87.07	/	66
4	2.93 79.86	0.5	1018	224	0.09 81.99	/	75
5	2.59 79.39	0.5	989	255	0.03 81.21	/	90
6	2.86 79.74	0.5	1002	225	0.08 81.29	/	120
7	2.96 80.11	6.5	1051	261	0.25 81.55	/	60
8	3.13 79.99	12.5	1114	269	0.37 81.49	/	60
9	2.84 79.70	18.5	1029	251	0.21 81.43	/	60
10	4.10 79.62	0.5	1115	280	0.25 81.72	0.190	60
11	4.07 80.02	0.5	963	228	0.09 81.99	0.214	60
12	4.52 79.93	0.5	1005	213	0.21 81.74	0.190	60
13	3.95 79.10	0.5	1063	302	0.88 81.54	0.189	60
14	4.14 79.65	0.5	1040	166	0.08 81.22	/	60
15	2.83 79.41	0.5	1018	238	0.04 80.86	0.159	60
16	2.81 85.23	0.5	930	196	0.32 85.42	0.140	60

FIG. (5.19)

Effect of screw speed on the upgrading of the Heavy Water component.

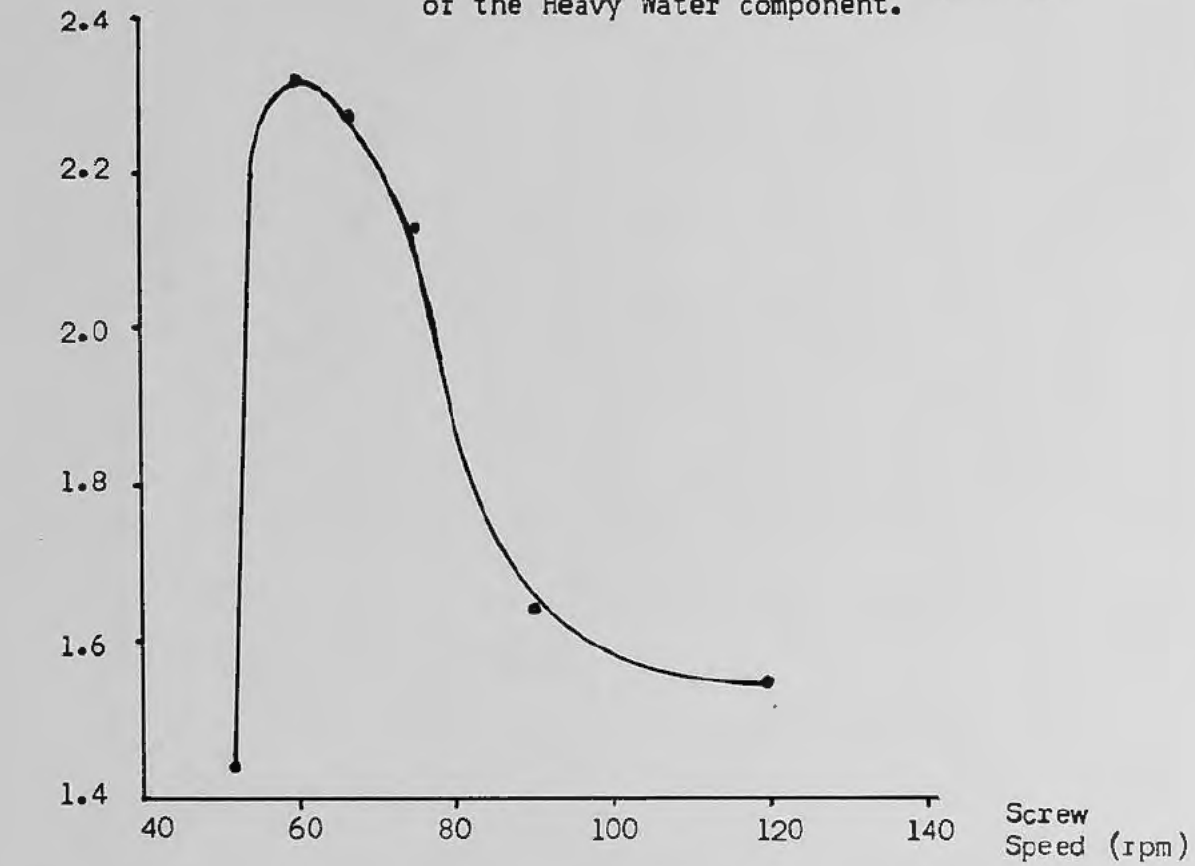

FIG. (5.20)

Variation in the maximum Heavy Water upgrading with change of feed position.

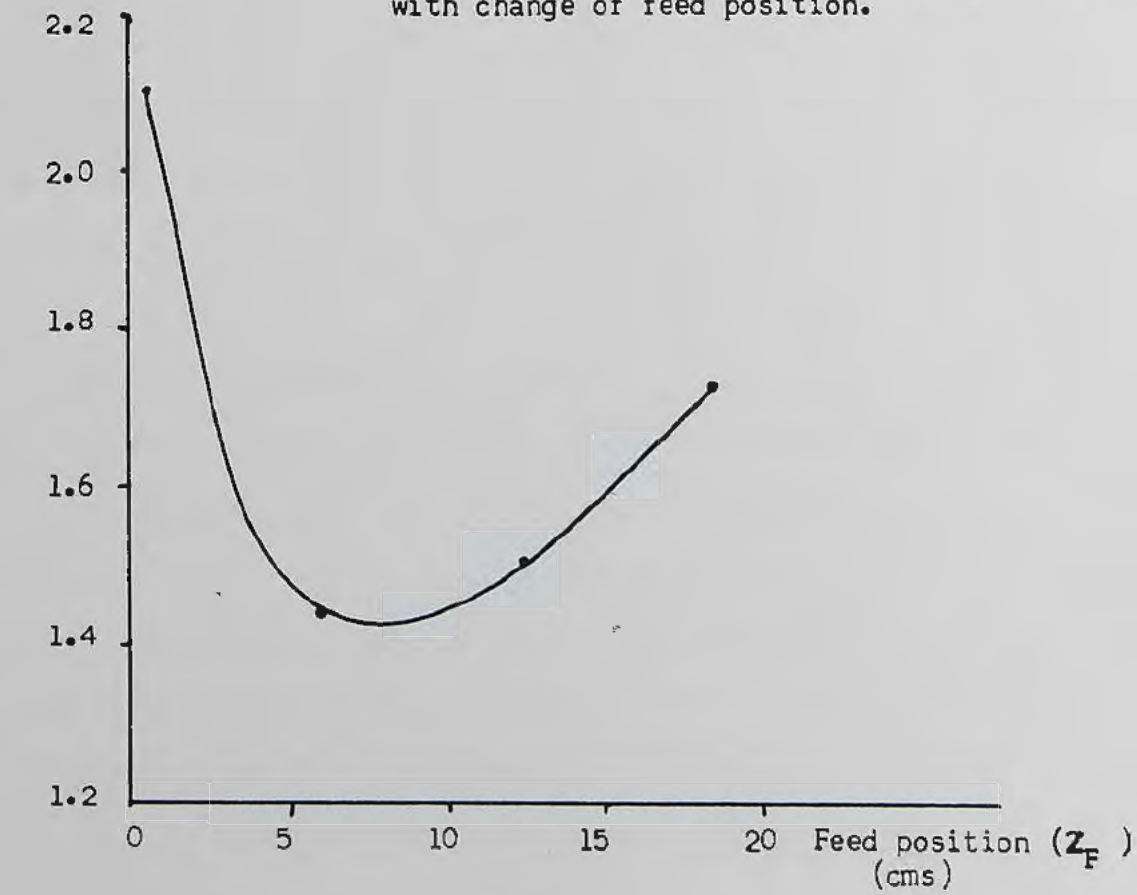

water to crystallise and be transported out of the freezing section together with water and ethanol impurity. As the crystals descend the column, the impurity level is reduced, the product being recovered essentially ethanol-free. As the screw speed is increased, the residence time for the crystals in the freezing section is reduced with the resultant decrease in heavy water concentration.

(b) Feed point variation The best upgrading of heavy water was achieved with the feed point located as close to the freezing section as possible. Fig (5.20) shows the rapid decrease in enrichment as the feed position is moved down the column. However the reduction in the final product concentration of heavy water was less than 0.7% of the highest concentration recorded.

(c) Product ratio (Fig (5.21))

Operating the column at constant feed rate whilst increasing the take-off of base product, produced the highest levels of heavy water enrichment. This is the reverse of the trends observed with the other systems investigated, where an increase in L_E produced a corresponding increase in Y_E. The variation in heavy water upgrading over the range of base product removal rates investigated, was approximately 0.9%.

(d) Crystal production rate Fig (5.22)

There was an initial rapid rise in the percentage increase of heavy water, this corresponding to a rapid reduction in impurity levels of the base product observed with the other systems. However once a crystal mass had been formed in the column, $C > 0.16$ g/sec an elevation of only 1% was observed up to a crystal rate of $C = 0.26$ g/sec.

FIG. (5.21)

Increase of the Heavy Water component with increasing product removal rate.

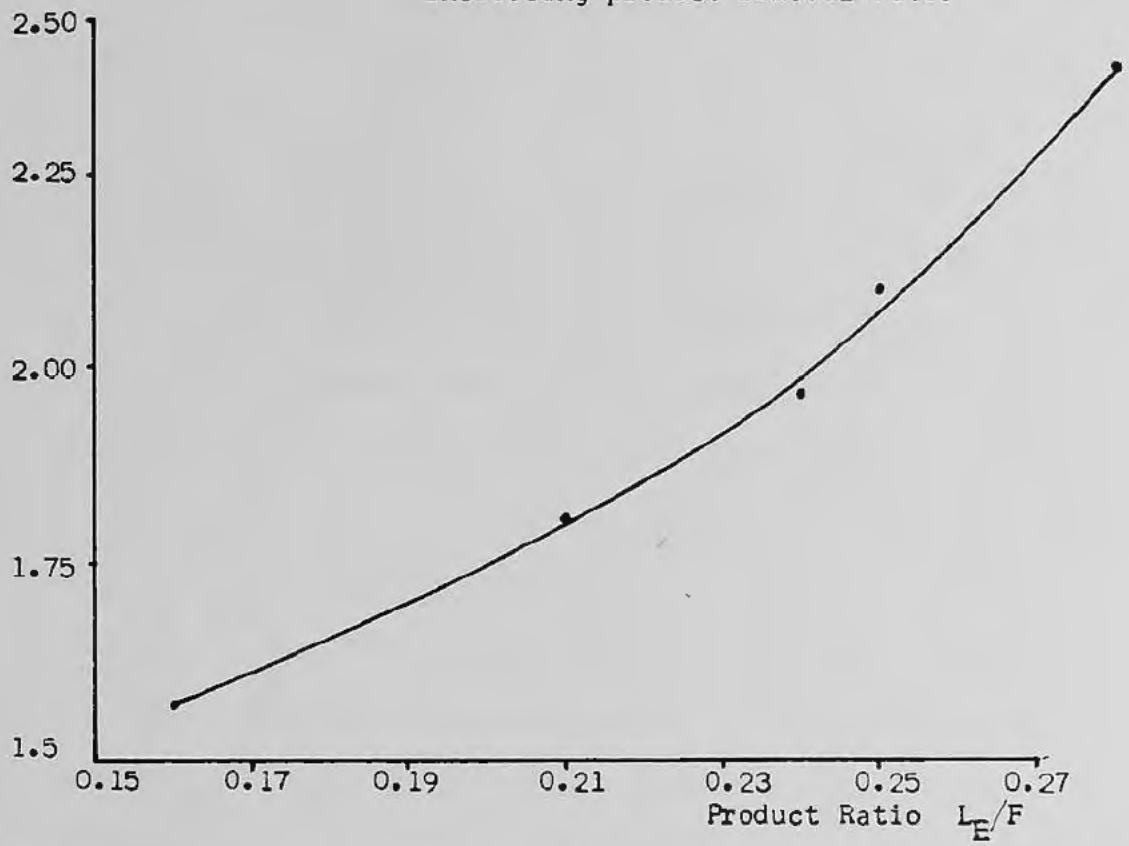

FIG. (5.22)

Effect of increasing crystal production rate on the percentage increase in Heavy Water.

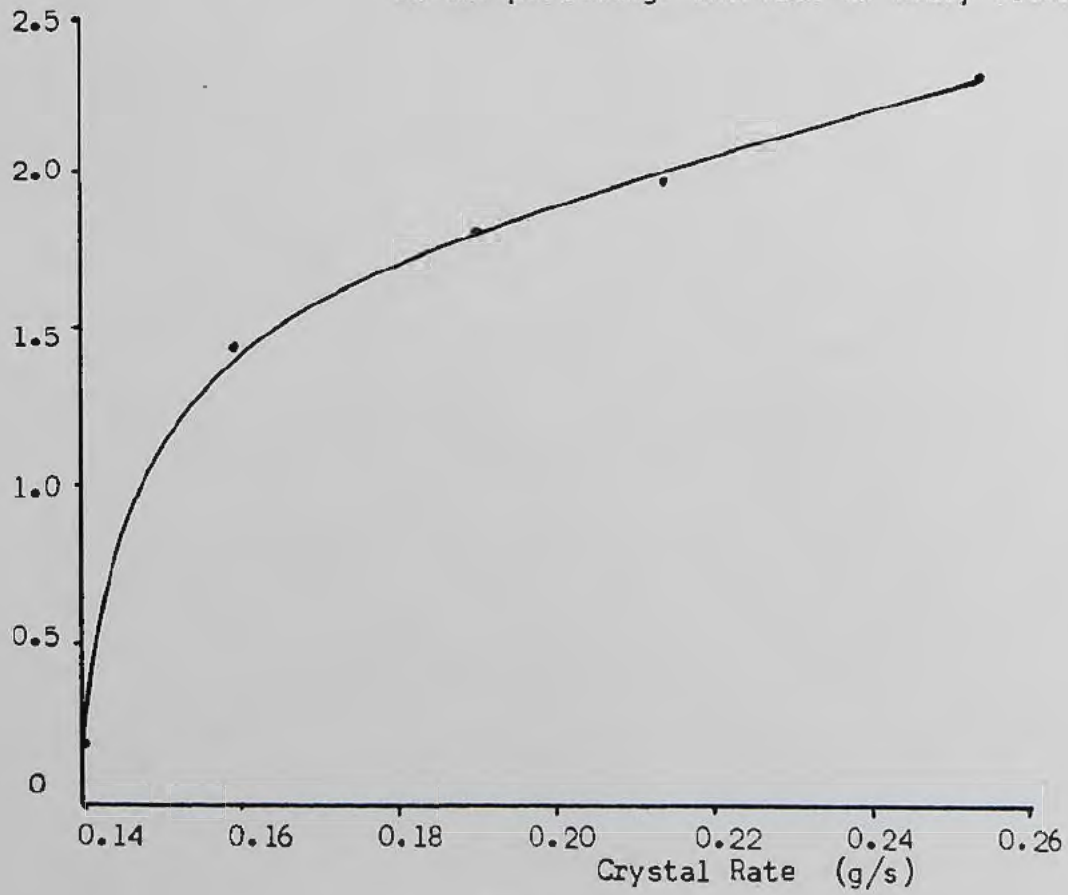

Chapter 6

General Discussion

(6.1) Effects of diffusion and mass transfer

The application of continuous column crystallisation to several aqueous systems was studied with a view to elucidating the dominating factors controlling column performance. A mathematical model has been utilised to give a comparison between experimental results and theoretical results generated from the model. The two parameters determining the separations achieved within the column, are the Axial Diffusion (D) and the Overall Mass Transfer rate (Ka). These two terms have been incorporated into the model, together with experimentally determined parameters, to give a final equation describing the separating power of the column (H_E and H_S). Calculating values for these two coefficients from experimental measurements allows subsequent theoretical evaluations to be carried out. From the series of experiments the values of D and Ka calculated have been used to generate theoretical concentration profiles and separation factors (See Appendices A2, A3, A4). This has allowed a comparison between the experimental results and the theoretical calculations.

The column process has been investigated in two modes , that is, to produce a low impurity enriched product (Desalination) and a concentrated, recovered product (Ethanol concentration). In the former this has required the suppression of diffusion down the column with maximisation of mass transfer between the adhering and reflux liquid. In the latter it is necessary to have the highest ethanol concentration possible entering the stripping section. Calculating the Diffusion and Mass Transfer Coefficients

gives an indication of which effect is predominant in the different systems. Several workers (52, 39, 42, 151, 153) have carried out somewhat similar analyses and their results are compared with those for the present studies. These are presented below in Table (6.1).

Column	Screw Speed (r.p.m)	Diffusion D ($cm^2\ s^{-1}$)	Overall Mass Transfer Ka (s^{-1})
Moyers[52] (Dense-Bed Crystalliser)	120	0.20 - 0.30	Uses a non-extractive washing model. No Mass Transfer term.
Ritter[52] (Countercurrent ice wash column)	-	0.025 - 0.17	-
Albertins[39] (Spiral conveyor-Total Reflux)	59	1.6 - 3.5	1.9×10^{-4}
Gates[42] (Spiral conveyor)	60	1.3 - 1.7	$0.075\text{-}0.64 \times 10^{-3}$
Cutts & Wells[151] (Spiral conveyor)	60**	0.25	0.26×10^{-2}
	90**	0.63	0.06×10^{-2}
50mm Column[153] (Spiral Conveyor)	60**	0.56	0.17×10^{-2}
	60T	1.24	0.74×10^{-3}
Desalination (	60	0.16	5.56×10^{-4}
	100	0.02	0.60×10^{-4}
100 mm Column (Spiral conveyor)	34T	0.71	0.27×10^{-3}
Desalination (	60	0.03	1.09×10^{-4}
	100	0.03	1.07×10^{-4}

** Benzene/Cyclohexane system
T Ethanol/Water system

Table (6.1)
A comparison of Diffusion and Mass Transfer coefficients

Previous work with packed extraction columns permits some general observations on the measurement of Mass Transfer coefficients to be made. Normally these cannot be predicted due to the complex flow patterns of the two phases, experimental data must be collected for each packing, as the packing itself plays an important role in determining the phase flow patters. Some of the inconsistencies often encountered with mass transfer data in packed columns is due to the manner in which the data were collected. In small diameter laboratory columns, uniform packing is not always achieved,especially when the packing is a significant fraction of the column diameter. This leads to preferential flow of phases, channelling, and gives rise to incomplete contacting of the phases. In large diameter columns it is extremely important to have the entering liquid phase uniformly distributed across the packing at the top of the column. Maldistribution of liquid can severely reduce the mass transfer rate because the two phases are not adequately contacted. Also if the packing is not carefully installed, there may be variations in void volume, which will encourage channelling or bypassing by the phase. To a greater or lesser extent these problems will exist in a packed crystallisation column, the situation being more complicated in that there is a liquid phase in contact with a mobile solid phase. The factors which influence the mass transfer rate can be summarised as follows:

1. The chemical system, the concentration of components, physical properties of liquids, solids.
2. Total flow rate of liquids through the column.
3. The ratio of liquid flows.
4. Which phase is continuous or dispersed.
5. The direction of transfer - from aqueous to organic, dispersed to continuous or reverse.

6. The materials of construction and its wetting characteristics.

7. The nature, whether rotary or pulsing, and intensity, whether fast or slow, of mechanical agitation, if any.

8. Size and size distribution of solid phase (crystals) or dispersed phase (droplets).

9. Phase hold-up.

10. Intrastage recycling of liquids.

11. End effects.

12. Axial mixing, or backmixing.

Only the overall mass transfer coefficients have been measured (K), these are made up of the individual phase coefficients, which are difficult to determine separately. Since it is also difficult to determine the interfacial area per unit volume, this has been considered in conjunction with the mass transfer coefficient.(Ka). Relating this to the crystallisation column, two parameters affecting the Diffusion and Overall Mass Transfer are the screw speed and crystal production rate. They control the extent of axial dispersion in the reflux liquid and the efficiency of impurity removal from the crystals. Increasing the screw speed produces higher levels of agitation within the column resulting in an increase in impurity dispersion. Reducing crystal production gives a less compacted crystal bed, that is, the slurry viscosity is reduced allowing easier transport of impurity along the column. A combination of the two extemes tends to destroy the concentration gradient in the column. This trend is observed in the previous table, the high values for D being obtained in systems where the spiral conveyor was rotated and oscillated [39] [42]. For systems using conveyor rotation only similar values were obtained for both coefficients in the same systems.

Comparing the 50mm and 100mm columns for ethanol concentration, the larger column showed a reduction of approximately half for both coefficients. This is expected, due to the larger working volume of the column, the lower levels of agitation for the same screw speed, and the less efficient washing action resulting from operating the column with a great solids production capacity. For the 50mm column, operating continuously with the desalination system, at a screw speed of 60 r.p.m, the fit between experimental and theoretical concentration profiles, calculated from the D and Ka values, was good. However, as the screw speed was increased to 100 r.p.m, the diffusional effects were reduced due to agglomeration of the crystals, which was also reflected in a reduction in the mass transfer between the adhering and free liquid. This is consistent with a reduction in crystal size observed in the larger column, for the desalination system. It is easier to remove impurity from larger crystals, the crystals having less tendency to pack tightly together, hence the much higher value for Ka at the lower screw speed.

Comparison with the values for the 100mm column, shows that the screw speed affects equally the axial dispersion and mass transfer processes. Both D and Ka values, for desalination, are lower than those for the other column, D being similar in magnitude to values obtained by Ritter for a countercurrent ice wash column. A comparison of the contribution of the diffusional group $D\rho A\eta$ and mass transfer groups $a(a+1)/KaA\rho$ and $a/KaA\rho$ for flow rate data (C, L_E) at the two screw speeds, showed the following trend:

At 60 rpm	Diffusional group	17%	Mass Transfer group	83%
At 100 rpm	"	"	32%	"	"	"	68%

Thus we would expect the mass transfer to be dominant in determining the separation factor (H_E), the diffusion becoming more important as the screw speed increased. In the more agitated columns the average contribution of the mass transfer term was 18%[43], indicating axial diffusion as the dominant effect determining the separation factor.

In the experimental work undertaken, a range of operating parameters have been studied allowing comparisons to be made between different chemical systems and the effects of increasing column size. The experimental observations together with a mathematical analysis have shown the optimum operating conditions for maximum separation. Several key parameters were identified, in chapter (5) they were discussed for individual systems and columns. Now it is necessary to make comparisons of the parameters and their effects generally on column performance.

(6.2) Screw Speed

For the different systems and columns, a range of screw speeds between 40-120rpm was studied. Previous work[153] on the 50mm column had shown that minimum levels of product impurity (or concentration improvement for ethanol) were achieved at 60rpm. It was concluded that at 60rpm (a slope of zero, FIG (5.2)(5.14)) the diffusion and mass transfer effects were balanced. This trend was observed in the mixed metal salts separation tests. However the levels of impurity in the product were higher than those obtained for desalination. Above this screw speed, the positive slope of the curve indicated that the diffusional effects dominated.

Study of the desalination system in the 100mm column produced different results. The extremes of product impurity over the screw speed range was 2-5 ($x10^{3}$ ppm) compared with 0.8-7 ($x10^{3}$ ppm) for the smaller column, the peak impurity arising at 80 rpm as in the 50mm system, but reducing only slightly through 60 rpm down to the minimum level at 52 rpm. This reflects the reduced response of the larger system, in its behaviour to tbe change of a parameter. Over this portion of the curve the mass transfer should be enhanced over the diffusion of impurity along the column. This is observed in the 50mm column as a rapid change in product impurity, whereas in the 100mm column, the washing efficiency being much reduced, giving a progressive response to increasing screw speed. When the screw speed reached 100 rpm the same product impurity levels as 60rpm were recorded, however the difference in the impurity levels at the two screw speeds was greater. At the greater screw speed and crystal production rate, the smaller crystals being produced, packed into a more dense-bed arrangement, making it harder for axial dispersion within the free liquid to occur.

A brief study[155] was made to investigate the effects of screw speed on base composition for the desalination system operating at Total Reflux. As screw speed was increased from 40 - 120 rpm, there was a minimum impurity level at 80 rpm, of a similar magnitude to that obtained for continuous operation. For similar screw speeds it was found that the impurity levels at the base of the column were significantly higher. This is to be expected since impurity levels in the stripping section are much higher giving greater amounts of impurity associated with the crystals. Axial dispersion of impurity is greater and it provides a more stringent test of the washing efficiency.

Comparing the two columns and the effect of screw speed on ethanol concentration, a different trend is observed. Ethanol enrichment in the L_S stream is maximised at 60 rpm, it being reduced at screw speeds above or below this in the smaller column, the trend for the larger column being a gradual reduction in top product concentration with increasing screw speed. The difference between the two extremes of flow for this column demonstrated the increased sensitivity of the stripping section to hydrodynamic considerations. This is to be expected if a comparison of the ratios of lengths of the stripping section : enriching section for the columns is made. For the 50 mm column it is 0.42 and for the 100mm column 0.27. Best results for the larger column are obtained at low screw speeds when the stripping section is being gently agitated and the take-off at the base (L_E) is high, giving reduced flow into the stripping section.

(6.3) Crystal Production Rate

Equation (3.54)
$$\frac{Y-Y_P}{Y_\emptyset-Y_P} = \exp.\ -\frac{(Z-Z_F)}{H_E}$$

describes the concentration profile in the column; at high levels of impurity removal, the value of Y is small. This is governed by the other terms, for a constant $Y_\emptyset$ and Y_P then a small value of H_E, Z_F and a high value of Z will give the lower value of Y. The values of Z_F and Z are dependent upon the equipment, the value of H_E being determined by equation (3.48). Terms held constant in this equation are ρ, A, η and α ; therefore at a set screw speed and product removal rate, L_E, the value of H_E is governed by C, D and Ka. As C increases, the term $1/(C-L_E)$ decreases, but $\alpha(1+\alpha)C^2 - \alpha L_E C / KaA\rho$ increases, other factors remaining constant. At low values of C, the contribution of the diffusional group, in equation (3.48), to the

separation factor, is greater. Increased transport of impurity down the column is predicted. The squared (C) in the second term ensures that the mass transfer group will assume greater importance as the crystal rate is increased. The limit of crystal production is reached when column blockage occurs. There is an optimum crystal rate for each system and operating conditions which gives a minimum value for the separation factor H_E.

A comparison of the effects of crystal production rate in the desalination system for the two columns, showed a reducing impurity level of the product for increasing values of crystal production. Both columns responded in a similar manner to solids flow, that is, the build up of a crystal slurry in the column. Efficient column operation requires effective washing of impurity from the crystals. If the crystals are present in a highly mobile slurry, then it is difficult for the reflux liquid to ascend the column in a uniform manner and it is much easier for impure liquid to be carried down the column. Operating the columns with packed beds improved the washing potential (c.f. the work on S.R.F desalination and pressurised counterwashers); however, a limit of crystal production was reached when bed density was so great that reflux liquid could no longer penetrate the crystal mass. For the 50mm column, a practical maximum value of C was 0.20 g/sec, and for the 100mm column C was 0.53 g/sec. Operating the 100mm column at values of C greater than this caused frequent blockage of the column to occur. This fall-off in separation is demonstrated in the waste efflucent recovery work on the 50mm column. Extending the crystal production rate, under carefully controlled conditions, to a maximum of C = 0.23 g/sec, produced no improvement in base impurity levels over those obtained at C = 0.20 g/sec. Carrying out similar investigations on the 100mm column[155] at Total Reflux, showed exactly the same trend as when the column was operated continuously. The range of impurity measured at

the base was much greater, the crystal production rate spanning a range of C = 0.30 to 0.35 g/sec.

A comparison of the effects of crystal production rate on the performance of the stripping section is provided with the ethanol water system. In the modified form, the equation describing the separation factor H_S, (3.57) has C in the form $^1/(C+L_S)$ and a squared term in the mass transfer group. Increasing crystal production gives a subsequent increase in H_S, hence the concentration of ethanol in the stripped stream is raised. Since there is no theoretical limit to the magnitude of H_S, ethanol enrichment should continue to increase as crystal production increases. This was observed in both columns, the limiting factor being the capacity of the cooling system to handle the increased load.

(6.4) Continuous column operation has been carried out, locating the feed point as near to the freezing section as possible. In the systems where the base product was required with minimum impurity, this proved to be the optimum location for the 50mm column. Examination of the experimental curves indicated that separation may be improved by feeding into the freezing section. To this end the 100mm column was fitted with a modified screw section in the freezing section, it being possible to accomplish this by feeding down a hollow central shaft, feed exit being provided at different locations down the shaft. Since the modified screw did not perform successfully, it was not possible to confirm this point.

Operating the columns for product concentration showed different trends. In the smaller column, a gradual reduction in ethanol concentration was

observed, while for the larger an initial fall in concentration was soon reversed as the feed point moved down the purification section. This increase in the value of Z_F effectively increased the length of the stripping section, also the impurity content of the free liquid in the column was higher, the rapid upturn in impurity levels occurring at or near the feed point. This effectively increased the concentration of ethanol into the stripping section.

(6.5) Another important parameter controlling column performance is product removal rate. This together with the crystal production rate controls the quantity of reflux (washing) liquid returned to the column. A comparison of the two columns with the desalination system [51] showed that as the ratio of product to feed (L_E/F) was reduced the concentration of sodium chloride in the enriched system was reduced. Projection of the curve to zero indicated the limiting concentration of the impurity the product would contain. This is to be expected, since reducing product removal gives a corresponding increase in washing potential, with the extra reflux liquid generated.

In the case of ethanol where the concentration of the top product is to be maximised, then it is required that the reflux liquid carries the highest ethanol concentration into the stripping section. This can be achieved by increasing the contact time between the reflux liquid and adhering liquid, that is, a low flow of free liquid along the column is required. Since L_S is determined by L_E, this can be achieved by increasing base stream removal rate. Generally, operating the columns at low product removal rates (L_E or L_S) will increase the purity (desalination, waste effluent recovery) or increase concentration (ethanol/water) of the product stream.

Chapter 7 Conclusions

Continuous column crystallisation has been shown to be an efficient separation technique suitable for processing a variety of aqueous and organic eutectic forming mixtures. The system appears viable for relatively small scale production of high purity crystals from eutectic systems. Efficient use of the column depends on the optimisation of important process parameters. These investigations have confirmed spiral rotation rate, crystal production rate and product removal rate to be the dominant parameters controlling the final impurity levels of the product.

The aim of the work was to construct a working continuous column crystalliser of a size comparable to a small scale industrial process. This has been achieved, the initial design being based upon operating experience gained with the small scale column. A study of equivalent systems on each column has enabled comparisons on the effects of scale up to be made, giving further understanding of the purification mechanism in the column. The important processes of mass transfer, axial diffusion and their effects on column performance have been investigated. Calculation of the coefficients has enabled the present study and the investigations of other workers to be compared.

The theoretical aspects of the study have been directed towards the continued development of a mathematical model. Ultimately the model would be used as a design equation, predicting column performance under various process conditions. The early work of Henry[43] with the benzene/cyclohexane system concluded that the model provided a good fit of his data when the axial dispersion and mass transfer, together with an estimation of the impurity associated with the crystal phase, was

used to describe column performance. The results obtained in the present study confirmed that these parameters, when incorporated into a mathematical model, described the purification mechanism adequately. A basic design equation has not yet been developed, however we have gained further insight into the mechanism of purification, which predominates under given conditions. Henry concluded that axial dispersion was the dominant mechanism limiting separation for continuous flow operation. The present studies showed a reversal in this dominance. Increasing column diameter to 50mm and working volume to one litre, showed the mass transfer to be of comparable importance to the axial dispersion in determining the separation. A further increase in diameter to 100mm and working volume to nine litres showed the mass transfer to be the dominant process limiting separation. As a consequence of increasing column size, the magnitude of the coefficients is reduced. In practical terms the larger column is less affected by diffusional effects but the washing of adhering impure liquid from the crystals is less efficient and complete. Hence the impurity levels of the product were higher for the larger column, at the increased throughput obtained. The production of very pure material would require the cascade operation of two columns.

A comparison of the experimental data and that generated from the mathematical model (see Appendix A2,3,4) showed a good fit, for experimental and theoretical concentration profiles for both columns. This was especially so at a screw speed of 60 r.p.m, therefore it is possible to use the calculated values of (D) and (Ka), to calculate the concentration profiles for other values of crystal production rate. A transport of impurity into the purification section, not reflected in the theoretical concentration profile, was observed in the 100mm column as the screw speed reached 100 r.p.m. The effect was more

pronounced at lower crystal production rates. Impurity penetration was limited to the top portion of the purification section, the levels rapidly falling to those of the theoretical concentration profile. The final product purity was similar to that obtained at the lower screw speed.

It is possible to draw some general conclusions on the optimum operating conditions for maximum column performance. The two parameters controlling separation in the column are screw speed and crystal production rate. Both columns gave the best results when operating at the lower screw speed and a high crystal production rate. Increasing screw speed promotes the axial diffusion of impurity along the column destroying the concentration gradient. A low crystal production rate does not allow the build-up of a packed crystal bed. Columns operating with a low solids content in the slurry allow easier transport of impurity along the column retarding the efficient washing of adhered impurity from the crystals. The lower the value of crystal production rate and the higher the value of screw speed, the greater is the tendency for the concentration gradient to be destroyed.

From the microscopic examination of the crystals it was concluded that a lower screw speed gave better crystal quality. As the screw speed was increased, there was a reduction in crystal size. Crystals produced at high screw speeds were observed to be more spherical compared to those at the lower screw speed which were observed as plate-shaped. Previous workers concluded that the washing of larger crystals was more efficient than equivalent smaller crystals. The different operational characteristics of the Archimedean screw were also observed. Its effect on the hydrodynamic conditions was more

pronounced in the smaller column. In this case it not only transported the crystals along the column but imparted a high degree of mixing and turbulence within the system. In the larger column, the level of agitation was reduced, the screw behaved as a transport device, providing little mixing of the phases, especially in the purification section operating with a packed crystal bed.

In an effort to reduce the lengthy procedure of a full systems analysis for the column, a design equation was derived to predict impurity levels in the product. Initially utilised with a binary organic system it was applied to the sodium chloride/water system on the 100mm column. From the experimental results, it was concluded that the equation was only valid at high values of R_E (>0.9); below this the simplifying assumptions were not valid. Operating the column with little reflux, that is, maximising product, the design equation gave a good estimation of the impurity content of the enriched stream. However this had only limited application since operating the column under these conditions gave a high impurity content in the enriched stream.

Suggestions for further work

A range of chemical systems have been investigated in each column crystalliser. Much data has been generated on the optimisation of the columns and utilised in a mathematical model to investigate the purification mechanisms in the columns. Concurrently with the present studies, computer investigations into the dynamic modelling and partial simulation of the 100mm diameter column were performed[156]. The initial attempts to predict column behaviour were confined to the freezing section, in which basic equations for heat and mass transfer were applied covering the different components. Much of the experimental data used for the computer work was generated on the 100 mm diameter column, however at the time, data on crystal sizes in the column was not available. This data is now available for use with the computer programme. There is still much work to carry out on the total simulation of the complete column. Further computer studies are necessary to predict concentration profiles, product impurities, etc, for comparison with experimental results obtained with the column.

As part of the continuing research into continuous column crystallisation, investigations have been undertaken into fundamental crystallisation studies. Operation of the two columns indicated several areas requiring in-depth study. Attempts have been made to take the freezing section in isolation, nucleate and grow ice crystals within it, and observe microscopically the crystals produced. Crystal washing experiments, relating product purity to mother liquor concentration, have been performed. Further work is required to refine and develop crystal size distribution and measurement techniques for use with an operational column. Ultimately it would be desirable to have an on-line sampling technique for crystal study, using particle sizing and counting, with back-up computing facilities for crystal size distribution analysis.

This would allow the detailed analysis of the variables affecting crystal quality.

A desirable modification to the present system would be the introduction of automatic control systems to monitor the column during operation. The rate of cooling, liquid stream flow rates and heat input in the melting section required constant manual adjustment to maintain constant conditions for the experimental runs. A basic system for automatic control would require the following:

(a) Base pressure control

(b) Base temperature control

(c) Refrigerant line temperature control

(d) Feed temperature control

(e) Bulk refrigerant control

(f) Feed pressure protection

(g) Current limiter for conveyor motor drive

To install the system would require the necessary controllers, temperature sensors, pressure transducers and electro-pneumatic valves.

References and Bibliography

1. Bennett, R.C. A.I.Ch.E. Symposium Series, No.95, 65, 34, (1969)

2. Nebbia, G. Menozzi, G. Desalination, 5, 49, (1968)

3. Buchanan, J.Y. Engineering, 85, 688, (1908)

4. Arnold, P.M. U.S. Patent, 2-540-083, Feb.6, (1951)

5. Arnold, P.M. U.S. Patent, 2-540-977, Feb.6, (1951)

6. McKay, D.L. Chap. 16, in Fractional Solidification Vol 1
   eds. M. Zief and W.R. Wilcox
   Edward Arnold (Publishers) Ltd. London (1967)

7. Schildknecht, H. Z. Analyt. Chem. 181, 254, (1961)

8. K.C.P. Crystal Purifier,
   Chemical Engineering, November 6, 67, (1978)

9. Ennis, C.E. Chemical Engineering Progress, 63, (1), 54, (1967)

10. Franks, F. Chemistry In Britain, 12, (9), 278, (1976)

11. Weiss, P.A. in The Practice of Desalination, 260,
    ed. R. Bakish, Noyes Data Corporation(Publishers)(1973)

12. Campbell, R.J. Emmermann, D.K.
    American Society of Mechanical Engineers, Paper 72-PID,
    (5) - (8), (1972)

13. Nyvlt, J. in Industrial Crystallisation from Solution,
    Butterworths, London, (1971)

14. Banforth, A.W. in Industrial Crystallisation, Leonard Hill,
    London, (1965)

15. Pfann, W.G. Journal of Metals, 194, 747, (1952)

16. Herington, E.F.G. in Zone Melting of Organic Compounds,
    Blackwell Scientific Publications, Oxford, (1963)

17. Anikin, A.G. in Zone Melting of Organic Compounds : The Work
    of Soviet Scientists.
    Translated from Russian by D.P. Bidelscomb,
    National Physical Laboratories, (1965)

18. Eldib, I.A. Industrial and Engineering Chemistry : Process
    design and development, 1, (1), 2, (1962)

19. Vol'pyan, A.E. Kurdyumov, G.M.
    Theoretical Foundations of Chemical Engineering, 4,
    266, (1970)

20. Fedorova, R.F. Fedorov, P.I.
    Russian Journal of Physical Chemistry, 45, (1),
    87, (1971)

21. Filippov, G.G. Nikolaev, D.A.
Theoretical Foundations of Chemical Engineering, 4, 264, (1970)

22. McKay, D.L. Dale, G.H. Weedman, J.A.
Industrial and Engineering Chemistry, 52, (3), 197, (1960)

23. Schildknecht, H. Vetter, H. Angew Chem., 73, (17/18), 612, (1961)

24. Yagi, S. Inoue, H. Kagaku Kogaku, 27, (6), 415, (1963)

25. McKay, D.L. Goard, H.W.
Chemical Engineering Progress, 61, (11), 99 (1965)

26. McKay, D.L. U.S. Patent, 3-212-281 (1965)

27. McKay, D.L. Goard, H.W. Industrial and Engineering Chemistry : Process Design and Development, 6, (1), 16, (1967)

28. McKay, D.L. Dale, G.H. Tabler, D.C.
Chemical Engineering Progress, 62, (11), 104 (1966)

29. Powers, J.E. Gates, W.C. Albertins, R. Chap. 11
in Fractional Solidification, eds M. Zief and W.R. Wilcox
Edward Arnold (Publishers) Ltd, London (1967)

30. Devyatykh, G.G.
Russian Journal of Physical Chemistry, 41, 507, (1967)

31. Arkenbout, G.J. Smit, W.M. Separation Science, 2, (5), 575, (1967)

32. Arkenbout, G.J. Smit, W.M. Separation Science, 3, (6), 501, (1968)

33. Malyusov, V.A. Kuznetsov, V.V. Borisenko, V.V.
Theoretical Foundations of Chemical Engineering, 2, 781, (1968)

34. Betts, W.D. Freeman, J.W. McNeil, D.
Journal of Applied Chemistry, 17, 180, (1968)

35. Richmond, S. Wright-Exley, D.
U.K. Patent 1-207-591, (1969)

36. Coal Tar Research Corporation, U.K. Patent 1-259-956, (1969)

37. Armstrong, R.M. British Chemical Engineer, 14,(5), 647, (1969)

38. Armstrong, R.M. The Chemical Engineer, October, 685, (1979)

39. Albertins, R. Powers, J.E.
American Institute of Chemical Engineers Journal, 15, (4), 554, (1969)

40. Player, M.R. Industrial and Engineering Chemistry : Process Design and Development, 8, (2), 210 , (1969)

41. Bolsaitis, P. Chemical Engineering Science, 24, 1813, (1969)

42. Gates, W.C. Powers, J.E.
American Institute of Chemical Engineers Journal, 16, (4), 648, (1970)

43. Henry, J.D. Powers, J.E.
American Institute of Chemical Engineers Journal, 16, (6), 1055, (1970)

44. Schildknecht, H. Breitter, J. Mass, K.
Separation Science, 5, (2), 99, (1970)

45. Brodie, J.A.
Mechanical and Chemical Engineer Transactions, May, 37, (1971)

46. Anonymous, Chemical Engineering, February, 40, (1972)

47. Kay, J. Processing, December, 25, (1978)

48. Matz, G. B.C.E. and Process Technology : Review, 17, (2), 99,(1972)

49. Arkenbout, G.J. Van Kuijk, A. Smit, W.M.
Chemtech, September, 596, (1976)

50. Hobson, M.D. McGrath, L. 4th International Symposium on Fresh Water from the Sea, 3, 357, (1973)

51. Bates, C. Gladwin, R.P. McGrath, L. 5th International Symposium on Fresh Water from the Sea, 3, 201, (1976)

52. Moyers, C.G. Olson, J.H.
American Institute of Chemical Engineers Journal, 20, (6), 1118, (1974)

53. Wells, G.L. Makin, A.C.I. Scarlett, P.
Transactions of the Institute of Chemical Engineers, 53, 136, (1975)

54. Devyatykh, G.G. Elliev, Yu.E. Scheplyagin, E.M.
Theoretical Foundations of Chemical Engineering, 11, 108, (1977)

55. Devyatykh, G.G. Elliev, Yu.E. Scheplyagin, E.M.
Theoretical Foundations of Chemical Engineering, 11, 156, (1977)

56. Kureha Chemical Co. Chemical Engineering, April, 109, (1979)

57. Encyclopedia of Chemical Technology, 2nd Edition, Kirk-Othmer, Vol.22, ed A. Standers, Interscience, N.Y. (1970)

58. Strobel, J.J. in Practice of Desalination, ed Dr. R Bakish, Noyes Data Corporation, (1973)

59. Morris, R.M. Chemistry and Industry, No. 15, 653, (1977)

60. Smith, M.J.S. Satchell, R.L.H. The Chemical Engineer, No. 256, 417, (1971)

61. Agarwal, A. New Scientist, 76, (1073), 96, (1977)

62. Desalination, H.M.S.O. (London), (1972)

63. Silver, R.A. Chemical Engineer, No.281-292, 35, (1974)

64. Butler, P. Process Engineering, No.117, 65, (1973)

65. Heckroth, C.W. Water and Wastes Engineering, 11, 20, (1974)

66. Porteous, A. Saline Water Distillation Processes, Longman Group Ltd, London, (1975)

67. Silver, R.S. Ch.3 in Principals of Desalination, ed K.S. Spiegler, Academic Press, N.Y. and London, (1966)

68. Frankel, A. Proceeding Institute of Mechanical Engineers, 174, (7), 312, (1960)

69. Pugh, O. Process Technology International, 18, 57, (1973)

70. Veenman, A.W. Desalination, 27, 21, (1978)

71. Sheth, N.J. Peck, R.E. Wason, D.T. Industrial and Engineering Chemistry : Process Design and Development, 14, 351, (1975)

72. Review 2nd European Symposium on Fresh Water from the Sea, Desalination, 2, 5, (1967)

73. Delyannis, A.A. Solar Energy, 12, 113, (1968)

74. Merten, U. Ch.8 in Principals of Desalination, ed. K.S. Spiegler, Academic Press, N.Y. and London, (1966)

75. Whitman, G.M. Caracciolo, V.P. in Practice of Desalination ed. R. Bakish, Noyes Data Corporation, (1973)

76. Podall, H.E. A.I.Ch.E. Symposium Series, No. 107, 67, 260, (1971)

77. Gutman, R.G. The Chemical Engineer, No.322, 510 and 521, (1977)

78. Kirkham, T.A. Mechanical Engineering, 90, March, 47, (1968)

79. Vermeer, D.J. Lynn, S. Vermeulen, T. Industrial and Engineering Chemistry : Process Design and Development, 14, 290, (1975)

80. Cable, P.J. Murtagh, R.W. Pilkington, N.H. The Chemical Engineer, No. 324, 624, (1977)

81. Fraser, J.H. American Water Works Association Journal, 64, 746, (1972)

82. Johnson, W.E. Water and Wastes Engineering, 6, 20, (1969)

83. Orcutt, J.C. Ch. 17 in Fractional Solidification Vol 1
eds, M. Zief and W.R. Wilcox
Edward Arnold (Publishers) Ltd, London (1967)

84. Pachter, M. Barak, A. Desalination, 2, 358, (1967)

85. Johnson, W. Pallone, A. Probstein, R.F. 4th International
Symposium on Fresh Water from the Sea, 3, 371, (1973)

86. Kennaway, T. Chemical and Process Engineering, 52, 91, (1971)

87. Wilson, J.H. Proceedings of the Institute of Refrigeration,
68, April, (1972)

88. Barduhn, A.J. Chemical Engineering Progress, 71, (11), 80, (1975)

89. Barduhn, A.J. Desalination, 5, 173, (1968)

90. Gibson, W.E. Desalination, 14, 249, (1974)

91. Barduhn, A,J. Chemical Engineering Progress, 63, (1), 98, (1967)

92. Bakker, N.A. Duncan, A.G. Hawtin, P.
The Chemical Engineer, No. 304, 769, (1975)

93. Schroeder, P.J. Chan, A.S. Rashid Khan, A.
Desalination, 21, 125, (1977)

94. Denton, W.H. Smith, M.J.S. Klaschka, J.T. Forgan, R. Diffy, H.R.
Rumany, C.H. Dawson, R.W. Desalination, 14, 263, (1974)

95. Grossman, G. American Institute of Chemical Engineers Journal,
22, (6), 1033, (1976)

96. Shwartz, J. Probstein, R.F. Desalination, 4, 5, (1968)

97. Shwartz, J. Probstein, R.F. Desalination, 6, 239, (1969)

98. Snyder, A.E. Ch. 7 in Principals of Desalination
ed. K.S. Spiegler, Academic Press, N.Y. and London, (1966)

99. Johnson, C.A. Lunde, P.T. in Desalination by Freeze Concentration
Noyes Data Corporation (Publishers) (1971)

100. Curran, H.M. Desalination, 7, (3) 273, (1970)

101. Stepakoff, G.L. Siegelman, D. Johnson, R. Gibson, W.
Desalination, 15, 25, (1974)

102. Lloyd, A.J. Desalination, 21, 137, (1977)

103. Harriott, P. American Institute of Chemical Engineers Journal,
13, (4), 755, (1967)

104. Umano, S. Kawasaki, S. from Tōkyō Kōgyō, Shikensho Hōkoku
U.K.A.E.A. Research Report Translation by R.A. Scutt,
54, (8), 233, (1969)

105. Orcutt, J.C. Desalination, 7, (1) 75, (1969)

106. Orcutt, J.C. Carey, T.P.
Industrial and Engineering Chemistry : Process Design and Development, 9, (1), 58, (1970)

107. Terwilliger, J.P. Dizio, S.F. Chemical Engineering Science, 25, 1331, (1970)

108. Janzow, E.F. Chao, B.T. Desalination, 12, (2), 141, (1973)

109. Janzow, E.F. Chao, B.T. Desalination, 12, (2), 163, (1973)

110. Margolis, G.M. Sherwood, T.K. Brian, P.L.T. Sarofim, A.F.
Industrial and Engineering Chemistry : Fundamentals, 10, (3), 439, (1971)

111. Wey, J.S. Estrin, J. Industrial and Engineering Chemistry : Process Design and Development, 12, (3), 236, (1973)

112. Akhtar, N. McGrath, L. Roberts, P.D. 6th International Symposium on Fresh Water from the Sea, 4, 13, (1978)

113. Kane, S.G. Evans, T.W. Brian, P.L.T. Sarofim, A.F.
Desalination, 17, 3, (1975)

114. Austin, C. in Science of Wine,
University of London Press Ltd, (1968)

115. Rieche, A. in Outline of Industrial Organic Chemistry,
3rd Edition, Butterworths, London, (1964)

116. Humphries, A.E. Chemical Engineering Progress, 73, (1), 85, (1977)

117. Sitton, O.C. Foutch, G.L. Book, N.L. Gaddy, J.L.
Chemical Engineering Progress, 75, (12,) 52, (1979)

118. Augood, D.R. The Industrial Chemist, 30, 585, (1954)

119. Selak, J. Finke, J. Chemical Engineering Progress, 50, (50), 221, (1954)

120. White, A.S. The Industrial Chemist, 34, 671, (1958)

121. Shay, E.G. Atlantic Refining Company, U.K. Patent 3-058-811 (1962)

122. United Kingdom Atomic Energy Authority, U.K. Patent 726-532 (1955)

123. United Kingdom Atomic Energy Authority, U.K. Patent 726-771 (1955)

124. Tronstad, L. U.K. Patent 581-908, (1946)

125. Taylor, H.S. Atomic Energy Commission (U.S.A.)
U.S. Patent 2-690-380, (1954)

126. Urey, H.C. Grosse, A.V. Atomic Energy Commission (U.S.A.)
U.S. Patent 2-690-379, (1954)

127. Barr, F.T. Drews, W.P.
Chemical Engineering Progress, 56, (3), 49, (1960)

128. Thayer, V.R. U.S. Patent, 3-411-884, (1968)

129. Bebbington, W.P. Thayer, V.R. Chemical Engineering Progress, 55, (9), 70, (1959)

130. Spevack, J.S. Atomic Energy Commission (U.S.A.) U.S. Patent 2-787-526, (1957)

131. Chopey, N.P. Chemical Engineering, February, 118 (1961)

132. Murphee, E.V. Atomic Energy Commission (U.S.A.) U.S. Patent 2-689-782, (1954)

133. Saito, T. Sonoda, S. Kurihara, Y. Tukamatsu, T. Morita, T. 3rd U.N. Conference, Geneva, Paper 433, (1964)

134. Schotten, W.C. Maher, R. Olcott, T.W. Burgess, M.P. Schwab, C. U.S. Atomic Energy Commission D.P. 470 (1960)

135. Besselievre, E.B. in The Treatment of Industrial Wastes, McGraw Hill (Publishers), (1969)

136. Fraser, J.H. Johnson, W.E. Avco Systems Division, Wilmington, M.A. in Applications of New Concepts of Physical-Chemical Waste water Treatment, Sept 18-22, (1972)

137. Ziering, M.B. Emmermann, D.K. Johnson, W.E. A.I.Ch.E. Symposium Series, No.136, 70, 550, (1974)

138. McNutty, K.J. A.I.Ch.E. Symposium Series, No.166, 73, (1977)

139. Vanhook, A. in Crystallisation, Reinhold (Publishers) N.Y. (1961)

140. Mullin, J.W. in Crystallisation, 2nd Edition, Butterworths, London, (1972)

141. Gibbs, J.W. in Collected Works, Longman and Green, London, (1928)

142. Nyvlt, J. in Industrial Crystallisation : The present state of the art, Verkag Chemie, Weinheim, N.Y. (1978)

143. Khamskii, E.V. in A special research report : Translated from Russian Consultants Bureau (Publishers), (1969)

144. Nielson, A.E. in Kinetics of Precipitation, Pergamon, Oxford, (1964)

145. Janse, A.H. DeJong, E.J. Transactions of the Institute of Chemical Engineers, 56, 187, (1978)

146. Wey, J.S. Estrin, J. Desalination, 14, (1) 103, (1974)

147. Strickland-Constable, R.F. in Kinetics and Mechanism of Crystallisation, Academic Press, London and N.Y. (1968)

148. Savanoe, H. Chemical Engineering Progress, 55, (5), 47, (1959)

149. Nakai, T. Miyake, T. Kagaku Kogaku Ronbunshu, 4, (1), 100, (1978)

150. Garrett, D.E. British Chemical Engineering, December, 673, (1959)

151. Cutts, G.G. Wells, G.L. Dechema-Monograph, 73, 253, (1973)

152. Powers, J.E. in Symposium uber Zonenschmelzen und Kolonnenkristallisiem II Schildknect, Kemforchungszentrum, Karlshrue, (1963)

153. Gladwin, R.P. Ph.D. Thesis, City University, (1975)

154. Betts, W.D. in Chemical Engineers' Handbook, 5th Edition, Ch.17-22, eds. Perry and Chilton

155. Arulapalam, G.T. Bates, C. Khaw, L.F. McGrath, L. Desalination, 36, 87, (1981)

156. Akhtar, N. McGrath, L. Roberts, P.D. Desalination, 28, 1, (1979)

APPENDIX

(A1) Derivation of the design equation (3.60) in chapter (3.6)

Under economic operating conditions, as defined by Wells et al[53],

$D\rho A\eta \gg LL'/K a\rho A$ especially at low refluxes.

This term can be neglected.

The assumption that the adhering liquid at the feed point has the same composition as the feed, permits the simplification of the overall component balances. Thus, from Chapter (3.6)

$$H_E \frac{dy}{dx} + Y = Y_P \qquad (3.43)$$

where $H_E = \frac{D\rho A\eta}{L-L'}$ (3.44) $\quad Y_P = \frac{C\varepsilon - L_E Y_E}{L-L'}$ (3.45)

and the solution is $$\frac{Y-Y_P}{Y_\phi - Y_P} = \exp.^{-Z/H_E} \qquad (3.54)$$

Applying the following conditions $Y = Y_E$ when $Z = L_P$ (L_P = purification section length), as demonstrated by Henry[43].

Then $$\frac{Y_E - Y_P}{Y_\phi - Y_P} = \exp.^{-L_P/H_E} \qquad A(3.54)$$

Now substituting (3.44) in the above:

$$\frac{Y_E - Y_P}{Y_\phi - Y_P} = \exp.\frac{-L_P(L-L')}{D\rho A\eta} \qquad (A1)$$

And from the initial assumptions, the following conditions apply for

a. component $L\,Y_\phi = C\varepsilon + L'\,Y_F - L_E\,Y_E$ (3.38)

b. overall balances $L = C + L' - L_E$ (3.39)

But $Y_E - Y_p = Y_E - \dfrac{C\varepsilon - L_E\,Y_E}{L-L'}$ using (3.45)

$$= \frac{(L - L' + L_E)\,Y_E - C\varepsilon}{L - L'}$$

ie $Y_E - Y_p = C\,\dfrac{(Y_E - \varepsilon)}{L - L'}$ using (3.39)′

Also $Y_\phi - Y_p = \underbrace{\left[\dfrac{C\varepsilon + L'Y_F - L_E\,Y_E}{L}\right]}_{\text{from (3.38)}} - \underbrace{\left[\dfrac{C\varepsilon - L_E\,Y_E}{L - L'}\right]}_{\text{from (3.45)}}$

$$Y_\phi - Y_p = \frac{(LL'Y_F - L'\,(C\varepsilon + L'Y_F - L_E\,Y_E))}{L\,(L - L')} \qquad (A2)$$

ie $$Y_\phi - Y_p = \frac{L'\,(L\,Y_F - (C\varepsilon + L'\,Y_F - L_E\,Y_E))}{L\,(L - L')} \qquad (A3)$$

Combining equations (3.39)′ (A3) (A1) gives,

$$\frac{L\,C\,(Y_E - \varepsilon)}{L'\,(L\,Y_F - C\varepsilon - L'\,Y_F + L_E\,Y_E)} = e.\,\frac{-L_p(L-L')}{D\rho A\eta} \qquad (A4)$$

Under conditions other than close to minimum reflux

$$(L - L')\, Y_F \gg L_E\, Y_E - C\varepsilon$$

so this term can be neglected in (A4)

$$\text{ie } \frac{L\, C(Y_E - \varepsilon)}{L'\,(L\, Y_F - L'\, Y_F)} = e^{\frac{-L_p(L-L')}{D\rho A\eta}} \qquad (A5)$$

$$\text{ie } \frac{L\, C\,(Y_E - \varepsilon)}{L'\, Y_F\,(L - L')} = e^{\frac{-L_p(L-L')}{D\rho A\eta}} \qquad (A6)$$

Applying the following conditions

$$R_E = \frac{L_E}{C} \qquad L' = aC \qquad (3.46)$$

and $L = C + L' - L_E$ (3.39)

Therefore $L - L' = C - L_E = C\,(1 - R_E)$ (A7)

and $L = L' + C\,(1 - R_E) = C\,(a + 1 - R_E)$ (A8)

Substituting in (A6) gives

$$\frac{C\,(a + 1 - R_E)\, C\,(Y_E - \varepsilon)}{a\, C\, Y_F\, C\,(1 - R_E)} = \exp.\frac{(-L_p\, C\,(1 - R_E)}{D\rho A\eta} \qquad (A9)$$

$$\text{ie } \frac{(a + 1 - R_E)\,(Y_E - \varepsilon)}{a\, Y_F\,(1 - R_E)} = \exp.\left[\frac{-L_p\,(1 - R_E)C}{D\,\rho\, A\eta}\right] \qquad (A10)$$

$$\text{ie } (Y_E - \varepsilon) = aY_F\frac{(1 - R_E)}{(a+1-R_E)} \exp.\left[\frac{-L_p(1-R_E)C}{D\rho A\eta}\right] \qquad (A11)$$

$$Y_E = \varepsilon + \left[\frac{1 - R_E}{a - R_E + 1}\right] a\, Y_F \exp.\left[\frac{-L_p(1 - R_E)C}{D\,\rho\, A\eta}\right] \qquad (3.60)$$

This expression relates product composition, product offtake ratio R_E, feed composition, Y_F, and purification section length, L_p. The term $D\rho A\eta$ is used to represent the axial dispersion of the impurity.

(A2) Desalination

Calculation of the separation factor H_E for experiment D.S(26)

The concentration profile for the column was constructed by plotting the impurity content in the free liquid (p.p.m), Y, against the distance (cms) from the feed point, Z*.

The point at which the graph crosses the zero point (feed point) reads a concentration of 38,750 p.p.m. This is the value of Y_ϕ.

In order to use equation (5.1), Z_1^*, and Z_2^* values were considered such that $\frac{Z_2^*}{Z_1^*} = 2$ and their corresponding concentration Y_1 and Y_2 were read from the graph.

$$Y_p = \frac{Y_1^2 - Y_2 Y_\phi}{2Y_1 - Y_2 - Y_\phi} \qquad (5.1)$$

Equation (5.1) was used to calculate the values of Y_p for each set of Y_1 and Y_2 values.

Y_p Average = 1650 ppm

Using this average value for Y_p, the $(Y - Y_p)$ values were calculated at each distance Z* (sample points).

Z*	19	39	59	79	89	108	113
$(Y-Y_p)\times10^3$	28.4	18.4	9.4	3.9	3.9	2.4	2.4

Then from equation (3.54)'

$$\ln (Y-Y_p) = \frac{-Z^*}{H_E} + \ln (Y_\phi - Y_p) \qquad (3.54)'$$

A plot of $(Y-Y_p)$ versus Z^* on log-linear paper gave a straight line, the gradient of which was the negative reciprocal of the separation factor H_E. (Fig A1). Gradient $= \frac{-1}{H_E} = -(\ln 30{,}000 - \ln 2{,}110)/90$

$= 0.0295$

That is, $H_E = 33.95$

Calculation of the Axial Diffusion (D) and Overall Masstransfer (Ka) coefficients

In order to evaluate D and Ka it is necessary to determine the following parameters: C, Y^*, α, η. The crystal rate was calculated using heat and mass balances on experimental measurements made over the freezing section of the column. The value of both α and η can be determined by consideration of the following equations:-

By definition in section (3) $\alpha = \frac{L'}{C}$, $\eta = \frac{L}{L + L' + C}$

Therefore to determine α and η, L and L' need first to be calculated. From equation (3.39)

$$L = C + L' - L_E \qquad (3.39)$$

A salt balance on the enriching section (Fig 3.13) gives the equation

$$LY = L'Y' - L_E Y_E \qquad \text{where } Y = Y_\phi$$

Then $$L Y_\phi = L' Y^* - L_E Y_E \qquad Y' = Y^*$$

Y^* is determined by plotting a graph of Y_S versus L_S and extrapolating back to cut the Y axis. At this point $L_S = 0$ and $Y_S = Y^*$, which for this case was 95,000 ppm. Knowing the value of Y and using the above equations, the values of L and L' can be calculated and hence those for α, η. The cross-sectional area of the column (A) and the density of the liquid phase are easily evaluated and the values of L_E and Y_E are determined experimentally.

The values of the parameters are:- At 60rpm Screw Speed)

$C = 0.530$ g/sec $L_E = 0.401$ g/sec

$Y_E = 4{,}000$ ppm $Y_\phi = 38{,}750$ ppm $Y^* = 95{,}000$ ppm

$A = 88.3\ cm^2$ $\rho = 1.03\ g/cm^3$

From the above equations $L' = 0.117$ and $L = 0.247$ which give values for $a = 0.22$, $\eta = 0.27$. Two more values for a and η were obtained from experimental runs and an average used in subsequent equations:

$$a = 0.26 \quad , \quad \eta = 0.28$$

The mathematical model was written as:

$$H_E = \frac{1}{(C-L_E)}\left[D\rho A\eta + \frac{a(1+a)C^2}{K^a A\rho} - \frac{a L_E C}{K^a A\rho}\right] \qquad (3.48)$$

substituting the above values into the equation

$$33.9 = \frac{1}{(0.530-0.401)}\left[D(0.28x88.3x1.03) + \frac{0.26(1+0.26)(0.530)^2}{Ka\ (88.3x1.03)} - \frac{0.26x0.40x0.530}{Ka\ (88.3x1.03)}\right]$$

which simplified to

$$(DS26)\quad 4.39 = 25.84D + \frac{4.03 \times 10^{-4}}{Ka}$$

Similar calculations were carried out for experimental runs (DS9) and (DS27) using the parameters below:

Values for the constants:

DS 9 > $A\rho = 90.95$ $a = 0.26$ $\eta = 0.28$
DS 27 >

Values of the experimental parameters:

(DS 9) $C = 0.574$ g/sec $L_E = 0.472$ g/sec $H_E = 43.80$

(DS 27) $C = 0.518$ g/sec $L_E = 0.358$ g/sec $H_E = 29.25$

Which yielded the following equations:

(DS 9) $4.47 = 25.84 + \frac{4.12 \times 10^{-4}}{Ka}$

(DS 27) $4.69 = 25.84 + \frac{4.36 \times 10^{-4}}{Ka}$

These three simultaneous equations were solved and values for the Diffusion and Overall Mass Transfer rate obtained.

$$\frac{D = 2.65 \times 10^{-2} \text{ cm}^2 \text{ s}^{-1}}{Ka = 1.09 \times 10^{-4} \text{ s}^{-1}}$$ (for a Screw Speed of 60 rpm)

Substitution of these values back into equation (3.48) allows the calculation of the theoretical value for the separation factor H_E to be determined and compared with that obtained experimentally. Thus for experimental runs

(DS 9) H_E (Theo) = 43.75 Percentage difference = 0.1%

(DS 26) H_E (Theo) = 33.97 Percentage difference = 0.1%

(DS 27) H_E (Theo) = 29.25 Percentage difference = 0.0%

Using these theoretical values of H_E in equation (3.54)

$$\frac{Y-Y_P}{Y_\phi - Y_P} = e. \frac{-(Z^*)}{H_E}$$

a theoretical concentration profile can be computed and compared to the experimentally measured concentration profile. The values of Y_P and Y_ϕ are estimated from the experimental measurements, the theoretical values of Y being computed at the sample point locations down the column, (Z^*).

Parameters for:	(p.p.m)	(p.p.m)
(DS 9)	$Y_P = 603$	$Y_\phi = 50,000$
(DS 26)	$Y_P = 1650$	$Y_\phi = 38,750$
(DS 27)	$Y_P = 968$	$Y_\phi = 45,000$

Position in column (Z*) cms	Theoretical concentration profiles ($x10^3$)p.p.m (DS 9)	(DS 26)	(DS 27)
19	32.98	23.17	24.36
39	21.09	13.59	12.77
59	13.57	8.28	6.93
79	8.82	5.33	3.98
89	7.14	4.39	3.10
108	4.84	3.22	2.08
113	4.34	3.00	1.91

The experimental concentration profiles are presented as follows ;

(DS 9) FIG. (A.2)

(DS 26) FIG. (A.3)

(DS 27) FIG. (A.4)

A comparison of the two sets of data is presented in Figs (A2), (A3), (A4). A similar mathematical analysis was carried out on another series of desalination runs, however this time the column was operated at a screw speed of 100 rpm, enabling a comparison with the 60 rpm data, to be made.

Values of constants: for (DS 31, DS 32, DS 33, DS 34)

$$A\rho = 90.95 \qquad a = 0.16 \qquad \eta = 0.18$$

Values for the experimental parameters:

(DS31)	C = 0.485 g/sec	L_E = 0.438 g/sec	H_E = 37.60
(DS32)	C = 0.520 g/sec	L_E = 0.470 g/sec	H_E = 35.44
(DS33)	C = 0.390 g/sec	L_E = 0.363 g/sec	H_E = 42.10
(DS34)	C = 0.443 g/sec	L_E = 0.401 g/sec	H_E = 37.34

Substituting the values into equation (3.48) yield the following simultaneous equations.

(DS31) $1.79 = 16.46D + 1.10 \times 10^{-4}/Ka$

(DS32) $1.75 = 16.46D + 1.25 \times 10^{-4}/Ka$

(DS33) $1.12 = 16.46D + 0.63 \times 10^{-4}/Ka$

(DS34) $1.59 = 16.46D + 0.91 \times 10^{-4}/Ka$

which when solved give the following values for the Diffusion and Overall Mass Transfer coefficients.

$D = 3.13 \times 10^{-2}\ cm^2\ s^{-1}$

$Ka = 1.07 \times 10^{-4}\ s^{-1}$

(at 100 rpm Screw Speed)

Theoretical values for the separation factor H_E can be calculated using these values and compared with the experimental values.

Run No	H_E(experimental)	H_E(theoretical)	Percentage difference
(DS31)	37.60	32.48	15.8 %
(DS32)	35.44	34.08	4.0 %
(DS33)	42.10	41.42	1.6 %
(DS34)	37.34	32.14	16.2 %

FIG. (A.1)

Log/Semi-Log plot of $(Y-Y_p)$ vs. Z^*

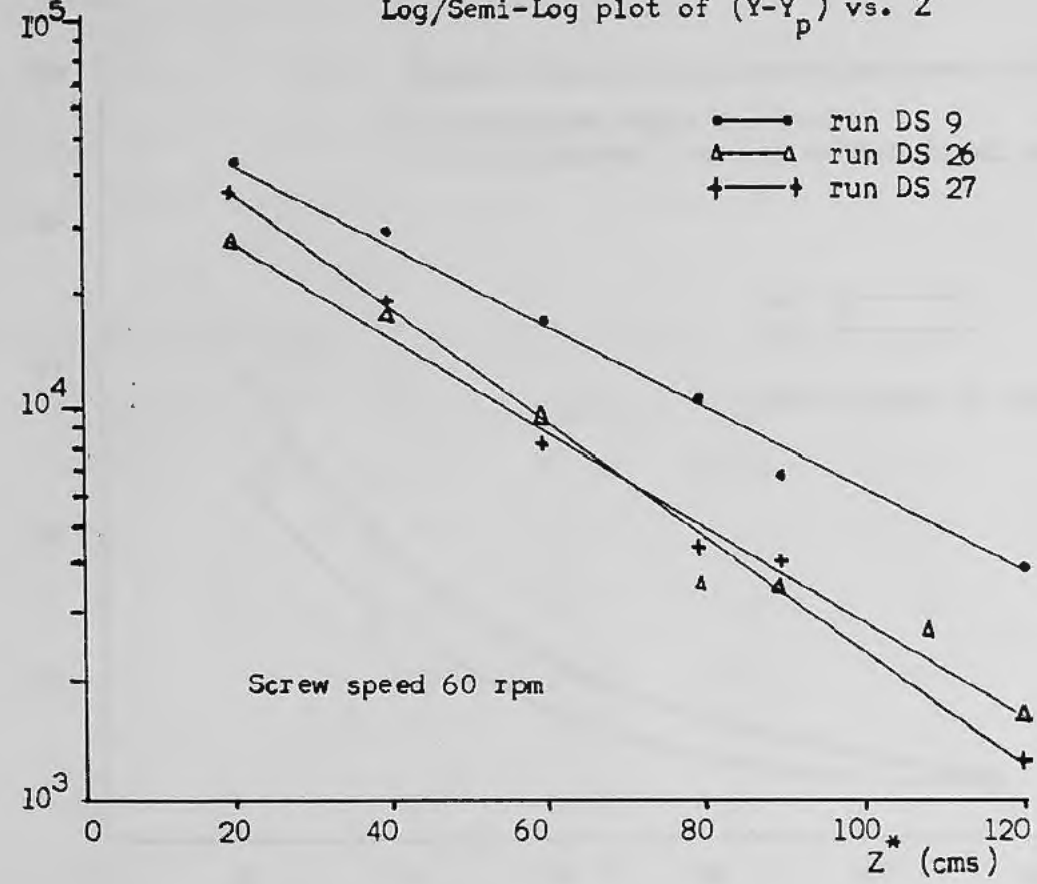

FIG. (A.2)

Sodium Chloride concentration down the column.

(a) measured experimentally

(b) calculated from the mathematical model

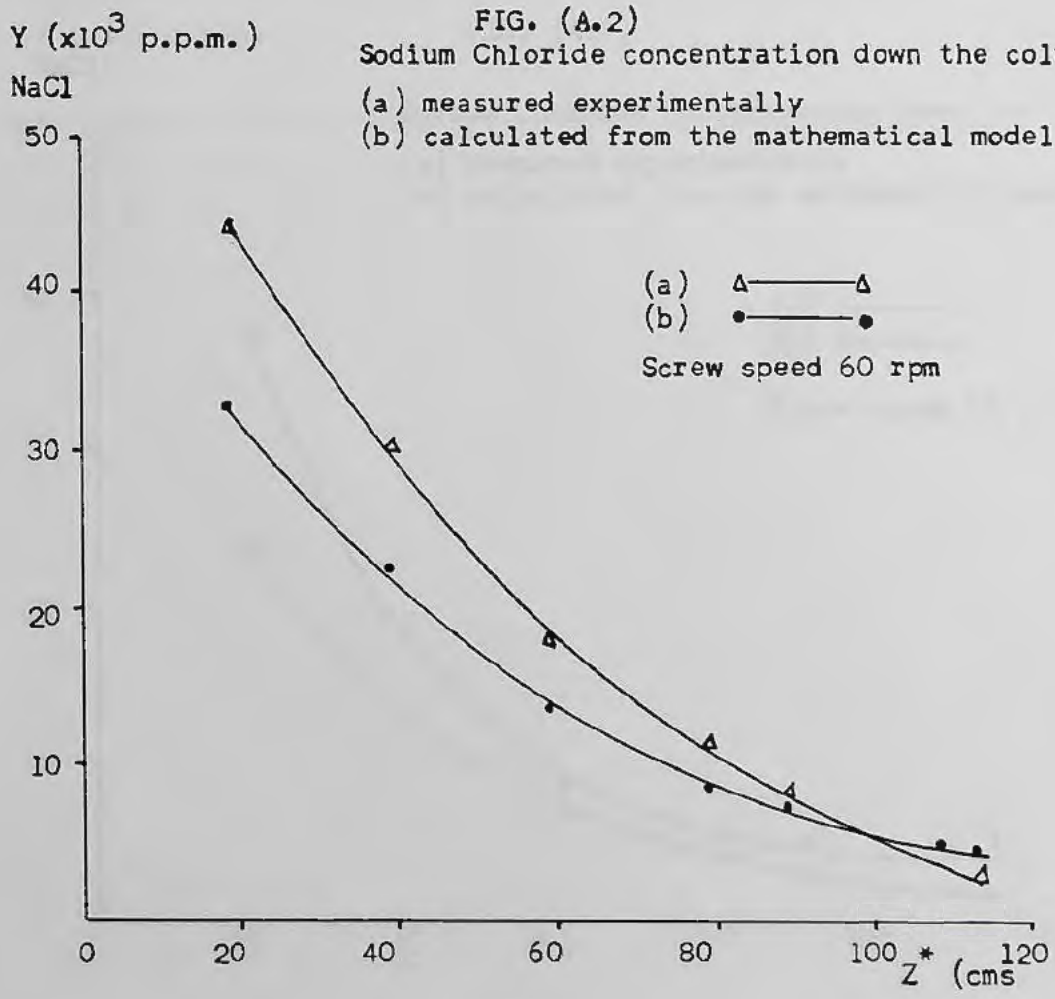

FIG. (A.3)

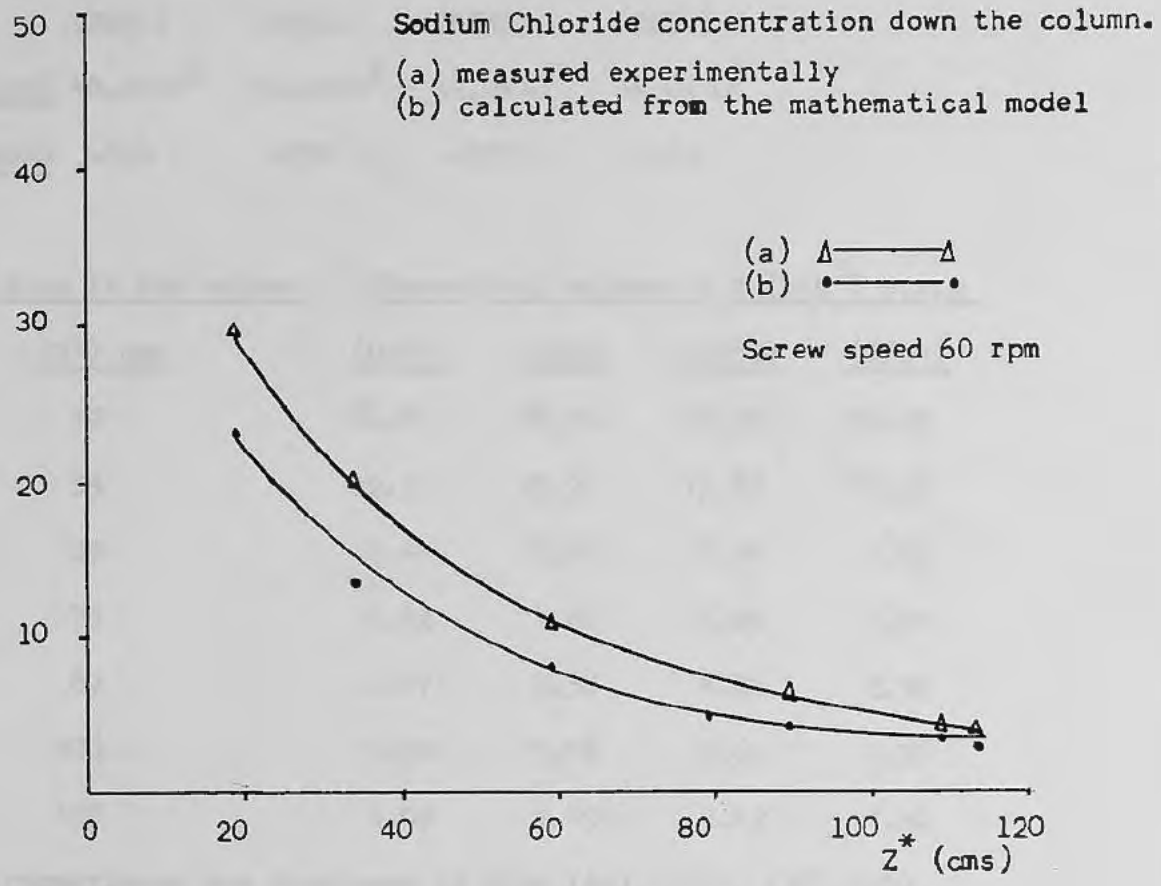
Y (x10³ p.p.m.)
NaCl
Sodium Chloride concentration down the column.
(a) measured experimentally
(b) calculated from the mathematical model
(a)
(b)
Screw speed 60 rpm
50
40
30
20
10
0
20
40
60
80
100
120
Z* (cms)

FIG. (A.4)

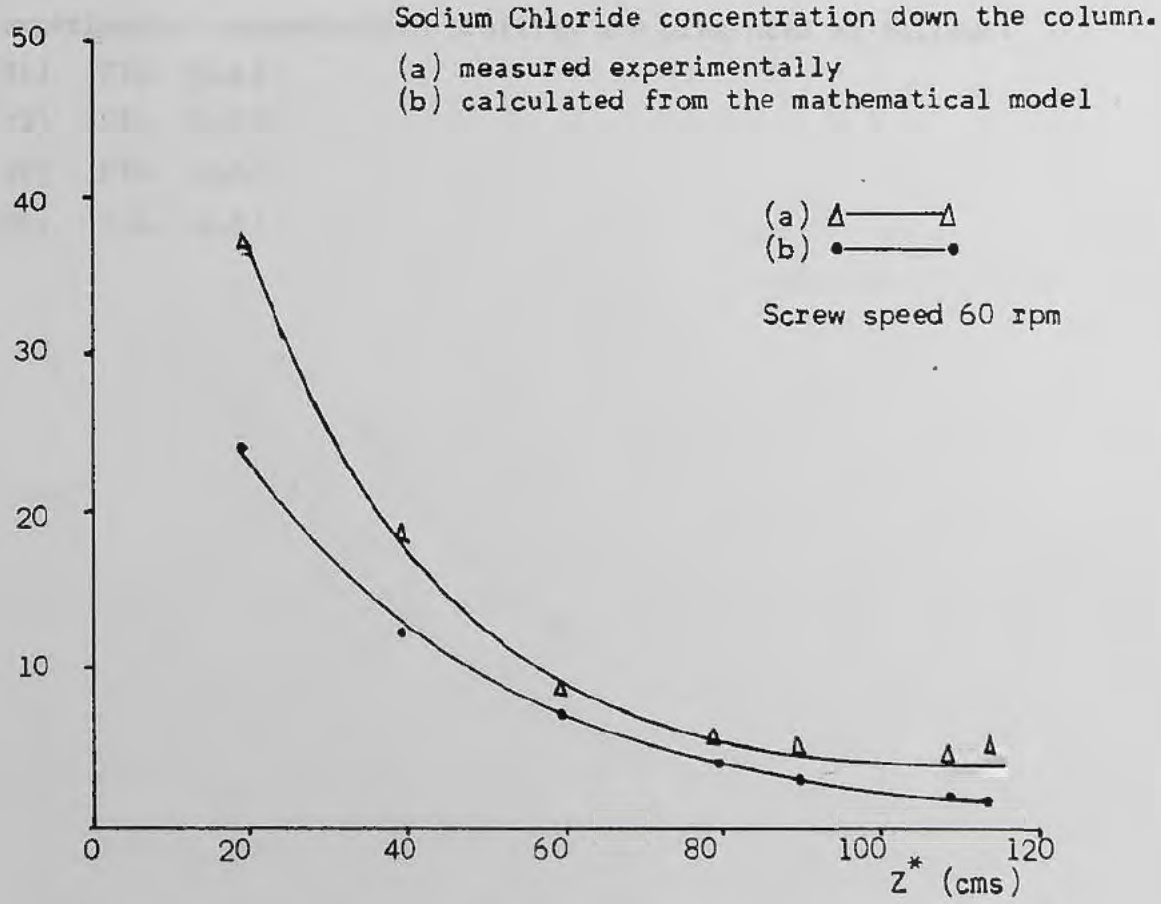
Y (x10³ p.p.m.)
NaCl
Sodium Chloride concentration down the column.
(a) measured experimentally
(b) calculated from the mathematical model
(a)
(b)
Screw speed 60 rpm
50
40
30
20
10
0
20
40
60
80
100
120
Z* (cms)

Using the calculated theoretical value of H_E, it is possible to compute the theoretical concentration profiles.

Run	(DS31)	(DS32)	(DS33)	(DS34)
Y_ϕ(ppm)	40.0×10^3	50.0×10^3	32.0×10^3	34.0×10^3
Y_p(ppm)	-165	-370	+325	+382

Position in the column	Theoretical values of Y ($\times 10^3$) p.p.m			
(Z*) cms	(DS31)	(DS32)	(DS33)	(DS34)
19	22.56	28.90	20.59	19.29
39	12.11	15.91	12.83	10.53
59	6.47	8.68	8.04	5.83
79	3.42	4.66	5.09	3.31
89	2.47	3.38	4.06	2.52
108	1.30	1.78	2.69	1.57
113	1.09	1.49	2.42	1.40

The comparisons are displayed in Figs (A6), (A7), (A8), (A9).

The experimental concentration profiles are presented as follows:

(DS 31) FIG. (A.6)

(DS 32) FIG. (A.7)

(DS 33) FIG. (A.8)

(DS 34) FIG. (A.9)

FIG. (A.5)

Log/Semi-Log plot of $(Y-Y_p)$ vs. Z^*

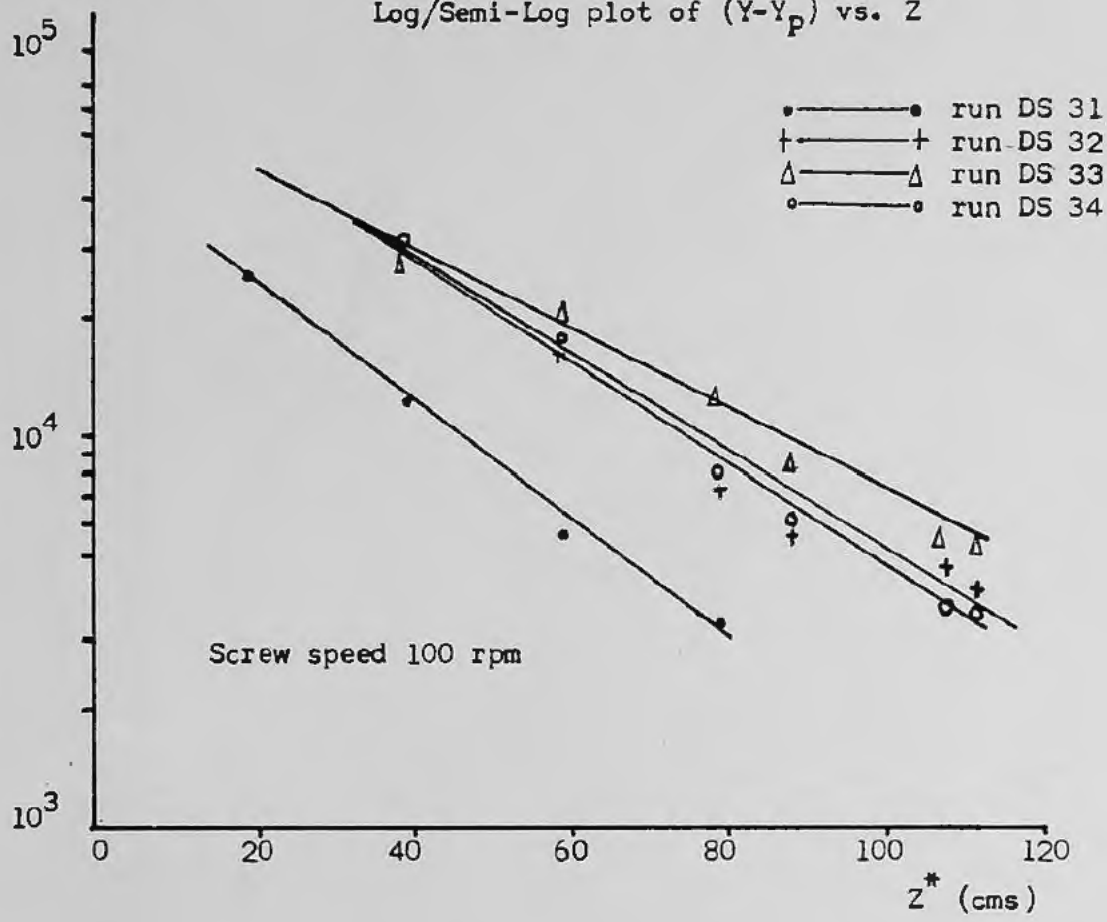

FIG. (A.6)

Sodium Chloride concentration down the column.

(a) measured experimentally
(b) calculated from the mathematical model

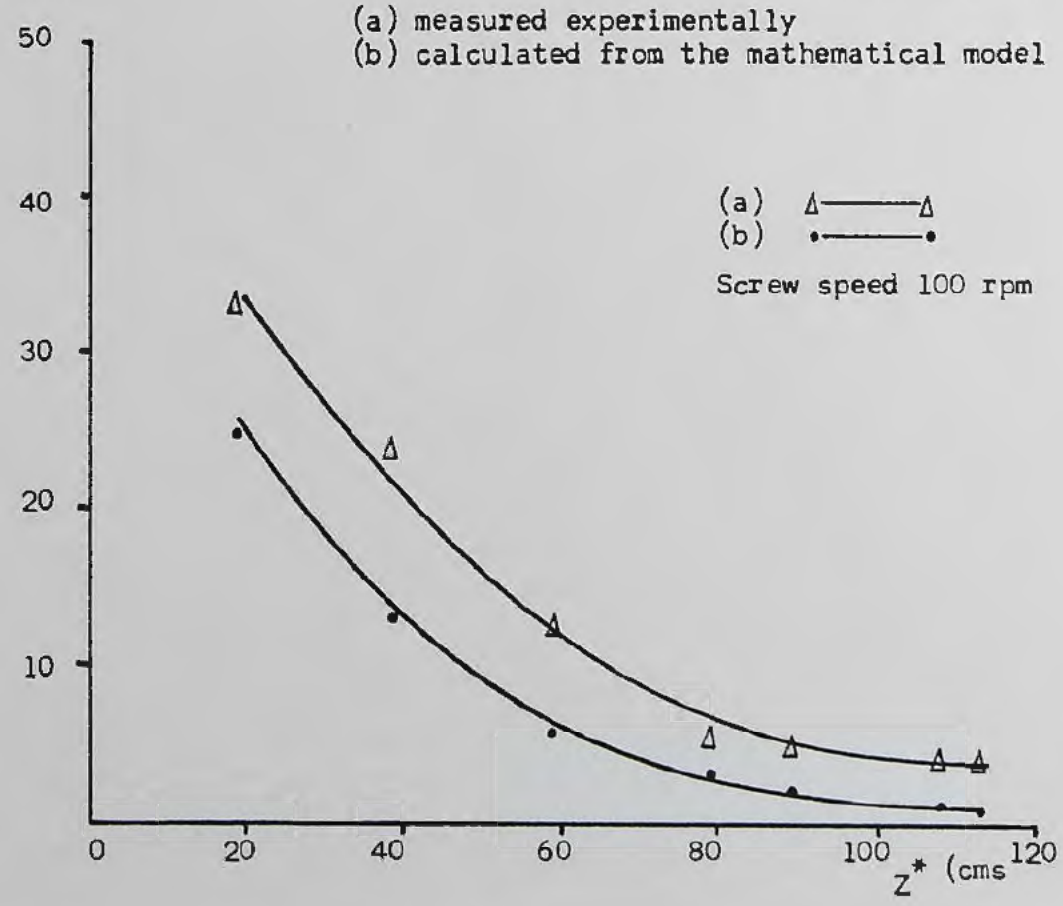

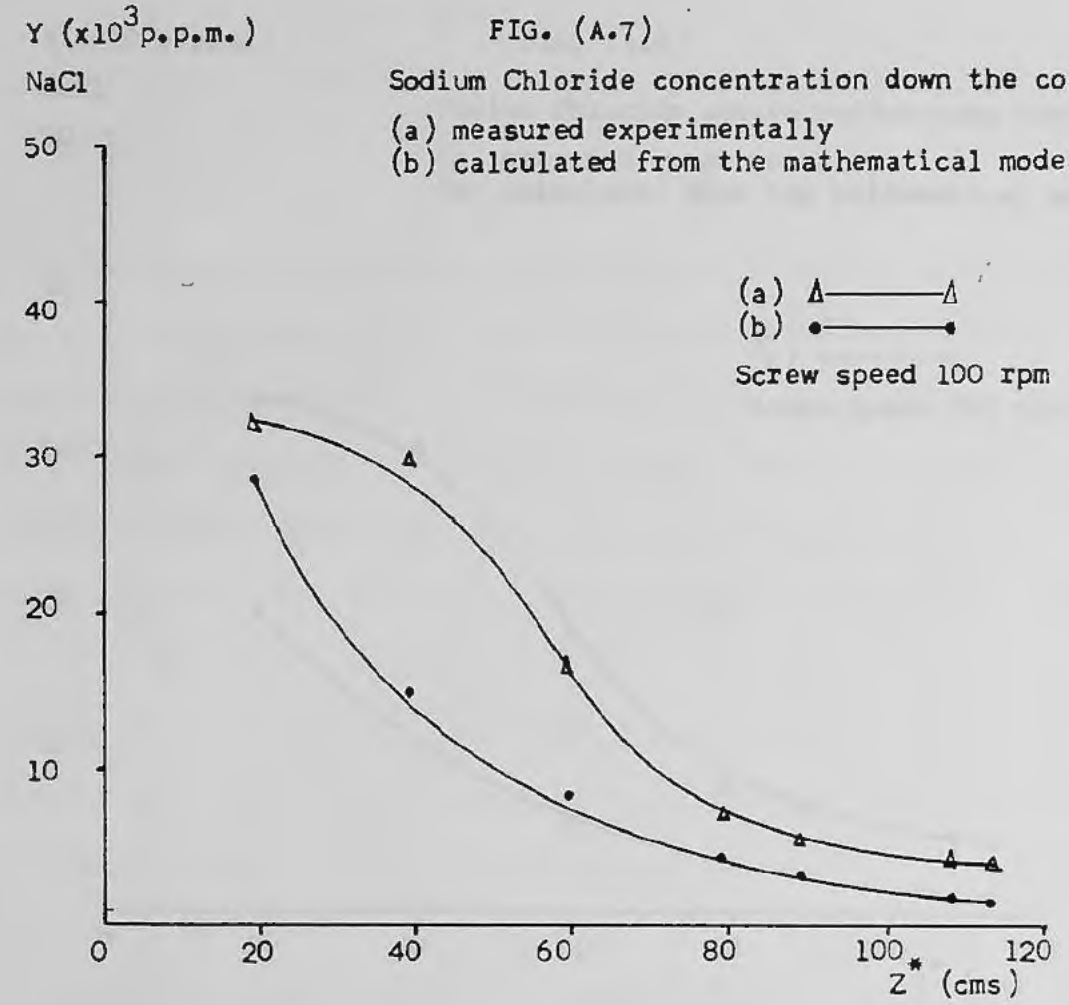

FIG. (A.7)

Sodium Chloride concentration down the column.

(a) measured experimentally
(b) calculated from the mathematical model

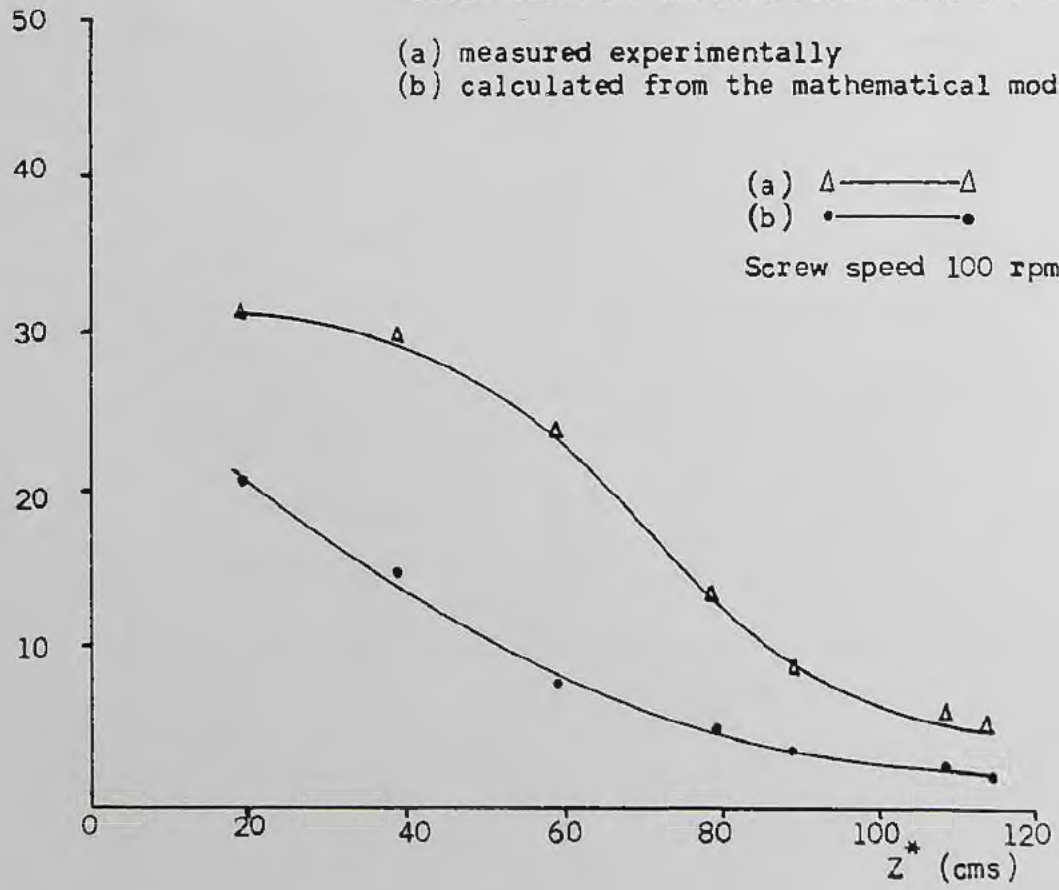

FIG. (A.8)

Sodium chloride concentration down the column.

(a) measured experimentally
(b) calculated from the mathematical model

FIG. (A.9)

Sodium Chloride concentration down the column.

(a) measured experimentally
(b) calculated from the mathematical model

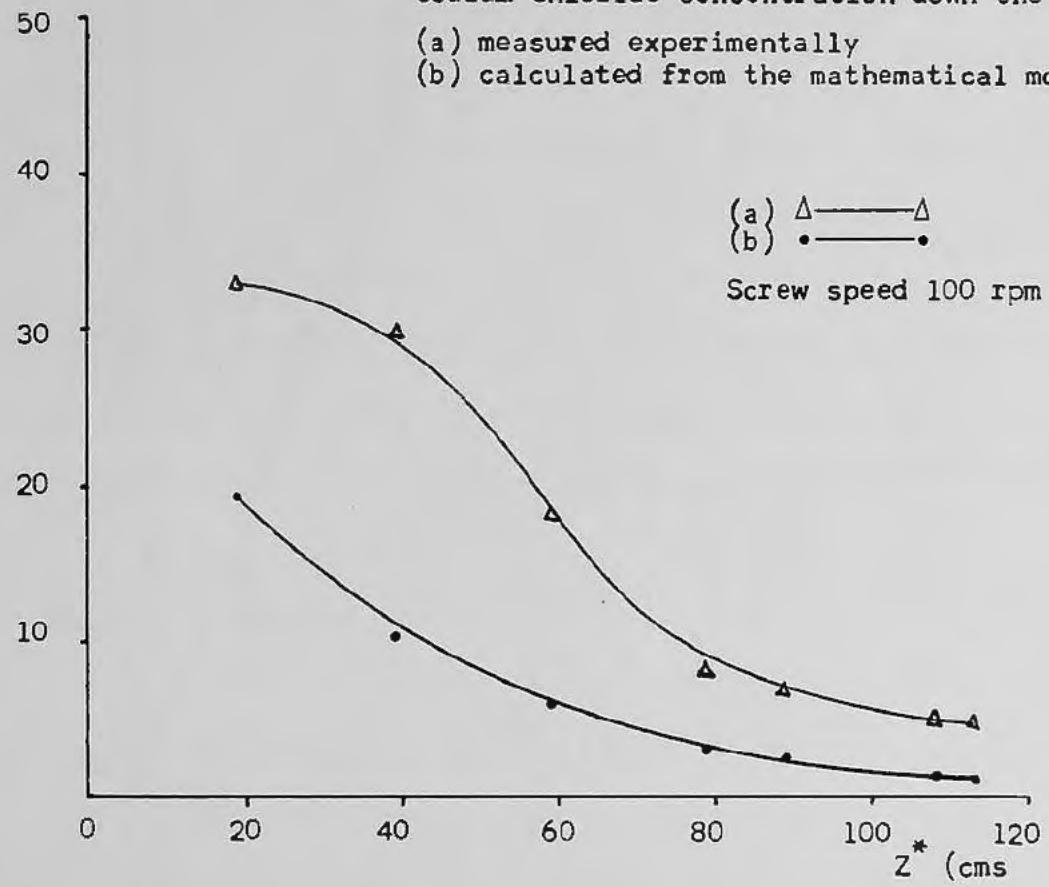

(A.3) Ethanol Concentration

Calculation of the Axial Diffusion (D) and Overall Mass transfer (Ka) coefficients

A mathematical analysis for the ethanol/water system is carried out for the stripping section. For the column configuration employed, only two concentrations can be measured accurately, the values for the ethanol entering and leaving the stripping section. This is performed at four different crystal production rates allowing average values for D and Ka to be computed. The value of $\bar{Y}p$ is calculated from equation (3.56)

$$\bar{Y}_p = (C\varepsilon + LsYs) / (C + Ls) \qquad (3.56)$$

The value of ε being determined from an analysis of the enriching section using the analogous equation to that above. The separation for the stripping section is given in equation (3.57)

$$H_S = \frac{1}{(C+Ls)}\left[D\eta A\rho + \frac{a(1+a)C^2 + aLsC}{KaA\rho} \right] \qquad (3.57)$$

The constants A, ρ , η , a were evaluated as before, the column being operated at four known crystal production rates, constant product removal rate (Ls), and the resulting value of Ys measured.

Values of the experimental parameters:

$A\rho$ = 85.77 a = 1.65 η = 0.41 Ls = 0.383 g/sec

Run (1) C = 0.324 g/sec Hs = 92.90 at 34 r.p.m

Run (23) C = 0.315 g/sec Hs = 71.20

Run (24) C = 0.301 g/sec Hs = 75.63

Run (25) C = 0.261 g/sec Hs = 69.60

Substitution of these values in (3.57) yields four simultaneous equations.

Run (1) $65.68 = 35.17D + \frac{0.77 \times 10^{-2}}{Ka}$

Run (23) $49.70 = 35.17D + \frac{0.74 \times 10^{-2}}{Ka}$

Run (24) $51.73 = 35.17D + \frac{0.68 \times 10^{-2}}{Ka}$

Run (25) $44.83 = 35.17D + \frac{0.54 \times 10^{-2}}{Ka}$

which when solved give the following values for the diffusion and overall mass transfer rates:

$$D = 0.71 \ cm^2 \ sec^{-1}$$

$$Ka = 2.67 \times 10^{-4} \ sec^{-1} \qquad \text{at } 34 \text{ r.p.m}$$

Substitution of these averaged values back into equation (3.57) allows the calculation of the theoretical value for the separation factor Hs to be determined, and compared with that obtained experimentally. Thus for the experimental runs, the following values were calculated:

Run No	Hs (experimental)	Hs (theoretical)	Percentage difference
(1)	92.90	76.29	21.8
(23)	71.20	75.35	5.5
(24)	75.63	73.94	2.3
(25)	69.60	70.21	0.9

Taking the theoretical values of Hs, it is possible to use them in equation (3.55), with the parameters below, to give an estimation of the concentration of ethanol (Ys) in the top product.

$$\ln(Y_s - \bar{Y}_p) = -(Z - Z_F)/Hs + \ln(Y_\phi - \bar{Y}_p) \qquad (3.55)$$

Run	(1)	(23)	(24)	(25)
Y_ϕ (%)	13.8	12.3	12.3	11.5
$\bar{Y}_p$ (%)	9.6	9.7	9.6	9.5

Giving the following values :

Run	(1)	(23)	(24)	(25)
(Ys)experimental	15.5	13.6	13.6	12.5
(Ys)theoretical	15.8	13.4	12.6	12.5

A comparison of the effect of crystal production rate on ethanol enrichment in the top product for experimental runs and corresponding theoretical estimations is presented in Fig (A.10).

FIG. (A.10)

Effect of crystal rate on the concentration of ethanol in the top product.

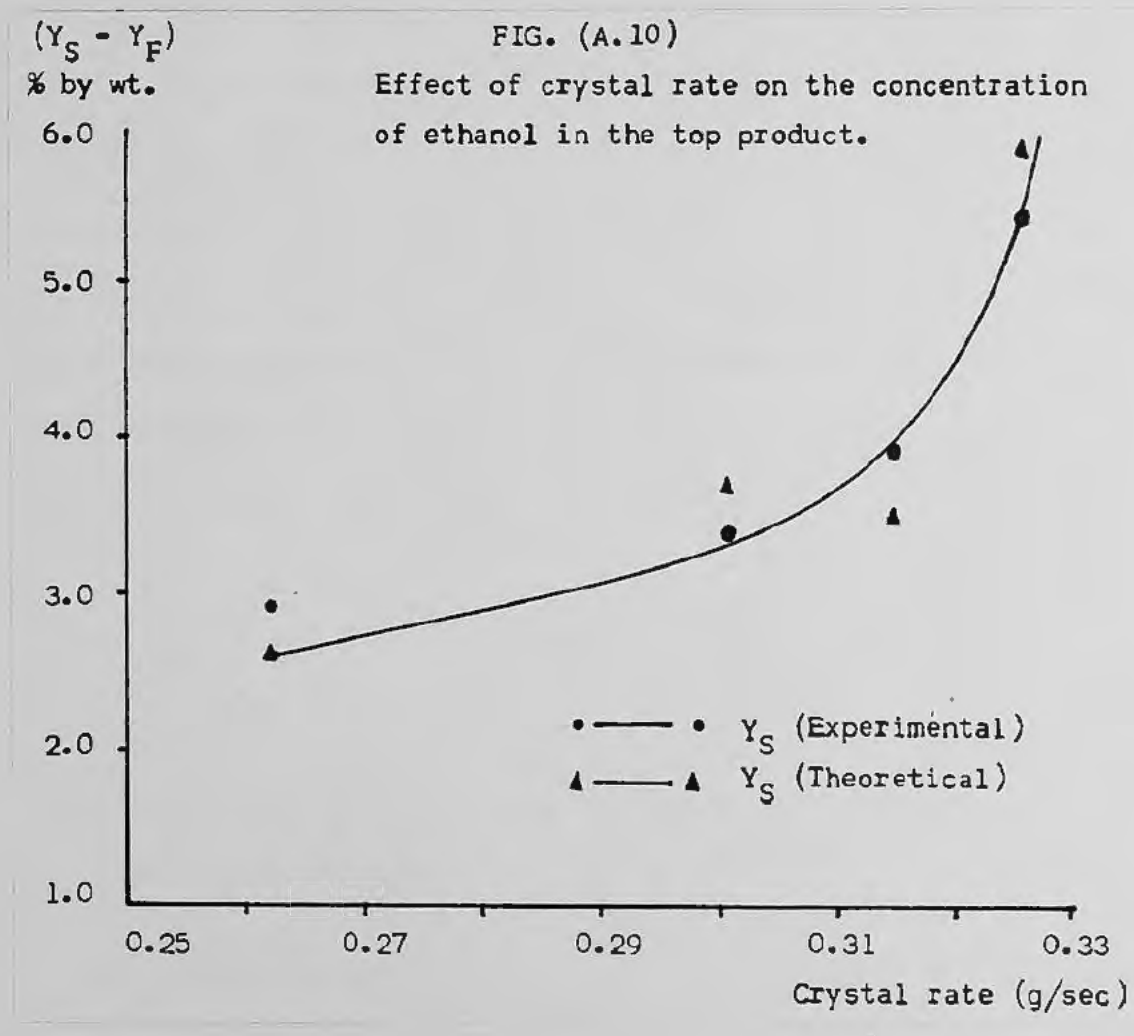

(A.4) Waste Effluent Recovery

Calculation of the Axial Diffusion (D) and Overall Mass transfer (Ka) coefficients

A mathematical analysis was carried out using the same procedure adopted in the calculation of the parameters for the desalination work. For three crystal production rates at constant product removal rates, the separation factor H_E was determined (Fig A.11).

Run (1) C = 0.178 g/sec L_E = 0.101 g/sec H_E = 31.46

Run (4) C = 0.193 g/sec L_E = 0.101 g/sec H_E = 26.53

Run (7) C = 0.226 g/sec L_E = 0.098 g/sec H_E = 19.62

Values of the experimental parameters:

A = 12.43 ρ = 1.016 α = 0.43 η = 0.42 at 60 r.p.m

Substitution of these values in (3.48) yields the following simultaneous equations,

Run (1) $2.43 = 5.33D + \frac{0.94\times10^{-3}}{Ka}$

Run (4) $2.45 = 5.33D + \frac{1.17\times10^{-3}}{Ka}$

Run (7) $2.51 = 5.33D + \frac{1.75\times10^{-3}}{Ka}$

which when solved give the following values for the diffusion and overall mass transfer rates:

$D = 0.44 \quad cm^2 sec^{-1}$

$Ka = 9.96\times10^{-3} \quad sec^{-1}$ at 60 r.p.m

Substitution of these values back into equation (3.48) allows the calculation of the theoretical value for the separation factor H_E to be determined and compared with that obtained experimentally.

Run (1)	H_E (experimental) = 31.46	H_E (theoretical) = 31.46
Run (4)	" = 26.53	H_E " = 26.52
Run (7)	" = 19.62	" = 19.63

The percentage difference in the two sets of values is negligible. Substitution of the H_E(Theoretical) values back into equation (3.54) (describes the concentration profile) allows a comparison to be made between the experimental data points and those calculated from the model.

Parameters for:

Run	(1)	(4)	(7)
$Y_{\emptyset}$ (ppm)x10^3	32.5	36.0	36.0
Y_P (ppm)	34	-115	1453

The theoretical concentration profiles are:

Pos^n in the column Z* (cms)	Run (1) x10^3 (p.p.m)	Run (4) x10^3 (p.p.m)	Run (7) x10^3 (p.p.m)
10	24.42	25.61	23.29
25	15.17	14.50	11.62
35	11.05	9.91	7.56
60	5.01	3.79	3.16

A comparison of the two sets of data is presented in Figs (A.12), (A.13), (A.14).

The experimental concentration profiles are presented as follows:

Run W.E. (1) FIG (A.12)

Run W.E. (4) FIG (A.13)

Run W.E. (7) FIG (A.14)

FIG. (A.11)

Log/Semi-Log plot of $(Y-Y_p)$ vs. Z^*

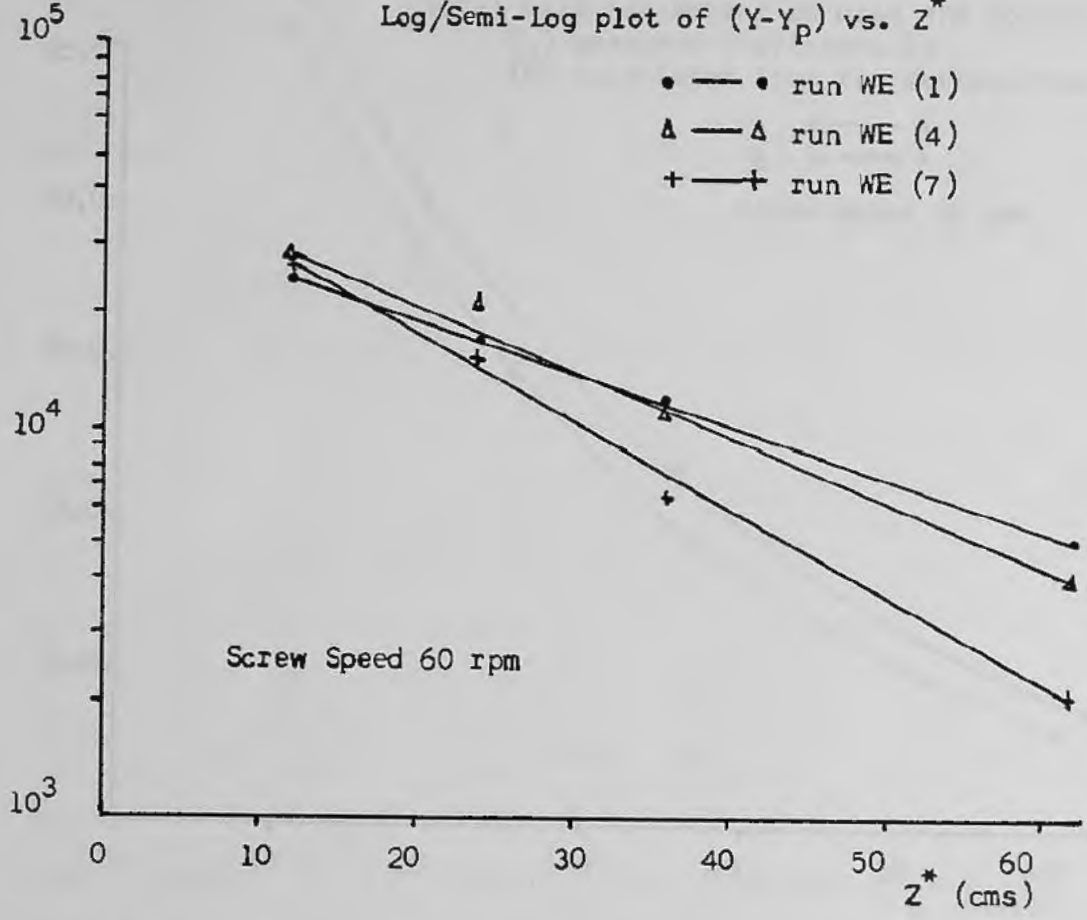

FIG. (A.12)

Total salt concentration down the column.
(a) measured experimentally
(b) calculated from the mathematical model

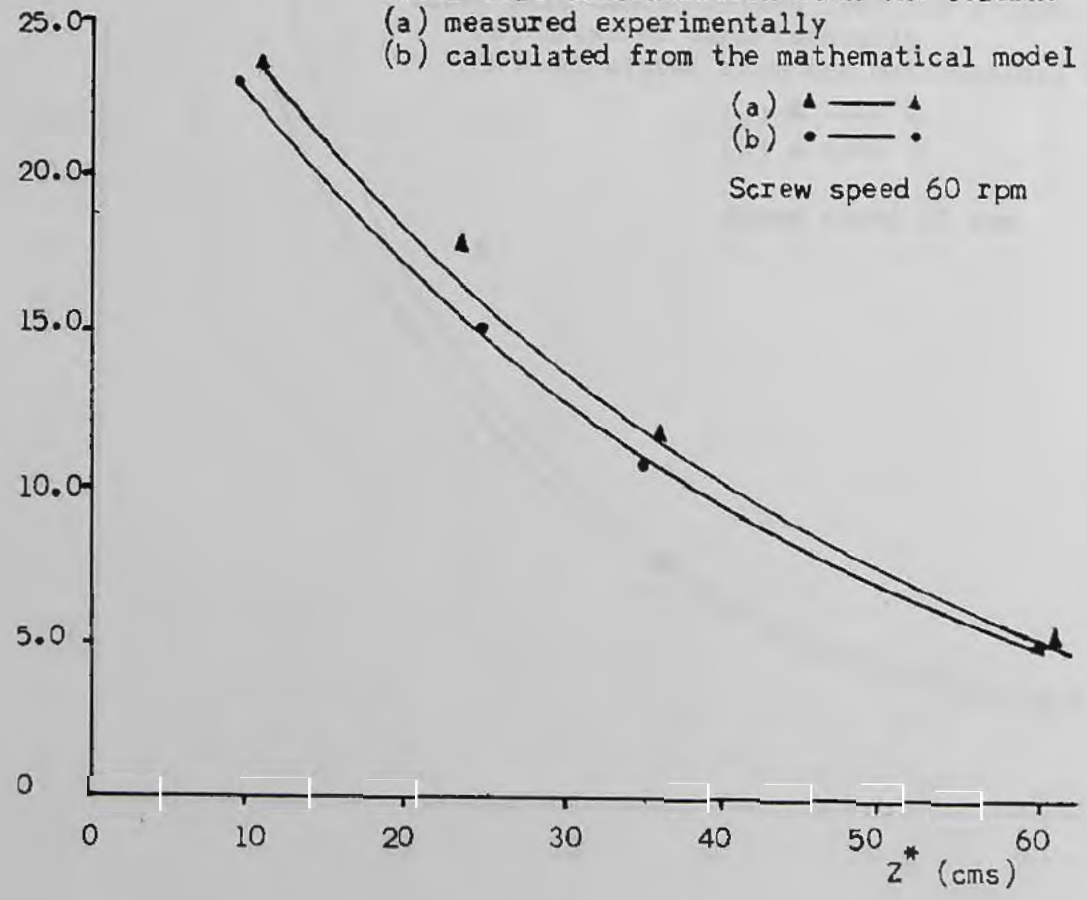

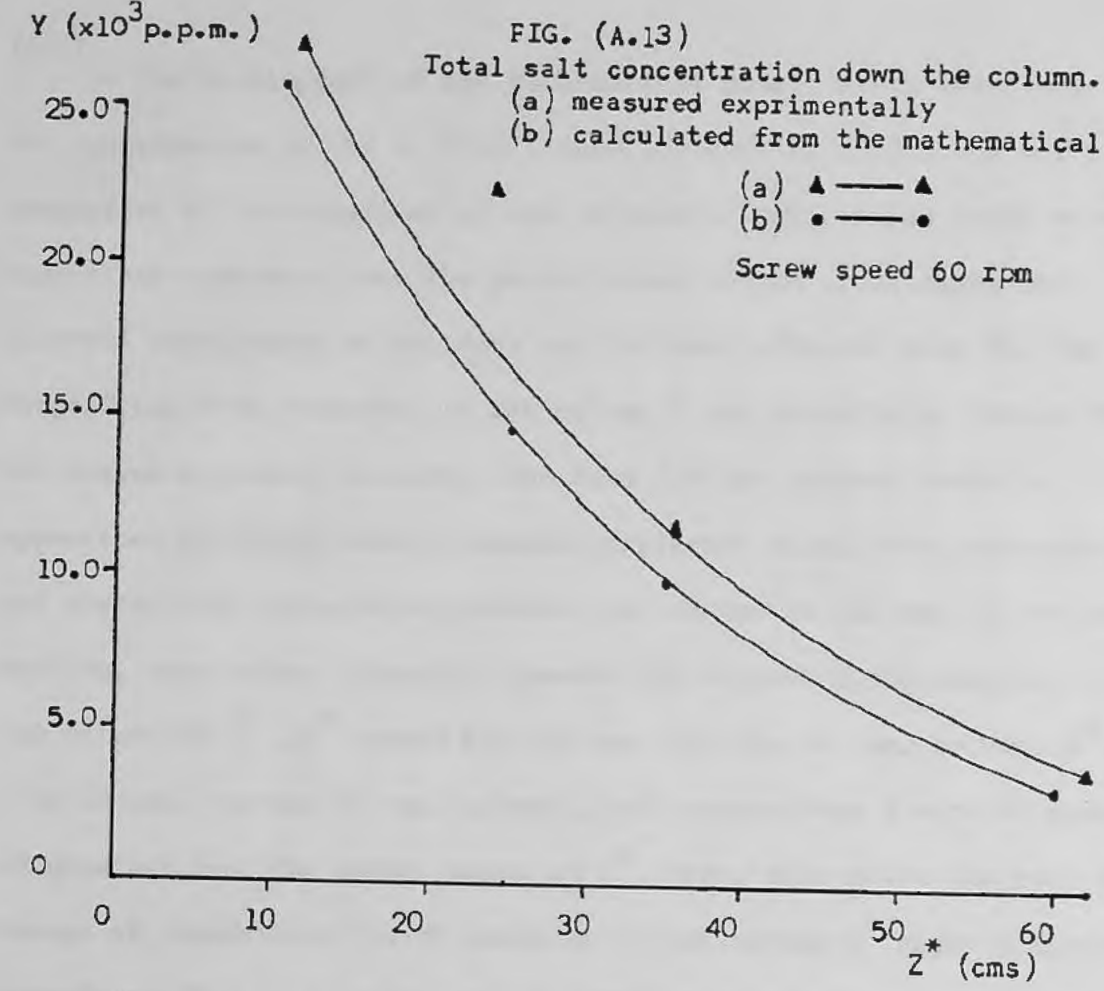

FIG. (A.13)
Total salt concentration down the column.
(a) measured exprimentally
(b) calculated from the mathematical model

(a) ▲——▲
(b) ●——●

Screw speed 60 rpm

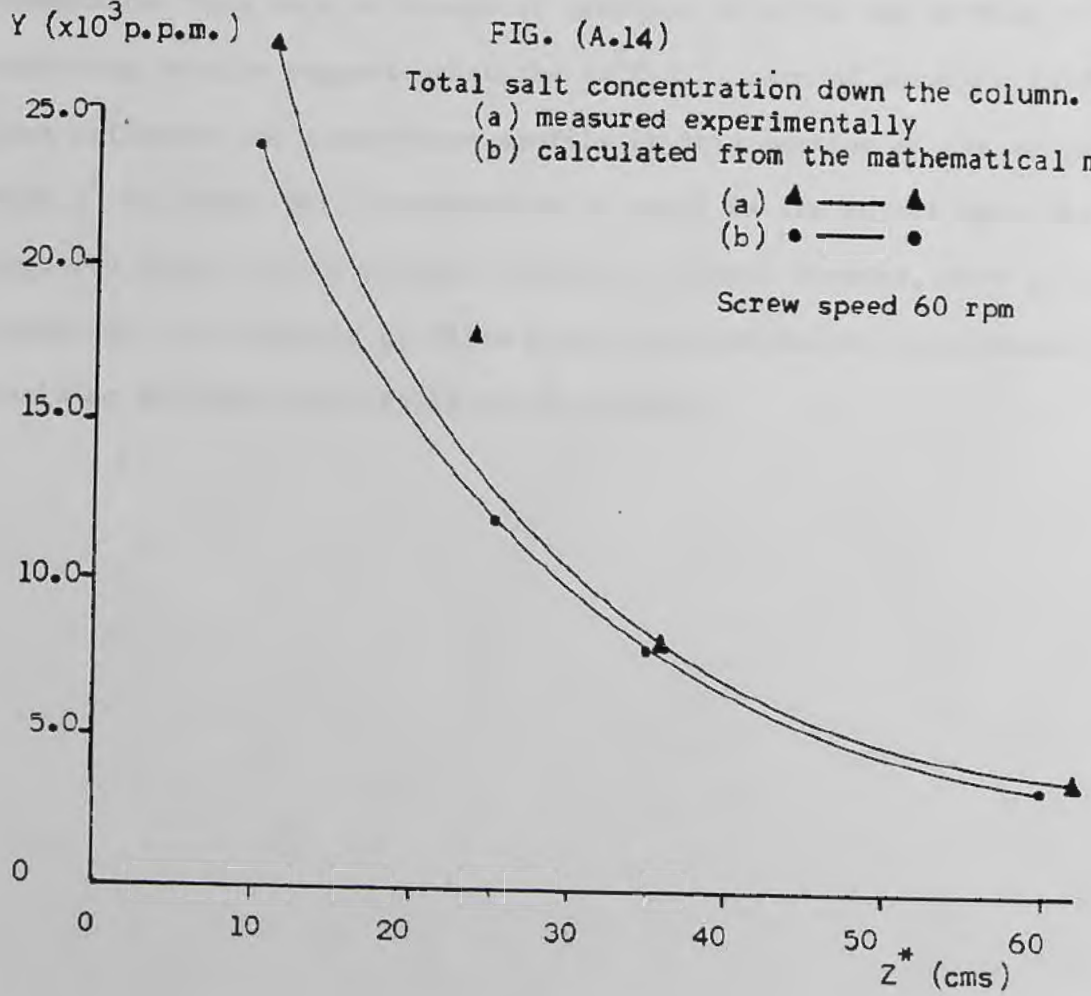

FIG. (A.14)
Total salt concentration down the column.
(a) measured experimentally
(b) calculated from the mathematical model

(a) ▲——▲
(b) ●——●

Screw speed 60 rpm

(A.5)

In the development of the mathematical model, Henry concluded that the contribution of the (d^2Y/dZ^2) term in equation (3.37) was negligible. Comparison of the experimental and calculated composition profiles showed very close agreement over the whole column length ,confirming the internal consistancy of the data and the model,(Henry's data for the composition Y vs. position in the column Z was essentially linear over the column enriching section). The data for the present study in Appendices (A.2,A.4) show a somewhat different trend. Both the experimental and theoretical composition profiles are curved at the top of the enriching section, approaching linearity towards the bottom of the section. For low values of Z^* ,(Z^* equals 0 to 50 cms. for the 100 mm. column, Z^* equals 0 to 25 cms. for the 50 mm. column), both curves show a rate of change of gradient over the above ranges of Z^*. After this point the rate of change of composition Y with position in the column Z^* shows a linear dependence. This rate of change of gradient over the top portion of the enriching section suggests that the (d^2Y/dZ^2) term of equation (3.37) does influence the composition profile in this portion of the column. When Z^* is large, this contribution is small in its effect upon the final impurity levels of the product. However, using a shorter, wide bore column, predicted concentration profiles would indicate better separations than could be achieved practically on the column.